




1981

Thermodynamics of Association and Catalysis of N-Acyl-Peptidyl-Phenylalanine Amide Substrates by Chymotrypsin

John Paul Huff
Loyola University Chicago

Follow this and additional works at: https://ecommons.luc.edu/luc_diss

 Part of the [Biochemistry, Biophysics, and Structural Biology Commons](#)

Recommended Citation

Huff, John Paul, "Thermodynamics of Association and Catalysis of N-Acyl-Peptidyl-Phenylalanine Amide Substrates by Chymotrypsin" (1981). *Dissertations*. 1987.

https://ecommons.luc.edu/luc_diss/1987

This Dissertation is brought to you for free and open access by the Theses and Dissertations at Loyola eCommons. It has been accepted for inclusion in Dissertations by an authorized administrator of Loyola eCommons. For more information, please contact ecommons@luc.edu.



This work is licensed under a [Creative Commons Attribution-NonCommercial-No Derivative Works 3.0 License](#).
Copyright © 1981 John Paul Huff

THERMODYNAMICS OF ASSOCIATION AND CATALYSIS
OF N-ACYL-PEPTIDYL-PHENYLALANINE AMIDE SUBSTRATES BY CHYMOTRYPSIN

by
John Paul Huff

A Dissertation Submitted to the Faculty of the Graduate School
of Loyola University of Chicago in Partial Fulfillment
of the Requirements for the Degree of
Doctor of Philosophy

February
1981

To Marcella

ACKNOWLEDGMENTS

I would like to acknowledge the guidance and support of my advisor, Dr. Richard M. Schultz. I would like to thank Alexa Cheerva, William Kennedy, William Treadway, and Pratibha Varma-Nelson for all their help. I would also like to thank my wife, Marcella, for all her help throughout our marriage. Lastly, I would like to thank my parents, Paul and Dorothy, for all their help and encouragement.

VITA

John Paul Huff was born to Paul and Dorothy Huff in Chicago, Illinois, on December 7, 1950.

He attended public grade and high school in Chicago. Upon graduation from Lindblom Technical High School in 1968, he was awarded an Illinois State Scholarship. He received a B.A. in Chemistry in 1974 from the University of Illinois at Chicago Circle.

In 1974, he began studies at Loyola University of Chicago towards the degree of Doctor of Philosophy in the Department of Biochemistry and Biophysics. While at Loyola, he was awarded a Basic Science Research Fellowship for the period of 1975-76 and a Basic Science Assistantship for the period 1976-79. In July of 1979, he began work towards the degree of Doctor of Medicine at the Loyola Stritch School of Medicine.

He has co-authored one publication:

Schultz, R.M., Huff, J.P., Tsay, S.-H.L., Kennedy, W.P. and Crumrine, D., "Thermodynamics of Association and Transition-State Formation in α -Chymotrypsin (Cht) Catalysis of N-Acyl-L-Phenylalanine Amide Substrates; Comparison of the sp^3 Hemiacetal Complex in Cht with N-Acyl-L-Phenylalaninals (Aldehydes)", Abstr. 180th Meeting Am. Chem. Soc., Biol. Chem., 33 (1980).

TABLE OF CONTENTS

	Page
ACKNOWLEDGEMENTS	iii
LIFE	iv
LIST OF TABLES	viii
LIST OF FIGURES	xi
LIST OF ABBREVIATIONS	xiv
CONTENTS OF APPENDICES	xvii
Chapter	
I. INTRODUCTION	1
A. Goals of this Dissertation	1
B. Basic Concepts and Theories of Enzymatic Catalysis	3
1. Basic Concepts of Enzyme Kinetics	3
2. Basic Concepts of Transition State Theory ...	8
3. Theories of Enzymatic Catalysis	12
C. Review of the Related Literature	21
1. α -Chymotrypsin	21
2. Thermodynamics of Productive and Non-Productive Association of Substrates with α -Chymotrypsin: "Association-Activation"	28
3. Thermodynamics of Association and Catalysis of Specific and Non-Specific Substrates by α -Chymotrypsin	33
4. Thermodynamoc, Kinetic, and Physical Evidence for Two Temperature Dependent Forms of Chymotrypsin	36
5. The Extended Binding Site of α -Chymotrypsin	39
6. Thermodynamics of Protein-Ligand and Protein-Protein Interactions	44
7. Model Solvent Partition and Enzyme Studies ..	48
8. Synthetic Catalytic Models	50
II. MATERIALS AND METHODS	53
A. General Materials and Sources	53
B. Synthesis of Derived Amino Acid and Peptide Substrates	55
1. Synthesis of N-Acetyl-L-Phenylalanine-Amide .	56
2. Synthesis of N-Acetyl-L-Phenylalanine-Glycine-Amide	59

3.	Synthesis of N-Acetyl-L-Proline-L-Phenylalanine-Amide	62
4.	Synthesis of N-Acetyl-L-Alanine-L-Proline-L-Phenylalanine-Amide	64
5.	Synthesis of N-Acetyl-L-Proline-L-Alanine-L-Proline-L-Phenylalanine-Amide	66
6.	Synthesis of N-Formyl-L-Phenylalanine-Amide.	67
7.	Synthesis of O-Acetoxy-L-Phenyllactic-Amide.	68
8.	Synthesis of L-(-)-keto-3-carboamide tetrahydroisoquinoline (L-(-)-KCAQ)	70
9.	Synthesis of L-(+)-3-Carboamide-3,4-Dihydroisocoumarin (CADIC)	72
C.	Synthesis of Nonapeptide Active Site Analog	75
1.	Removal of Ethyl Ester Group from Tripeptide	75
2.	Removal of t-Boc Protecting Group from hexapeptide	78
3.	Coupling of Tripeptide and Hexapeptide	78
4.	Deprotection of Nonapeptide Amino Acid Side Chains by Sodium-Liquid Ammonia Reduction ..	80
5.	Cyclization of the Nonapeptide	83
6.	Purification of Cyclic Nonapeptide	84
D.	Physical Techniques for Measuring Thermodynamic and Kinetic Parameters	85
1.	Model Partition Experiments Between Water and Chloroform	85
2.	Ninhydrin Assay for Hydrolysis Experiments .	90
3.	Enzyme Hydrolysis Procedure	91
4.	N-Acetyl-L-Tyrosine Ethyl Ester Activity Assays	93
5.	p-Nitrophenyl Acetate Active Site Titrations	93
6.	N-trans-Cinnamoylimidazole Active Site Titrations	94
7.	Sulphydryl Group Determination	95
8.	Detection Methods for Thin-Layer Chromatography	95
9.	pH Stat Titration of Nonapeptide	96
E.	Model Partition System and Calculations	97
III.	RESULTS	101
A.	Model Partition Experiments	101
1.	Amino Acid Analogs and DMSO Results	
2.	Peptide Series Results	127
B.	Enzyme-Peptide Amide Substrate Interactions	129
1.	Steady-State Associations and Catalysis of N-Acyl-Peptidyl-L-Phenylalanine Amide Substrates by α -Chymotrypsin	134
2.	Thermodynamics of the Steady-State Association and Catalysis of N-Acyl-L-Phenylalanine Amide Substrates by α -Chymotrypsin	171
C.	Nonapeptide Results	181
1.	pH Stat Titration of Nonapeptide	181

2.	Kinetics of Nonapeptide Catalyzed Hydrolysis of p-Nitrophenyl Acetate	181
3.	Proflavin Binding to Nonapeptide	185
IV.	DISCUSSION	187
A.	Conclusions	187
B.	Two Temperature Dependent Forms of α -Chymotrypsin	190
1.	Kinetic and Thermodynamic Evidence for Two Temperature Dependent Forms of α -Chymotrypsin	190
2.	Enthalpy and Entropy Change Effects in Generating a Non-Linear Van't Hoff Plot	192
3.	Interpretation of Curved Van't Hoff Plots ..	212
4.	Model Partition Studies Versus Enzyme-Substrate Association	214
5.	Thermodynamics of Peptide Substrate Binding and Catalysis: Productive Binding, Association-Activation	224
a.	Association-Activation is Not Observed in the Free Energy of Binding	224
b.	Can Association-Activation be Observed in the Enthalpy and Entropy of Binding? ..	226
c.	Is Substrate Specificity Enthalpy or Entropy Controlled?	230
6.	Model Partition Corrections for Substrate Desolvation in the Enzyme-Substrate Association Process	237
7.	Catalytic Efficiency in α -Chymotrypsin from a Thermodynamic and Evolutionary Perspective	241
8.	Evidence and a Unifying Theory for Association-Activation Mechanisms	246
C.	The Nonapeptide as a Synthetic Catalyst	259
REFERENCES	263
APPENDIX A	277
APPENDIX B	281

LIST OF TABLES

Table	Page
1. Thermodynamic Parameters for the Binding of Substrate Analogues to Native and Modified Forms of Cht at 25°C According to Schultz	30
2. Binding and Catalytic Constants for Tyrosine Peptide Substrates with α -Chymotrypsin	41
3. Selected Physical Constants for Synthesized Compounds	74
4. Specific Activity and Concentrations for Partition Experiments	86
5. Correction Factors for Quenching	88
6. Percent Counts Due to Hydrolyzed Compound	89
7. Extinction Coefficients for Ninhydrin Assay of Ammonia and Glycine	92
8. Thermodynamic Parameters for the Transfer Process of Phenylalanine Substrate Analogs from Aqueous Buffer to Chloroform at 25°C	122
9. Thermodynamic Parameters for the Transfer Process of Phenylalanine Substrate Analogs from Aqueous Buffer (5% DMSO) to Chloroform at 25°C	123
10. Changes in Thermodynamic Parameters for the Transfer Process of Phenylalanine Substrate Analogs from Aqueous Buffer to Chloroform at 25°C Due to Changes in Analog Structure	125
11. Thermodynamic Parameters for the Transfer Process of Peptide Substrates from Aqueous Buffer to Chloroform at 25°C	128
12. Change in ΔG_{\ddagger}^0 for Peptide Side Chains at 25°C: A Hydrophobicity Scale for Side Chain Residues	130
13. Comparison of Active Sites and Stability of G-25 Sephadex Purified and Non-G-25 Sephadex Purified Cht at pH 3.0 and 7.8	132
14. Steady-State Kinetic Parameters for the Association and Catalysis of Peptide Substrates by α -Chymotrypsin	135
15. Comparison of the Kinetic Parameters of Amide and Peptide Hydrolysis of this Work with the Literature	139

16.	Thermodynamics of the Steady-State Association of Amide and Peptide Substrates by α -Chymotrypsin at 25°C	172
17.	Differences in Thermodynamic Parameters at 25°C for the Association of Amide and Peptide Substrates with the Two Temperature Dependent Forms of α -Chymotrypsin	173
18.	Changes in Heat Capacity Due to Association of Amide and Peptide Substrates with α -Chymotrypsin	177
19.	Thermodynamics of Activation for the Steady-State Catalysis of Amide and Peptide Substrates by α -Chymotrypsin at 25°C	178
20.	Thermodynamics of Activation for the Second Order Rate Constant k_{cat}/K_m at 25°C	180
21.	Proflavin Binding Constants and Second Order Rate Constants for the Hydrolysis of p-Nitrophenyl Acetate by the Nonapeptide: Comparison with α -Chymotrypsin and Model Systems ...	184
22.	Effects of Changes in ΔG^0 on the Equilibrium of Enzyme X Between a High and Low Temperature Form	197
23.	Changes in K_m Due to a Positive Heat Capacity Change	199
24.	Thermodynamic Parameters for Two Temperature Dependent Forms of Enzyme 'X' Based Upon Compensating Changes in ΔH^0 and ΔS^0	202
25.	Changes in K_m Due to a Positive Heat Capacity Change and a Positive Temperature Dependent Change in ΔS^0	203
26.	Thermodynamic Parameters and Association Constants for the Association of N-ac-Ala-Pro-Phe-NH ₂ with the Two Temperature Dependent Forms of Cht from 5° to 37°C	207
27.	Predicted Observed Association Constants for N-ac-Ala-Pro-Phe-NH ₂ with Cht Based Upon Two Temperature Dependent Forms of Cht in Equilibrium	209
28.	Comparison of Binding Constants for the Phenylalanine Substrate Analog Series	221
29.	Comparison of Model Partition and α -Chymotrypsin Binding Free Energy Data for the Contribution of Peptide Residues of the Peptide Amide Substrate Series at 25°C	223
30.	Thermodynamic Parameters for the Association and Activation of Five Specific Peptide Amide Substrates with α -Chymotrypsin at 37°C	233
31.	Model Partition Versus Enzymatic Contributions to the Energy of Binding by Amino Acid Residues at 25°C	234

32.	Thermodynamic Parameters for the Second Order Rate Constants for the Cht Catalyzed Hydrolysis of Five Peptide Amide Substrates at 37°C	236
33.	Thermodynamic Parameters in Unitary Units for the Steady-State Association of Amide and Peptide Substrates by Cht at 25°C ..	238
34.	Thermodynamic Parameters for the Association of Amide Substrates to Cht at 25°C Corrected for Thermodynamic Contributions Due to the Transfer Process as Found by Model Partition Studies	240
35.	Comparison of the Thermodynamics of α -Chymotrypsin Catalyzed Hydrolysis of the Amide Bond with Non-Catalyzed Hydrolysis at 25°C	245
36.	Free Energies of Binding and Activation for Six Peptides of the Series N-ac-Pro-Ala-Pro-X-NH ₂	250
37.	Model Partition Data Versus Enzyme Binding Data for P ₁ Residue Side Chains of Six Peptides of the Series N-ac-Pro-Ala-Pro-X-NH ₂	251

LIST OF FIGURES AND DIAGRAMS

Figure or Diagram	Page
1. Free Energy vs. Reaction Coordinate Diagram with $k_{-1} \gg k_2$	6
2. Difference Free Energy vs. Reaction Coordinate Diagram Comparing an Uncatalyzed with an Enzymatically Catalyzed Unimolecular Reaction	13
3. Diagrammatic Representation of the Contribution of "Association-Activation" Mechanisms to Enzymatic Catalysis	16
4. Diagrammatic Representation of "Transition State Complementarity"	19
5. Productive Association of L Enantiomers of Esters of α Substituted β -Phenylpropionic Acids with the Primary Binding Site in Cht	23
6. Synthetic Scheme for Nonapeptide	76
7. Set Up for Sodium-Liquid Ammonia Reduction of Nonapeptide	81
8. Phenylalanine Analog Series for Model Partition Studies	102
9. van't Hoff Plot of the Temperature Dependence of the Model Partition Studies between Aqueous Buffer and Chloroform for N-Acetyl-Phenylalanine-Amide	104
10. van't Hoff Plot of the Temperature Dependence of the Model Partition Studies between Aqueous Buffer and Chloroform of N-Formyl-Phenylalanine-Amide	106
11. van't Hoff Plot of the Temperature Dependence of the Model Partition Studies between Aqueous Buffer and Chloroform for L-(-)-keto-3-Carboamide Tetrahydroisoquinoline. L-(-)-KCAQ	108
12. van't Hoff Plot of the Temperature Dependence of the Model Partition Studies between Aqueous Buffer and Chloroform for O-Acetoxy-L-Phenyllactic-Amide	110
13. van't Hoff Plot of the Temperature Dependence of the Model Partition Studies between Aqueous Buffer and Chloroform for L-(+)-3-Carboamide-3,4-Dihydroisocoumarin. (CADIC)	112

14.	van't Hoff Plot of the Temperature Dependence of the Model Partition Studies between Aqueous Buffer and Chloroform for DMSO	114
15.	van't Hoff Plot of the Temperature Dependence of the Model Partition Studies between Aqueous Buffer and Chloroform for N-Acetyl-Proline-Phenylalanine-Amide .	116
16.	van't Hoff Plot of the Temperature Dependence of the Model Partition Studies between Aqueous Buffer and Chloroform for N-Acetyl-Alanine-Proline-Phenylalanine-Amide	118
17.	van't Hoff Plot of the Temperature Dependence of the Model Partition Studies between Aqueous Buffer and Chloroform for N-Acetyl-Proline-Alanine-Proline-Phenylalanine-Amide	120
18.	Typical Lineweaver-Burk Plot	137
19.	van't Hoff Plot of the Temperature Dependence of the Dissociation Constant (K_m) of N-ac-Phe-NH ₂ with Cht .	141
20.	van't Hoff Plot of the Temperature Dependence of the Dissociation Constant (K_m) of N-ac-Pro-Phe-NH ₂ with Cht	143
21.	van't Hoff Plot of the Temperature Dependence of the Dissociation Constant (K_m) of N-ac-Ala-Pro-Phe-NH ₂ with Cht	145
22.	van't Hoff Plot of the Temperature Dependence of the Dissociation Constant (K_m) of N-ac-Pro-Ala-Pro-Phe-NH ₂ with Cht	147
23.	van't Hoff Plot of the Temperature Dependence of the Dissociation Constnat (K_m) of N-ac-Phe-Gly-NH ₂ with Cht	149
24.	Arrhenius Plot of the Temperature Dependence of the Catalytic Rate Constant (kcat) of N-ac-Phe-NH ₂	151
25.	Arrhenius Plot of the Temperature Dependence of the Catalytic Rate Constant (kcat) of N-ac-Pro-Phe-NH ₂ ...	153
26.	Arrhenius Plot of the Temperature Dependence of the Catalytic Rate Constnat (kcat) of N-ac-Ala-Pro-Phe-NH ₂	155
27.	Arrhenius Plot of the Temperature Dependence of the Catalytic Rate Constant (kcat) of N-ac-Pro-Ala-Pro-Phe-NH ₂	157

28.	Arrhenius Plot of the Temperature Dependence of the Catalytic Rate Constant (k_{cat}) of N-ac-Phe-Gly-NH ₂	159
29.	Arrhenius Plot of the Temperature Dependence of the Second Order Rate Constant (k_{cat}/K_m) of N-ac-Phe-NH ₂ ..	161
30.	Arrhenius Plot of the Temperature Dependence of the Second Order Rate Constant (k_{cat}/K_m) of N-ac-Pro-Phe-NH ₂	163
31.	Arrhenius Plot of the Temperature Dependence of the Second Order Rate Constant (k_{cat}/K_m) of N-ac-Ala-Pro-Phe-NH ₂	165
32.	Arrhenius Plot of the Temperature Dependence of the Second Order Rate Constant (k_{cat}/K_m) of N-ac-Pro-Ala-Pro-Phe-NH ₂	167
33.	Arrhenius Plot of the Temperature Dependence of the Second Order Rate Constant (k_{cat}/K_m) of N-ac-Phe-Gly-NH ₂	169
34.	Change in the Enthalpy of Association (ΔH_a^0) with Temperature for the Five Specific Amide and Peptide Substrates	175
35.	pH Stat Titration of Nonapeptide	182
36.	Change in Binding Constants of Two Temperature Dependent Forms of Enzyme 'X' Due to a Positive Heat Capacity Change	200
37.	Change in Binding Constants of Two Temperature Dependent Forms of Enzyme 'X' Due to a Positive Heat Capacity Change and a Compensating Positive Temperature Dependent Change in ΔS^0	204
38.	van't Hoff Plot of Predicted Observed Binding Constants for N-ac-Ala-Pro-Phe-NH ₂ with Cht Versus Actual Observed Data	210
39.	The Nonapeptide Active Site	261

LIST OF ABBREVIATIONS

()	- reference
ac	- acetyl
ala	- alanine
brine	- saturated NaCl solution
bz	- benzyl
$^{\circ}\text{C}$	- degrees Centigrade
CADIC	- L-(+)-3-Carboamide-3,4-dihydroisocoumarin
CaSO_4	- calcium sulfate
CBZ	- benzyloxycarbonyl protecting group
CCl_4	- carbon tetrachloride
CHCl_3	- chloroform
CH_2Cl_2	- dichloromethane
Cht	- bovine α -chymotrypsin
cys	- cysteine
DCC	- dicyclohexylidiimide
DCU	- dicyclohexylurea
DMF	- dimethylformamide
DMSO	- dimethylsulfoxide
E	- enzyme
ϵ	- extinction coefficient
g	- grams
glu	- glutumate
gly	- glycine
HCl	- hydrogen chloride

his	- histidine
$\text{ICH}_2\text{CH}_2\text{I}$	- diiodoethane
im	- imidazole
$^{\circ}\text{K}$	- degrees Kelvin
KCAQ	- L-(-)-keto-3-Carboamide tetrahydroisoquinoline
lit.	- literature value
<u>M</u>	- molar
MeOH	- methanol
mg	- milligram
MgSO_4	- magnesium sulfate
ml	- milliliter
<u>mM</u>	- millimolar
m.p.	- melting point
N	- nitrogen
<u>N</u>	- normal
N_2	- nitrogen gas
NaHCO_3	- sodium bicarbonate
NaOH	- sodium hydroxide
NCI	- N-trans cinnamoylimidazole
NH_2	- amide
NH_3	- ammonia
NMM	- N-methylmorpholine
P	- product
O	- oxygen
OEt	- ethyl ester
OMe	- methyl ester
phe	- phenylalanine

pNPA	- p-nitrophenyl acetate
pro	- proline
p.s.i.	- pounds/square inch
R_f	- thin layer chromatography value = (distance traveled by a compound on a TLC plate)/(distance traveled by the solvent on a TLC plate)
S	- substrate
ser	- serine
S_0	- initial substrate concentration
TLC	- thin layer chromatography
v/v	- volume/volume
w/v	- weight/volume

CONTENTS FOR APPENDICES

	Page
APPENDIX A Derivation of an Equation to Describe the Effect on the Equilibrium Between Two Conformations of an Enzyme Upon Addition of Substrate	277
APPENDIX B Rate Equations for Enzymes Possessing Two Catalytic Sites	281

CHAPTER I

INTRODUCTION

I A. Goals of this Dissertation.

The purpose of this dissertation is to extend the current knowledge of the thermodynamics of substrate binding and turnover in enzyme reactions in an attempt to understand the energetic relationships that lead to a lowering of the energy of activation for enzyme catalyzed reactions. In these studies we utilize the well characterized enzyme bovine α -chymotrypsin (Cht).

A group of specific peptide substrates for Cht have been synthesized which sequentially increase the interactions between the substrate and enzyme from the primary binding site to the fully extended secondary binding regions of the enzyme active site. Furthermore, these enzyme studies have been correlated with model partition studies to help delineate contributions to the thermodynamic parameters of the enzymatic process that arise from the enzyme molecule itself and from substrate desolvation upon binding to the enzyme active site. In addition, acyclic substrates and their rigid cyclized analogs have been synthesized and studied to determine the effect of rotational degrees of freedom in the substrate on the transfer process from solvent to a hydrophobic model binding site as a part of a study on the effect of loss of rotational degrees of freedom in a substrate on its thermodynamics of enzyme

association.

An additional approach to the interpretation of thermodynamic data in enzyme substrate interactions is to utilize a small peptide model that has the features of the protein-enzyme active site. The study of binding and catalysis in this simple compound can be used to determine some of the essential features of catalysis of more complex protein systems. Accordingly, a model peptide containing the features of the Cht active site has been synthesized and studied.

It is a contention of this proposal that free energy data alone is insufficient support for an enzymatic mechanism. An understanding of catalysis can be clear only with an understanding of the enthalpy and entropy contributions to the free energy of the individual steps of the enzymatic process. However, the contribution of enthalpy and entropy to the individual steps of enzymatic mechanisms in substrate catalysis has not been fully elucidated in any one enzyme. It is hoped that a study of these parameters will allow the resolution of conflicting theories of enzymatic catalysis such as strain and distortion, induced fit, and non-productive binding may hopefully be elucidated.

I B. Basic Concepts and Theories of Enzyme Catalysis.

I B-1. Basic Concepts of Enzyme Kinetics.

A unique complementarity of enzymes and their substrates has been suggested since the mid 19th Century to explain the unusually favorable affinity between them. As an understanding of the unique chemical structural features of enzyme and substrate complexes has grown, they have been recognized to supply the integral forces necessary to drive catalysis (1-4).

It is generally agreed that enzymatic catalysis principally involves a stereochemically precise and coherent arrangement of forces during the reversible step of enzyme-substrate complexation prior to and/or during the rate limiting step of catalysis. The simple scheme shows the possible kinetic consequences of the complexation:



where enzyme (E) and substrate (S) complex to form the non-covalent Michaelis complex (ES) and are catalyzed to free enzyme and product (P) and k_2 is the catalytic rate constant k_{cat} . Accordingly, the rate of substrate turnover is proportional to the concentration of ES,

$$\frac{-d(S)}{dt} = k_{cat} (ES), \quad (1.2)$$

where,

$$(ES) = \frac{(E)(S)}{K_s}, \quad (1.3)$$

and K_s is the equilibrium dissociation constant for formation of so-called Michaelis complex,

$$K_s = \frac{k_{-1}}{k_1}, \quad (1.4)$$

If, in addition, we make the following assumptions:

- i) there is a single substrate;
- ii) there is no significant back reaction from P;
- iii) $S_0 \gg E_0$;
- iv) $k_{-1} \gg k_2$;

then we obtain the mathematical relationship called the Michaelis-Menten equation:

$$V = \frac{V_{\max} (S_0)}{K_s + (S_0)} \quad (V_{\max} = k_{\text{cat}} (E)). \quad (1.5)$$

In the case where assumption (iv) does not hold, we can alternatively assume a steady-state in the Michaelis complex (ES) over short ranges of substrate concentration,

$$d \frac{(ES)}{dt} = 0. \quad (1.6)$$

However, since assumption (iv) no longer is true then the Michaelis constant no longer equals K_s (equation 1.4) and instead is equal to K_m :

$$K_m = \frac{k_{-1} + k_2}{k_1}. \quad (1.7)$$

The Briggs-Haldane or Steady-State equation then is

$$V = \frac{V_{\max} (S_0)}{K_m + (S_0)} \quad (1.8)$$

Experimentally k_{cat} and K_m can be determined by taking the reciprocal of equation 1.8

$$\frac{1}{V} = \frac{K_m}{V_{\max} (S_0)} + \frac{(S_0)}{V_{\max} (S_0)} \quad (1.9)$$

which simplifies to:

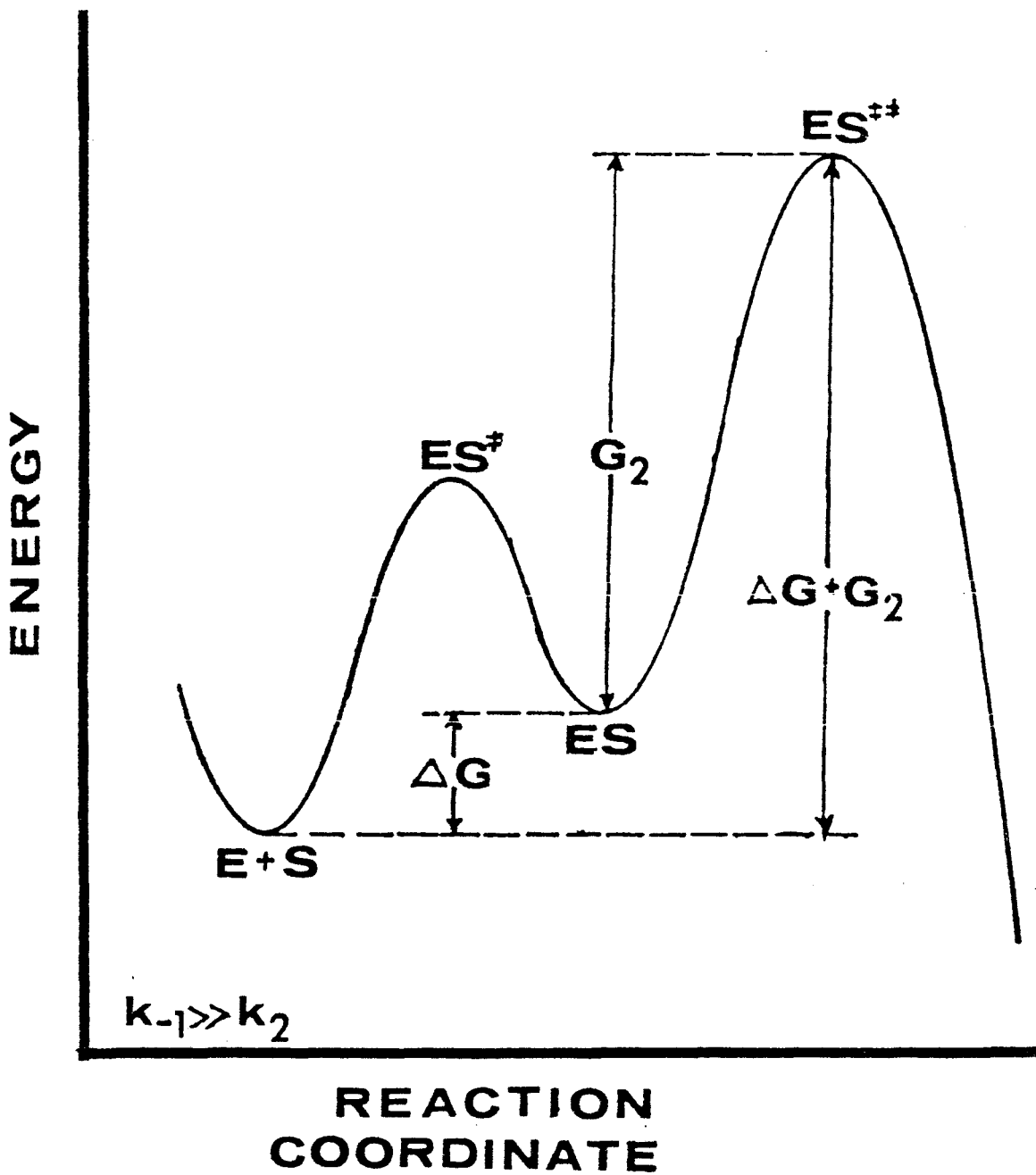
$$\frac{1}{V} = \frac{K_m}{V_{\max} (S_0)} + \frac{1}{V_{\max}} \quad (1.10)$$

This is the Lineweaver-Burk equation (5) which characterizes the graphical representation of the reciprocal of the velocity as a function of the reciprocal of the substrate. The slope of this line is equal to the Michaelis constant, K_m , divided by the maximum velocity, V_{\max} , and the intercept on the Y axis is equal to the reciprocal of the maximum velocity (V_{\max}). Other algebraic forms of the Michaelis-Menten or Briggs-Haldane equation give alternative graphical analyses that may be used to obtain these kinetic parameters, perhaps with a greater statistical accuracy (5).

LEGEND

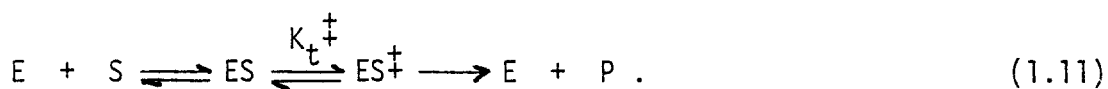
Figure 1. Free Energy vs. Reaction Coordinate Diagram with
 $k_{-1} \gg k_2$.

K_S is proportional to ΔG , the rate constant k_2 is proportional to G_2 , and rate constant k_2/K_S is proportional to $\Delta G + G_2$. Note that the free energy expression for K_S and k_2/K_S must incorporate the free enzyme (E).



I B-2. Basic Concepts of Transition State Theory.

The thermodynamic parameters of a catalytic process can give us information on the nature of the process. Transition state theory relates the rate of a reaction to the difference in Gibbs energy (ΔG) between the transition state and the ground state (fig.1). Equation 1.1 can be rewritten to include the transition state (ES^\ddagger) for the enzymatic catalysis of substrate (S) to product (P) as follows:



Equation 1.11 describes an equilibrium between the reactant and the transition state, under conditions in which the back reaction from product to transition state is negligible, with a small amount of transition state (ES^\ddagger) decomposing to product as shown.

Classical kinetic theory states that the rate of formation of a product in a unimolecular reaction is equal to the concentration of the reactant times a constant (6,7), so that for equation 1.11,

$$\frac{d(P)}{dt} = k_t^\ddagger (ES^\ddagger) . \quad (1.12)$$

The rate of breakdown of the transition state complex (ES^\ddagger) can be equated with the vibrational mode of the molecular complex that is on the pathway to product (7). Since from classical physics (6,7):

$$\nu = \frac{kT}{h} , \quad (1.13)$$

where ν is the vibrational frequency along the reaction pathway, k is

Boltzman's constant, T is the temperature in $^{\circ}\text{K}$, and h is Planck's constant, we then can relate the rate with the vibrational frequency,

$$k^{\ddagger} = \frac{kT}{h}, \quad (1.14)$$

where k^{\ddagger} is the rate constant from equation 1.12. If we arrange the equation defining the equilibrium constant

$$K^{\ddagger} = \frac{(ES^{\ddagger})}{(ES)}, \quad (1.15)$$

to

$$(ES^{\ddagger}) = K^{\ddagger} (ES), \quad (1.16)$$

we can then substitute equations 1.16 and 1.14 into equation 1.12 to obtain

$$\frac{d(P)}{dt} = \frac{kT}{h} K^{\ddagger} (ES). \quad (1.17)$$

From the thermodynamic formula:

$$\Delta G^{\circ} = -RT \ln K, \quad (1.18)$$

where ΔG° is the standard free energy change and R is the universal gas constant we obtain:

$$K = e^{\frac{-\Delta G^{\circ}}{RT}}. \quad (1.19)$$

Substituting into equation 1.17 we obtain

$$\frac{d(P)}{dt} = \frac{kT}{h} e^{-\frac{\Delta G^\ddagger}{RT}} (ES), \quad (1.20)$$

where ΔG^\ddagger is the free energy of activation between the ground state and transition state and since from equation 1.2

$$\frac{d(P)}{dt} = k_2(ES), \quad (1.21)$$

substituting equation 1.21 into 1.20 we obtain

$$k_2 = \frac{kT}{h} e^{-\frac{\Delta G^\ddagger}{RT}}. \quad (1.22)$$

Rearranging equation 1.22, and taking the log to the base 10, we obtain at $T = 298^\circ\text{K}$ (2):

$$\Delta G^\ddagger = -1360 \log k_2 + 17,400 \text{ cal/mole.} \quad (1.23)$$

Also by substituting the equation:

$$\Delta G = \Delta H - T \Delta S, \quad (1.24)$$

where ΔH is the enthalpy change, ΔS is the entropy change into equation 1.23 we obtain

$$k_2 = \frac{kT}{h} \left(e^{\frac{\Delta S^\ddagger}{R}} \right) \left(e^{-\frac{\Delta H^\ddagger}{RT}} \right), \quad (1.25)$$

taking the logarithm and differentiating with respect to temperature we obtain

$$d \frac{\ln k_2}{dT} = \frac{\Delta H^\ddagger}{RT^2} + \frac{1}{T}. \quad (1.26)$$

Comparing equation 1.26 with the empirical equation proposed by Arrhenius (6) to show the relationship of the reaction rate to temperature,

$$\frac{d \ln k_2}{dT} = \frac{\Delta E_a}{RT^2}, \quad (1.27)$$

(ΔE_a is the Arrhenius activation energy for the reaction.) We find that the Arrhenius activation energy, ΔE_a , can be described by the equation:

$$\Delta E_a = \Delta H^\ddagger + RT. \quad (1.28)$$

Integration of equation 1.27 gives

$$\ln k = \ln A - \frac{\Delta E_a}{RT}, \quad (1.29)$$

where $\ln A$ is a constant of integration. Plotting $\ln k_2$ versus $1/T$ we can solve for E_a/R (8) or ΔH^\ddagger can be calculated directly from the slope of the line,

$$\text{slope} = \frac{\Delta H^\ddagger}{R} + RT. \quad (1.30)$$

ΔS^\ddagger can be calculated from equation 1.24.

I B-3. Theories of Enzymatic Catalysis.

The forces associated with the high affinity and structural complementarity of enzymes and substrates on binding of substrate to enzyme are now thought to be the driving force of catalysis (1-4). That a linkage exists between the favorable free energy of association ($\Delta G_a < 0$) that occurs upon formation of the enzyme-substrate complex and the fast rates observed in an enzyme-catalyzed reaction is more clearly understood from a thermodynamic approach to the process.

The rate of a reaction (such as equation 1.1) is inversely proportional to the free energy content of an energy barrier that exists between the reactants and products (2). A catalyst lowers this proposed barrier or "activation energy". Therefore, for the catalyzed reaction to have a faster rate of reaction than the uncatalyzed rate, the activation energy for the catalyzed reaction must be less with respect to its ground state energy than the activation energy for the non-catalyzed reaction with respect to its ground state energy (fig. 2).

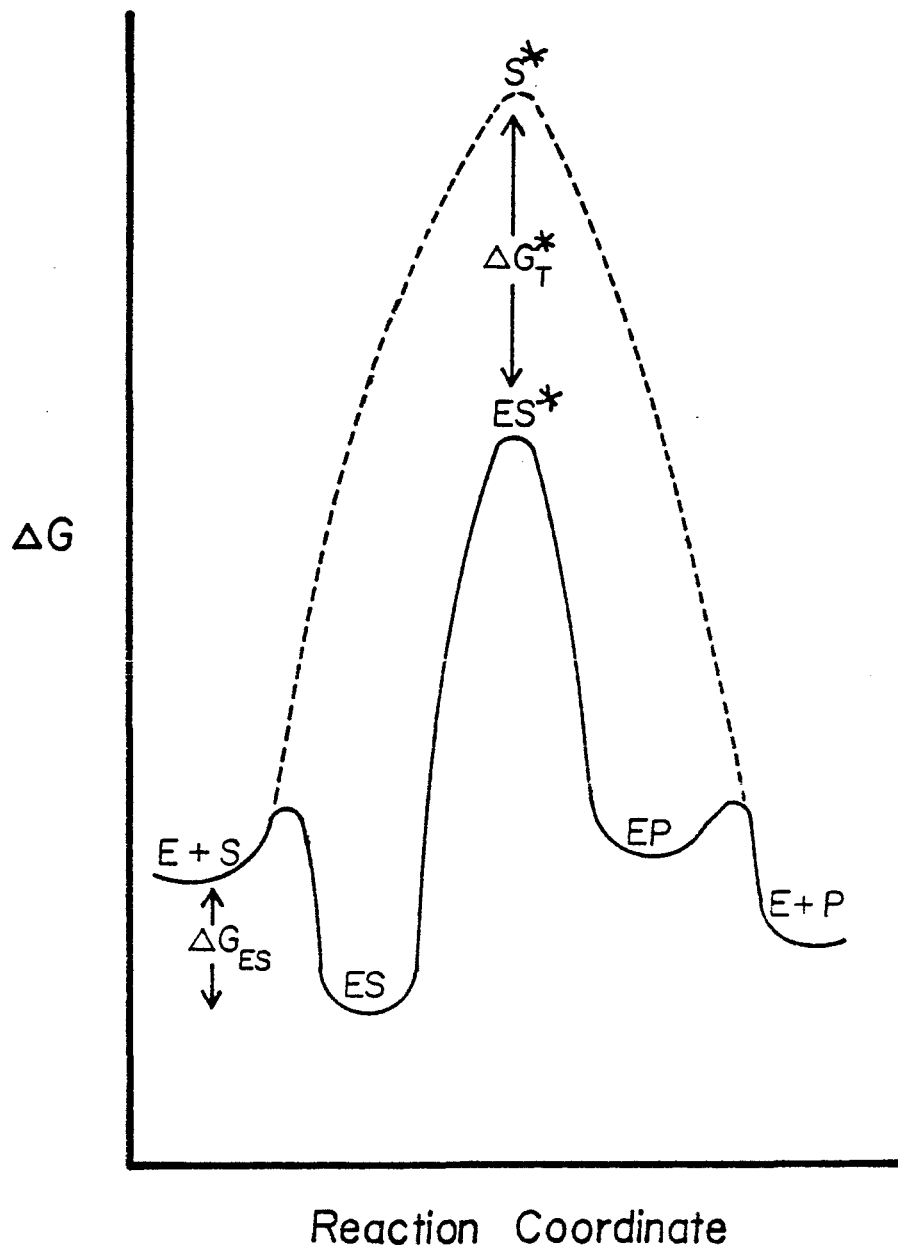
Many of the currently proposed hypotheses on the mechanisms of enzymatic catalysis state that a portion of the favorable free energy associated with formation of the non-covalent enzyme-substrate complex is utilized to lower the energy of activation of the succeeding bond making and/or breaking steps of the reaction (1-4). These "association-activation" mechanisms (9) attempt to explain the fast rates observed in enzymatically catalyzed reactions. Three current hypotheses of enzyme mechanisms are:

- i) Induced fit (2,3). The binding of a substrate to an enzyme caused a conformational change in the enzyme leading to a pre-

LEGEND

Figure 2. Difference Free Energy Versus Reaction Coordinate
Diagram Comparing an Uncatalyzed with an Enzymatically
Catalyzed Unimolecular Reaction.

S and P are the substrate and product, respectively, and ES and EP are their respective complexes with the enzyme. For catalysis to occur in the enzymatic case, the difference free energy between the enzymatically catalyzed "activated" state (ES*) and the activated state for the uncatalyzed reaction (S*) ($= \Delta G_T$) must be greater than the favorable free energy of S + E complexation (ΔG_{ES}).



cise orientation of the catalytic groups of the enzyme with the sensitive bond(s) of the substrate.

- ii) Rack or strain and distortion (1,2). The binding substrate with enzyme causes a distortion of the substrate along the catalytic pathway towards the transition state.
- iii) Propinquity (2,4). The entropic demands of the reaction are reduced prior to the rate limiting step upon binding, or the formation of the non-covalent enzyme-substrate complex (Michaelis complex) causes restricted rotational and translational degrees of freedom about the scissile bond of the substrate within close proximity to the catalytic residues of the enzyme active site.

These "association" mechanisms propose that the observed standard free energy for the non-covalent association of enzyme and substrate is:

$$\Delta G_{\text{obs}} = -RT \ln K_{s,\text{obs}}, \quad (1.31)$$

where K_s is the binding equilibrium constant. The observed binding free energy can then be written as two terms, the true or intrinsic binding free energy (ΔG_i) and the free energy used to lower the energy of activation (ΔG_{aa}) for succeeding bond making or breaking steps on the reaction pathway (fig. 3):

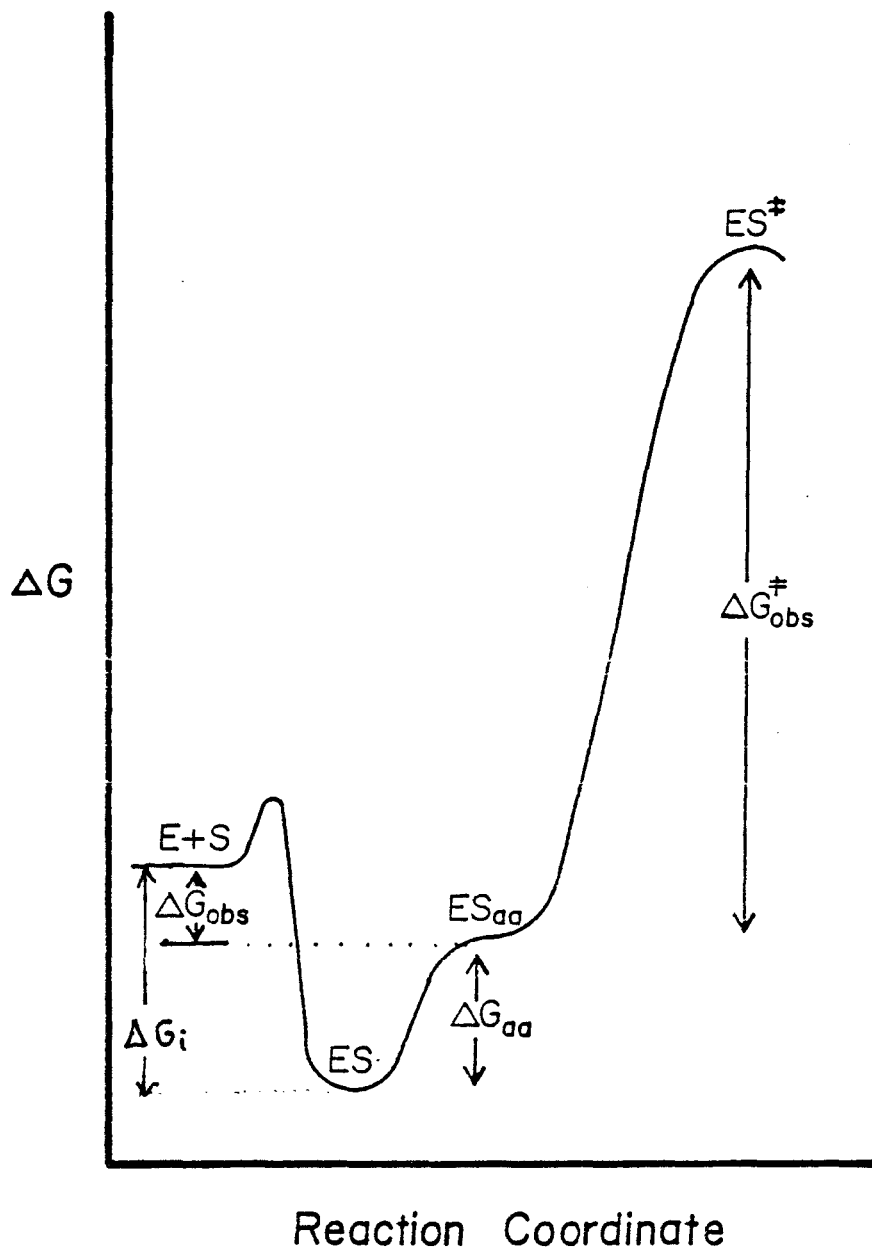
$$\Delta G_{\text{obs}} = \Delta G_i + \Delta G_{aa}. \quad (1.32)$$

In kinetic terms, "association-activation" mechanisms would then predict that specific substrates with fast or large values of k_{cat} would have poorer values of $K_{m(\text{obs})}$ (more positive values of ΔG_{obs}) than less

LEGEND

Figure 3. Diagrammatic Representation of the Contribution of "Association-Activation" Mechanisms to Enzymatic Catalysis.

Part of the favorable free energy of enzyme (E) - substrate (S) complexation (ΔG_i) is proposedly utilized to activate the ground state of the initial Michaelis complex (ES to ES_{aa}) towards the transition state (ES[‡]). Accordingly, the observed difference free energy in the non-covalent interactions of the ES complexation (ΔG_{obs}) is less favorable by the factor ΔG_{aa} , but the energy necessary to reach the transition state for the subsequent, rate limiting step, ΔG^{\ddagger} , is lowered by the contribution of ΔG_{aa} .



or non-specific substrates (2,10). Experimental evidence in support of this prediction, however, are generally not conclusive.

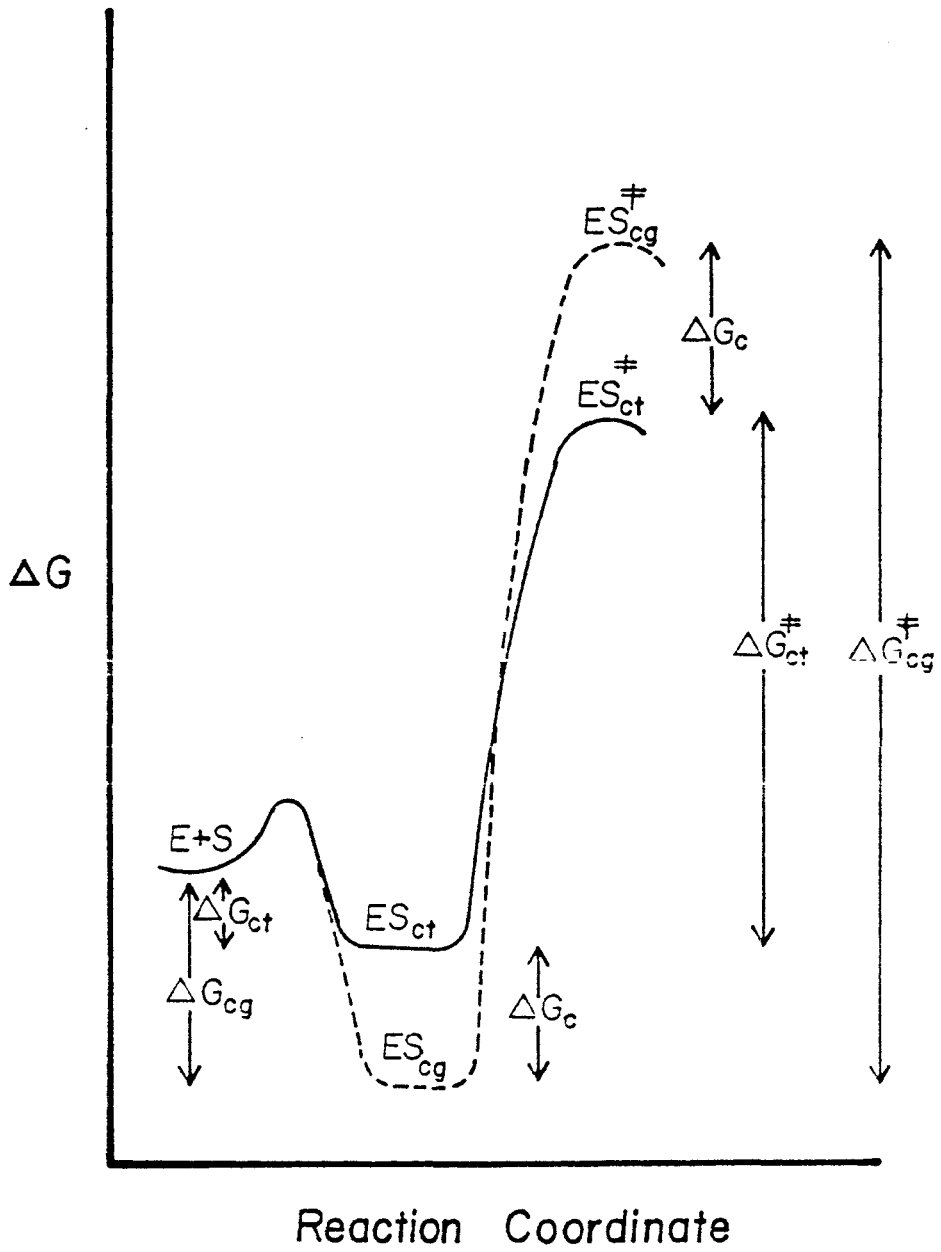
Other hypotheses, such as non-productive binding, may explain the sometimes inverse relationship between k_{cat} and K_m . In non-productive binding the substrate binds in an alternate unreactive binding mode or modes at the active site of the enzyme, in competition with the reactive or productive mode of binding. The effect of this is to lower both k_{cat} and K_m , while the ratio of the two constants (the second order rate constant k_{cat}/K_m) would change very little (2,11,12).

In addition, while "association-activation" mechanisms may propose destabilization of the ground state of the substrate and/or enzyme to lower the activation energy of succeeding steps in the reaction at the expense of binding energies (1,3,4,9,13), the concept of transition state "complementarity" (13,14) suggests that all of the potential energies associated with the binding of a substrate with the active site of an enzyme and its subsequent conversion to product will not be fully realized until the "transition state" is reached (fig. 4). Accordingly, the rate of an enzymatically catalyzed reaction may principally depend upon the efficiency of interactions occurring in the enzyme-substrate "transition state" complex, not those observed in the binding step. Substrate specificity will be manifested as an increased k_{cat} . The favorable energies of formation of the Michaelis complex may also be attributed to features of the substrate interacting with the enzyme remote from the reactive bond or bonds. These remote interactions may remain unperturbed as the transition state is formed.

LEGEND

Figure 4. Diagrammatic Representation of "Transition State Complementarity".

----- represents the reaction pathway occurring when the enzyme's (E) binding site is complementary to substrate in its ground state configuration (S). _____ represents the reaction pathway when E is complementary to substrate in its "transition state" structure (S). ΔG_{ct} and ΔG_{cg} are the observed difference free energies for formation of the Michaelis complex for the enzyme complementary to the ground state (cg) and for the enzyme complementary to the transition state (ct), respectively. ΔG_{ct}^{\ddagger} and ΔG_{cg}^{\ddagger} are the respective free energies of activation.



I C. Review of the Related Literature.

I C-1. α -Chymotrypsin.

Bovine α -chymotrypsin (Cht) is one of the most characterized of the enzymes. It was first purified and crystallized by Kunitz and Northrop in 1935 (15) and was one of the first enzymes to be studied for mechanism and specificity (16). Its physiologic role is to digest food proteins in the intestinal tract, in which it acts along with other proteolytic enzymes (17).

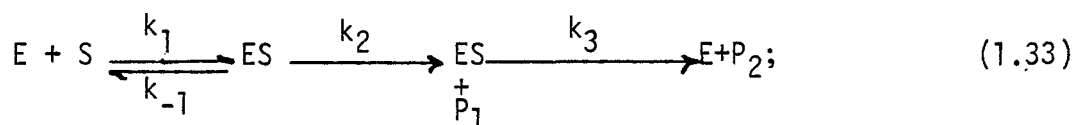
The inactive zymogen of α -chymotrypsin, chymotrypsinogen-A, is synthesized in the pancreatic islet cells. The zymogen molecule, consisting of 245 amino acids and 5 intrachain disulfide bonds, is secreted into the duodenum, and is then activated to form the active enzyme (18). The mechanism of activation to the most stable form is by specific proteolysis to form α -Cht (18), which consists of 241 amino acids in three polypeptide chains interconnected by two interchain and three intrachain cystine disulfide bonds (19).

Chemical modifications experiments (20) show the Serine-195 and the Histidine-57 to be essential to catalytic activity. In addition, Aspartate-102 has been inferred as an essential catalytic residue from X-ray crystallographic data (21). The experimental data suggest that the Ser-195 OH γ is acylated by substrates forming an acylenzyme intermediate during the hydrolysis of ester and amide substrates (22,23). The N ^{ϵ 2} of the imidazole ring of His-57, found in the active site near the Ser-195 OH γ , is thought to act as a general acid-general base catalyst during the formation of the acylserine intermediate and in its

ensuing hydrolysis to product (24). The Asp-102 is hydrogen bonded to the N¹ of the His-57 (21) where it may delocalize the incipient positive charge on the imidazole ring when it acts as a general base catalyst. This would explain the unusual reactivity of the Ser-195 as a nucleophilic catalyst. Similar systems consisting of a serine, histidine, and glutamate or aspartate have been reported for other proteases (25).

Chymotrypsin has a fairly broad specificity, preferably hydrolyzing peptide bonds C-terminal to the aromatic amino acids tyrosine, tryptophan, and phenylalanine, and with decreasing specificity the peptide bonds for aliphatic amino acids (26). The topology of the enzyme primary substrate binding site S₁ (where S_i refers to the amino acid binding site in the active site for residue P_i in the substrate (27))¹ has been schematically deduced (fig. 5) from its specificity and reactivity towards small ester and amide substrates (28,29).

Based upon a mechanism involving an acylserine intermediate, the following simple kinetic scheme has been proposed for Cht catalyzed hydrolysis of ester and amide substrates at pH 7.8,



where

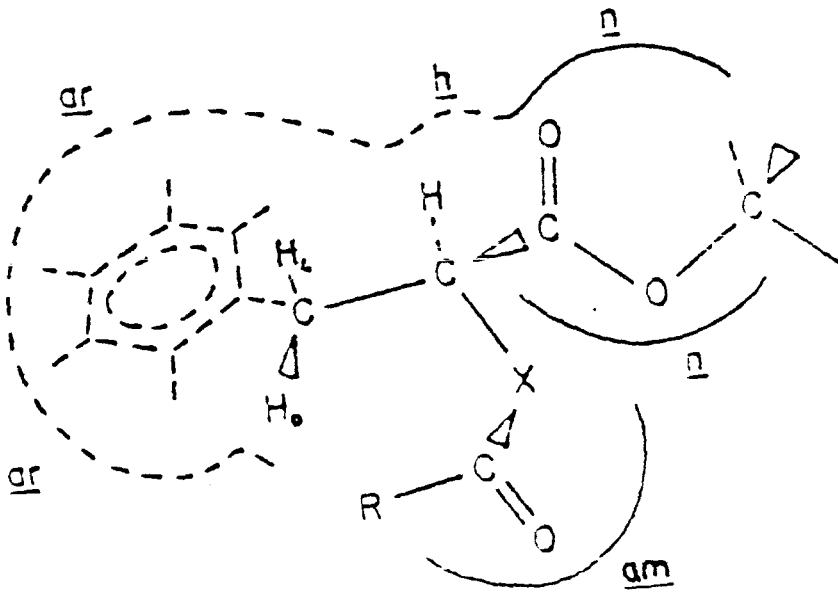
$$K_S = \frac{k_{-1}}{k_1} = \frac{(E)(S)}{(ES)}, \quad (1.34)$$

¹ Nomenclature is according to Schechter and Berger (27). S_i refers to the amino acid binding site in the active site for amino acid residue P_i in the substrate. Based on this nomenclature, a hexapeptide substrates hydrolyzable bond between S₁-S₁.

LEGEND

Figure 5. Productive Association of L Enantiomers of Esters of α -Substituted β -Phenylpropionic Acids with the Primary Binding Site in Cht.

Compound L-APME, X = NH, R = CH₃, L-N-acetylphenylalanine methyl ester (28,29); ar is the aromatic binding site, am is the acylamide binding site, h is the hydrogen binding site, and n is the nucleophilic binding site where the scissile bond is cleaved.



ES in the non-covalent Michaelis complex between enzyme and substrate, ES the acylserine intermediate, P_1 the first product (either alcohol or amine) and P_2 the carboxylic acid product of the hydrolysis reaction (22,24). Furthermore, the Michaelis-Menten parameter $K_m(\text{app})$ is equal to K_s for amide and peptide substrates, with step k_2 rate limiting (23,30). Bender (22), Hess (23), and co-workers have determined the rate constants of the steps for the kinetic scheme represented in equation 1.33 for small specific and non-specific substrates of the enzyme. Other workers have suggested additional intermediates in the catalytic mechanism (20,24), but evidence for these additional steps remains speculative.

Hess et al. (23) and Zerner and Bender (30) showed that for a series of N-acetyl-aromatic amino acid methyl and ethyl esters and amide substrates the binding was primarily determined by the amino acid moiety with the ester or amide group contributing very little to the binding process. The deacylation step k_3 would be the same for a given aromatic acid derivative series of esters and amides since the acyl-enzyme intermediate ES (equation 1.33) would be the same for both ester and amide derivatives. The acylation step k_2 , however, would reflect the greater reactivity of the ester as compared to the less reactive amide bond. They found that the ester substrates had about a 1,000 times greater reactivity than the amide substrates and that for ester substrates k_3 was the rate determining step and that

$$k_{\text{cat}} = k_3. \quad (1.35)$$

Therefore, the equation for the binding constant $K_{m(\text{app})}$,

$$K_{m(\text{app})} = \left(\frac{k_3}{k_2 + k_3} \right) K_s, \quad (1.36)$$

reduced to

$$K_{m(\text{app})} = \left(\frac{k_3}{k_2} \right) K_s. \quad (1.37)$$

For the amide substrate, the acylation step, k_2 , was rate limiting:

$$k_{\text{cat}} = k_2, \quad (1.38)$$

and equation 1.35 simplified to

$$K_{m(\text{app})} = K_s. \quad (1.39)$$

The three dimensional structure of the enzyme has been obtained from X-ray crystallographic data at low resolution with virtual substrates and inhibitors bound (31,32). Model building from the X-ray data has supported hypotheses on substrate specificity advanced from solution studies of the enzyme (31). The X-ray data show the primary binding site to be a hydrophobic cleft into the interior of the enzyme, with the acylamide binding site (am) on the surface of the enzyme forming a hydrogen bond from the carboxyl oxygen of the Ser-214 residue to the α -acylamide nitrogen of the substrate. The nucleophilic site (\underline{n} , fig. 5) is towards the surface of the enzyme and contains the catalytically essential His-57 and Ser-195 side chains.

In a recent reinterpretation of X-ray crystallographic data, Matthews et al. (33) show that the Ser-195 OH is not hydrogen bonded to

$N^{\epsilon 2}$ of His-57 in the native enzyme as was previously proposed (31). Additional reinterpretation of the X-ray data showed an artifactual $SO_4^{=}$ bound in the active site within van der Waals contact radii of the charge relay system, making interpretations from the X-ray structure speculative. Data from X-ray crystallographic studies in Tulinsky's laboratory (32) have shown previously unnoted significant differences between the two monomeric units that make up the dimeric molecular units of the crystalline structure, indicating that previously proposed structures were in fact averaged structures. These studies have also shown that a conformational change characterized by 30 to 40 atomic displacements occur upon substrate association. These displacements differ for the two monomers within the dimer crystalline unit cell. Accordingly, these data show Cht to be a dynamic molecule that undergoes atomic position (conformational) changes upon substrate association.

I C-2. Thermodynamics of Productive and Non-productive Association of Substrates with α -Chymotrypsin: "Association-Activation".

Simple hydrophobic bond formation has been shown to be characterized thermodynamically by an enthalpy (ΔH_b^0) near zero and a positive entropy (ΔS_b^0) (2,34). Productive association of substrate with Cht (pH > 7) has been shown to be characterized by both a negative enthalpy and entropy of association (9,11,35-40). Many authors have taken these thermodynamic values to be indicative of a conformation change upon substrate association (2,3,9,11,28,29,36-40). Association-activation mechanisms have been proposed suggesting that this conformational change orders or activates the enzyme-substrate complex toward the transition state (2,3,9,11), lowering the energy barriers (fig. 3), and, thus, increasing the rate of the enzymatically catalyzed reaction (6,7: fig. 2).

An example is found in the early thermodynamic studies of Vaslow and Doherty in 1953. They studied the association of the L and D isomers of the specific virtual substrate N-acetyl-3,5-dibromo-tyrosine with Cht at 20°C and pH 7.5 (active) or pH 5.0 (inactive) (35). They found at pH 7.5 the L isomer, which binds productively, had a $\Delta G_a^0 = -2.3$ kcal/mole, a $\Delta H_a^0 = -5.5$ kcal/mole, and a $\Delta S_a^0 = -12$ e.u. However, the D isomer which binds non-productively and acts as a competitive inhibitor of Cht had a similar ΔG_a^0 , but a $\Delta H_a^0 = -0.5$ kcal/mole and a $\Delta S_a^0 = +5$ e.u. At pH 5.0 (inactive) the L isomer again gave a similar ΔG_a^0 but, the $\Delta H_a^0 = -0.5$ kcal/mole and $\Delta S_a^0 = +9$ e.u. Therefore, productive association was characterized by a negative ΔG_a^0 , a large negative ΔH_a^0 , and a negative ΔS_a^0 . Non-productive association was characterized by a negative ΔG_a^0 , a ΔH_a^0 near zero, and a positive ΔS_a^0 , values similar to

those expected for simple hydrophobic bond formation (2,34).

These conclusions are supported by the 1970 studies of Shiao on binding of the L and D isomers of the specific virtual substrate N-acetyl-tryptophane to Cht at 25°C at pH 7.8 or pH 5.6 using microcalorimetric techniques (36). At pH 7.8, he found that association of the L isomer was characterized by a $\Delta G_a^0 = -3.0$ kcal/mole, a $\Delta H_a^0 = -21$ kcal/mole, and a $\Delta S_a^0 = -61$ e.u. The D isomer had slightly more positive values of ΔH_a^0 and ΔS_a^0 with a $\Delta G_a^0 = -3.3$ kcal/mole, a $\Delta H_a^0 = -19$ kcal/mole, and a $\Delta S_a^0 = -52$ e.u. Binding of the D isomer to Cht at pH 5.6, however, yielded a $\Delta G_a^0 = -3.7$ kcal/mole, a $\Delta H_a^0 = -5.5$ kcal/mole, and a $\Delta S_a^0 = -6$ e.u.; values more positive than at pH 7.8 by 15 kcal/mole for ΔH_a^0 and 45 e.u. for ΔS_a^0 .

Data from X-ray crystallographic studies indicate Ser-195 and His-57 have a high probability of participating in the association-activation process (20). Modification of these residues should give less productive or non-productive association of substrate and modified enzyme compared to that found for substrate and native enzyme. In 1977, Schultz et al. studied the binding of the L and D isomers of N-acetyl tryptophane by the proflavin displacement method with forms of Cht in which Ser-195 and His-57 had been chemically modified (9). These modified forms of Cht, (dehydroalaninyl-195) α -Cht (ACht) which had less than 0.1% the activity of native (9,41) and N^{ε2}-methyl-(histidinyl-57) α -Cht (MCht) which had less than 1% the activity of native, both showed a more positive ΔH_a^0 ($\Delta\Delta H = +10$ kcal/mole) and ΔS_a^0 ($\Delta\Delta S = +30$ e.u.) with substrate than was found for the association of substrate with native enzyme (Table 1). In ACht, which had been lyophilized during

TABLE 1

Thermodynamic Parameters for the Binding of Substrate Analogues
to Native and Modified Forms of Cht at 25°C According to Schultz^a

ENZYME	SUBSTRATE ANALOG	ΔG_a^0 kcal/mole	ΔH_a^0 kcal/mole	ΔS_a^0 e.u.
α -Cht ^b	Proflavin	-6.23 [±] 0.01	-8.01 [±] 1.09	- 6 [±] 4
	L-Ac-Trp	-2.94 [±] 0.07	-9.06 [±] 0.96	-21 [±] 3
	D-Ac-Trp	-3.23 [±] 0.10	-10.0 [±] 1.3	-23 [±] 4.5
ACht ^c	Proflavin	-4.36 [±] 0.07	- 0.38 [±] 1.45	+13 [±] 5
	L-Ac-Trp	-2.98 [±] 0.24	+ 1.29 [±] 0.79	+14 [±] 3
	D-Ac-Trp	-2.14 [±] 0.12	+ 0.58 [±] 0.39	+ 9.1 [±] 1.7
MCht ^d	Proflavin	-6.24 [±] 0.04	- 2.99 [±] 0.70	+11 [±] 2.5
	L-Ac-Trp	-2.52 [±] 0.16	+ 1.38 [±] 1.36	+12 [±] 4
	D-Ac-Trp	-2.92 [±] 0.05	- 2.66 [±] 0.77	+0.9 [±] 2.5

^a Schultz et al. (9); 0.05M sodium phosphate, 0.1M NaCl, pH 7.8.

^b Unmodified α -Chymotrypsin; 25.3°C.

^c Dehydroalaninyl-195 α -Cht; 25°C.

^d N ϵ^2 -methyl-(histidiny1-57) α -Cht; 25°C.

the purification process, binding of the virtual substrates had enthalpies near zero ($\Delta H_a^0 = +1.29$ kcal/mole and $+0.58$ kcal/mole for the L and D isomer respectively) and a positive entropy ($\Delta S_a^0 = +14$ e.u. and $+9$ e.u. for the L and D isomers respectively). These values were again what one would expect for simple hydrophobic bond formation (2, 34).

Schultz et al. (9) interpreted their results as showing that the association-activation process had been disrupted in the two modified forms of the enzyme and the enzyme-substrate complex was therefore not being activated or ordered for the catalytic process. Fastrez and Houyet (43) studied the rate of deacylation of N-acetyl-L-phenylalanine-MCht and found rates much slower than those for native Cht. In addition, they found an entropy of activation for the deacylation step of MCht 15 e.u. more negative than for native enzyme, thus giving some support to the contention that these modified forms were not ordered for catalysis as in the native enzyme.

It has been shown and/or noted by Lumry and co-workers (37-40), Schultz and co-workers (9,44), and others (35,36,45) that, while association of substrate to Cht perturbed by changes in solution pH, substrate structure, and/or protein structure may be characterized by large changes in the enthalpy and entropy of association, these changes are compensating and result in only minimal changes in the free energy of association. If such enthalpy and entropy changes are plotted according to equation 1.40:

$$\Delta H_a^0 = T_c \Delta S^0 + \text{constant}, \quad (1.40)$$

then a linear relationship is found with values for the slope, which is T_C (the compensation temperature) ranging from 270°K to 300°K. These T_C values are characteristic of values found for small solute reactions in water (37,38,40,46).

It has been argued that an observed linear correlation between compensating enthalpy and entropy changes are often due to experimental error and represent a statistical artifact (47,48). While the data from kinetic and binding studies, discussed above, have not been analyzed according to the recently published statistical criteria of Krug et al. (47,48) these compensation effects were analyzed by the criteria of Exner (38,49) and Lumry (39). These analyses indicated that the compensation in enthalpy and entropy is real and not due to statistical error. Recently, Luscher and Ruegg have analyzed an enthalpy and entropy compensation for the interaction of water with Cht by the method of Krug et al., and found the compensation to be real by the Krug analysis (50). The value of T_C of 291°K found in this later work is similar to the values of T_C found in the kinetic and substrate association experiments, and suggest a common source for both compensation phenomena (50).

Productive binding then has been shown to be characterized thermodynamically by negative enthalpies and entropies of association. Non-productive binding has been shown to have varied enthalpies and entropies of association which often were similar to values found for simple hydrophobic bond formation (2,34). However, both productive and non-productive binding have similar free energies of association which many authors feel by itself cannot explain the mechanism of enzyme catalysis (1-5,9, 11,12,37,44,45).

I C-3. Thermodynamics of Association and Catalysis of Specific and Non-Specific Substrates by α -Chymotrypsin.

As the negative enthalpy and entropy values obtained upon productive association to the S_1 site have been interpreted to be evidence for a protein conformational change on substrate association (2,3,9,11, 29,36-40), one could interpret productive association as a process leading to a highly ordered substrate-enzyme complex "activated" for catalysis. If, indeed, productive binding characterized by negative enthalpies and entropies of binding does lead to an activated enzyme-substrate complex as proposed by association-activation hypotheses then this activation should be apparent in the kinetic thermodynamic parameters (1-4,9).

Detailed kinetic and thermodynamic data for the individual steps of catalysis by Cht have been limited mainly to the more easily studied substrate analog binding step (9,36,44) and the deacylation step (22,51, 52), while only very limited studies of the more difficult to study acylation step have been reported (39,53-56).

Inagami et al. (54) studied the binding (K_S) and acylation of Cht by anilide substituted N-acetyl-L-tyrosine analide at 15^o, 25^o, and 35^oC. They found enthalpies of association near zero and small positive entropies of association for all derivatives studied. The acylation step in turn showed large positive enthalpies of activation (10-17 kcal/mole) and small negative entropies of activation (-3, to -8 e.u.).

Kunugi et al. (56) studied the pre-steady state catalysis of N-(2-furyl) acrylayl (Fa) derivatives of amino acid esters specific for the Cht S_1 site. They found the entropies of activation for the acylation

step k_2 to be near zero or positive (-4 e.u. and +10 e.u. for the Fa-L-Phe-OMe and acetyl-L-Trp p-nitrophenyl ester (ONp) derivatives respectively). The deacylation step k_3 had similar enthalpies of activation for five amino acid analogs ($\Delta H^\ddagger \cong 11.5$ kcal/mole), while the entropy of activation for the deacylation step varied from -11.3 e.u. for the tyrosine derivative to -22.6 e.u. for the leucine derivative. Therefore, the deacylation step specificity appeared entropically controlled. The association process had seemingly ordered the enzyme-substrate complex for the acylation step but, not the deacylation step as is shown by the positive and negative entropies of activation for the steps, respectively.

In studying the Cht catalysis of the non-specific substrates series of fatty acid p-nitrophenyl esters, Marshall and Chen (51) found that the deacylation step was enthalpically controlled, opposite to what had been found for specific amino acid substrates by Kunugi et al. However Marshall and Chen also studied the deacylation of two specific acyl amino acid ester substrates of the homologous protease enzyme elastase and also found that specificity for specific substrates was entropically controlled as had been found for specific substrates of Cht (56). The entropy of activation values for the deacylation step varied from 10 e.u. to 16 e.u. for the specific acyl amino acid ester and fatty acid p-nitrophenyl ester substrates, respectively, while the enthalpy of activation remained fairly constant around 10 kcal/mole. However, Baggott and Klapper (52) studied the deacylation step of the non-specific substrate series of 2(5-n alkyl) furoyl p-nitrophenyl esters and found that the deacylation step was enthalpically controlled at low temperatures

($\ll 25^{\circ}\text{C}$). They found that at low temperatures the enthalpy of activation for the deacylation step became more negative (favorable) by 4 kcal/mole upon going from shorter chain to longer alkyl chain (more specific) derivatives. The entropy of activation also became more negative (unfavorable) by 13 e.u. for the more specific substrates at low temperatures. The opposite relationship was found for the high temperature form with the enthalpy increasing by 3 kcal/mole (unfavorable) and the entropy increasing by 8.5 e.u. (favorable) for the more specific longer alkyl chain derivatives. This led Baggott and Klapper to propose two thermally induced forms of Cht with a transition temperature around 25°C .

I C-4. Thermodynamic, Kinetic, and Physical Evidence for Two Temperature Dependent Forms of Chymotrypsin.

As previously discussed, Baggott and Klapper (52) studied the deacylation step of the non-specific substrate series of 2 (5n-alkyl) furoyl p-nitrophenyl esters and found two thermodynamically distinct kinetic temperature dependent forms of Cht. The deacylation step was enthalpically controlled at low temperatures ($<25^{\circ}\text{C}$) and entropically controlled at high temperatures ($>25^{\circ}\text{C}$). Adams and Swart (55) studied the binding and catalysis of non-specific alkyl p-nitrophenyl esters and also proposed two temperature dependent forms of Cht, with a sharp transition range of 3° for the enzyme around 25°C . Thermodynamic studies of K_m and k_{cat} for specific ester substrates also showed two temperature dependent forms of the enzyme with a transition around 25°C (45,57). Glick (45) reported the hydrolysis of N-acetyl-L-tryosine ethyl ester (ATEE) by Cht in nine different solvent systems of different buffer salt and organic solvent combinations. Based upon a sharp discontinuity in the van't Hoff plots near 25°C , he proposed two temperature dependent forms of the enzyme with a transition point around 25°C . Wedler et al. (57) studied the binding and catalysis of N-acetyl amino acid methyl esters and also found a sharp discontinuity around 25°C in their data for both the association and catalytic steps (K_m and k_{cat}).

However, in many instances two temperature dependent forms of Cht were not observed. Inagami et al. (54) did not report a discontinuity in their studies of binding and acylation of Cht at 15° , 25° , and 35°C by N-acetyl-L-tyrosine anilides. Kunugi et al. (56) did not ob-

serve a discontinuity in their studies of the deacylation step from 5° to 40°C for the specific N-(2-furyl) acryloyl aromatic and aliphatic amino acids. Marshall and Chen (51) reported data for fatty acid p-nitrophenyl ester substrates at four temperatures from 10° to 37°C and did not observe a discontinuity. Baggott and Klapper (52) only saw the discontinuity for the larger analogs of the 2(5n-alkyl) furoyl p-nitrophenyl ester series. Schultz et al. (9) reported only a small discontinuity for binding of proflavin and the virtual substrate N-acetyl tryptophanes from 5° to 37°C.

Adams and Swart (55) did not see a discontinuity in the deacylation step of the non-specific alkyl p-nitrophenyl ester substrates. Since the discontinuity was present in the K_s , k_2/K_s kinetic parameters but, not in k_3 , they reasoned that the p-nitrophenyl ester group contributed a binding point to the enzyme which, when lost in the deacylation step, correlated with the amelioration of thermodynamic differences between the two forms of the enzyme.

Direct physical methods have clearly demonstrated two conformational forms of Cht with a transition around 25°C. The temperature dependence of the intrinsic fluorescence of native Cht was studied by Kim and Lumry (58) and showed two temperature dependent forms of the enzyme with the discontinuity around 25°C. Recently, Kennedy (59) has repeated these fluorescent studies for native free Cht and for Cht with N-acetyl-L-phenylalaninal (aldehyde) bound and found two forms with the discontinuity around 25°C. Havesteen et al. (60) studied the absorbance changes of native free Cht, monoacetyl-Cht, and isopropylacetyl-Cht at pH 2.0, and found a reversible temperature induced conformational change

that started around 25°C. The temperature dependence of the peroxide oxidation of surface methionine of Cht and chymotrypsinogen at pH 3.0 was studied by Wasi and Hofmann (61). They found a sharp increase in oxidation rate of protein methionine over free methionine at 25°C for Cht and 30°C for chymotrypsinogen. In addition, the recent study of the temperature dependence of water sorption by Cht by Ruegg and co-workers (50,62) clearly shows a high and low temperature conformation of the enzyme with the change in conformation occurring around 23°C.

These physical, kinetic, and thermodynamic data have been interpreted first by Lumry and co-workers (37,38,58) and more recently by others (45,50,52,55,57,59-62) as being indicative of a thermally induced conformational change in Cht near 25°C.

I C-5. The Extended Binding Site of α -Chymotrypsin.

Serine proteases have been classified by Fruton (63) into three general categories according to their primary and secondary site binding and catalytic specificity:

- i) Primary site binding and catalytic specificity. Interactions beyond the primary binding site S_1 have little or no effect on binding affinity or catalytic efficiency.
- ii) Primary and secondary site binding and catalytic specificity. Significant increases in both binding affinity and catalytic efficiency occur upon binding to secondary sites outside the primary binding site.
- iii) Secondary site catalytic specificity. Secondary binding site interactions beyond S_1 show large increases in catalytic efficiency, whereas binding only to S_1 is insufficient for significant catalytic rates.

Enzymes from category (i) such as trypsin (64), would be an efficient catalyst for short peptides. Enzymes from category (ii) such as Cht (65,66), subtilisin (67), and elastase (10) would be efficient catalysts for short and medium sized peptides. Enzymes from category (iii) such as pepsin (68) would be an efficient catalyst for large peptides and proteins. However, Fruton (63) does allow for a possible fourth class of serine restriction proteases such as thrombin (69) that have trypsin like primary specificity, but very exacting secondary specificity.

Bovine α -chymotrypsin is a type 2 serine protease according to Fruton's classification system (63). It shows both primary site and

secondary site binding and catalytic specificity (26,66,67,70,71). The primary binding site S_1 has both an increased binding affinity and catalytic efficiency for aromatic amino acids, and to a lesser extent aliphatic amino acids (26,71).

Catalytic studies of the extended binding site of Cht (S_4-S_4') show varying effects on the kinetic parameters K_m and k_{cat} depending on the amino acid residues of the substrate (65,66,70-72) and even the conformation of the substrate (73). Studies of Cht catalyzed hydrolyses of $(\text{glycyl})_n\text{-L-tyr ethyl ester}$ and $(\text{glycyl})_n\text{-L-tyr-(glycyl)}_n$ for sites S_4-S_4' , where tyrosine is in position P_1 and binds in the S_1 site, by Yoshida et al. (70) and others (66,74-77, Table 2) show varying effects upon K_m and k_{cat} for sites S_3-S_4 . Kinetic studies by Bauer et al. (72) and X-ray crystallographic studies of Cht with peptide chloromethyl ketone inhibitors bound by Segal et al. (78) also showed little or no interaction beyond the S_3 site.

Bauer et al. (72) and others (65,66,79) found that binding of a proline residue was favorable in sites S_2 and possibly S_4 and unfavorable in sites S_1 and S_3 to the extent that the large favorable binding of aromatic amino acids in S_1 (26,71) was overcome and hydrolysis of the peptide N-acetyl-L-Pro-L-Ala-L-Phe-NH₂ would occur at the Ala-Phe bond at a small, but significant rate (72). These studies by Bauer et al. of the Cht hydrolysis and the serine protease Streptomyces griseus protease 3 (SGP-3) hydrolysis of the peptide series N-ac-Phe, Pro-Phe, Ala-Pro-Phe, Pro-Ala-Pro-Phe amides at 37°C showed a similar restriction for proline in the P_2 position. A similar restriction in the S_2 binding of proline has been found for the analogous serine protease elastase by

LEGEND

Table 2. Binding and Catalytic Constants for Tyrosine PeptideSubstrates with α -Chymotrypsin.

- a Yoshida and Ishii (74), pH 8.0, 30^oC
- b Yamamoto and Izumiya (75), pH 8.3, 30^oC
- c Yoshida et al. (70), pH 8.3, 30^oC
- d Yoshida et al. (70), pH 7.7, 30^oC
- e Baumann et al. (76), pH 7.9, 25^oC
- f Izumiya and Yamashita (77), pH 8.0, 30^oC
- g Baumann et al. (66), pH 7.9, 25^oC

BINDING AND CATALYTIC CONSTANTS FOR TYROSINE PEPTIDE SUBSTRATES WITH
 α -CHYMOTRYPSIN.

COMPOUNDS	SOURCES AND CONDITIONS	K _m (mM)	k _{cat} moles/min/gN	k _{cat} s ⁻¹
Ac-Tyr-OEt	a	1.30		271
Ac-Tyr-OEt	b	0.40	1.71	
Gly ₂ -Tyr-OEt	b	1.63	5.5	
Gly-Ala-Tyr-OEt	b	1.40	3.7	
Gly ₃ -Tyr-OEt	c	7.4	7.0	
Gly ₄ -Tyr-OEt	c	6.2	5.1	
Gly-Tyr-Gly ₂	d	3.2	0.006	
Gly ₂ -Tyr-Gly ₂	d	2.7	0.030	
Gly ₃ -Tyr-Gly ₂	d	1.7	0.065	
Gly ₄ -Tyr-Gly ₂	d	23	0.007	
Gly ₂ -Tyr-Gly ₃	d	20	0.045	
Gly ₂ -Tyr-Gly ₄	d	6.7	0.027	
Ac-Tyr-NH ₂	b	153	0.0168	
Ac-Tyr-NH ₂	e	32 _{±4}		0.17 _{±0.02}
Gly-Tyr-NH ₂	f	150	0.0028	
Ala-Tyr-NH ₂	f	180	0.034	
Gly ₂ -Tyr-NH ₂	b	41	0.015	
Gly-Ala-Tyr-NH ₂	b	95	0.15	
Ac-Tyr-Gly-NH ₂	e	23.3 _{±2.8}		0.64 _{±0.10}
Ac-Tyr-Ala-NH ₂	e	17.2 _{±0.9}		7.5 _{±0.5}
Ac-Gly-Tyr-Gly-NH ₂	g	7.8 _{±0.5}		0.48 _{±0.04}
Ac-Ala-Tyr-Gly-NH ₂	g	29.1 _{±1.2}		1.41 _{±0.08}

Thompson and Blout (80). These data (72,80) and other X-ray (79) and kinetic data (65,66) led Bauer et al. to hypothesize that binding of proline in the S_2 and S_4 sites was favorable over the S_1 and S_3 sites and that this substrate sequence would severely curtail non-productive modes of binding.

I C-6. Thermodynamic of Protein-Ligand and Protein-Protein Interactions.

According to association-activation hypotheses of enzyme catalysis (1-4,9) binding of the substrate to the active site of the enzyme activates the enzyme-substrate complex towards catalysis. Productive association of enzyme and substrate was found to be characterized thermodynamically by negative ΔG_a^0 , ΔH_a^0 , and ΔS_a^0 , while non-productive binding was variable (9,11,35-40; see section I C-2). Non-catalytic protein association with specific ligands as in the case of hemoglobin association with O_2 and immunoglobulin association with antibody are non-productive in the catalytic sense but, are "productive" in a functional sense.

Mills et al. (81) studied the binding of oxygen by the α and β monomer units of the human hemoglobin tetramer, $\alpha_2\beta_2$. They found that the binding of O_2 by the α and β monomers was characterized at 25°C and pH 7.4 by a $\Delta G_u^0 = -8.20$ kcal/mole, $\Delta H^0 = -15.55$ kcal/mole, and $\Delta S_u^0 = -2.45$ e.u. (expressed in unitary units to eliminate the contributions due to mixing (34,82)). Studies of the association of two oxygenated monomer units at 21.5°C and pH 7.4 gave a $\Delta G_u^0 = -5.28$ kcal/mole, $\Delta H^0 = +4.3$ kcal/mole, and a $\Delta S_u^0 = +40.6$ e.u., values that are similar to the association of two oxygenated $\alpha\beta$ dimers to form $\alpha_2\beta_2$ hemoglobin (83) ($\Delta G_u^0 = -8.1$ kcal/mole, $\Delta H^0 = +3.8$ kcal/mole, and $\Delta S_u^0 = +48.4$ e.u.). However, association of two unoxxygenated $\alpha\beta$ dimers to form unoxxygenated $\alpha_2\beta_2$ hemoglobin gave thermodynamic values of $\Delta G_u^0 = -14.2$ kcal/mole, $\Delta H^0 = -28.9$ kcal/mole, and $\Delta S_u^0 = -41.8$ e.u. (84), values that differ from the oxygenated association process by a $\Delta\Delta G_u^0 = -6.1$ kcal/mole, $\Delta\Delta H^0 = -32.7$ kcal/mole, and $\Delta\Delta S_u^0 = -90.2$ e.u. Association of un-

oxygenated dimers (84), therefore, yielded thermodynamic parameters similar to those found for productive enzyme-substrate association ($\Delta G_a^0 < 0$, $\Delta H_a^0 < 0$, $\Delta S_a^0 < 0$), while association of O_2 with monomer units and association of oxygenated monomers and dimers (81,83) yielded values that were similar to those found for non-productive association of enzyme and substrate ($\Delta G_a^0 < 0$, $\Delta H_a^0 = 0$ or $+$, $\Delta S_a^0 > 0$). Valdes and Ackers (83) proposed that since the values for association of oxygenated dimers were similar to those found for simple hydrophobic bond formation, the values were the result of solvation and water structure changes. Interesting, therefore, the oxygenated forms seem to be the more constrained structure in that association results in no apparent conformational change, while the unoxygenated submits undergo a conformational change upon self-association (85).

The thermodynamic of hapten-antibody association over a 70°C temperature range was studied by Mukkur and Szewczuk (86,88). A plot of the temperature dependence of the logarithm of the association constant for ϵ -DNP-L-lysine and rabbit anti DNP IgG (van't Hoff plot) gave a curvilinear concave shaped line with a minimum at 40°C. The thermodynamic parameters ΔH^0 and ΔS_u^0 were negative at -3°C (-14.22 kcal/mole and -18.34 e.u., respectively) and increased to positive values at 67°C (+18.88 kcal/mole and +90.69 e.u., respectively). Accordingly, the binding process was enthalpy driven at low temperatures ($< 25^\circ\text{C}$) and entropy driven at high temperatures ($> 25^\circ\text{C}$). In addition, the changes in enthalpy and entropy were found to be compensating and the change in heat capacity, ΔC_p , was positive ($\Delta C_p = + 470$ cal/deg/mole). In a review by Tanford (89) he showed similar curved van't Hoff plots and heat ca-

capacity changes ($\Delta C_p > 0$) for the protein denaturation process.¹ The urea denaturation of B-lactoglobulin and the thermal denaturation of ribonuclease and chymotrypsinogen were all found to be enthalpy driven processes at low temperature ($\Delta H < 0$) and an entropy driven process at high temperature ($\Delta S > 0$).

Cuatrecacas studied the binding of insulin to its receptor on fat cell membranes (90) at four temperatures and found the van't Hoff analysis also showed a positive ΔC_p , resulting in an enthalpy driven process at low temperatures and an entropy driven process at higher temperatures.

The dimerization of Cht was studied by Aune et al. (91) at pH 5.5 (inactive). They found a curvilinear temperature dependence, however the curve showed a maximum instead of a minimum giving a negative ΔC_p for the association process. In addition, they found that the equilibrium constant for the dimerization reaction was increased as the ionic strength was increased, indicating the involvement of hydrophobic forces (2,34,82,89).

Pancreatic trypsin inhibitor (PTI) is the natural large protein inhibitor for Cht in the pancreatic islet cells (92). X-ray crystallographic data has shown that PTI binds at the active site of Cht and that the structure of the inhibitor and Cht changes very little from free in-

¹ Tanford (89) defined the denaturation process as simply being a major change from the original native structure, without alteration of the amino acid sequence. Unfolding of the protein is an example of a denaturation process.

hibitor and enzyme as compared to complex (93,94). At low concentrations a two step binding process is discernable, with a fast diffusion rate limited first step and a slow second step (95). Quast et al. (96) studied the association of PTI with Cht at pH 7 and 8 and found that the fast initial binding step was characterized thermodynamically at 25°C by a $\Delta G^0 = -4.4$ kcal/mole, $\Delta H^0 = +3.4$ kcal/mole, and $\Delta S^0 = +26$ e.u. The slow second rearrangement step was characterized by a $\Delta G^0 = -7.6$ kcal/mole, $\Delta H^0 = -1$ kcal/mole, and $\Delta S^0 = +22$ e.u. They interpreted their results to indicate that both reactions were entropy driven and that, since conformational transitions upon binding were small (93,94), the process was due to solvation and water structure changes (96).

I C-7. Model Solvent Partition and Enzyme Studies.

Model partition studies have shown that transfer of hydrophobic moieties from an aqueous to a non-polar hydrophobic environment, as in hydrophobic bond formation, are characterized thermodynamically by a negative standard free energy change, an enthalpy change near zero, a positive entropy change, and a positive heat capacity change (2,34,97). Association of aromatic moieties in the S_1 site of Cht has been shown to be characterized by a negative standard free energy change, a negative enthalpy change, a negative entropy change and is an enthalpy driven process (1-4,9,36,98) unlike partition studies between aqueous and hydrophobic solvent systems (2,3,4,97).

Wildnauer and Canady (99) carried out partition studies between aqueous and organic phases, and between the aqueous phase and the S_1 site of Cht for the non-specific aromatic compound series: benzene, toluene, ethylbenzene, etc.. They found that plots of the free energy of transfer versus surface area of the compounds gave almost identical linear relationships for partitioning and binding of these non-specific Cht inhibitors. Gill et al. (97) found that the transfer of benzene from aqueous to benzene at 25°C was characterized by a $\Delta G_t^0 = -4.6$ kcal/mole, a $\Delta H_t^0 = -0.5$ kcal/mole, and a $\Delta S_t^0 = +14$ e.u.. Berezin et al. found that the transfer or binding of benzene from aqueous buffer (pH 8.0) to the S_1 site of Cht at 25°C was characterized by a $\Delta G_t^0 = -3.0$ kcal/mole, a $\Delta H_t^0 = -4.5$ kcal/mole, and a $\Delta S_t^0 = -5$ e.u. The transfer of benzene to benzene was, therefore, an entropy driven process while the transfer of benzene to the S_1 site of Cht was an enthalpy driven process.

Nozaki and Tanford (100) found that the benzyl side chain of the amino acid phenylalanine has a $\Delta G_t^0 = -2.6$ kcal/mole for transfer from aqueous solution to pure ethanol and a $\Delta G_t^0 = -2.32$ kcal/mole for transfer to pure ethylene glycol at 25°C. Nandi (101) found that for transfer to n-hexanol from an aqueous solution the benzyl side chain of phenylalanine had a $\Delta G_t^0 = -1.8$ kcal/mole at 25°C. Bauer et al. (71) found that the free energy of association of a tetrapeptide specific for Cht with glycine in the P₁-S₁ position, with respect to the same peptide containing a phenylalanine in the P₁-S₁ position, gave a value of $\Delta G_a^0 = -2.2$ kcal/mole for binding of the phenyl side chain to the S₁ site.

Association-activation mechanisms of enzyme catalysis predict that a specific substrate that binds productively to an enzyme will be characterized thermodynamically by a negative standard free energy, a negative enthalpy, and a negative entropy of association (1-4,9). Wedler et al. (57) found that the substrate N-acetyl-L-leucine methyl ester, which binds productively with Cht, was characterized by a $\Delta G_a^0 = -1.85$ kcal/mole, a $\Delta H_a^0 = -7.5$ kcal/mole, and a $\Delta S_a^0 = -18.95$ e.u. at pH 8.0 and 25°C. Nandi (101) found that transfer of the substrate N-acetyl-L-leucine ethyl ester from aqueous to n-hexanol at 25°C was characterized by a $\Delta G_t^0 = -1.90$ kcal/mole, a $\Delta H_t^0 = +4.7$ kcal/mole, and a $\Delta S_t^0 = +22.2$ e.u..

Accordingly, enthalpy and entropy values of hydrophobic moieties binding to the S₁ site of Cht were found to be more negative than values found for the simple transfer process to a hydrophobic solvent.

I C-8. Synthetic Catalytic Models.

Enzymes catalyze reactions by bringing reactant(s) and/or reactive catalytic groups together under conditions more favorable for catalysis (1-4,9,11,14). Synthetic catalytic models including micelles, organic molecules, polymers, and peptides have shown an ability to catalyze certain reactions by rates up to 10^6 times faster than the corresponding non-catalyzed reaction (11,102-108).

Micelles utilize the binding energy of a compound to bring reactive groups together at the micelle solvent interphase (11). The reaction of m-bromobenzaldoxime with p-nitrophenyl acetate (pNPA) and p-nitrophenyl salicylate in the presence of hexadecyltrimethylammonium bromide micelles showed rate increases of 10^3 and 1.7×10^4 over the water hydrolytic rate alone by Berezin and co-workers (11,102). Similarly, Hogan and Gandour (103) have shown that glymes (open chain poly-ethers, molecular weight 1,000 or less) catalyze the butylamine aminolysis of pNPA at a rate 1,900 times faster in chlorobenzene than the same non-catalyzed reaction in chlorobenzene. In addition, they found that while the more flexible glymes showed poorer binding by the substrates of 10^4 times ($\Delta G = 5.9$ kcal/mole more positive) than the more rigid closed chain poly-ethers (crowns) the reaction was catalyzed three times faster by the more flexible glymes.

More recently Breslow et al. (104) showed a rate enhancement of 10^6 times ($\Delta\Delta G^\ddagger = -7.8$ kcal/mole) for the hydrolysis of the ester bond of ferrocenylacrylic p-nitrophenyl ester by hydroxyl containing B-cyclodextrin. These investigation systematically varied the structure of the substrates and by using molecular models they were able to pre-

dict that ferrocenyloxylic p-nitrophenyl ester would be more stabilized in the transition state than in the ground state association to the cyclodextrins, as calculated from percent occupancy of the cyclodextrin cavity from molecular models of substrate in the ground state and substrate in the proposed transition state within the cyclodextrin catalyst. Thermodynamic parameters for the catalyzed reaction of p-nitrophenyl ferrocenacrylate by cyclodextrin showed a large decrease at 25°C in both the enthalpy and entropy ($\Delta H_C^\ddagger = 5.7$ kcal/mole, $\Delta S_C^\ddagger = -42.4$ e.u.) over the non-catalyzed reaction of p-nitrophenyl ferrocenacrylate in 60% Me₂SO₄/40% H₂O, pH 6.8 ($\Delta H^\ddagger = 19.9$ kcal/mole, $\Delta S^\ddagger = -23.6$ e.u.). Similar studies of ester hydrolysis by the polymer polyethyleneimine with imidazole bound showed significant rate enhancements (101, 102). Klotz *et al.* (101) found a 300 fold increase for the hydrolysis of pNPA by imidazole polymer that had been dodecylated to provide hydrophobic binding regions. Mirejovsky (102) found a 600 times increase in the rate of p-nitrophenyl caproate hydrolysis by acetylated imidazole polymer. In addition, he found that the reaction rate actually decreased with increased bound imidazole and postulated that only certain imidazole groups near polar-apolar interphases were catalytically active.

Small peptides with the catalytically active amino acid residues cysteine and histidine have also shown significant rate enhancements in ester hydrolysis (107-109). Fridkin and Goren studied the heptapeptide L-Ser-L-Pro-L-Cys-L-Ser-L-Glu-L-Thr-L-Tyr catalyzed hydrolysis of pNPA (107). They found that the benzyl-cysteine derivative of the heptapeptide had no activity while, the free cysteine derivative showed a rate increase between pH 7 and 8 of five times that of free thiol and ten

times that of the cysteine containing peptide glutathione.

Petz and schneider (108) studied the hydrolysis of pNPA by cysteine containing di-, tri-, and pentapeptides. They found that the presence of the amino acid histidine led to a cooperative effect that increased the reactivity of the cysteine-SH group, while a peptide with histidine and no cysteine had a rate 40 fold less than peptide with cysteine and no histidine and 120 fold less than a peptide with both cysteine and histidine. In addition, presence of an acidic amino acid such as aspartate one amino acid residue from histidine perturbed the pKa of histidine from 6.42 to 6.82, increasing the rate enhancement of the peptide through increased cooperative effects with the cysteine-SH group.

Goren et al. (109) studied the hydrolysis of pNPA by poly (L-histidyl-L-alanyl- α -L-glutamic acid). They found that free imidazole had two times the catalytic rate of polymer histidine at solvent conditions of 2% trifluoroethanol in water and that as the percentage of trifluoroethanol was increased the rate of hydrolysis by free imidazole dropped while the polymer imidazole hydrolysis rate increased by 60% until they were equal at 40% trifluoroethanol/water concentration. At this concentration of trifluoroethanol there are large amounts of α -helix conformation present, and the Glu could hydrogen bond to one of the nitrogens of the histidine. As such it could be a model for the Asp-His "charge relay system" of serine protease enzymes. In addition, they found that the value of the rate constant for a bound imidazole is only 0.2 to 0.3 times that of solution free imidazole due to steric and/or electrostatic differences (109,110).

CHAPTER II

MATERIALS AND METHODS

II A. General Materials and Sources

The sources of chemicals and solvents were the Eastman Chemical Company, Scientific Products (S/P), Mallinckrodt Chemical Works, Aldrich Chemical Company, and Sigma, Chemical Company, and were reagent grade or better. Specialty chemicals are as noted.

All amino acids and derivatives are of the L conformation unless otherwise noted and were purchased from the Sigma Chemical Company. The generally labeled tritiated L-phenylalanine (Batch No. 16) was purchased from Amersham/Searle Corporation as was the carbon-14 labeled dimethyl sulfoxide (DMSO).

Dimethyl sulfoxide (DMSO), purchased from the Eastman Chemical Company, was twice redistilled under vacuum over lithium hydride (Matheson Coleman and Bell) and stored under nitrogen at 4°C (solid form) until used.

Bovine pancreatic α -chymotrypsin (three times crystallized) was purchased from Worthington Biochemical Corporation. Lot No. CDI 35P693 (67U/mg) was used exclusively throughout this work. All chymotrypsin was further purified by the method of Yapel et al. (111) using G-25 (superfine) Sephadex purchased from Pharmacia Fine Chemicals. The concentration of this enzyme was accurately determined from its UV absorbance at 280 nm in 10^{-3} N HCl (pH 3.0) solution using the molecular absorbance coefficient (E) of 5×10^4 absorbance units /M/cm (112).

The chromatographic system used to check all organic reactions was done by thin-layer chromatography (TLC) using silica gel plates (Q 1) purchased from Quantum Industries and were developed in a 9:1 (V/V) chloroform to methanol system, unless otherwise noted.

A ninhydrin spray reagent (113) was prepared at 0.2% in acetone (0.2 g/100 ml) and was used to check for free amine groups. Upon heating the development of a red color indicated presence of free amine, a positive reaction.

All radioactive compounds to be used in the model studies were synthesized by the substitution of the generally labeled tritiated -L-phenylalanine in the synthetic procedures. All enzymatic hydrolyses experiments were done with non-radioactive substrates.

Elemental analyses were performed by Galbraith Laboratories, Incorporated of Knoxville, Tennessee.

Amino acid analyses were done by Dr. Charles Lange of the Department of Microbiology at Loyola - Stritch School of Medicine.

II B. Synthesis of Derived Amino Acid and Peptide Substrates.

Syntheses of all substrates were performed as indicated in the referenced literature except where modifications are noted. Maintenance of enantiomeric integrity is discussed in the literature. Identification and purity of products was done on the basis of physical constants and techniques noted in the literature. Infrared (IR) spectra were recorded on a Perkin-Elmer model 337 IR-spectrophotometer.

In the synthesis of these substrates several steps are repeated for the different substrates. These steps will be given in detail the first time and then referred to each additional time they are used.

II B-1. Synthesis of N-Acetyl-L-Phenylalanine-Amide.

The methyl ester hydrochloride of L-phenylalanine (PheOMe HCl) was synthesized by standard procedures (113). Anhydrous HCl gas (Matheson) was bubbled through a vigorously stirring slurry of 10 g (0.06 moles) of crystalline Phe in 150 ml of anhydrous methanol (MeOH) until the solute was completely dissolved. The solvent was then cooled to 0°C in an ice bath and HCl added for an additional 30 minutes with vigorous stirring. The solution was then stoppered and allowed to stand at room temperature for 3 hours. The solvent was then rotary evaporated under vacuum and the resulting solids recrystallized from MeOH yielding 11.7 g (89% yield) of fine, white needle crystals (m.p. 162-163°C, m.p. lit. (114) 162-163°C, TLC $R_f = 0.4$).

The phenylalanine methyl ester hydrochloride was then N-acetylated by the procedures of Baumann et al. (66) with one modification. The 0.7 g of phenylalanine methyl ester (0.053 moles) was dissolved in 100 ml of vigorously stirring dimethylformamide (DMF) instead of water as in the Baumann procedure, 6.04 ml (0.053 moles) of N-methylmorpholine (NMM) was then added. N-acetoxysuccinimide (7.54 g, 0.053 moles, synthetic procedure is given following complete synthesis of N-ac-phe-NH₂) was then added to the solution and the reaction was allowed to proceed for 4 hours at room temperature with stirring. The DMF was then rotary evaporated under vacuum using a dry ice-acetone trap. The residue was dissolved in ethyl acetate (100 ml), filtered through a scintered glass filter to remove any NMM·HCl and the solution washed 3 times with cold 0.1 N HCl, 3 times with cold 4% NaHCO₃ (W/V) solution, and 2 times with a

cold saturated saline solution (NaCl). The solution was dried with anhydrous MgSO_4 , filtered, the volume reduced to one half, hexanes added to the cloud point, and the round bottom was then stoppered and placed in the refrigerator. After several hours 10.8 g (92% yield) of white crystals were filtered off. (m.p. 89-90°C, m.p. lit. (115) 90-91°C, TLC $R_f = 0.92$). Crystals gave a negative ninhydrin test while starting materials was positive.

The 10.8 g of N-ac-Phe OMe was then dissolved in 100 ml of anhydrous MeOH with stirring for the amidation step. The solution was brought to 0°C and anhydrous NH_3 gas (Matheson) bubbled through for 3 hours. The round bottom was then stoppered and the solution allowed to stir at room temperature for 2 days. The MeOH was then rotary evaporated under vacuum, the solid was dissolved in an ethanol-ethyl methyl ketone mixture, the volume was reduced by one half, chilled to 0°C and yielded needle crystals upon being scratched and placed in the refrigerator overnight. Yield 9.5 g (94%) of fine needle crystals. (m.p. 179-181°C, m.p. lit (115) 176-177°C TLC $R_f = 0.55$ visualized under I_2). Product was used without further purification.

N-acetoxysuccinamide for the acetylation step by the Baumann et al. procedure (66) was prepared by dissolving 10 g of N-hydroxysuccinimide (0.087 moles) in 250 ml of acetone. Acetic anhydride (4.2 ml, 0.087 moles) was added dropwise at room temperature with vigorous stirring. The reaction was allowed to proceed for 160 minutes. The acetone was then rotary evaporated off leaving a crystalline residue which was redissolved in absolute ethanol at 45°C. The solution was then placed in the refrigerator overnight. Fine crystalline needles (10.4 g, 88%

yield) were filtered off the following day. (m.p. 129-130°C, m.p. lit.
(66) 132-133°C, TLC R_f = 0.9).

II B-2. Synthesis of N-Acetyl-L-Phenylalanine-Glycine-Amide.

N-ac-Phe-Gly-NH₂ was synthesized by the method of Vaughn and Osato (116) with modifications. DMF was used as the solvent rather than toluene, NMM was used rather than triethylamine as suggested by Anderson (117) to reduce activation time for the carboxyl group, and the use of one equivalent less 6% of isobutyl chloroformate to prevent blocking of the amino group by excess chloroformate as suggested by Tilak et al. (118).

CBZ-L-Phe (10 g, 0.034 moles) was added to 100 ml of DMF in a three neck round bottom flask fitted with a CaSO₄ filled ground glass joint drying tube, a thermometer through a fitting, and a stopper. One equivalent NMM (3.75 ml, 0.034 moles) was added with stirring and the solution brought to -15°C in a CCl₄-dry ice bath. Isobutyl chloroformate (4.18 ml, 0.032 moles) was added with vigorous stirring. The activation was allowed to proceed for 10 minutes. A solution of Gly-OET HCL (4.68 g, 0.034 moles) and NMM (3.75 ml., 0.034 moles) in 50 ml of DMF at -15°C was then added. The solution was allowed to slowly warm to room temperature and left overnight with stirring. The solution turned yellow overnight with a white precipitate (NMM·HCl) which was filtered off and the solution rotary evaporated to a solid. The solid was dissolved in 100 ml of ethyl acetate and any additional solid filtered off. The solution was then washed three times each with 50 ml aliquots of cold 0.1N HCl, 4% NaHCO₃, and brine (saturated saline). Each aqueous wash was washed with 10 ml of ethyl acetate which was added back to the original solution. The entire ethyl acetate solution was dried over MgSO₄, filtered, and the volume reduced. Hexanes were then added to the

cloud point and the solution placed in the refrigerator for several hours. The crystals were filtered (m.p. 107-108°C, m.p. lit. (116) 108-110°C, TLC R_f = 0.94 in 97:3, CHCl_3 :MeOH) yielding 3.27 g. Addition of more hexanes and cooling produced 3 additional crops of crystals with similar melting points for a total of 8.95 g (67% yield) of CBZ-L-Phe-Gly-OEt.

The CBZ (benzyloxycarbonyl) protecting group was then removed, the peptide acetylated and finally amidated by the method of Baumann et al. (66) with several modifications. These were the use of t-butyl alcohol instead of ethanol in the hydrogenation step, the use of DMF instead of water in the acetylation step and crystallization from ethyl methyl ketone-ethanol instead of water.

CBZ-L-Phe-Gly-OEt (8.95 g, 0.0275 moles) was dissolved in 250 ml of t-butyl alcohol in a Parr hydrogenator flask. An equivalent of 6N HCl (4.85 ml, 0.0275 moles) was added to prevent formation of diketopiperazines, followed by 9 g of 5% palladium on charcoal catalyst (Matheson Coleman and Bell). The flask was then placed on the Parr hydrogenator and purged 3 times with 20 p.s.i. hydrogen gas, the flask refilled to 20 p.s.i., and then the solution was shook overnight (>12 hours) at a maintained pressure of 20 p.s.i. hydrogen gas. The following morning the flask was evacuated and purged 3 times with room air, the catalyst was filtered off, and the solution rotary evaporated to an oily residue. Addition of cold hexanes produced crystalline hygroscopic solids (R_f = 0.37, 97:3, CHCl_3 :MeOH) which were ninhydrin positive.

The solids were then acetylated by the N-acetoxysuccinamide method as described in section II B-1. Assuming 100% hydrogenation,

N-acetoxysuccinamide (3.87 g, 0.0275 moles) and NMM (3.01 ml, 0.0275 moles) were dissolved in 200 ml of DMF containing Phe-Gly-OEt·HCl (0.0275 moles) with stirring and the reaction allowed to proceed for 6 hours at room temperature. The solution was then rotary evaporated and worked up as described in section II B-1. Yield from the ethyl acetate-hexanes crystallization was 4.52 g of ninhydrin negative solids. (50% yield, m.p. 138-140°C, m.p. lit. (116) 133-135°C, TLC R_f = 0.91, 97:3, CHCl₃:MeOH).

Amidation of ac-Phe-Gly-OEt (4.52 g, 0.014 moles) was done as described in section II B-1 in 100 ml of anhydrous MeOH. Solids were recrystallized from ethyl methyl ketone-ethanol yielding 3.92 g. (96% yield, m.p. 182-184°C, m.p. lit. (116) 183-184°C, TLC R_f = 0.70, 4:1, CHCl₃:MeOH). Product was used without further purification.

II B-3. Synthesis of N-Acetyl-L-Proline-L-Phenylalanine-Amide.

N-ac-Pro-Phe-NH₂ was synthesized by coupling N-ac-Pro directly as described by Bauer et al. (72). PheOMe·HCl was used instead of Phe-NH₂ for ease of extraction as the ion exchange purification method as described by Bauer et al was not used in this synthesis. Phe-OMe·HCl was synthesized as described in section II B-1.

The methyl ester hydrochloride of proline (20 g, 0.153 moles) was synthesized by standard procedure as for Phe in section II B-1 resulting in a clear colorless oil after rotary evaporation of MeOH. Crystallization was from MeOH-ethyl ether. (25.4 g, 91% yield, m.p. 70-71°C, m.p. lit. (119) 71°C, TLC R_f = 0.25).

N-acetylation of ProOMe·HCl was done by standard procedure (113). ProOMe HCl (25.4 g, 0.139 moles) was dissolved in 150 ml of anhydrous MeOH and 10.42 ml (0.139 moles) of dry pyridine were added and the solution cooled to 0°C in an ice bath. Acetic anhydride (12.2 ml, 0.139 moles) was then added dropwise with stirring, the solution allowed to slowly warm to room temperature and then stirred for an additional 3 hours. The solvents were rotary evaporated under vacuum and the resulting oil was dissolved in 250 ml of CH₂Cl₂ (dichloromethane). The organic layer was washed 2 times each with 30 ml aliquots of cold 0.1 N HCl, 4% NaHCO₃, and brine. Each aqueous wash was counterextracted with two 50 ml aliquots of CH₂Cl₂ which were then added to the original solution. The solvent was then dried over MgSO₄, filtered, and rotary evaporated resulting in a ninhydrin negative solid (TLC R_f = 0.45).

The methyl ester was hydrolyzed by standard procedure (113). The solid from the acetylation step was dissolved in 150 ml of 1:1, 0.1N

NaOH/MeOH at room temperature with stirring and the pH was maintained at 13 by dropwise addition of 10N NaOH for 1 hour. The reaction was then acidified to pH 3.0 with concentrated HCl, the volume reduced to 75 ml and extracted ten times with 100 ml aliquots of CH_2Cl_2 . The solution was then dried with MgSO_4 , filtered, and the solvent rotary evaporated to yield a solid. Crystallization from MeOH-ethyl ether yielded 10.77 g (0.063 moles, 40.9% overall yield). (m.p. 113-114°C. m.p. Vega Biochemicals 111-113°C, TLC R_f = 0.2). The N-ac-Pro was pure by TLC, had a short range for the melting point, and was used without further purification.

Coupling by the mixed anhydride method was done as in section II B-2 except only a five minute activation time was allowed following addition of isobutyl chloroformate and an excess of N-ac-Pro was used to increase the yield (118). N-ac-Pro (4.09 g, 0.025 moles), NMM (2.91 ml, 0.025 moles), isobutyl chloroformate (3.25 ml, 0.024 moles) in 50 ml DMF at -15°C. Phe-OMe HCl (4.66 g, 0.0215 moles), NMM (2.41 ml, 0.0215 moles) in 50 ml DMF. DMF was rotary evaporated and solids dissolved in CH_2Cl_2 for aqueous washes. Crystallization of N-ac-Pro-Phe-OMe was from hot CHCl_3 -hexanes, 5.2 g (0.0156 moles, 65% yield, m.p. 107.5-109°C, TLC R_f = 0.9).

Amidation was done as in section II B-1 in 100 ml of MeOH. Crystallization from hot ethyl acetate yielded 4.72 g (0.0148 moles, m.p. 178-179°C, m.p. lit (72) 178-179°C, TLC R_f = 0.4).

II B-4. Synthesis of N-Acetyl-L-Alanine-L-Proline-L-Phenylalanine-Amide.

In the synthesis of N-ac-Ala-Pro-Phe-NH₂, CBZ-Ala was first coupled to Pro-OMe HCl by the mixed anhydride method as described in section II B-2. Pro-OMe·HCl was synthesized as described in section II B-3. CBZ-Ala (8.7 g, 0.039 moles, NMM (4.36 ml, 0.039 moles) and isobutyl chloroformate (4.93 ml, 0.037 moles) were dissolved in 50 ml DMF at -15°C. Pro-OMe HCl (6.46 g, 0.039 moles) and NMM (4.36 ml, 0.039 moles) in 50 ml DMF at -15°C was added after a 5 minutes activation time. Reaction was run overnight, DMF rotary evaporated under vacuum, and resulting oil (TLC R_f = 0.95) was dissolved in 100 ml ethyl acetate for aqueous washes and the ethyl acetate was rotary evaporated under vacuum. The resulting oil product, CBZ-Ala-Pro-OMe, was dissolved in 150 ml of 1:1, 0.1N NaOH:MeOH and held at pH 13 by dropwise addition of 10N NaOH for 2 hours. TLC showed the spot at R_f = 0.95 disappeared with time and one at R_f = 0.4 appeared with time. The solution was then acidified to pH 3.0, the volume reduced to 75 ml and the aqueous layer extracted 5 times with 50 ml aliquots of ethyl acetate. The ethyl acetate was rotary evaporated under vacuum to yield an oil, CBZ-Ala-Pro (10.0 g, 0.0312 moles, TLC R_f = 0.4).

CBZ-Ala-Pro was coupled to Phe-OMe HCl (prepared by the esterification procedure as described in section II B-1) by the mixed anhydride method as described in section II B-2. CBZ-Ala-Pro (10 g, 0.0312 moles), NMM (3.69 ml, 0.032 moles), and isobutyl chloroformate (3.99 ml, 0.03 moles) were added to 50 ml DMF at -15°C and allowed to stand 5 minutes. Phe-OMe HCl (7.12 g, 0.033 moles) and NMM (3.69, 0.032 moles) in 50 ml

DMF precooled to -15°C was then added with stirring. The reaction was allowed to proceed overnight. After rotary evaporation of the DMF under vacuum, the solid residue was dissolved in CH_2Cl_2 for the aqueous washes as described in section II B-2. Crystallization from ethyl acetate-hexanes gave 12.76 g (79% yield, 0.0246 moles) of CBZ-Ala-Pro-Phe-OMe (TLC $R_f = 0.90$).

The CBZ group was then removed by hydrogenation as described in section II B-2. CBZ-Ala-Pro-Phe-OMe (12.76 g, 0.0246 moles), 6N HCl (4.1 ml, 0.0246 moles) and 5% palladium on charcoal (12 g) were dissolved in 250 ml of t-butyl alcohol and shook overnight at 20 p.s.i. of H_2 . The following day the H_2 gas was purged, the catalyst filtered off, and t-butyl alcohol was rotary evaporated under vacuum leaving a hygroscopic solid (TLC $R_f = 0.2$) which was ninhydrin positive.

Ala-Pro-Phe-OMe HCl (0.012 moles), NMM (1.35 ml, 0.0125 moles) and N-acetoxysuccinamide (1.693 g, 0.012 moles) were added to 100 ml DMF with stirring for the acetylation reaction as described in section II B-1. The ac-Ala-Pro-Phe-OMe was worked up in CH_2Cl_2 as described in the same section. The product was then amidated in 100 ml MeOH, as described in section II B-1, and crystallized from ethyl acetate-hexanes to give white hygroscopic solids of N-ac-Ala-Pro-Phe- NH_2 . (2.69 g, 0.0072 moles, m.p. $100-102^{\circ}\text{C}$, m.p. lit. (72) $94-97^{\circ}\text{C}$, TLC, 9:1, CHCl_3 :MeOH, $R_f = 0.4$; TLC, 4:1:1, 1-butanol:acetic acid:water, $R_f = 0.45$; TLC lit. (72,80), 4:1:1, $R_f = 0.5$). Product was used without further purification.

II B-5. Synthesis of N-Acety-L-Proline-L-Alanine-L-Proline-L-Phenylalanine Amide.

N-ac-Pro-Ala-Pro-Phe-NH₂ was synthesized by coupling N-ac-Pro to Ala-Pro-Phe-OMe·HCl and then amidating the peptide as in sections II B-2 and II B-1, respectively.

N-ac-Pro (2.2 g, 0.041 moles) from the synthesis in section II B-3, NMM (1.57 ml, 0.014 moles) and isobutyl chloroformate (1.75 g, 0.0132 moles) were dissolved in 50 ml DMF at -15°C as described in the coupling procedure in section II B-2. Ala-Pro-Phe-OMe·HCl (3.06 g, 0.008 moles) and NMM (0.9 ml, 0.008 moles) in 50 ml DMF at -15°C was added after 5 minutes with stirring and allowed to proceed overnight. The following day excess mixed anhydride was hydrolyzed by the addition of 5 ml of saturated NaHCO₃ (118) at 0°C with stirring for one half hour. The solvent was then rotary evaporated under vacuum to give an oily residue. The residue was dissolved in 250 ml CH₂Cl₂ and 30 ml 4% NaHCO₃. The solution was then washed with an additional 30 ml aliquot of cold 4% NaHCO₃, followed by two 30 ml aliquots of cold 0.1N HCl, and cold brine. Each aqueous wash was in turn washed with three 50 ml aliquots of CH₂Cl₂ which were returned to the original solution after every wash. The CH₂Cl₂ was then rotary evaporated and the hygroscopic residue (TLC R_f = 0.45) was amidated in 100 ml of MeOH as described in section II B-1. After 3 days the MeOH was rotary evaporated under vacuum and the hygroscopic residue from the amidation step was triturated in ethyl-ether to give approximately 1.5 g of ninhydrin negative hygroscopic solid (0.003 moles, 37% yield). (m.p. 76-78°C TLC, 9:1, CHCl₃:MeOH, R_f = 0.36: TLC, 4:1:1, 1-butanol:acetic acid: water, R_f = 0.5 TLC lit (72,80), 4:1:1, R_f

= 0.5). Product was used without further purification.

II B-6. Synthesis of N-Formyl-L-Phenylalanine-Amide.

N-formyl-Phe-NH₂ was prepared by formylation of Phe-NH₂·HCl by the procedure of Sheehan and Yang (120). Phenylalanine (1.0 g, 0.006 moles) was first esterified, the product crystallized, and then amidated by the procedures as described in section II B-1. After rotary evaporation of the MeOH the resulting solids (TLC R_f = 0.35) of Phe-NH₂·HCl were dissolved in 12.6 ml of 98% formic acid at 5°C with stirring, triethylamine (8.3 ml, 0.006 moles) was added following by acetic anhydride (4.2 ml, 0.045 moles) over a 1 hour period, after which the temperature was allowed to go to room temperature. After an additional hour, TLC indicated that all starting material had reacted to product, N-formyl-Phe-NH₂ (TLC R_f = 0.55), ninhydrin negative. Ice water (6 g) was then added to kill the reaction. The solvents were evaporated and the product crystallized from water-ethanol. Overall yield was 67% of N-formyl-Phe-NH₂ (0.75 g, 0.004 moles, m.p. 159-161°C, TLC R_f = 0.55). Elemental analysis was performed by Galbraith Laboratories, Inc. N-formyl-L-phenylalanine-NH₂ theoretical calculation: C, 62.5; H, 6.25; N, 14.58; found C, 62.36; H, 6.34; N, 14.42. Product was used without further purification.

II B-7. Synthesis of O-Acetoxy-L-Phenyllactic-Amide.

Phenyllactic acid was first prepared from L-Phe by the method of Dakin and Dudley (121). Silver nitrite was first prepared by standard procedure. A warm concentrated aqueous solution of KNO_2 (5 g, 0.055 moles) was added with stirring to a warm concentrated solution of AgNO_3 (8 g, 0.047 moles), the solution was then cooled to 0°C and the yellow crystal precipitate was collected and washed with water. The entire amount of wet AgNO_2 was then added over a one hour period with stirring to a solution of L-Phe (4.0 g, 0.024 moles) in 104 ml of 0.5N HCl (0.052 moles) at 0°C . The reaction was allowed to proceed overnight, coming slowly to room temperature. The solution was then filtered and the solution extracted 9 times with 100 ml aliquots of ethyl ether. The ethyl ether solution was then rotary evaporated under vacuum to dryness, re-dissolved in 200 ml anhydrous ethyl ether, dried with MgSO_4 , filtered and the volume reduced leading to product. The L-phenyllactic acid was recrystallized from CCl_4 -ethanol (1.4 g, 0.0084 moles, 35.1% yield, m.p. $117-119^\circ\text{C}$, m.p. lit. (121) $123-125^\circ\text{C}$, TLC $R_f = 0.5$)

L-Phenyllactic acid (1.4 g, 0.0084 moles) was then esterified in 50 ml MeOH as described in section II B-1 (TLC $R_f = 0.98$) and amidated (TLC $R_f = 0.55$). After rotary evaporation of the MeOH the residue was dissolved in 50 ml of ethyl acetate to be O-acetylated by the procedure of Ingles and Knowles (122). Pyridine (0.68 ml, 0.0085 moles) was added at room temperature with stirring followed by acetic anhydride (0.79 ml, 0.0084 moles). The round bottom was fitted with a reflux condensor and the solution heated to 40°C . TLC indicated that no product was being formed so an additional equivalent of acetic anhydride was added after

90 minutes and the heating increased. After 3 hours of additional refluxing TLC indicated the acetylation had taken place. (TLC R_f = 0.85). The acetic anhydride was then rotary evaporated, the residue dissolved in 50 ml ethyl acetate and washed three times with cold 0.001N HCl, 4% NaHCO₃, and brine. The ethyl acetate was dried with MgSO₄, filtered and evaporated yielding 0.6 g of material.

Repeated attempts to crystallize the product were unsuccessful. Purification was done on a large prepacked silica gel column purchased from Quantum Industries. The column was first washed with 250 ml of absolute thanol, followed by 250 ml of CHCl₃ and was dried overnight under a stream of filtered, dried compressed air. The column was then wet with 250 ml of 97:3, CHCl₃:MeOH and the residue from the acetoxy-L-phenyllactic-NH₂ synthesis was layered on in 1.5 ml of 97:3. The 1.5 ml was forced onto the column under 20 p.s.i. of dry N₂ and was then chased by 450 ml of 97:3 under 20 p.s.i. N₂ giving a flow rate of approximately 4 ml per minute. The first 250 ml was collected in bulk and the remaining solution was collected in 8 ml fractions by an Isco Model 273 fraction collector. Product was found by spotting solution from the fractions on TLC. Tubes 13 through 22 yield 0.2 g of O-acetoxy-phenyllactic-NH₂ (0.001 moles, 12% yield, TLC R_f = 0.85, 97:3 CHCl₃:MeOH). However, crystallization still could not be accomplished. Elemental analysis calculated:C, 63.77; H, 6.28; N, 6.76; found: C, 63.43; H, 6.60; N, 6.53. The compound was used without further purification.

II B-8. Synthesis of L-(-)- keto-3-carboamide tetrahydroisoquinoline
(L-(-)-KCAQ).

L-(-)-KCAQ was synthesized by the method of Cohen and Schultz (123) with modifications resulting in a doubling of product. After the cyclization step the ester product is hydrolyzed to the acid and is worked up with the acid and MeOH-HCl is used for esterification instead of thionyl chloride.

Phe-OMe·HCl (7.56 g, 0.035 moles) was prepared as described in section II B-1, was dissolved in 57.33 ml of a 12.5% COCl₂ (phosgene) in benzene solution (0.07 moles) followed by 5.8 ml of dry pyridine (0.072 moles) which was added slowly with initial cooling and stirring. The reaction was stirred at room temperature for three hours, at the end of which a stream of dry nitrogen was passed through the solution for one hour to remove any excess phosgene. The pyridine hydrochloride precipitate was then filtered from the solution and the benzene rotary evaporated, resulting in an orange oil, 6.18 g. This intermediate was then dissolved in 10 ml dry CS₂ and added slowly over a half hour to a refluxing suspension of 10.27 g AlCl₃ (0.07 moles) in 40 ml dry CS₂. Refluxing was continued for an additional 2½ hours. The solvent was then blown off under N₂ (gas) at room temperature and 50 g of an ice-water slurry was added slowly. This was followed by 3 ml of concentrated HCl (0.035 moles) and a trace of ether. The mixture was filtered and the solution extracted five times with ethyl ether, the ether was dried with MgSO₄, filtered, and evaporated leading to an orange oil consisting of some acid but mostly ester of the cyclized product.

This crude product was then dissolved in 100 ml of a 1:1, MeOH: 0.2N NaOH solution at room temperature and stirred for 1 hour. TLC in 9:1 showed disappearance of ester spot at $R_f = 0.8$ and strengthening of acid spot at $R_f = 0.1$. The solution was brought to pH 7.0, with 1N HCl MeOH evaporated, and the solution extracted three times with ethyl-ether to remove any ether soluble impurities. The aqueous phase was then acidified to pH 1.5 where large amounts of acid crystallized immediately. This was filtered off and dried, yielding 2.5 g of acid (0.015 moles, 42% yield, m.p. 200-202°C, m.p. lit. (123) 240-242°C).

The entire amount of material was then reesterified in MeOH-HCl and then amidated as described in section II B-1. After rotary evaporating the MeOH under vacuum 0.5 g of L-(-)-KCAQ was recrystallized from boiling water. (0.35 g, 0.0011 moles, m.p. 216-218°C, TLC $R_f = 0.4$). Elemental analysis calculated: C, 63.32; H, 5.26; N, 14.74; found: C, 62.95; H, 5.26; N, 14.74. Compound was used without further purification.

II B-9. Synthesis of L-(+)-3-Carboamide-3,4-Dihydroisocoumarin(CADIC).

CADIC was synthesized by the method of Cohen and Schultz (123). L-phenyllactic acid was prepared as described in section II B-7.

The intermediate, O-hydroxymethylphenyllactic acid was then synthesized by adding to a stirring suspension of 1.0 g L-phenyllactic acid at 0°C in 10 ml dry CS₂, 0.8 ml of chloromethyl methyl ether (0.01 moles) and 0.7 ml stannic chloride (0.006 moles) in 5 ml dry CS₂ over a one hour period. The mixture was stirred for two hours at room temperature, an orange solid precipitating. The solvent was decanted, ice water added, and the solution stirred vigorously leading to a white solid, O-hydroxy-methylphenyllactic acid. This was recrystallized from ethyl ether after addition of two drops of water and being placed in the freezer for three days (m.p. 69-71°C, m.p. lit. (123) 70-72°C).

To a solution of 0.215 g (0.0011 moles) of this product in 10 ml acetic acid, 0.43 g of CrO₃ in 5 ml 80% acetic acid was added over a 5 minute period. The solution was stirred for an additional hour at room temperature, then 20 ml water was added, the solution extracted four times with CHCl₃, the CHCl₃ dried and concentrated, leading to an oil which, on scratching with CHCl₃-hexanes and cooling, led to a solid, 0.08 g of cyclized acid.

The p-nitrophenyl ester of the isocoumarin was prepared by standard procedure. Cyclized acid (0.2 g, 0.001 moles) was dissolved in 6 ml of 2:1, acetonitrile:tetrahydrofuran along with 0.174 g, 0.0013 moles p-nitrophenol. After several minutes, 0.18 g (0.0012 moles) of DCC (dicyclohexyldiimide) in 1.5 ml acetonitrile was added at 0°C with

stirring. White crystals of DCU (dicyclohexylurea) began to precipitate immediately and the mixture was stirred in the cold room at 5°C for two hours. Then two drops of acetic acid were added and stirring continued for one hour. The solution was then filtered and concentrated, recrystallization from CHCl_3 -hexanes yielded product L-(+)-3,4-dihydroisocoumarin-3-carboxylate p-nitrophenyl ester. (0.16 g, 0.0005 moles, m.p. 190-192°C, m.p. lit. (123) 180-182°C).

Amidation of the ester was done by dissolving the ester in CHCl_3 at 0°C. Anhydrous NH_3 was then passed through the solution for 45 seconds and a yellowish precipitate formed immediately (p-nitrophenol). The mixture was stirred for 4 minutes, NH_3 again passed through for 45 seconds, the solution stirred for 3 additional minutes and the solvent immediately evaporated on a rotary evaporator. TLC indicated formation of amide at $R_f = 0.8$. The resulting material was then washed with ether three times, the ether dried, and evaporated. Attempts were then made to crystallize from ethyl acetate-hexanes. Crystallizations failed and product was finally purified on the silica gel column as described in section II B-7, using a solvent of 49:1, CHCl_3 :MeOH, yield was 0.011 g (5.6×10^{-5} moles, m.p. 183-184°C, TLC $R_f = 0.8$). Elemental analysis calculated: C, 62.82; H, 4.74; N, 7.33; found: C, 62.68; H, 4.75; N, 7.09. Compound was used without further purification.

TABLE 3

SELECTED PHYSICAL CONSTANTS FOR SYNTHESIZED COMPOUNDS

COMPOUND	MOL. WT. ^a	M.P. °C ^b	Lit. ^c M.P. °C	R _f	TLC ^d SOLVENT
IIB 1. Ac-Phe-NH ₂	206.24	179-181	176-177	0.55	e
IIB 2. Ac-Phe-Gly-NH ₂	273.26	182-184	183-184	0.7	f
IIB 3. Ac-Pro-Phe-NH ₂	303.36	178-179	178-179	0.4	e
IIB 4. Ac-Ala-Pro-Phe-NH ₂	374.43	100-102	100-102	0.4	e
				0.45	g
IIB 5. Ac-Pro-Ala-Pro-Phe-NH ₂	471.55	76- 78		0.36	e
				0.5	g
IIB 6. N-formyl-Phe-NH ₂	192.19	159-161	i	0.59	e
IIB 7. O-acetoxy-Phenyllactic-NH ₂	207.19	j	i	0.85	h
IIB 8. L-(-)-KCAO	189.2	216-218	i	0.4	e
IIB 9. CADIC	190.2	183-184	i	0.8	e

^a Molecular weight.

^b Melting points for these syntheses.

^c As described in the text.

^d Thin layer chromatography.

^e 9:1, CHCl₃:MeOH, solvent system.

^f 4:1, CHCl₃:MeOH, solvent system.

^g 4:1:1, 1-butanol:acetic acid:water, solvent system.

^h 97:3, CHCl₃:MeOH, solvent system.

ⁱ Elemental analysis performed. See text.

^j Used as oil as described in text.

II C. Synthesis of Nonapeptide Active Site Analog.

Synthesis of the cyclic nonapeptide:

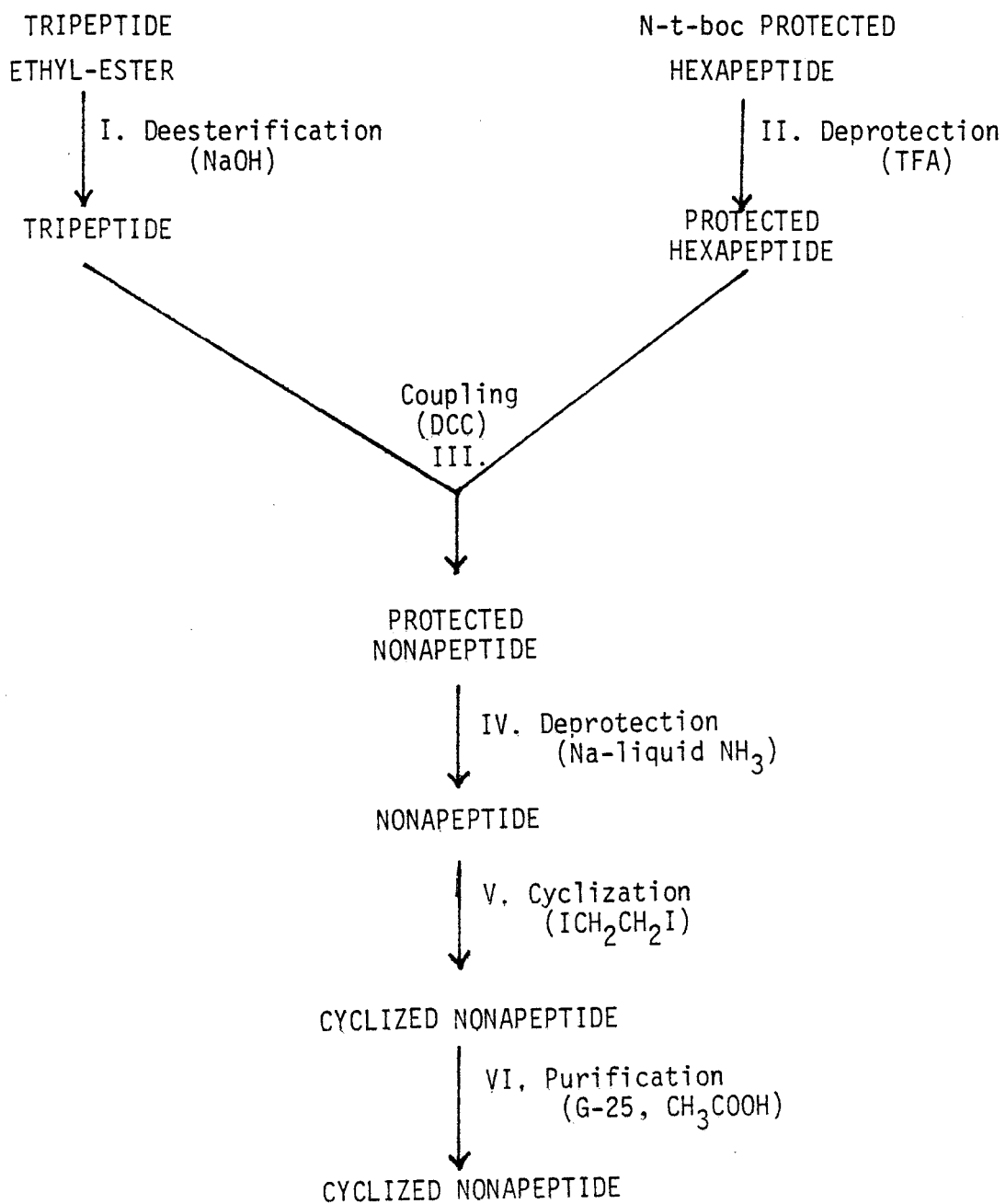
Ac-His-Phe-Gly-Cys-D-Phe-Ser-Gly-Glu-Cys-NH₂ was carried out by coupling the tripeptide Ac-His (N-im-Bzl) -Phe-Gly with the hexapeptide Cys (S-Bzl)-D-Phe-Ser(O-Bzl)-Gly-Glu(O-Bzl)-Cys(S-Bzl)-NH₂. The tripeptide ethyl ester and N-t-boc protected hexapeptide were obtained from Dr. Richard M. Schultz. Syntheses of both compounds were confirmed by elemental analysis. The hexapeptide synthesis was also confirmed by amino acid analysis. The synthetic scheme for coupling and purification of the nonapeptide is shown in figure 6.

II C-1. Removal of Ethyl Ester Group from Tripeptide.

The ethyl ester group was hydrolyzed from the tripeptide (Ac-His (N-im-Bzl)-Phe-GlyOEt) by standard procedure (124). Tripeptide ethyl ester (0.4 g, 7.4×10^{-4} moles, TLC 9:1, CHCl₃:MeOH R_f = 0.7, TLC 4:1:1, 1-butanol:acetic acid:water R_f = 0.6) pure by TLC was added to 80 ml of 3:2, MeOH:0.1N NaOH at 0°C with stirring, was brought to 5°C and allowed to proceed. TLCs in 9:1, CHCl₃:MeOH of the solution during the hydrolysis showed a gradual disappearance of the reactant at R_f = 0.7 and appearance of the product at R_f = 0.1. After 2½ hours the reaction was stopped by adjusting the pH to 4.5 and rotary evaporating the solution under vacuum. The solid residue was then taken up in 150 ml of warm 95% ethanol, the volume reduced to 30 ml, and the flask placed in the refrigerator for 3 days. Crystalline product (0.28 g, 5.7×10^{-4} moles, 77% yield, m.p. 229-231°C, TLC R_f = 0.1). TLC sensitivity was increased by Cl₂ o-tolidine (125).

LEGEND

Figure 6. Synthetic Scheme for Nonapeptide



II C-2. Removal of t-Boc Protecting Group from Hexapeptide.

T-boc-hexapeptide was first recrystallized from hot ethanol. The protected hexapeptide (0.30 g, 2.72×10^{-4} moles) was then placed in a round bottom flask, 3 ml of TFA (trifluoroacetic acid) was added for removal of the t-boc protecting group (126) and 0.2 ml of anisole as a scavenger (124). The solution was stirred for 30 minutes at room temperature. TLC in 9:1, CHCl_3 :MeOH of starting material and after 30 minutes showed the disappearance of the ninhydrin negative spot at $R_f = 0.7$ and appearance of ninhydrin positive spot at $R_f = 0.3$ with time. The TFA was rotary evaporated under vacuum, the peptide precipitated with ethyl ether and the solution placed in the freezer for 30 minutes. The precipitate was then filtered and placed in a dessicator overnight.

II C-3. Coupling of Tripeptide and Hexapeptide.

Tripeptide (0.147 g, 3×10^{-4} moles) was dissolved in 5 ml DMF in a 50 ml round bottom flask followed by 0.063 g (4.9×10^{-4} moles) of 1-hydroxybenzotriazole (124). The flask was placed in a CCl_4 -dry ice bath at -15°C . After 10 minutes 0.067 g (3.25×10^{-4}) DCC was added with stirring and the solution was allowed to activate for 30 minutes. Hexapeptide (0.3 g, 2.72×10^{-4} moles) was dissolved in a second flask containing 5 ml DMF. NMM (0.031 ml, 2.8×10^{-4} moles) was added to the hexapeptide solution and the solution cooled to -15°C . After 30 minutes activation time the hexapeptide solution was added to the tripeptide solution with stirring. Cooling was continued for an additional 2 hours and then the reaction was allowed to proceed overnight at room temperature with stirring (total time of reaction approximately

18 hours). TLC of reactants in 9:1, CHCl_3 :MeOH gave tripeptide $R_f = 0.10$ and hexapeptide $R_f = 0.3$ ninhydrin positive. TLC of reaction showed disappearance of hexapeptide with time and appearance of spot at $R_f = 0.7$ with time.

The following day 0.5 ml of acetic acid was added to decompose excess DCC and the solution was filtered after 5 minutes to remove DCU (dicyclohexylurea). The DMF was rotary evaporated under vacuum with an acetone-dry ice trap. The residue was redissolved in 4 ml of DMF and DCU was again filtered off. The DMF was again rotary evaporated off and the solid residue rinsed from the flask onto a scintered glass filter with 5% NaHCO_3 . The solid was then washed with 50 ml 5% NaHCO_3 , 25 ml distilled deionized water, 50 ml 10^{-5}N HCl, 50 ml distilled deionized water and 50 ml ethyl ether. Total crude product was 0.346 g. TLC in 4:1:1, 1-butanol, acetic acid, H_2O showed 2 spots $R_f = 0.95$ (DCU) and $R_f = 0.7$ (nonapeptide). Melting point of crude product was 209-212°C. Product was left in vacuum dessicator overnight. Trituration with hot ethanol the following day yielded 0.25 g of product, m.p. 229-233°C. A second trituration on the following day yielded 0.236 g (1.6×10^{-4} moles, 57% yield) of protected nonapeptide, m.p. 231-234°C. which was pure by TLC and was placed in a vacuum dessicator overnight under high vacuum over CaSO_4 for the deprotection step.

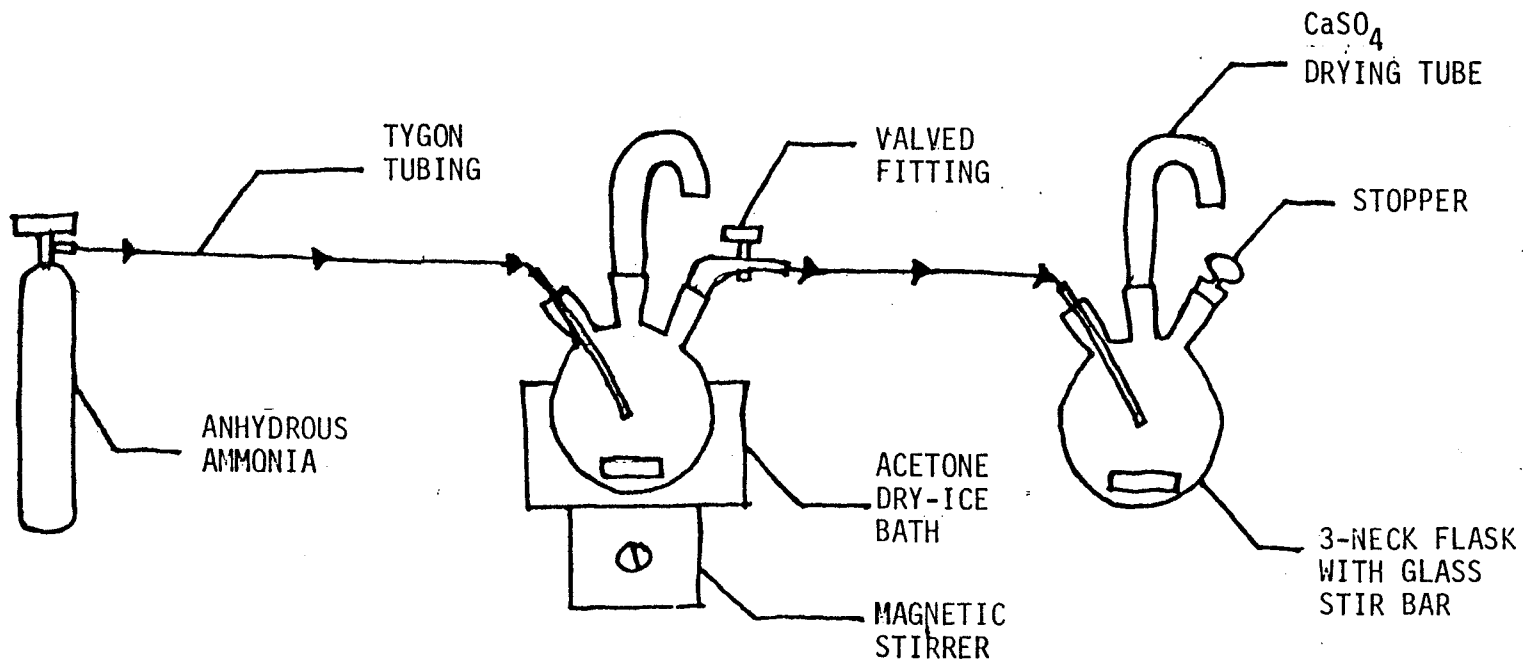
II C-4. Deprotection of Nonapeptide Amino Acid Side Chains by Sodium
Liquid Ammonia Reduction.

The 5 benzyl (Bzl) protecting groups were removed from the nonapeptide by the sodium-liquid ammonia reduction method (124,127). A 200 ml 3-neck round bottom flask was fitted with a glass magnetic stir bar, an inlet port for the NH_3 , a CaSO_4 drying tube, and a valved fitting with Tygon tubing leading to a second 200 ml 3-neck flask. The second flask was fitted with a glass magnetic stir bar, an inlet port for distilled NH_3 from the first flask, a CaSO_4 drying tube, and a stopper (see figure 7). The entire setup was flamed prior to the reaction and sealed from atmospheric moisture.

Approximately 100 ml of anhydrous NH_3 (Matheson) was condensed to a liquid in the first flask which had been placed in an acetone-dry ice bath. Freshly cut slivers of metallic Na under toluene were then added to the NH_3 with stirring to maintain a bright blue color for 30 minutes. The acetone-dry ice bath was removed and placed under the second flask, the drying tube was removed and the opening stoppered, and the valve leading to the second flask was opened. The NH_3 was allowed to slowly vaporize and distill over to the second flask where it was again condensed to a liquid. The distillation tube was removed from the second flask and the opening stoppered after all the NH_3 had been distilled. Protected nonapeptide (0.100 g, 6.76×10^{-5} moles) was then added to the liquid ammonia with stirring. Small slivers of freshly cut metallic Na under toluene were then added until a bright blue color could be maintained for 2-3 minutes. NH_4Cl was then added to stop the

LEGEND

Figure 7. Set Up for Sodium-Liquid Ammonia Reduction
of Nonapeptide.



reaction (approximately 20 minutes total time). The acetone-dry ice bath was then removed and the NH_3 allowed to evaporate. Residual NH_3 was then removed under vacuum after which the flask was opened under N_2 .

II C-5. Cyclization of the Nonapeptide.

Cyclization of the nonapeptide was carried out by oxidation with 1,2-diiodoethane (126). A 200 ml solution of 1:1, $\text{MeOH}:\text{H}_2\text{O}$, previously deaerated for 1 hour under N_2 , was added to the nonapeptide (6.76×10^{-5} moles) in the 3-neck flask immediately after the flask was opened under N_2 . An aliquot was taken to perform an Ellman test (128) to follow the cyclization by quantating the disappearance of sulfhydryl groups. A slight excess of $\text{ICH}_2\text{CH}_2\text{I}$ (TRIDOM/FLUKA; 0.021 g, 7.45×10^{-5} moles) was then added to the solution with vigorous stirring under N_2 . After 3 hours the Ellman test indicated total disappearance of sulfhydryl groups, 10 ml of acetic acid were added and the solution rotary evaporated under vacuum to dryness. The residue was redissolved in 50 ml of 30% acetic acid and lyophilized.

II C-6. Purification of Cyclic Nonapeptide.

The nonapeptide was purified on a column (1.5 cm x 95 cm) of Sephadex G-25 superfine (126,129). The lyophilized residue from the cyclization step (II C-5) was eluted in 50% acetic acid at a flow rate of 15 ml/hour. Product detection was done on a LKB recorder and Uvicord II UV Detector type 8303A. Fractions were collected on a Savant fraction collector. The sample was eluted as a peak with a leading hump which should have been polymer. Fractions were taken from the main peak to maximize purity of the product and lyophilized to give 0.027 g of nonapeptide (2.61×10^{-5} moles, 39% yield). Amino acid analysis of 6N HCl hydrolysis gave Gly, 2.00; Glu, 1.00; His, 0.94; Ser, 0.79; Phe, 2.04; Cys 0.66; a performic acid oxidation gave Gly, 1.00; Cys, 0.99. Product was pure by TLC in 4:1:1, 1-butanol:acetic acid:water and was used without further purification.

II D. Physical Techniques for Measuring Thermodynamic and Kinetic Parameters.

II D-1. Model Partition Experiments Between Water and Chloroform.

The partition method employed by Nandi (101) and discussed by Tanford (34) was used to determine the thermodynamic parameters of transfer of solutes from an aqueous buffer solution to CHCl_3 . Partition coefficients for 8 compounds (II B 1,3,4,5,6,7,8,9) synthesized with tritiated phenylalanine were determined over a 35° temperature range between 0.05 M sodium phosphate, 0.1 M sodium chloride, pH 7.8 buffer and nanograde CHCl_3 . Partition coefficients were further determined between a 5% DMSO-buffer solution (V/V) and nanograde CHCl_3 for 4 of these compounds (II B 1,6,7,8) and DMSO.

Solutions of labeled compounds were first made up (see Table 4) by dissolving peptide and nitrogen analog compounds (II B 1,2,3,4,5,6,8) in aqueous buffer and nonlabeled 5% DMSO-aqueous buffer. Oxygen analog compounds (II B 7,9) were dissolved in nanograde CHCl_3 (Mallinckrodt) to minimize hydrolysis. Carbon 14 DMSO was made up as a 5% DMSO-buffer solution directly. After the solutions were prepared, 3 ml each of the CHCl_3 and aqueous solutions (DMSO or no DMSO) were pipetted into 5 pyrex glass vials (15 ml with teflon lined screw caps). The vials were in a horizontal position in a temperature controlled shaker bath (Blue M model 3222A-1) and were shaken for 23 hours at a given temperature, and then allowed to stand in the bath for one hour for good phase separation. Aliquots (0.1 ml) were then taken from each phase in the 5 vials, placed in liquid scintillation vials containing 10 ml of scintillation fluor,

TABLE 4
SPECIFIC ACTIVITY AND CONCENTRATIONS
FOR PARTITION EXPERIMENTS

COMPOUND	Spec. Act. ^a Ci/ <u>M</u>	Conc. ^b x10 ³ <u>M</u>
IIB 1. Ac-Phe-NH ₂	5.56	0.49
IIB 3. Ac-Pro-Phe-NH ₂	2.5	1.0
IIB 4. Ac-Ala-Pro-Phe-NH ₂	2.5	1.0
IIB 5. Ac-Pro-Ala-Pro-Phe-NH ₂	2.5	1.0
IIB 6. N-formyl-Phe-NH ₂	2.5	0.98
IIB 7. O-acetoxy-Phenyllactic-NH ₂	1.8	0.97
IIB 8. L-(-)-KCAQ	3.48	0.65
IIB 9. CADIC	1.14	1.5
10. DMSO ^c	70.9	704.9

^a Specific activity.

^b Concentration for a solution of 3ml of nanograde CHCl₃ and 3ml of 0.05M phosphate, 0.1M NaCl, pH 7.8. Same concentrations were used for experiments using 3ml nanograde CHCl₃ and 3ml 0.05M phosphate, 0.1M NaCl, pH 7.8, 5% DMSO.

^c Experiments with DMSO were done using 5% DMSO directly.

and the activity of the samples determined on a liquid scintillation counter (Beckman model LS-250).

Partition data for each compound was determined over the temperature range of 5° to 40°C at fairly evenly spaced temperatures. Fresh solutions were used at each determination. Temperature of the bath was determined by a total immersion thermometer accurate to $\pm 0.05^\circ\text{C}$. Samples were taken with a 100 μ ($\pm 1\%$) Oxford pipettor or a Dade micro pipet ($\pm 0.3\%$). Scintillation fluor consisted of 100 ml toluene, 20 ml of BBS-3 (detergent), and 0.5 g PPO (all purchased from Beckman). Counts were taken for 20 minutes per vial using a tritium window giving 10,000 counts per sample ($\pm 1\%$ error). Quench corrections for the various solutions (Table 5) were determined by spiking 10 ml of fluor with a given activity and then adding 100 μ of each cold solution to determine percent quench. Activities of the various solutions were then multiplied by the correction factor: 100/percent quench. The oxygen analog compounds (II B 7,9) were further corrected for activity due to hydrolyzed material. Percent hydrolyzed compound was determined by spotting samples of the two partitioned phases on plastic backed silica gel plates with fluorescent indicator (Eastman Chromogram Sheet # 6060), developing the plates in 9:1, CHCl_3 :MeOH, cutting out the spots of compound ($R_f = 0.9$) and hydrolyzed contaminant ($R_f = 0.6$), placing them in scintillation vials with 10 ml of fluor and determining the relative activity on the scintillation counter (Table 6).

TABLE 5
CORRECTION FACTORS FOR QUENCHING

SYSTEM	PHASE	ISOTOPE	CORR. FACTOR ^a
CHCl ₃ -Buffer ^b	CHCl ₃	³ H	1.723 ± 0.049
CHCl ₃ -Buffer ^b	Buffer	³ H	1.027 ± 0.021
CHCl ₃ -Buffer (5% DMSO) ^c	CHCl ₃	³ H	1.708 ± 0.038
CHCl ₃ -Buffer (5% DMSO) ^c	CHCl ₃	¹⁴ C	2.651 ± 0.063
CHCl ₃ -Buffer (5% DMSO) ^c	Buffer (5% DMSO)	³ H	1.035 ± 0.018
CHCl ₃ -Buffer (5% DMSO) _c	Buffer (5% DMSO)	¹⁴ C	1.048 ± 0.012

^a Correction factor = 100/percent quench.

^b 0.05M sodium phosphate, 0.1M sodium chloride, pH 7.8

^c 0.05M sodium phosphate, 0.1M sodium chloride, 5% DMSO, pH 7.8.

TABLE 6

PERCENT COUNTS DUE TO HYDROLYSED COMPOUNDS

COMPOUND	SOL. SYS.	TEMP. °C	% HYDROLYSED	
			BUFFER	CHCl ₃
O-Acetoxy-L-Phenyllactic-Amide (IIB 7)	a	5.9	0	0
		13.1	0	0
		20.1	1.01 ± 0.30	0.04 ± 0.11
		24.6	5.09 ± 0.50	0.23 ± 0.25
		31.45	9.05 ± 0.62	0.85 ± 0.63
		37.45	11.34 ± 0.58	3.55 ± 0.81
" " " " " "	b	5.0	0	0
		12.0	0	0
		19.0	0.85 ± 0.60	0
		25.0	4.75 ± 0.71	0.2 ± 0.09
		31.0	7.95 ± 0.85	0.72 ± 0.21
		37.0	10.5 ± 0.77	3.28 ± 0.63
CADIC (IIB 9)	a	5.9	4.0 ± 0.62	0.1 ± 0.13
		13.1	12.4 ± 0.91	0.3 ± 0.20
		20.1	21.9 ± 0.53	0.8 ± 0.31
		24.8	37.7 ± 0.98	1.1 ± 0.28
		31.75	52.0 ± 1.08	2.5 ± 0.42
		38.3	73.7 ± 1.01	4.0 ± 0.33

^a CHCl₃ / 0.05M sodium phosphate, 0.1M sodium chloride, pH 7.8.

^b CHCl₃ / 0.05M sodium phosphate, 0.1M sodium chloride, 5% DMSO, pH 7.8.

II D-2. Ninhydrin Assay for Hydrolysis Experiments.

Determination of NH_3 and Gly was done by the method of Moore and Stein (130) with one modification. Determination of Gly was done at pH 4.65 as suggested by Blackburn (131) instead of pH 5.5.

Hydrindantin was first made by reducing ninhydrin with ascorbic acid (130). Ninhydrin (80 g, 0.449 moles) was dissolved in 2 liters of water at 90°C with stirring. Ascorbic acid (80 g, 0.454 moles) in 400 ml of water at 40°C was then added to the ninhydrin solution with stirring and the reaction was allowed to proceed for 30 minutes without further heating. Crystals began to precipitate almost immediately. After 30 minutes, the solution was cooled to room temperature for 1 hour under running tap water. The hydrindantin was then filtered off, washed with plenty of water, and dried over P_2O_5 in a vacuum dessicator overnight to yield 73.4 g (0.228 moles, 51% yield, m.p. $251\text{--}252^\circ\text{C}$).

Ninhydrin reagent solution was prepared fresh daily by dissolving ninhydrin (2 g, 0.011 moles) and hydrindantin (0.3 g, 9.3×10^{-4} moles) in 75 ml of methyl cellosolve followed by 25 ml of 4 N sodium acetate buffer (pH 4.65 for NH_3 , pH 5.5 for Gly).

Ninhydrin assay for free amine (NH_3 and Gly) was done by pipetting 0.1 ml of free amine containing solution to 1.0 ml of ninhydrin reagent solution in a 10 ml disposable test tube. The tube was stoppered and placed in a boiling water bath for 20 minutes. The test tube was then removed and cooled to room temperature in a water bath for 10 minutes. The sample was then diluted with 5.3 ml of a 1:1, isopropyl alcohol:water solution. The solution was mixed and the absorbance measured at 570 nm on a Beckman DU spectrophotometer

(model 2400).

Extinction coefficients for NH_3 and Gly (Table 7) were determined by assaying NH_4Cl (ammonium chloride) and free Gly solutions over the concentration range 10^{-4} M to 10^{-3} M.

II D-3. Enzyme Hydrolysis Procedure.

Chymotrypsin (Cht) was further purified on a G-25 (superfine) Sephadex column as suggested by Yapel et al. (111). Enzyme concentration was determined from its UV absorbance at 280 nm in 10^{-3} N HCl (pH 3.0) solution using the molecular absorbtivity coefficient (E) of 5×10^4 absorbance units /M/cm (112).

Enzymatic hydrolysis of substrate was assayed initially at 25°C for each substrate at 4 different concentration with aliquots taken at 5 intermittent times during the course of the reaction. A linear relationship was found in all cases. Six percent or less of total substrate was hydrolyzed during the assay time period. Subsequent assays were done on only 2 points, an initial and final time. Each point in each assay was determined in triplicate by assay of three 0.1 ml aliquots and at least 2 assays were done per substrate per temperature. Assays were done at 4 substrate concentrations ranging from approximately 0.5 Km to 2 times Km.

TABLE 7
EXTINCTION COEFFICIENTS FOR NINHYDRIN ASSAY
OF AMMONIA AND GLYCINE

COMPOUND	pH ^a	E ^b
NH ₃	5.5	1.69 x 10 ⁴
NH ₃	4.65	2.17 x 10 ⁴
Gly	5.5	1.97 x 10 ⁴

^a pH of acetate buffer.

^b Extinction coefficient in absorbance units /M/cm.

II D-4. N-Acetyl-L-Tyrosine Ethyl Ester Activity Assays.

Activity assays for Cht were carried out with ATEE (N-ac-Tyr-OET) according to a modified procedure of Schwert and Takenaka (132). ATEE solution (1×10^{-3} M) was prepared by dissolving 0.0252 g in 100 ml of buffer (0.067 M phosphate, pH 7.0) and storing at 20°C. Decreases in absorbance at 237 nm were measured with time at 25°C between a reference cell and enzyme solution. The reference cell contained 3.0 ml of ATEE solution and 0.1 ml of the same buffer as CHT was dissolved in. A straight baseline between the reference cell and assay cell was obtained after addition of 3.0 ml of ATEE solution to the assay cell. Enzyme solution (0.1 ml, 4×10^{-7} M) was then added and the solution manually mixed. Assays were done on a Cary 15. A difference extinction coefficient of 292/M/cm was determined by total hydrolysis of sample ATEE solutions by CHT.

II D-5. p-Nitrophenyl Acetate Active Site Titrations.

p-Nitrophenyl acetate (pNPA) active site assays were done by a modification of the procedure of Bender et al. (133). Assays were done in 0.067 M phosphate, pH 7.8 buffer on a Cary 15 spectrophotometer at 400 nm. A Cht solution (approximately 2×10^{-5} M) was made up in buffer and 2.9 ml pipetted into a cuvette and a baseline recorded at a slow chart speed. A 0.1 ml aliquot of pNPA (4×10^{-3} M) in acetonitrile was then added and the contents of the cuvette mixed manually. The increase in absorbance with time was then recorded. After steady state conditions were reached, extrapolation back to zero time gave the increase in ab-

sorbance due to the pNPA burst. Concentration was determined by dividing the absorbance by the extinction coefficient (E). The extinction coefficient was determined by measuring the absorbance of stock solutions of p-nitrophenol at pH 7.8. ($\epsilon = 15,066$ absorbance units/M/cm).

II D-6. N-trans-Cinmamoylimidazole Active Site Titrations.

N-trans-cinmamoylimidazole (NCI) active site titrations were performed by the method of Schonbaum et al.(134). A Cht solution (approximately 7×10^{-4} M) was made up in buffer (0.1 M acetate, pH 5.0). Buffer, 3 ml, was placed in a sample cuvette and a straight baseline was then obtained on the Cary 15 at 335 mm against a reference cuvette also containing 3 ml of buffer. A 0.01 ml aliquot of NCI solution (0.01 M in acetonitrile) was then added to the sample cuvette, the solution mixed and the absorbance recorded until a straight line could be extrapolated back to the time of addition (A_2). A 0.01 ml aliquot of enzyme solution was then added, the solution mixed and the absorbance recorded until a straight line could be extrapolated back to the time of enzyme addition (A_3). The normality of the enzyme solution was then calculated from the equation $N = (0.969 A_2 - A_3)/279.9$, where 0.969 is a correction for dilution due to the enzyme addition, and 279.9 is the extinction coefficient for NCI with the dilution due to enzyme taken into account.

II D-7. Sulfhydryl Group Determination.

Determination of free sulfhydryl groups during the cyclization step of the nonapeptide was done by the method of Ellman (128). A 1.5 ml aliquot of solution containing free sulfhydryl groups was combined with 1.0 ml phosphate buffer (0.05 M, pH 8.0) and 2.5 ml of water. A 0.02 ml (1×10^{-2} M) aliquot of DTNB (5,5-dithiobis (2-nitrobenzoic acid)) in phosphate buffer (0.05 M, pH 7.0) was then added. After 2 minutes at room temperature the absorbance was read at 412 nm on a GCA/McPherson Spectrophotometer (model 700).

II D-8. Detection Methods for Thin-Layer Chromatography.

Thin layer chromatography (TLC) using silica gel plates (Q 1) with fluorescent indicator for visualization under UV were purchased from Quantum Industries and used to check organic reactions. Plates were developed in a 9:1 (V/V) chloroform to methanol system unless otherwise noted.

A ninhydrin reagent spray (113) was prepared for visualization of free amines on TLC plates. A 0.2% solution (0.2g/100ml) of ninhydrin in acetone was prepared and lightly sprayed on the chromatogram after excess developing solvent had been blown off. Upon heating development of a red color indicated presence of free amine, a positive reaction.

An iodine (I_2) vapor chamber (125) was used for detection of compounds on TLC plates when the compounds could not be detected under UV or were ninhydrin negative. After excess developing solvent was blown off the chromatogram was placed in a closed container containing crystals of iodine (I_2) for several minutes. The chromatogram was then

removed and excess iodine blown off. Most organic compounds yielded yellow or brown spots.

A more sensitive test for organic compounds is the chlorine-tolidine test(125). Chlorine gas (Cl_2) was evolved in a closed chamber by addition of 10ml of 6N HCl to 10ml of a saturated KMnO_4 solution. Excess developing solvent was blown off the chromatogram and the chromatogram was then placed in the closed chamber for 15-20 minutes. A spray reagent of o-tolidine was prepared by dissolving 0.160g of o-tolidine in 30ml glacial acetic acid, diluting the solution to 500ml with distilled water, and then adding 1.0g of potassium iodide (KI). The chromatogram was removed from the Cl_2 chamber after the 15-20 minutes and excess Cl_2 was blown off for 2-3 minutes or until no Cl_2 could be detected. The chromatogram was then lightly sprayed with tolidine solution. Presence of compound was denoted by appearance of a yellow color.

II D-9. pH Stat Titration of Nonapeptide.

Titration of the nonapeptide was done on a Radiometer pH Stat (model TTT-2) equipped with a 0.25ml burette. Nonapeptide (0.00112g, (1.03×10^{-6}) moles) was dissolved in 5ml of degassed 0.1N NaCl to give a 2.06×10^{-4} M solution. Nonapeptide solution (3.0ml, 6.18×10^{-7} moles) was titrated at 25°C under N_2 with 0.01N NaOH which was standardized against potassium acid phthalate.

II E. Model Partition System and Calculations.

Various model systems have been studied in an attempt to explain both the role and process of substrate binding in enzymatic catalysis (2, 11,34,104). Physical methods employed to characterize the thermodynamics of the transfer process have included surface tension (135); solubility (100), and partition techniques (101). The partition technique of Nandi (101), described in section II D-1, is employed to study the transfer process, since dilute solutions of $10^{-3}M$ could be employed thus sparing substrate and allowing for a simplification of equation 3.5 (vide infra). Since the purpose of the model is to separate the thermodynamics of the nonspecific transfer process from the thermodynamics of the specific enzymatic binding process, an additional requirement of the model is non-specificity in binding. Hence, the differences between the thermodynamic data obtained from the model transfer process and the enzymatic transfer process would be due to the specific interaction between the enzyme and substrate on binding.

Tanford has suggested ethanol with its hydrogen bonding capability and its structure of hydrophilic and hydrophobic areas as a 'good' model for the interior of a protein (136). This close analogy, however, may be a disadvantage of ethanol as our model system due to its ability to be a general hydrogen bond donor which may generate specific interactions with some substrates and not other substrates. The relatively disordered structure of a low dielectric aprotic hydrophobic solvent such as chloroform may better meet the requirements of a nondiscriminate hydrophobic model.

The thermodynamic paraters ΔG_t^0 (standard free energy of trans-

fer), ΔH_t^0 (standard enthalpy of transfer), and ΔS_t^0 (standard entropy of transfer) are calculated in unitary units, which simply means that the solute concentration in the equation for the chemical potential is expressed in mole fraction units (34,82). Calculating the chemical potential in mole fraction units eliminates the statistical contribution to the standard chemical potential (μ^0) due to the entropy of mixing solute and solvent molecules in the dissociation process. Therefore, μ^0 calculated in unitary units, eliminates the mixing contribution and only contains contributions due to internal free energy of the solute molecule and the free energy of its interaction with the solvent. The chemical potential in unitary units for a solute molecule dissolved in water can be calculated from the procedure described by Tanford (34),

$$\mu_w = \mu_w^0 + RT \ln X_w + RT \ln f_w, \quad (2.1)$$

where μ_w is the chemical potential, μ_w^0 is the standard chemical potential, X_w is the concentration of the solute in mole fraction units, and f_w is the activity coefficient at that concentration. The same equation can be written for a solute molecule in an organic solvent (34),

$$\mu_i = \mu_i^0 + RT \ln X_i + RT \ln f_i. \quad (2.2)$$

When the two solvents are interphased and the solute molecules allowed to partition to equilibrium

$$\mu_w = \mu_i, \quad (2.3)$$

so that

$$\mu_i^0 + RT \ln X_i + RT \ln f_i = \mu_w^0 + RT \ln X_w + RT \ln f_w, \quad (2.4)$$

and, after rearranging, we obtain

$$\mu_i^0 - \mu_w^0 = -RT \ln \frac{X_i}{X_w} - RT \ln \frac{f_i}{f_w}. \quad (2.5)$$

At dilute concentrations the activity coefficient approaches one and thus

$$RT \ln \frac{f_i}{f_w} = 0. \quad (2.6)$$

Hence

$$\mu_i^0 - \mu_w^0 = -RT \ln \frac{X_i}{X_w}. \quad (2.7)$$

In other words, the difference in standard chemical potential for the transfer of a solute molecule from water to an organic solvent is equal to the negative product of the gas constant, the temperature in degrees Kelvin, and the natural logarithm of the quotient of the solute concentration in the organic solvent divided by the solute concentration in the water phase expressed in mole fraction units. The difference in standard chemical potential is the change in free energy (ΔG_t^0) for the transfer process in unitary units. The parameter ΔH_t^0 is calculated from the temperature dependence of the partition coefficients (5). The parameter ΔS_t^0 is calculated from the standard thermodynamic relationship (5):

$$\Delta G = \Delta H - T \Delta S. \quad (2.8)$$

Uncertainty in ΔG_t^0 is expressed as the standard error of the mean, uncertainty is ΔH_t^0 in standard error of the slope from a computer assisted least squares analysis, and uncertainty in ΔS_t^0 is calculated from the uncertainty in ΔG_t^0 and ΔH_t^0 .

CHAPTER III

RESULTS

III A. Model Partition Experiments

III A-1. Amino Acid Analogs and DMSO Results.

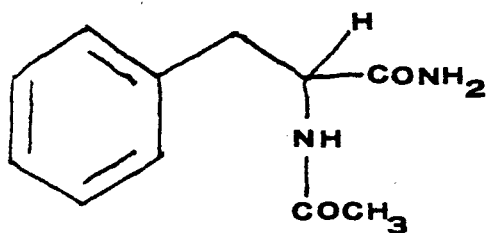
van't Hoff plots for the transfer process from aqueous buffer to CHCl_3 of the natural alpha nitrogen and substituted alpha oxygen amino acid analogs (fig. 8), peptides, and DMSO are presented in figures 9-17. Lines drawn through the data points are those derived from the computer assisted least squares analysis. Partition experiments for N-ac-Phe- NH_2 , N-formyl-Phe- NH_2 , L-(-)-KCAQ, O-acetoxy-L-Phenylactic- NH_2 , and CADIC in aqueous buffer without 5% DMSO were carried out using a $100 \mu\text{l} \pm 0.3\%$ Dade micro pipet and gave more consistent data as determined by statistical analysis than the remaining experiments which were done with an Oxford Sampler pipet, $100 \mu\text{l} \pm 1.0\%$.

Data from the partition experiments between non-DMSO and 5% DMSO aqueous buffer solvent system and CHCl_3 are presented in Tables 8 and 9. If we first look at the non-DMSO buffer partition experiments (Table 8) several trends in the data are evident. In the phenylalanine analog series nitrogen containing analogs have a small positive (unfavorable) ΔG_t^0 for the transfer process from aqueous buffer solution to chloroform. All three analogs have a positive ΔH_t^0 (unfavorable) and positive ΔS_t^0 (favorable) for the transfer process. The unfavorable positive ΔH_t^0 is the major contributor to the free energy term,

LEGEND

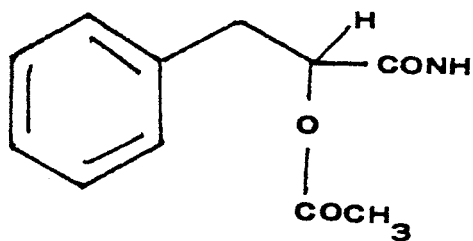
Figure 8. Phenylalanine Analog Series for Model Partition Studies.

IIB-1



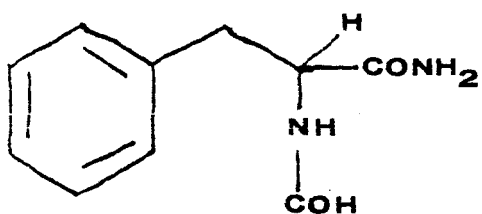
N-acetyl-L-phenylalanine amide

IIB-7



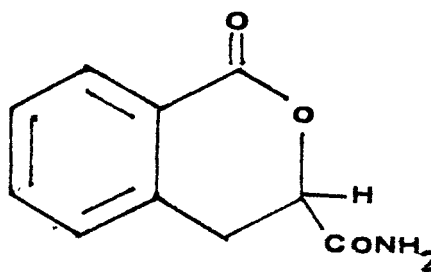
O-acetyl-L-phenyllactic amide

IIB-6



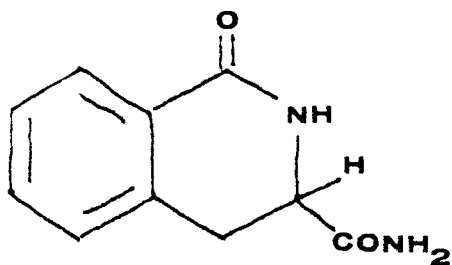
N-formyl-L-phenylalanine amide

IIB-9



D-3-carboamido-3,4-dihydroisocoumarin

IIB-8

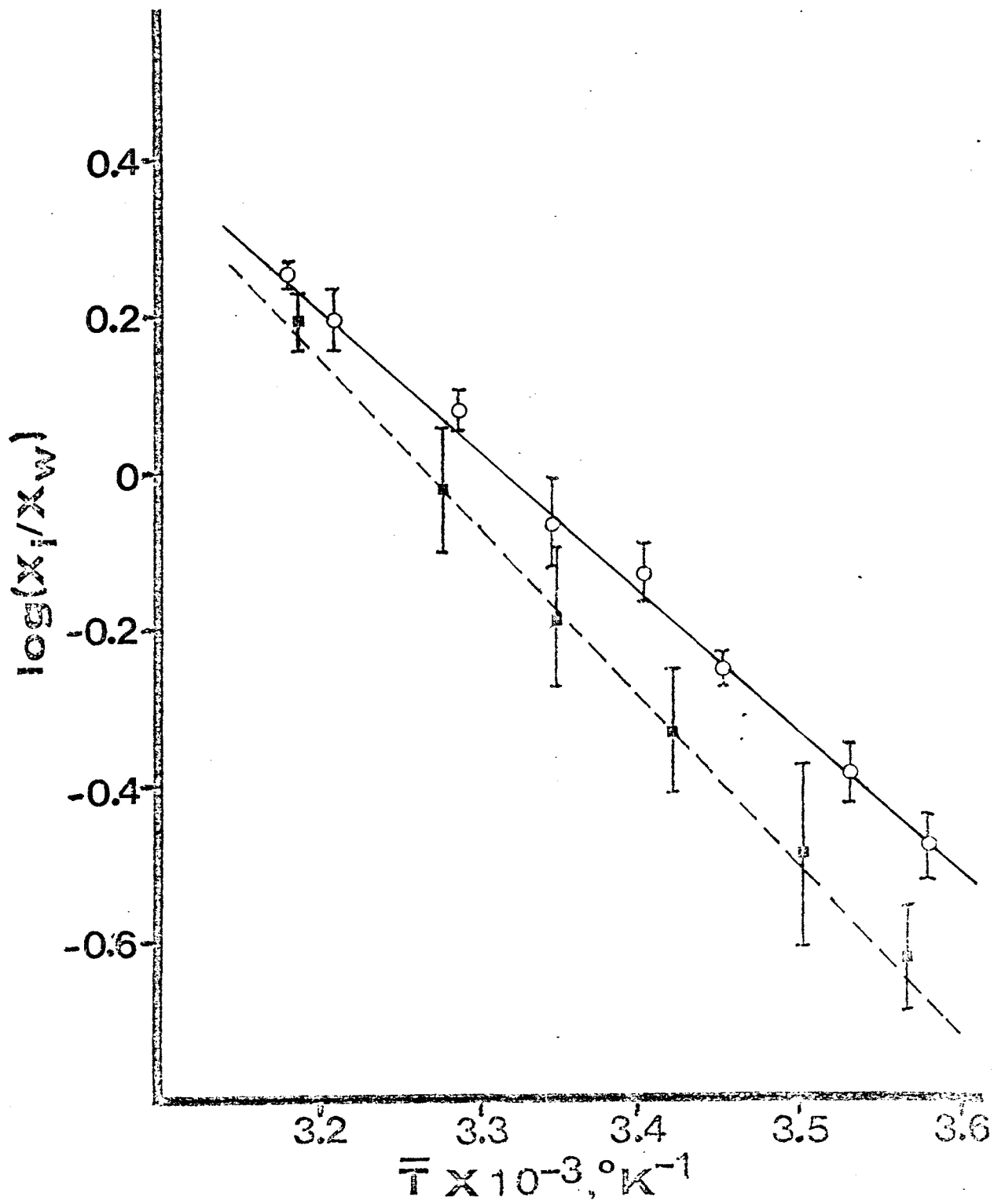


D-3-carboamido-3,4-dihydroisocarbostyryl

LEGEND

Figure 9. van't Hoff Plot of the Temperature Dependence of the Model Partition Studies between Aqueous Buffer and Chloroform N-Acetyl-Phenylalanine Amide.

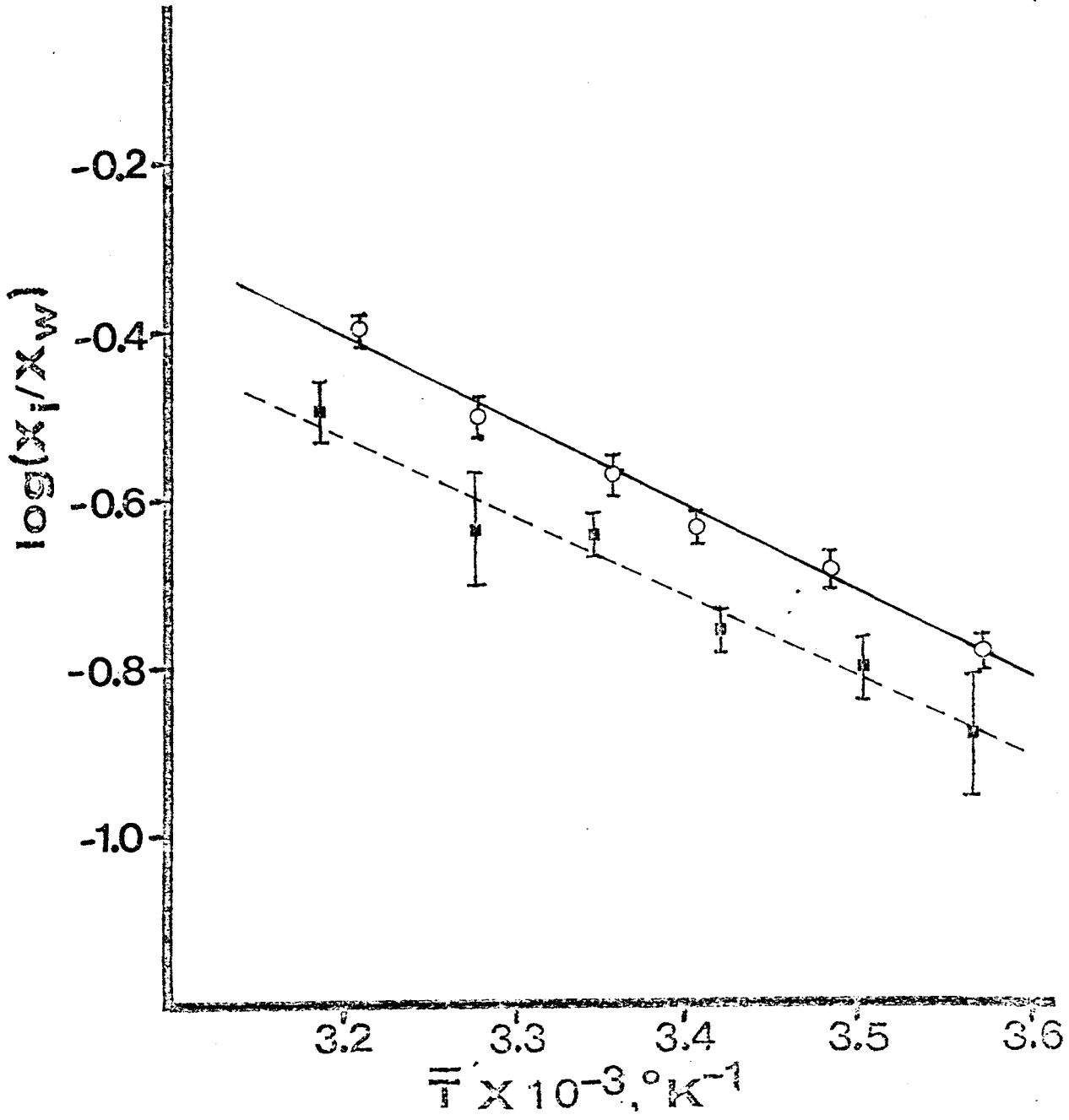
Conditions for partition experiments were: solid line, 0.05M sodium phosphate, 0.1N NaCl, pH 7.8/CHCl₃; broken line, 0.05M sodium phosphate, 0.1N NaCl, 5% DMSO, pH 7.8/CHCl₃.



LEGEND

Figure 10. van't Hoff Plot of the Temperature Dependence of the Model Partition Studies between Aqueous Buffer and Chloroform for N-Formyl-Phenylalanine Amide.

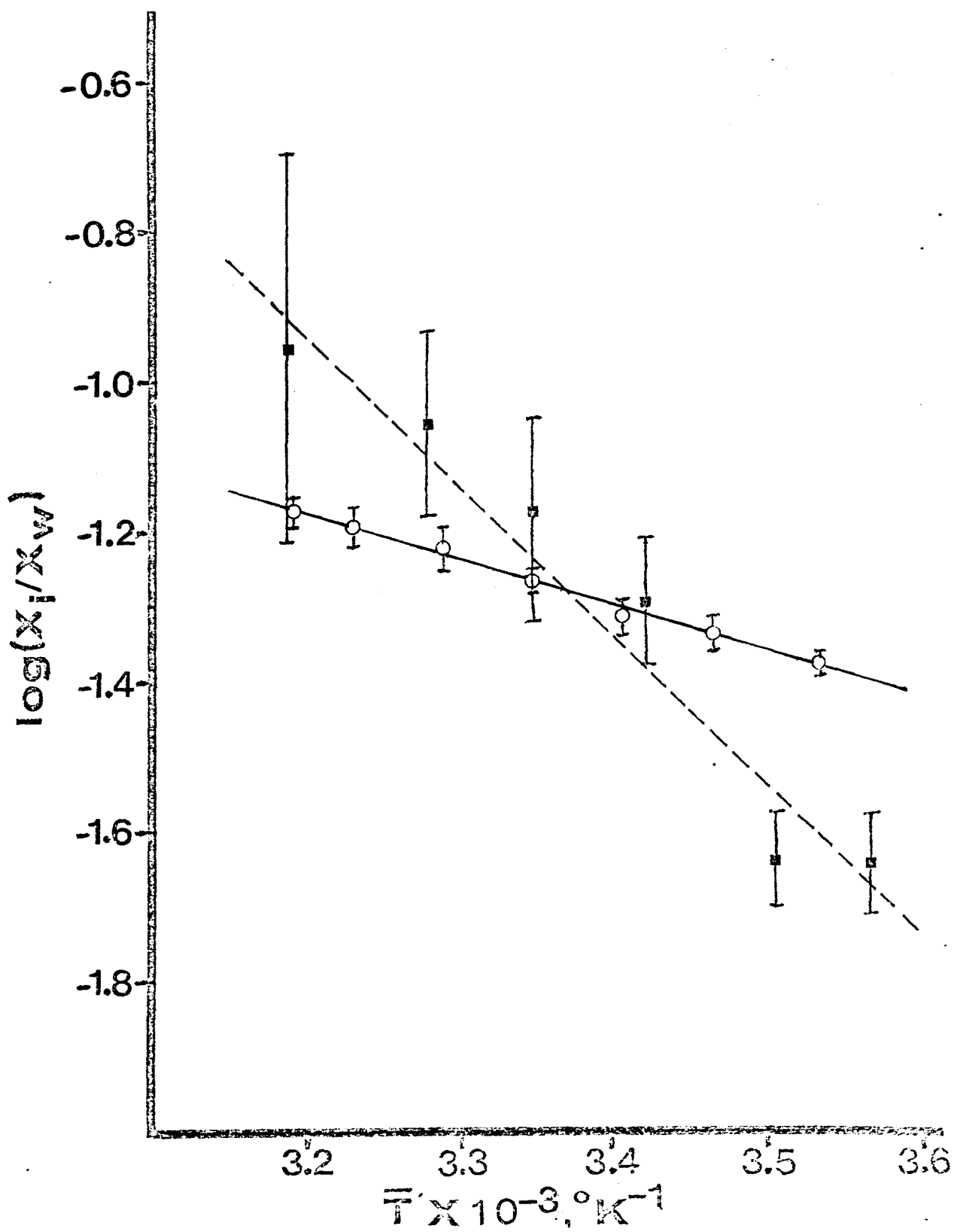
Conditions for partition experiments were: solid line, 0.05M sodium phosphate, 0.1N NaCl, pH 7.8/CHCl₃; broken line, 0.05M sodium phosphate, 0.1N NaCl, 5% DMSO pH 7.8/CHCl₃.



LEGEND

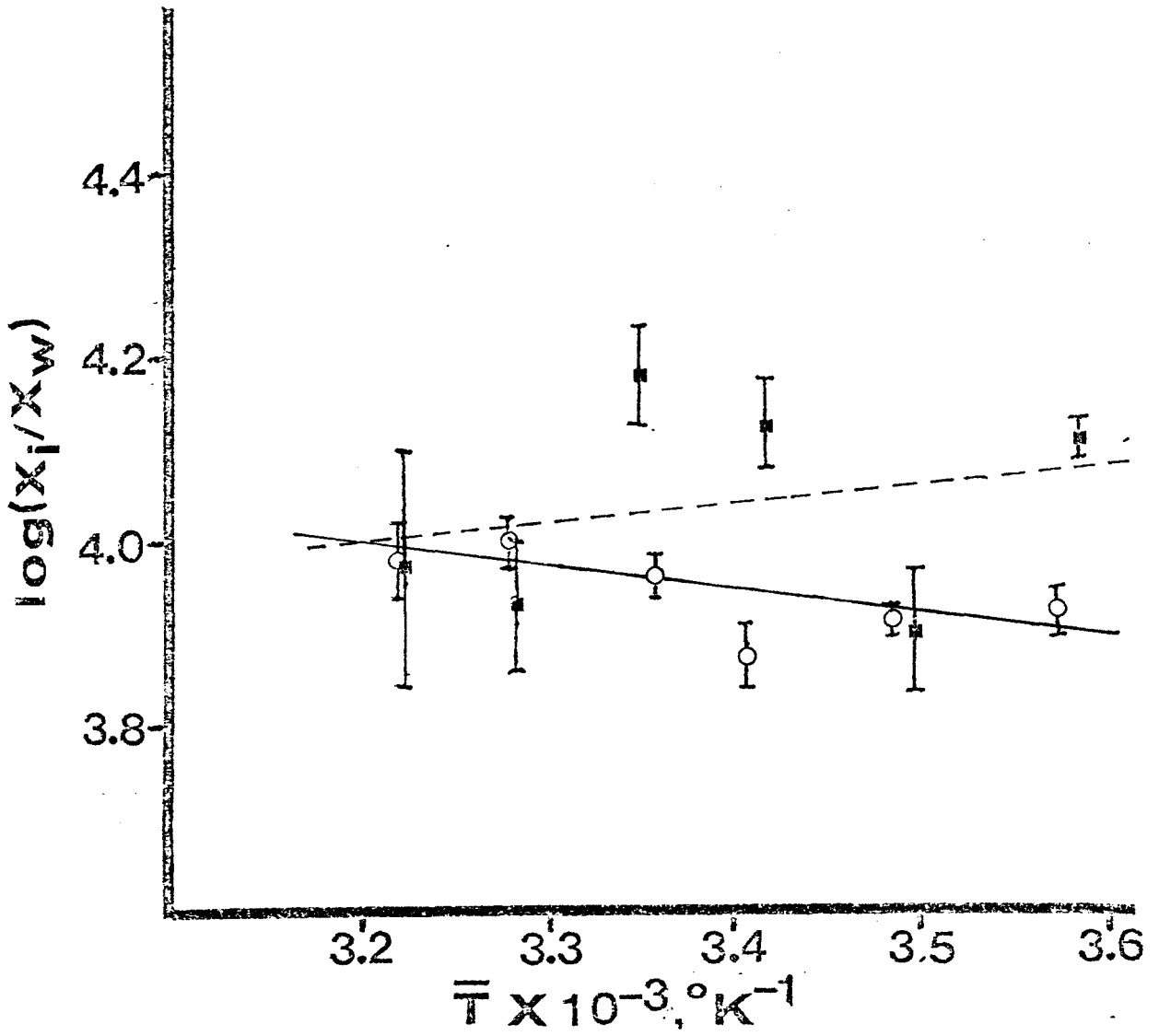
Figure 11. van't Hoff Plot of the Temperature Dependence of the Model Partition Studies between Aqueous Buffer and Chloroform for L-(-)-Keto-3-Carboamide Tetrahydroisoquiniline. (L-(-)-KCAQ).

Conditions for partition experiments were: solid line, 0.05M sodium phosphate, 0.1N NaCl, pH 7.8/CHCl₃; broken line, 0.05M sodium phosphate, 0.1N NaCl, 5% DMSO, pH 7.8/CHCl₃.



LEGEND

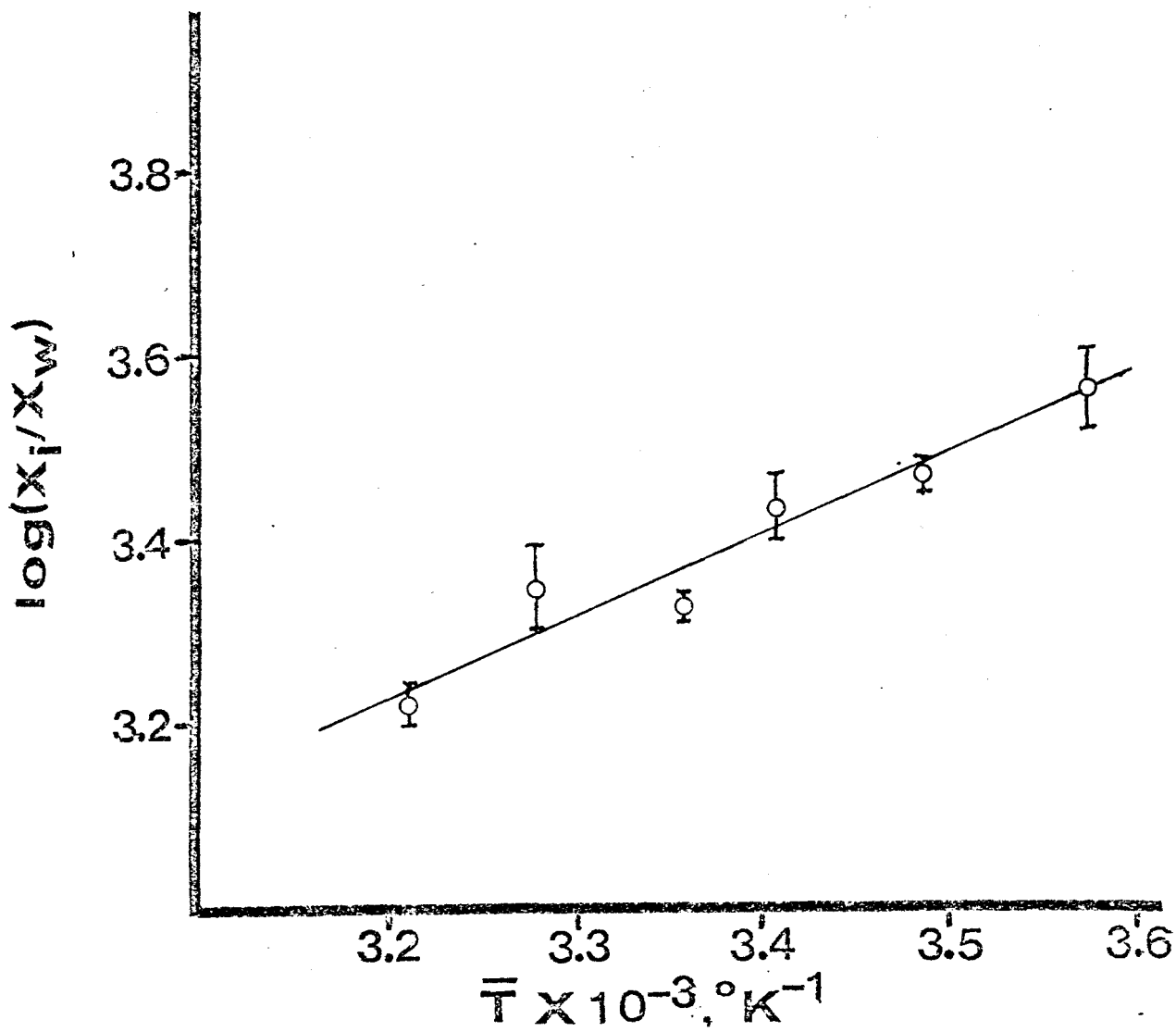
Figure 12. van't Hoff Plot of the Temperature Dependence of the Model Partition Studies between Aqueous Buffer and Chloroform for O-Acetoxy-L-Phenyllactic Amide.
Conditions for partition experiments were: solid line, 0.05M sodium phosphate, 0.1N NaCl, pH 7.8/CHCl₃; broken line, 0.05M sodium phosphate, 0.1N NaCl, 5% DMSO, pH 7.8/CHCl₃.



LEGEND

Figure 13. van't Hoff Plot of the Temperature Dependence of the Model Partition Studies between Aqueous Buffer and Chloroform for L-(+)-3-Carboamide-3,4-Dihydroisocoumarin (CADIC).

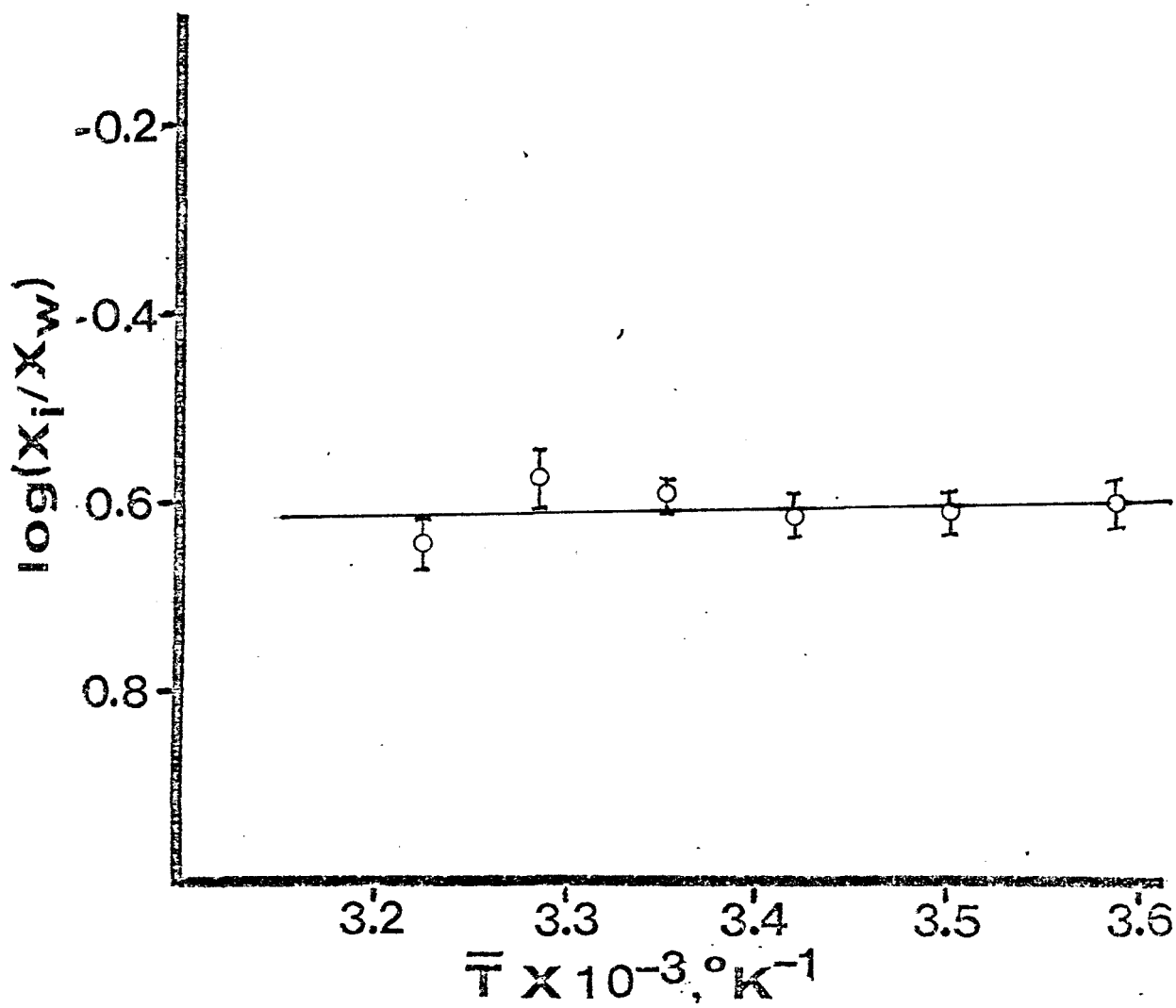
Conditions for partition experiment were: 0.05M sodium phosphate, 0.1N NaCl, pH 7.8/CHCl₃.



LEGEND

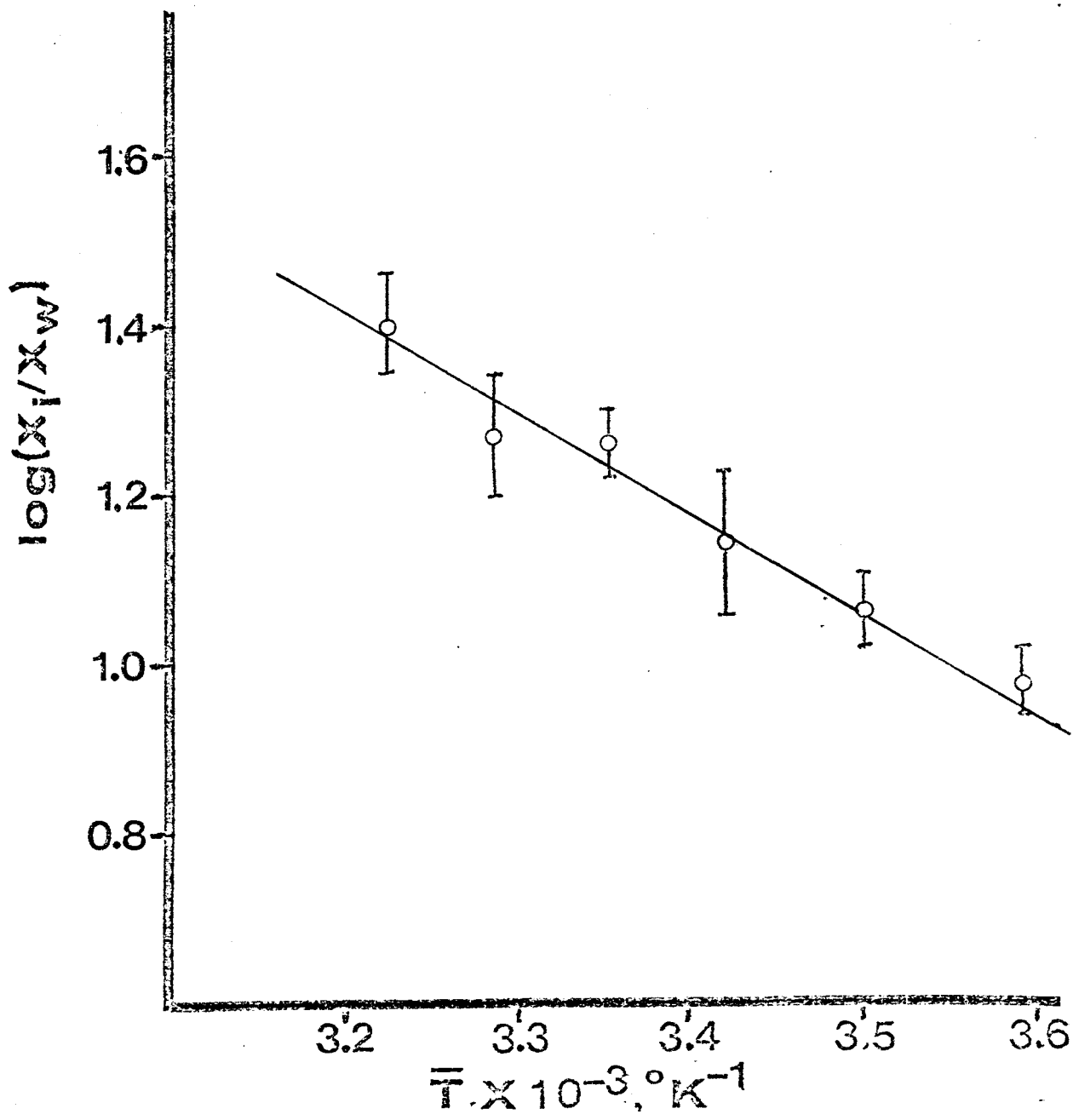
Figure 14. van't Hoff Plot of the Temperature Dependence of the Model Partition Studies between Aqueous Buffer and Chloroform for DMSO.

Conditions for partition experiments were: 0.05M sodium phosphate, 0.1N NaCl, 5% DMSO, pH 7.8/CHCl₃.



LEGEND

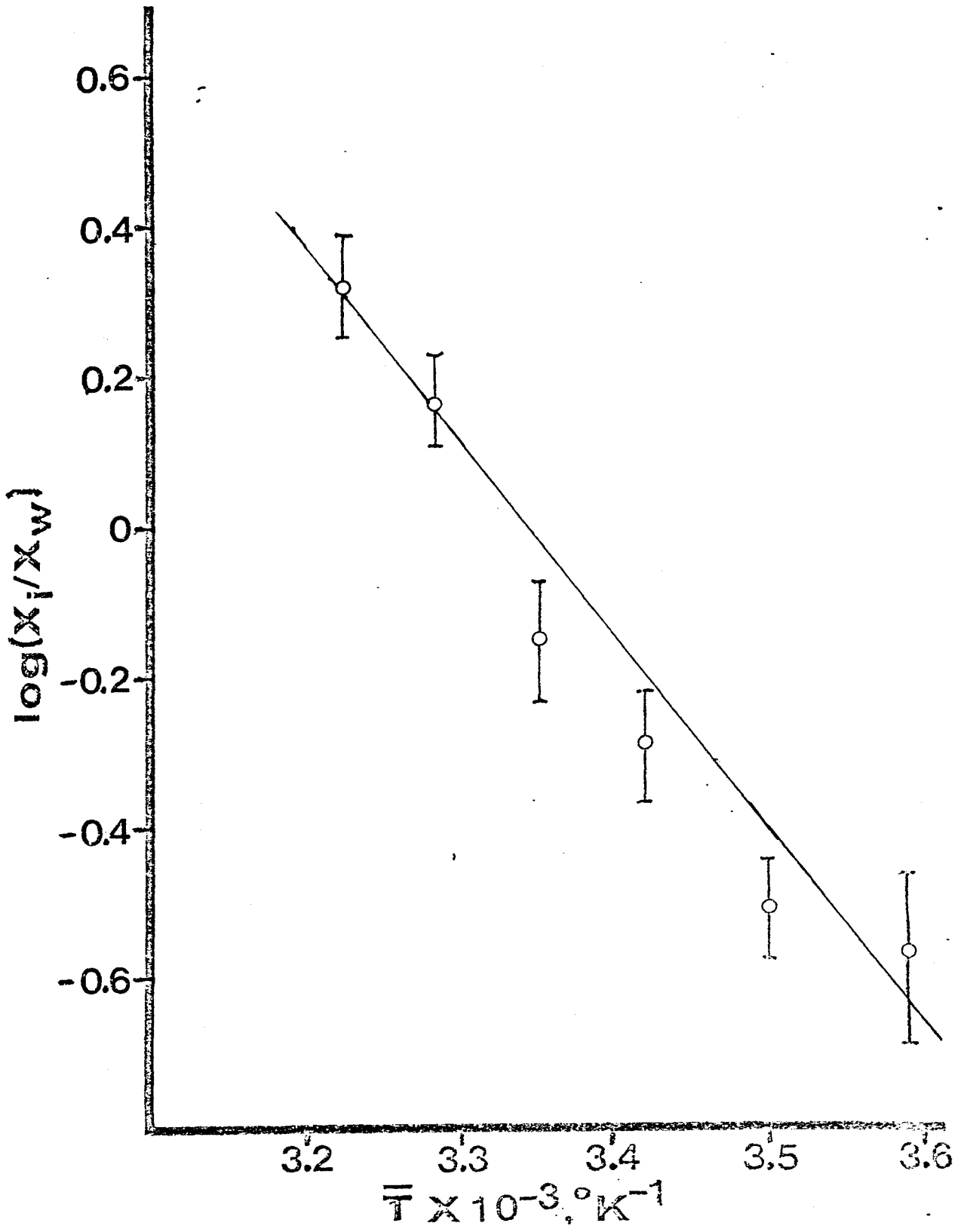
Figure 15. van't Hoff Plot of the Temperature Dependence of the Model Partition Studies between Aqueous Buffer and Chloroform for N-Acetyl-Proline-Phenylalanine Amide.
Conditions for partition experiments were: 0.05M sodium phosphate, 0.1N NaCl, pH 7.8/CHCl₃.



LEGEND

Figure 16. van't Hoff Plot of the Temperature Dependence of the Model Partition Studies between Aqueous Buffer and Chloroform for N-Acetyl-Alanine-Proline-Phenylalanine-Amide.

Conditions for partition experiments were: 0.05M sodium phosphate, 0.1N NaCl, pH 7.8/CHCl₃.



LEGEND

Figure 17. van't Hoff Plot of the Temperature Dependence of the Model Partition Studies between Aqueous Buffer and Chloroform for N-Acetyl-Proline-Alanine-Proline-Phenylalanine-Amide.

Conditions for partition experiments were: 0.05M sodium phosphate, 0.1N NaCl, pH 7.8/CHCl₃.

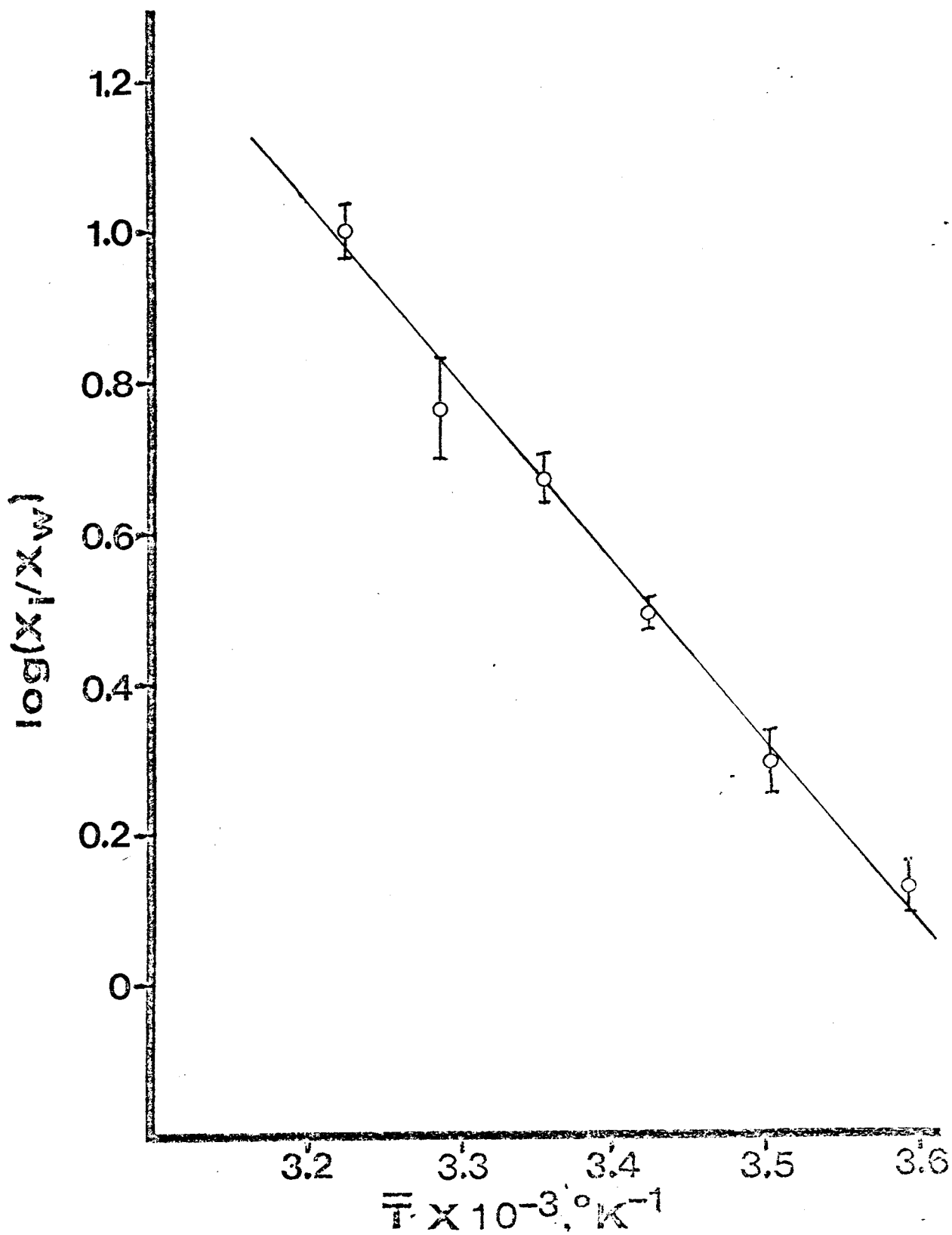


TABLE 8

THERMODYNAMIC PARAMETERS FOR THE TRANSFER PROCESS OF PHENYLALANINE SUBSTRATE

ANALOGS FROM AQUEOUS BUFFER^a TO CHLOROFORM^b AT 25°C

COMPOUND	RATIO OF MOLE FRACTIONS ^c	ΔG_t° cal/mole	ΔH_t° cal/mole	ΔS_t° e.u.
IIB-1, N-ac-Phe-NH ₂	0.94 ±0.05	35±30	3,570± 80	11.8 ±0.4
IIB-6. N-formyl-Phe-NH ₂	0.568±0.015	335±10	2,000±110	5.6 ±0.4
IIB-8. L-(-)-KCAQ	0.283±0.008	750± 5	1,200± 40	1.5 ±0.2
IIB-7. O-acetoxy-L-Phenyllactic NH ₂	52.9 ±0.9	-2,350± 5	500±300	9.6 ±1.0
IIB-9. CADIC	27.9 ±0.3	-1,970± 5	-1,700±200	0.80±0.8

^a 0.05M sodium phosphate, 0.1M NaCl, pH 7.8. Uncertainty expressed as ± standard error of the mean.

^b Ethanol free nanograde chloroform purchased from Mallinckrodt.

^c X_i/X_w where X_i and X_w are the mole fractions of solute in chloroform and aqueous buffer respectively.

TABLE 9

THERMODYNAMIC PARAMETERS FOR THE TRANSFER PROCESS OF PHENYLALANINE SUBSTRATE

ANALOGS FROM AQUEOUS BUFFER^a (5% DMSO) TO CHLOROFORM^b AT 25°C

COMPOUND	RATIO OF MOLE FRACTIONS ^c	ΔG_t° cal/mole	ΔH_t° cal/mole	ΔS_t° e.u.
IIB-1. N-ac-Phe-NH ₂	0.835±0.078	110±25	4,135±115	13.5±0.5
IIB-6. N-formyl-Phe-NH ₂	0.529±0.012	375±10	1,870±155	5.0±0.6
IIB-8. L-(-)-KCAQ	0.313±0.051	695±45	3,885±470	10.7±1.7
IIB-7. O-acetoxy-L-Phenyllactic-NH ₂	65.8 ±3.5	-2,490± 5	-395±835	7.0±2.8
10. DMSO	0.557±0.008	345± 5	55±170	- 1.0±0.6

^a 0.05M sodium phosphate, 0.1M NaCl, pH 7.8, 5% DMSO. Uncertainty expressed as ± standard error of the mean.

^b Ethanol free nanograde chloroform purchased from Mallinckrodt.

^c X_i/X_w where X_i and X_w are the mole fractions of solute in chloroform and aqueous buffer respectively.

overcoming the favorable positive entropy term. In contrast, the two oxygen analogs have a negative (favorable) ΔG_t^0 of -2.0 kcal/mole or greater (Tables 8,9,10). The acyclic oxygen analog, O-acetoxy-L-Phenyl-lactic-amide, has a slightly positive ΔH_t^0 (unfavorable) and a large positive ΔS_t^0 (favorable). The transfer process from aqueous to chloroform for the acyclic oxygen analog O-acetoxy-L-Phenyl-lactic-amide (II B-7) is entropy driven as is the nitrogen analogs. The cyclic oxygen analog, however, has a large negative ΔH_t^0 (favorable) and a ΔS_t^0 near zero and the transfer process is therefore, enthalpy driven, unlike the other analogs. Overall, the data show that the most significant difference in the partition process between the nitrogen and oxygen analogs are due to the changes in the enthalpy term (ΔH_t^0). The enthalpy term varies from highly positive, unfavorable values for the nitrogen analogs to a negative, favorable value for the cyclized oxygen analog (Tables 8,10).

Perturbation of the aqueous buffer solution with the organic solvent DMSO showed a large change only in thermodynamic parameters for the cyclic nitrogen analog (Table 9). The ΔG_t^0 for the transfer process of the cyclic nitrogen analog remained fairly constant while both the ΔH_t^0 and ΔS_t^0 increased compensatingly from small positive values to larger positive values. The overall process remained unfavorable with the predominating positive enthalpy opposing the transfer process and the positive entropy favoring the transfer process. The transfer process for DMSO shows no temperature dependence with both ΔH_t^0 and ΔS_t^0 being near zero.

The changes in thermodynamic parameters for the transfer process

TABLE 10

CHANGES IN THERMODYNAMIC PARAMETERS FOR THE TRANSFER
OF PHENYLALANINE SUBSTRATE ANALOGS FROM AQUEOUS
BUFFER TO CHLOROFORM AT 25°C DUE TO CHANGES IN ANALOG STRUCTURE

NUMBER	STRUCTURES ^a AND CONDITIONS COMPARED	$\Delta\Delta G_t^{\circ}$ cal/mole	$\Delta\Delta H_t^{\circ}$ cal/mole	$\Delta\Delta S_t^{\circ}$ e.u.
1	IIB8-IIB1 ^b	735 \pm 35	-2,360 \pm 120	-10.3 \pm 0.67
2	IIB8-IIB1 ^c	585 \pm 75	- 250 \pm 585	- 2.8 \pm 2.5
3	IIB8-IIB6 ^b	415 \pm 10	- 795 \pm 150	- 4.1 \pm 0.60
4	IIB8-IIB6 ^c	320 \pm 50	+2,015 \pm 625	+ 5.7 \pm 2.3
5	IIB6-IIB1 ^b	300 \pm 40	-1,565 \pm 190	- 6.25 \pm 0.8
6	IIB6-IIB1 ^c	265 \pm 50	-2,265 \pm 270	- 8.5 \pm 1.0
7	IIB9-IIB7 ^b	380 \pm 10	-2,335 \pm 510	- 8.8 \pm 1.7
8	IIB7-IIB1 ^b	-2,385 \pm 35	-3,065 \pm 355	- 2.3 \pm 1.30
9	IIB9-IIB8 ^b	-2,720 \pm 10	-2,940 \pm 275	0.70 \pm 1.0

^a Values are calculated using the least derived or lower numbered substrate as the reference point. Uncertainty expressed as \pm standard error of the differences of the means.
 IIB-1, N-acetyl-Phe-NH₂; IIB-6, N-formyl-Phe-NH₂; IIB-8, L-(-)-KCAQ; IIB-7, O-acetoxy-L-Phenyllactic-NH₂; IIB-9, CADIC.

^b Values and conditions from Table 8, non-DMSO system.

^c Values and conditions from Table 9, 5% DMSO system.

due to changes in analog structure are presented in Table 10. Comparison of the thermodynamic parameters for the transfer process shows that transfer of the cyclic compounds from aqueous to CHCl_3 has a more positive ΔG_t^0 (unfavorable than their homologous acyclic compounds (Table 10, items 1-7)). This is shown for the nitrogen and oxygen analogs in the non-DMSO aqueous system (Table 10, items 1,3,5,7) and the 5% DMSO system (Table 10, items 2,4,6). The data for the nitrogen and oxygen analogs shows that as the analogs change from acetyl derivatives to formyl to the cyclic derivatives in the nitrogen analog series the transfer process from non-DMSO aqueous solution to CHCl_3 is characterized by an increasing unfavorable positive $\Delta \Delta G_t^0$ which is composed of a favorable vasculating negative $\Delta \Delta H_t^0$ and a more predominant unfavorable negative $\Delta \Delta S_t^0$ which vasculates in an almost compensating manner with $\Delta \Delta H_t^0$. The same trend is seen in the 5% DMSO-aqueous results upon going from the acetyl to the formyl derivative of the nitrogen analogs. On cyclization of the alpha nitrogen derivative the ΔG_t^0 is still unfavorable, however, the parameters ΔH_t^0 and ΔS_t^0 have both become more positive and ΔH_t^0 is the predominant factor (Table 10, item 4).

While literature values for the thermodynamics of transfer of these compounds are generally not available, a few comparisons can be made. The data of Gill et al. (97) suggests a value for ΔG_t^0 of -800 cal/mole for the transfer of the methyl group of toluene and -765 cal/mole for the transfer of an aromatic methylene group. Tanford suggested (34) that the hydrophobicity of a hydrophobic group covalently bonded to another hydrophobic group was greater than the hydrophobicity

of the same group covalently bonded to a polar group and, therefore, the hydrophobic group bonded to the hydrophobic group would have a more negative ΔG_t^0 for the transfer process from aqueous to hydrophobic solvent. Accordingly, these data suggest a value of ΔG_t^0 for the methyl group in N-acetyl-Phenylalanine amide (when compared to N-Formyl-Phenylalanine amide) of -300 ± 40 cal/mole (Table 10, item 5) as compared to -800 cal/mole found by Gill et al. (97) for the transfer of a similar methyl group. These data also yield a value of -415 ± 10 cal/mole (Table 10, item 3) as compared to -765 cal/mole (97) for the contribution of an aromatic benzyl methylene group which is bonded to the hydrophilic peptide bond upon cyclization.

III A-2. Peptide Series Results.

van't Hoff plots of the partition experiments for the peptide substrate series are presented in figures 9 and 15-17. Thermodynamic parameters found for the transfer process of the peptide series, N-ac-Phe-NH₂, N-ac-Pro-Phe-NH₂, N-ac-Ala-Pro-Phe-NH₂, and N-ac-Pro-Ala-Pro-Phe-NH₂ are presented in Table 11. The mono amino acid substrate N-ac-Phe-NH₂ has a ΔG_t^0 near zero (35 ± 70 cal/mole) with a large positive ΔH_t^0 and ΔS_t^0 . Addition of proline to make the dipeptide changes the slightly unfavorable positive ΔG_t^0 to a negative ΔG_t^0 . Addition of alanine to the dipeptide again makes the overall transfer process slightly unfavorable ($\Delta G_t^0 = 90 \pm 50$ cal/mole), while addition of the second proline, to make the tetrapeptide, makes the transfer process slightly favorable ($\Delta G_t^0 = -400 \pm 20$ cal/mole), as for the dipeptide. The variance in ΔG_t^0 is within 1 kcal/mole and all four compounds have

TABLE 11

THERMODYNAMIC PARAMETERS FOR THE TRANSFER PROCESS OF PEPTIDE SUBSTRATES FROM
AQUEOUS BUFFER^a TO CHLOROFORM^b AT 25°C

COMPOUND	RATIO OF MOLE FRACTIONS ^c	ΔG_t° cal/mole	ΔH_t° cal/mole	ΔS_t° e.u.
IIB-1. N-ac-Phe-NH ₂ ^d	0.94 ±0.05	35±30	3,570± 80	11.8±0.4
IIB-3. N-ac-Pro-Phe-NH ₂	3.55 ±0.13	-750±10	2,200±200	10.0±0.7
IIB-4. N-ac-Ala-Pro-Phe-NH ₂	0.865±0.074	90±25	5,000±570	16.6±2.0
IIB-5. N-ac-Pro-Ala-Pro-Phe-NH ₂	1.96 ±0.06	-400±10	4,600±245	16.8±0.8

^a 0.05M sodium phosphate, 0.1M NaCl, pH 7.8. Uncertainty expressed as ± standard error of the mean.

^b Ethanol free nanograde chloroform purchased from Mallinckrodt.

^c X_i/X_w where X_i and X_w are the mole fractions of solute in chloroform and aqueous buffer respectively.

^d From Table 8.

both a positive ΔH_t^0 and a positive ΔS_t^0 for the transfer process from aqueous buffer to chloroform at 25°C, which is in agreement with the work of Nandi (101).

A comparison of the hydrophobicity of the amino acids can be made with literature values. Nandi (101) gives a value of $\Delta G_t^0 = 1.8$ kcal/mole for the transfer of a glycine peptide unit from aqueous solution to chloroform at 25°C. If we assume that N-ac-Phe-NH₂ has two glycine peptide units, then the side chain of phenylalanine contributes about -3.5 kcal/mole to ΔG_t^0 , as compared to -2.6 kcal/mole shown by Nozaki and Tanford (100) for transfer from aqueous to 100% ethanol. Adding 1.8 kcal/ for each additional glycine peptide unit gives us a rough value of ΔG_t^0 for each side chain (Table 12) and a hydrophobicity scale for the side chains of Phe > Pro > Ala which is consistent with literature values (100,135).

In summary, the transfer process of the peptide substrates from aqueous buffer to chloroform at 25°C is characterized by a position ΔH_t^0 (unfavorable) and a positive ΔS_t^0 (favorable) and is an entropy driven process.

III B. Enzyme-Peptide Amide Substrate Interactions.

Standard steady-state kinetic assays (5) were utilized to obtain the kinetic parameters which characterize binding and catalysis of substrates by α -chymotrypsin (51,52,55,72). In these procedures the ninhydrin assay method of Moore and Stein (129) is used to follow the rate of amide and peptide hydrolysis in 0.05M sodium phosphate, 0.1M NaCl, pH 7.8. The ninhydrin method's advantage over other methods is

TABLE 12

CHANGE IN ΔG_t° FOR PEPTIDE SIDE CHAINS AT 25°C: A HYDROPHOBICITY SCALE
FOR SIDE CHAIN RESIDUES

SIDE CHAIN	RESIDUE ^b	ΔG_t° SIDE CHAIN cal/mole	Lit. ^c ΔG_t° cal/mole
Phenylalanine	P ₁	- 3,565	- 2,600
Proline	P ₂	- 2,585	
Alanine	P ₃	- 960	- 520
Proline	P ₄	- 2,290	

^a Data from Table 11. See text for discussion.

^b Nomenclature from Schechter and Berger (27).

^c Nozaki and Tanford (100) from aqueous solution to 100% Ethanol.

that it directly measures the amount of free ammonia and amine in solution without necessary corrections for concurrent reactions as in the pH stat (72) and proflavin displacement (9) methods. The kinetic parameters K_s and k_2 were then calculated from a weighted Lineweaver-Burk computer analysis (5). In addition, a computer assisted analysis of the initial rate data was performed by the methods of Hanes (5), Augustinsson (5) and Lumry (39). The kinetic parameters K_s and k_2 calculated by all methods were found to be within experimental error of the value calculated by the weighted Lineweaver-Burk method.

Ninhydrin solution was prepared fresh daily as some inconsistency was noted when a solution was used the following day. Bovine pancreatic α -chymotrypsin (3X crystallized Worthington Biochemical Corp.) was prepared fresh daily and further purified by passing enzyme solution (8×10^{-4} M dissolved in 10^{-3} N HCl) over a G-25 (superfine) Sephadex column as suggested by Yapel et al. (111) to remove any small molecular weight contaminants.

Kennedy (59) found large changes in the fluorescent spectra of Cht sitting in solution at pH 7.8 and restricted his studies to less than ten minutes. This work studies Cht that has been further purified over G-25 and Cht straight from the bottle without further purification (Cht (G-25) and Cht (Bt1), respectively). The studies indicated that Cht (G-25) was stable at pH 3.0 throughout the length of the day's experiments (Table 13). However, a study of the activity of both Cht (G-25) and Cht (Bt1) at pH 7.8 showed an initial drop in activity within the first ten minutes which then plateaued to a constant activity for the remainder of the time (three hours). Similar results were re-

TABLE 13

COMPARISON OF ACTIVE SITES AND STABILITY OF G-25 SEPHADEX PURIFIED
AND NON-G-25 SEPHADEX PURIFIED CHT AT pH 3.0 AND 7.8

Cht Source ^a	<u>% Active Sites</u>		<u>STABILITY</u>				
	pNPA ^b	NCI ^c	Stock Solution		% Activity		Total Time of Study (MINS.)
			pH	Conc.	T _o	T _f	
Cht (Bt1)	86.0±0.0	100.0±1.6	7.8	4x10 ⁻⁶ M	100	88.1±1.8	180
Cht (G-25)	87.0±2.0	-----	7.8	1.27x10 ⁻⁵ M	100	80.3±1.6	180
			3.0	2.04x10 ⁻⁵ M	100	100. ±2.6	2,796

^a See text. Uncertainty expressed as ± one standard deviation.

^b p-Nitrophenylacetate.

^c N-trans-Cinnomayl Imidazole.

^d Work done in conjunction with Dr. Pratibha Varma-Nelson.

^e Activity determined by ATEE assay (N-acetyl-L-tyrosine-ethyl ester). T_o is the activity at time zero. T_f is the activity at the end of the total time of the study.

ported by Pandit and Norosinga-Rao (137), who found that the activity of pure Cht decreased by 17% to a plateau level after 45 minutes (pH 8.3, tris buffer). Cht with autocatalyzed product added, would plateau after 10% of the initial Cht was autocatalyzed (as compared with 19.7% and 11.9% autocatalyzed products found in this work for Cht (G-25) and Cht (Bt1), respectively (Table 13)). Other workers have reported a continuous second order autocatalytic process at high pHs and an almost indefinite stability at acidic pH (pH < 5.0) (138,139).

Prior to Kunugi et al. (56) in 1979 no direct study of the enthalpy and entropy for K_s and k_2 for a series of amino acid substrates had been reported. These prior studies all utilized ester substrates of the specific amino acids, Trp, Tyr, Phe, and Leu, and not the more natural peptide and amide substrates with k_2 rate controlling (equation 1.33).

The series of Cht specific N-acyl-peptidyl-phenylalanine-amide substrates studied by Bauer et al. (72) at 37°C were used in this work because of their high specificity for Cht and ease of synthesis over the tryptophan or tyrosine derivatives. In addition, proline in position P_2 and P_4 should prevent non-productive binding modes of the substrate to Cht (see section I C-5).

III B-1. Steady-State Association and Catalysis of N-Acyl-Peptidyl-L-Phenylalanine Amide Substrates by α -Chymotrypsin.

Kinetic parameters K_s , k_2 , and k_2/K_s , for the steady-state association and catalysis of the five specific substrates by Cht (0.05M sodium phosphate, 0.1N NaCl, pH 7.8) over the temperature range 5° to 37°C (45°C for N-ac-Phe-NH₂) are presented in Table 14. The dissociation constant, K_s , and the catalytic rate constant, k_2 , were calculated from the intercept and slope, respectively from a computer assisted weighted Lineweaver-Burk analysis (fig. 18; section III B). The uncertainty in K_s and k_2 are expressed as plus or minus the standard error of the mean. Comparison of data with available literature values shows a good correlation (Table 15).

The peptide series of Bauer et al. (72) systematically increases the enzyme-substrate interactions from the P₁ site to the P₄ site on going from the mono amino acid to the tetrapeptide substrate. Upon going from the mono amino acid to the tetrapeptide, an increase in catalytic specificity is observed. Addition of proline to the P₂ and P₄ positions shows little or no difference in the binding specificity. However, Bauer et al. (72) showed that addition of proline in the P₂ position was highly restrictive to productive modes of binding. Accordingly, this restriction in non-productive modes of binding would result in a decrease in the contribution of these non-productive modes of binding to the binding constant K_m . The dipeptide N-ac-Phe-Gly-NH₂, which binds in the P₁-P₁' site and is hydrolyzed at the Phe-Gly bond (66,76), shows a twofold increase in binding and catalytic specificity

TABLE 14

STEADY-STATE KINETIC PARAMETERS FOR THE ASSOCIATION AND CATALYSIS OF PEPTIDE SUBSTRATES

BY α -CHYMOTRYPSIN^a

COMPOUND	TEMP. °C	NUMBER OF DETERMINATIONS ^b	K_m (mM)	k_{cat} ($S^{-1} \times 10^3$)	k_{cat}/K_m ($M^{-1} S^{-1}$)	[S] ^c (mM)
N-ac-Phe-NH ₂ ^d	4.5	6	20.7 \pm 2.2	5.25 \pm 0.37	0.254 \pm 0.040	7.23-50.9
	12	5	28.6 \pm 1.4	15.4 \pm 0.8	0.54 \pm 0.05	
	18	7	28.3 \pm 2.2	30.2 \pm 0.2	1.06 \pm 0.08	
	25	7	29.3 \pm 1.5	56.1 \pm 3.0	1.91 \pm 0.19	
	31	7	24.4 \pm 1.3	83.4 \pm 3.2	3.42 \pm 0.30	
	37	12	32.3 \pm 1.9	119. \pm 9.	3.69 \pm 0.47	
	45	7	28.6 \pm 2.2	121. \pm 9.	4.22 \pm 0.59	
N-ac-Pro-Phe-NH ₂	5	1	25.4 \pm 4.0	76.0 \pm 8.8	3.00 \pm 0.71	10.8 -50.08
	12	1	27.8 \pm 0.9	141. \pm 4.	5.08 \pm 0.28	
	19	1	29.2 \pm 1.7	269. \pm 13.	9.21 \pm 0.95	
	25	3	21.1 \pm 2.8	323. \pm 30.	15.3 \pm 3.1	
	31	1	29.8 \pm 1.6	559. \pm 25.	18.8 \pm 1.8	
	37	2	28.4 \pm 2.7	748. \pm 58.	26.4 \pm 4.2	
N-ac-Ala-Pro-Phe-NH ₂	5	3	3.75 \pm 0.58	245. \pm 25.	65.3 \pm 14.5	1.33- 9.48
	12	3	3.95 \pm 0.2	455. \pm 17.	115. \pm 10.	
	19	2	3.09 \pm 0.13	767. \pm 21.	248. \pm 17.	
	25	2	2.39 \pm 0.27	1170. \pm 90.	491. \pm 82.	
	31	2	3.25 \pm 0.35	1940. \pm 150.	595. \pm 100.	
	37	3	3.89 \pm 0.38	2830. \pm 200.	728. \pm 111.	
N-ac-Pro-Ala-Pro-Phe-NH ₂	5	3	3.99 \pm 0.41	232. \pm 19.	58.2 \pm 9.7	1.41- 9.93
	12	3	4.20 \pm 0.78	484. \pm 67.	115. \pm 32.	
	19	2	3.43 \pm 0.43	843. \pm 75.	246. \pm 47.	
	25	3	3.03 \pm 0.24	1290. \pm 70.	425. \pm 54.	
	31	6	4.22 \pm 0.26	2050. \pm 100.	485. \pm 50.	
	37	6	4.58 \pm 0.38	3160. \pm 220.	690. \pm 97.	

TABLE 14

STEADY-STATE KINETIC PARAMETERS FOR THE ASSOCIATION AND CATALYSIS OF PEPTIDE SUBSTRATES
BY α -CHYMOTRYPSIN^a
(cont'd)

COMPOUND	TEMP. °C	NUMBER OF DETERMINATIONS ^b	K_m (mM)	k_{cat} ($S^{-1} \times 10^3$)	k_{cat} / K_m ($M^{-1} S^{-1}$)	[S] ^c (mM)
N-ac-Phe-Gly-NH ₂	5	2	22.7 ± 1.3	17.4 ± 1.6	0.766 ± 0.108	6.58-25.12
	12	3	16.1 ± 1.5	34.0 ± 3.4	2.11 ± 0.37	
	19	3	16.9 ± 1.5	68.3 ± 7.7	4.03 ± 0.74	
	25	2	15.7 ± 0.6	94.8 ± 5.0	6.03 ± 0.54	
	31	3	20.1 ± 0.9	164. ± 11.	8.15 ± 0.88	
	37	2	25.6 ± 0.9	249. ± 14.	9.72 ± 0.83	

^a 0.05M sodium phosphate, 0.1N NaCl, pH 7.8. Uncertainty expressed as ± standard error of the mean.

^b Each run was done independently and in duplicate, except for N-ac-Phe-NH₂ where the number indicates the number of single runs at that temperature.

^c Range of peptide concentration used to determine K_m and k_{cat} .

^d Two runs at each temperature were done independently by Dr. Shu-Hsien Lui Tsay.

LEGEND

Figure 18. Typical Lineweaver-Burk Plot.

N-Ac-Pro-Phe-NH₂ at 37°C

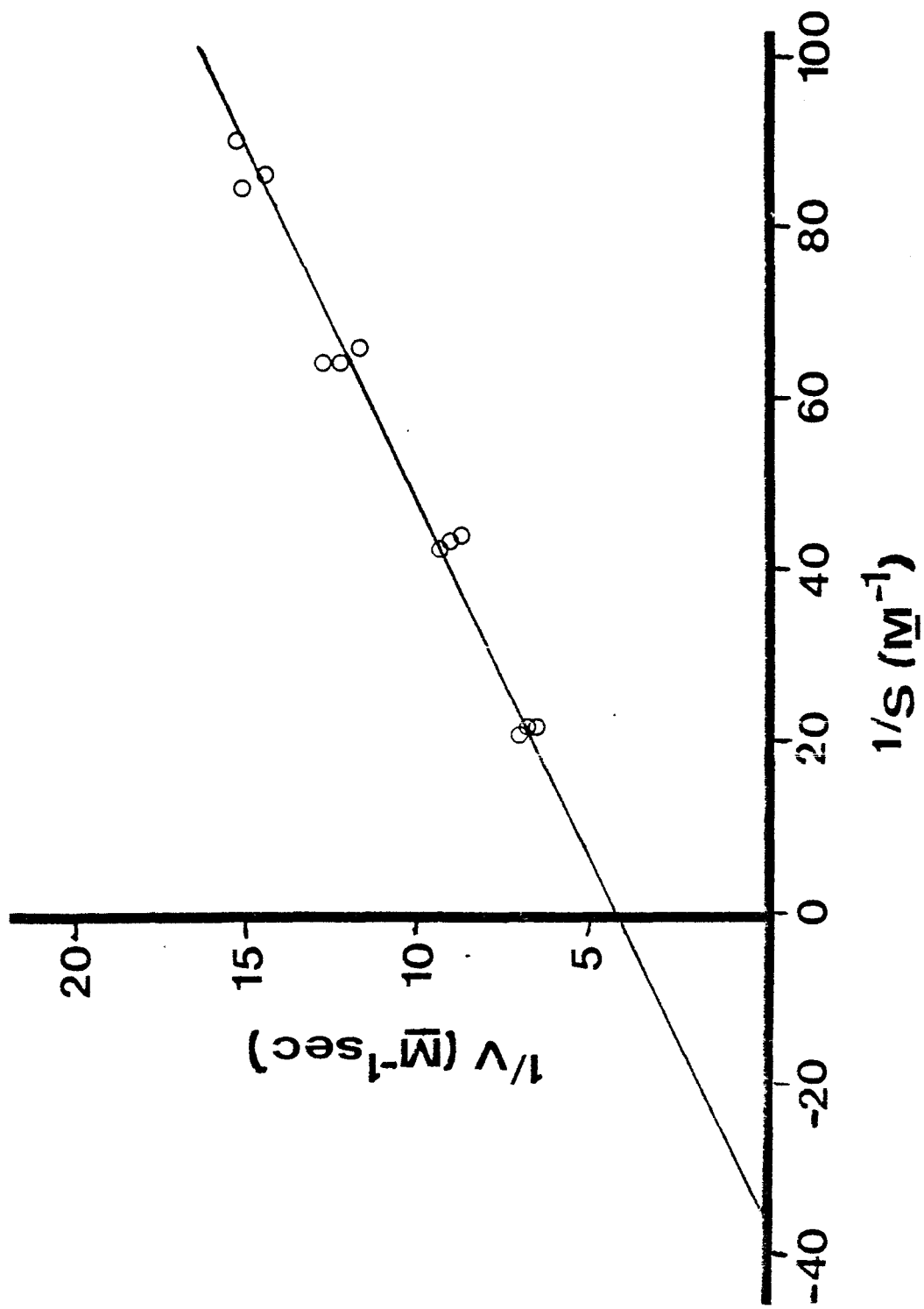


TABLE 15

COMPARISON OF THE KINETIC PARAMETERS OF AMIDE AND PEPTIDE HYDROLYSIS
OF THIS WORK WITH THE LITERATURE

COMPOUND	TEMP. °C	THIS WORK		LITERATURE		REFERENCE
		k_{cat} s ⁻¹	K_m mM	k_{cat} s ⁻¹	K_m mM	
N-ac-Phe-NH ₂	25	0.056±0.003	29.3 ±1.5	0.055	31 ±3	140
	25	0.056±0.003	29.3 ±1.5	0.046	30	141 ^a
	37	0.119±0.009	32.3 ±1.9	0.22 ±0.01	21 ±2	72
N-ac-Pro-Phe-NH ₂	37	0.748±0.058	28.4 ±2.7	0.70 ±0.02	24 ±1	72
N-ac-Ala-Pro-Phe-NH ₂	37	2.83 ±0.198	3.89±0.38	2.3 ±0.1	2.2±0.2	72
N-ac-Pro-Ala-Pro-Phe-NH ₂	37	3.16 ±0.22	4.58±0.38	2.8 ±0.2	3.4±0.4	72
N-ac-Phe-Gly-NH ₂	25	0.095±0.005	15.7 ±0.6	0.140±0.006	14.6±0.3	76

^a 0.02M Tris Buffer, pH 7.9.

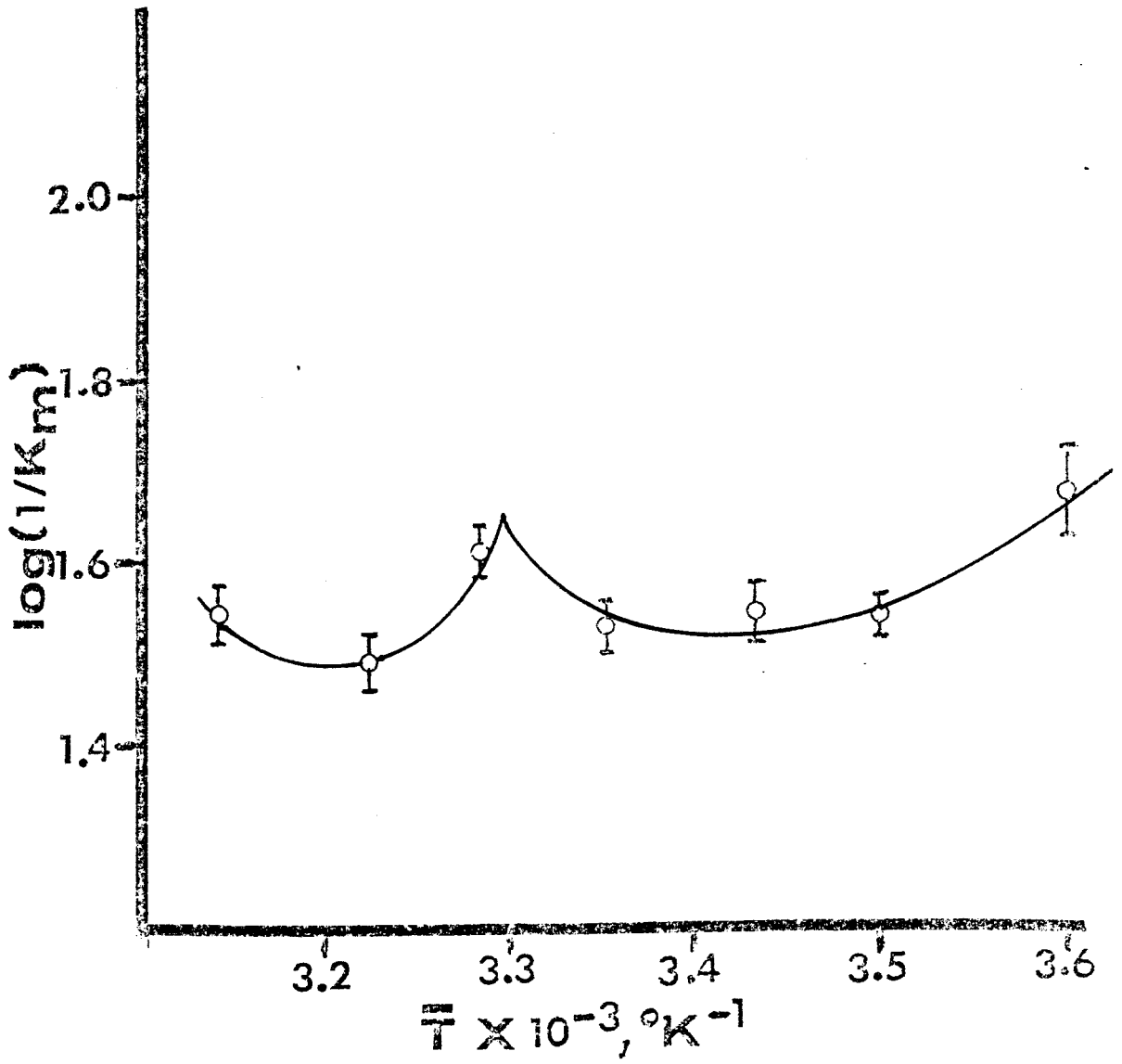
over N-ac-Phe-NH₂ (Table 14).

van't Hoff plots of the temperature dependence of the dissociation constant, $K_m = K_s$, for the five peptide substrates all show a discontinuity (figs. 19-23). The discontinuity gives a maximum affinity near 31°C for N-ac-Phe-NH₂ and near 25°C for the remaining four peptide substrates. Two curves have, therefore, been drawn through the graphs to give two temperature dependent forms of Cht.

Arrhenius plots of the catalytic rate constant, $k_{cat} = k_2$, show a similar discontinuity at 31°C and 25°C for the mono and poly amino acid substrates, respectively (figs. 24-28). However, there is no statistical preference for drawing the plots as one or two curves. The Arrhenius plot of N-ac-Phe-NH₂ (fig. 24) can be drawn as one curvilinear line while Arrhenius plots of the remaining substrates can be drawn as a single straight line. However, Arrhenius plots of k_{cat}/K_m (figs. 29-33) show two linear temperature dependent relationships. Therefore, since the van't Hoff plots of K_m displayed two curvilinear lines, the Arrhenius plots of k_{cat} must also be resolvable to two curvilinear lines that cancel out for the second order rate constant k_{cat}/K_m .

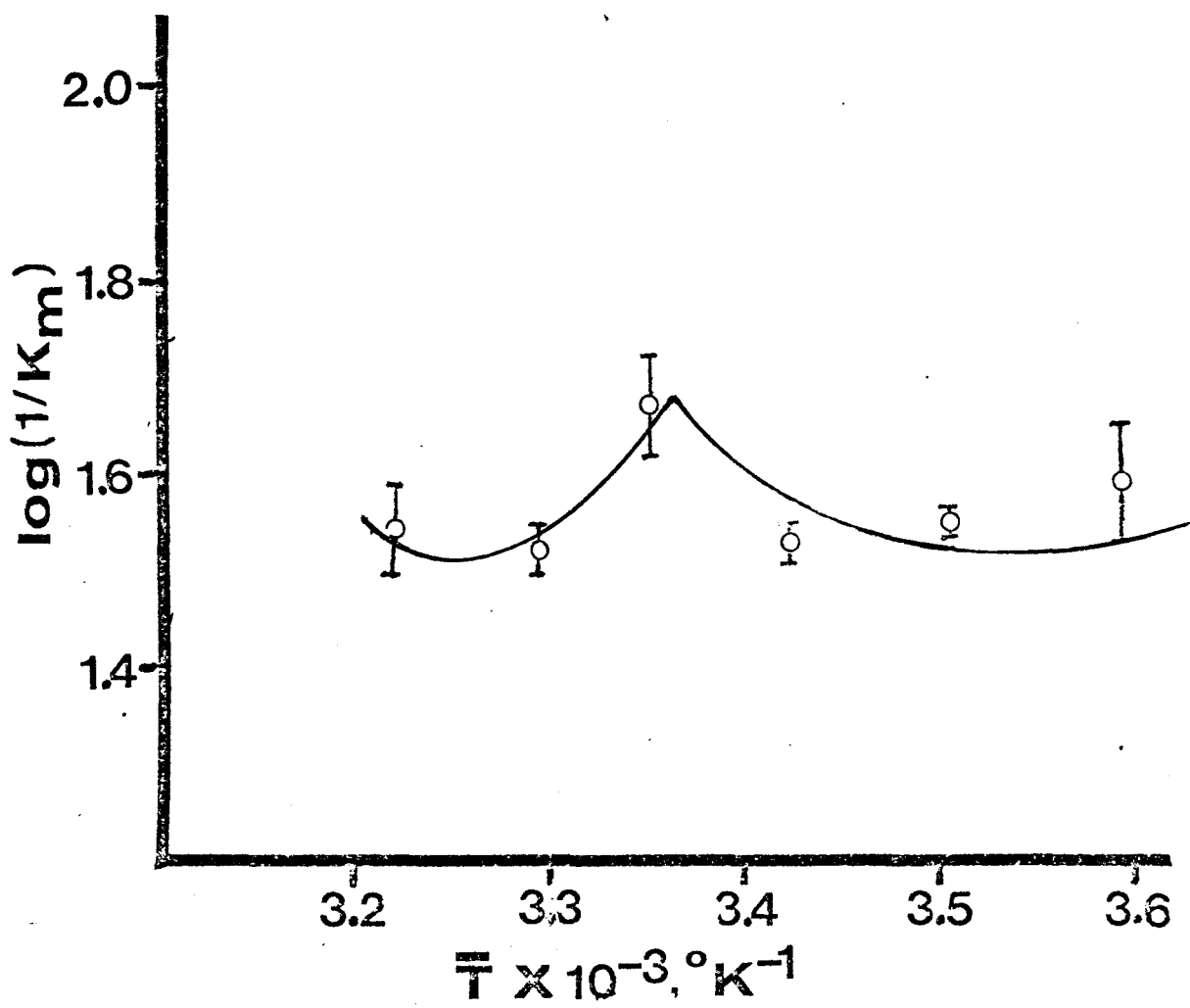
LEGEND

Figure 19. van't Hoff Plot of the Temperature Dependence of the
Dissociation Constant (K_m) of N-Ac-Phe-NH₂ with Cht.



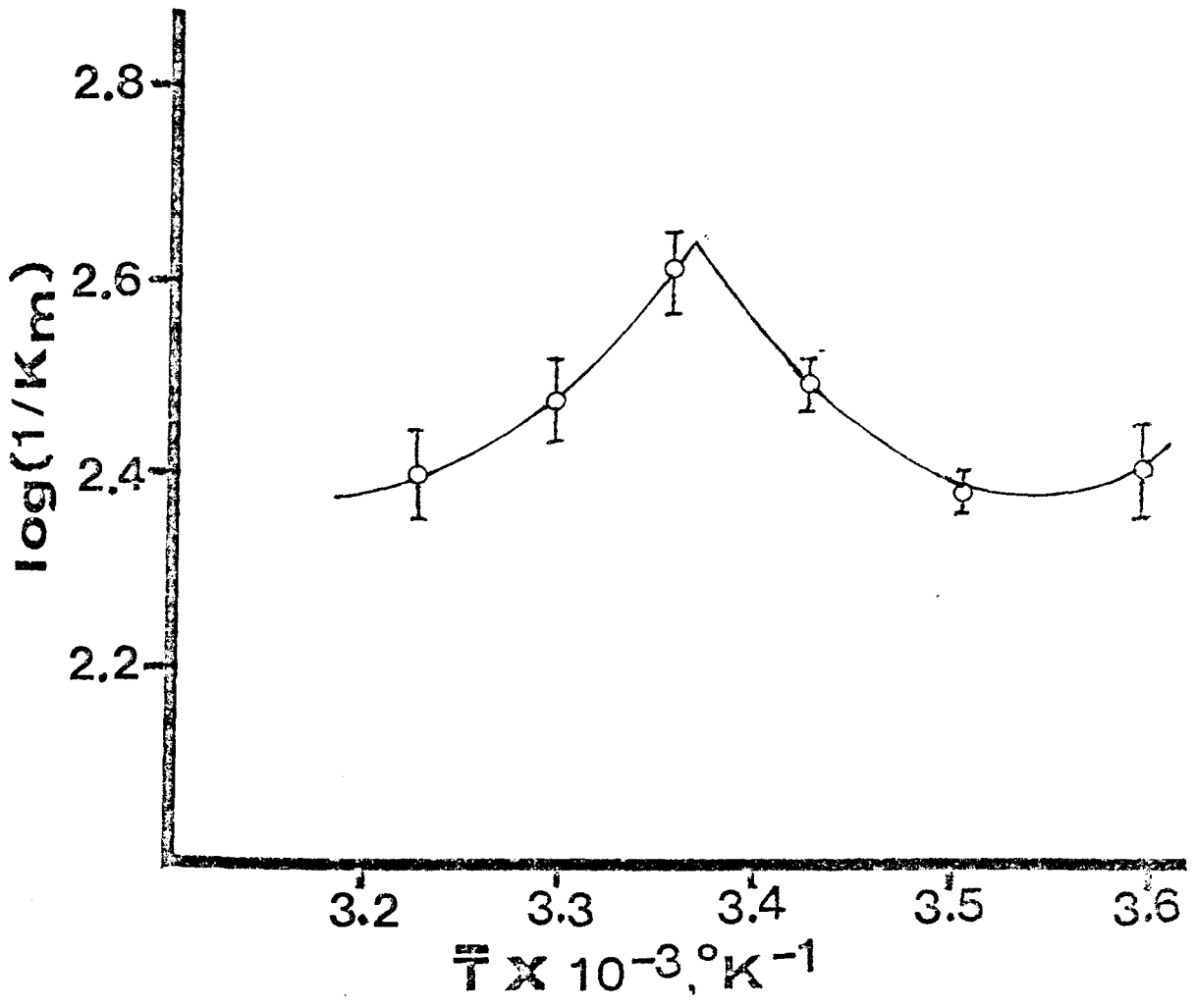
LEGEND

Figure 20. van't Hoff Plot of the Temperature Dependence of the
Dissociation Constant (K_m) of N-Ac-Pro-Phe-NH₂ with Cht.



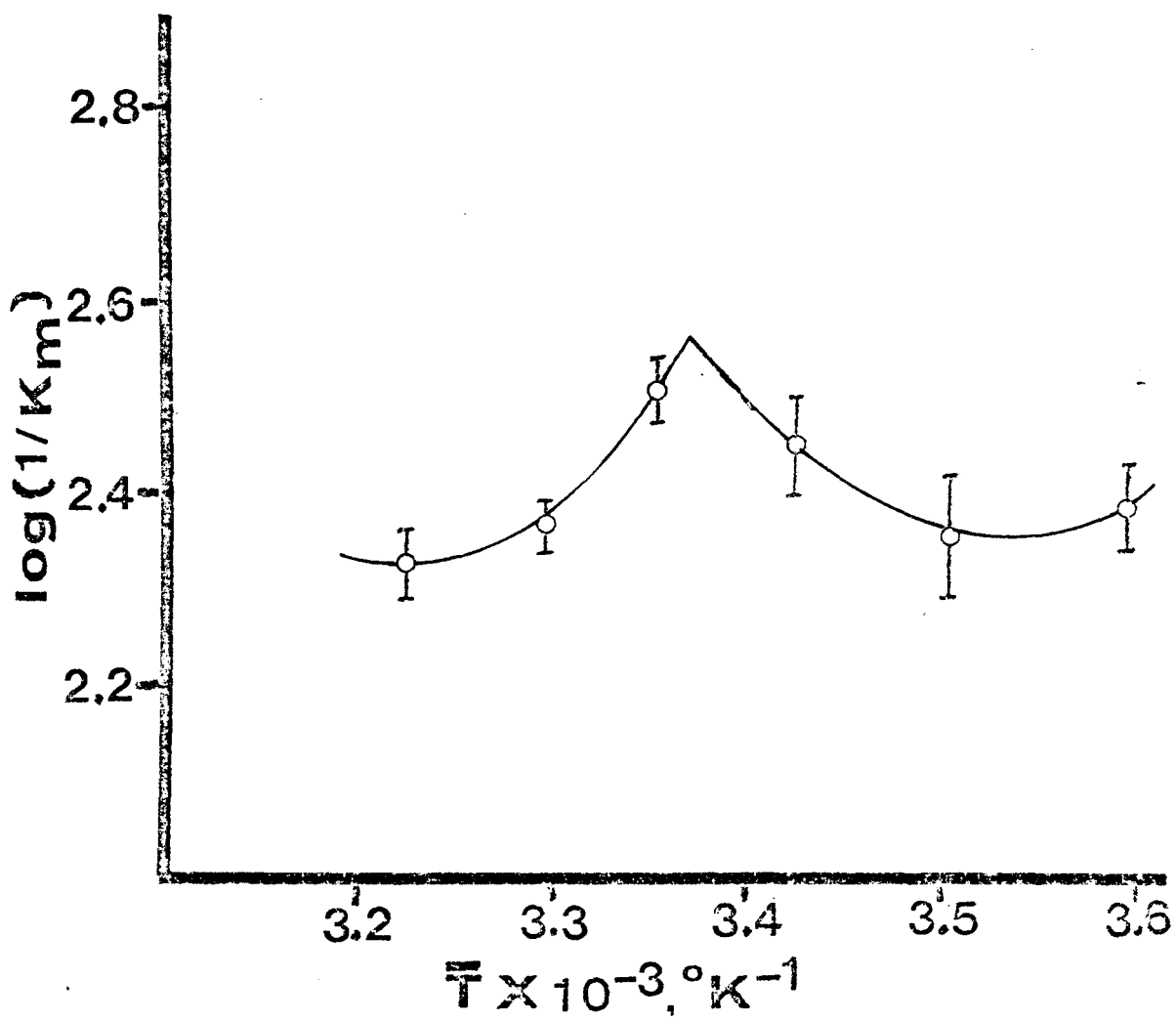
LEGEND

Figure 21. van't Hoff Plot of the Temperature Dependence of the
Dissociation Constant (K_m) of N-Ac-Ala-Pro-Phe-NH₂
with Cht.



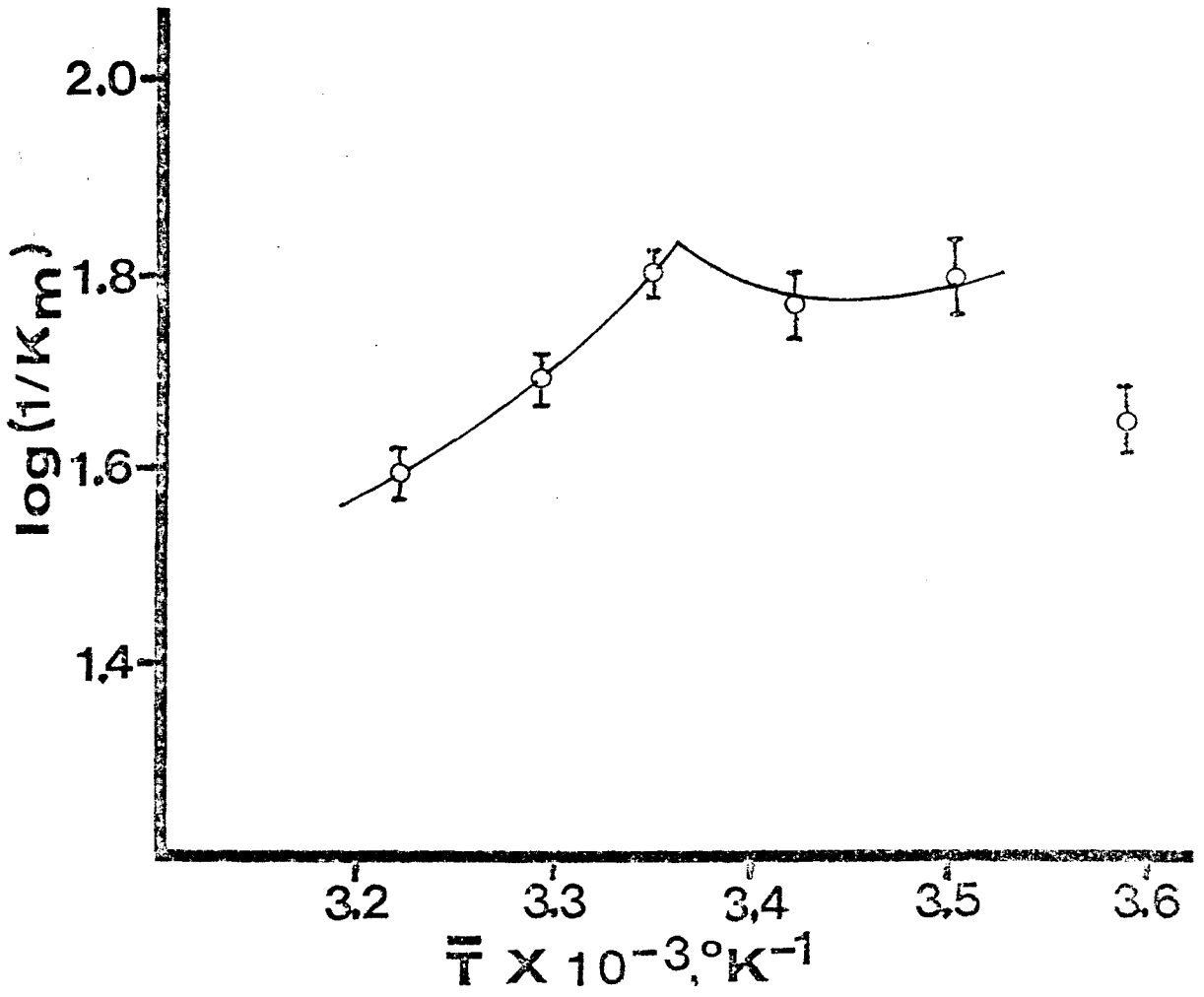
LEGEND

Figure 22. van't Hoff Plot of the Temperature Dependence of the Dissociation Constant (K_m) of N-Ac-Pro-Ala-Pro-Phe-NH₂ with Cht.



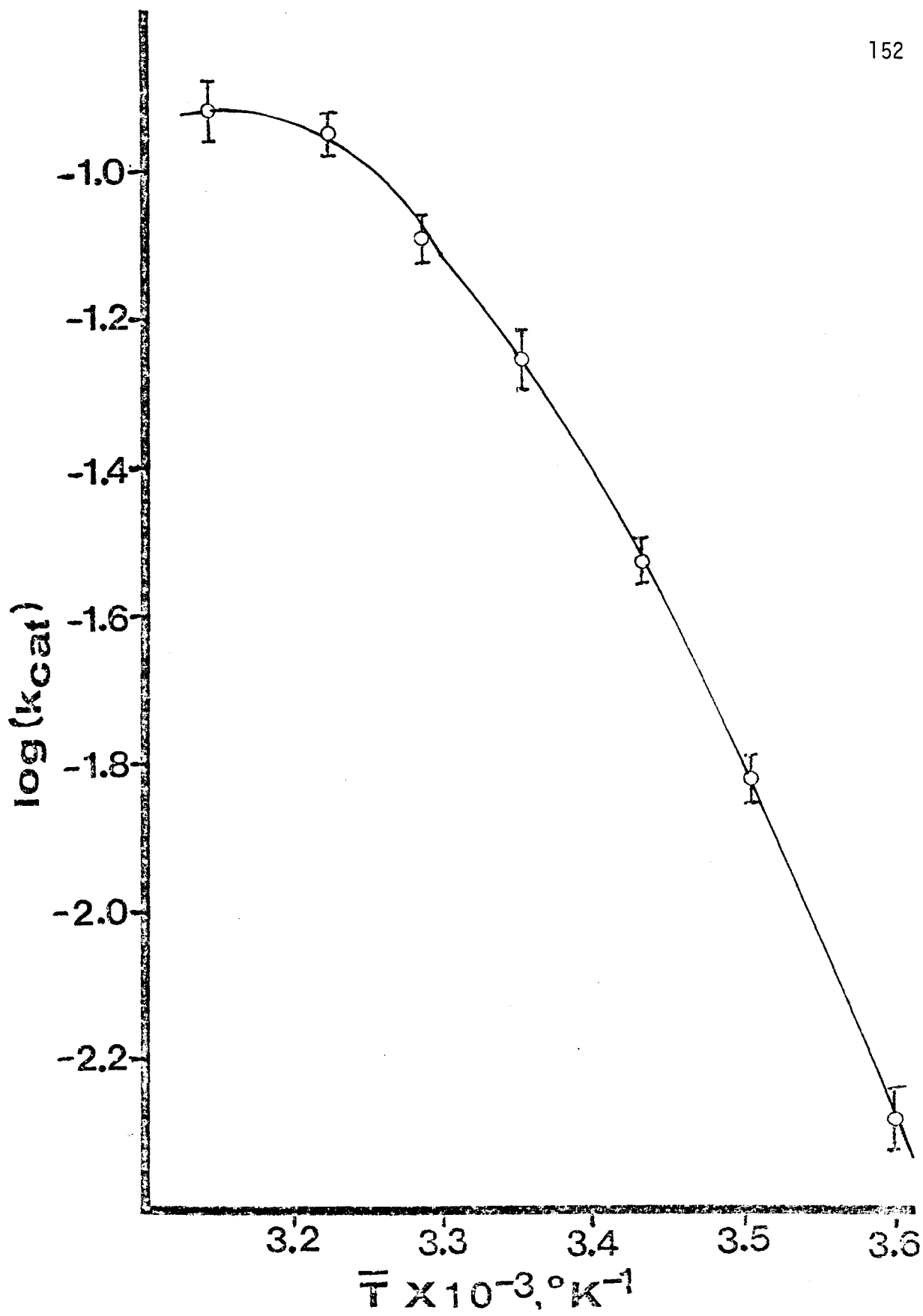
LEGEND

Figure 23. van't Hoff Plot of the Temperature Dependence of the Dissociation Constant (K_m) of N-Ac-Phe-Gly-NH₂ with Cht.



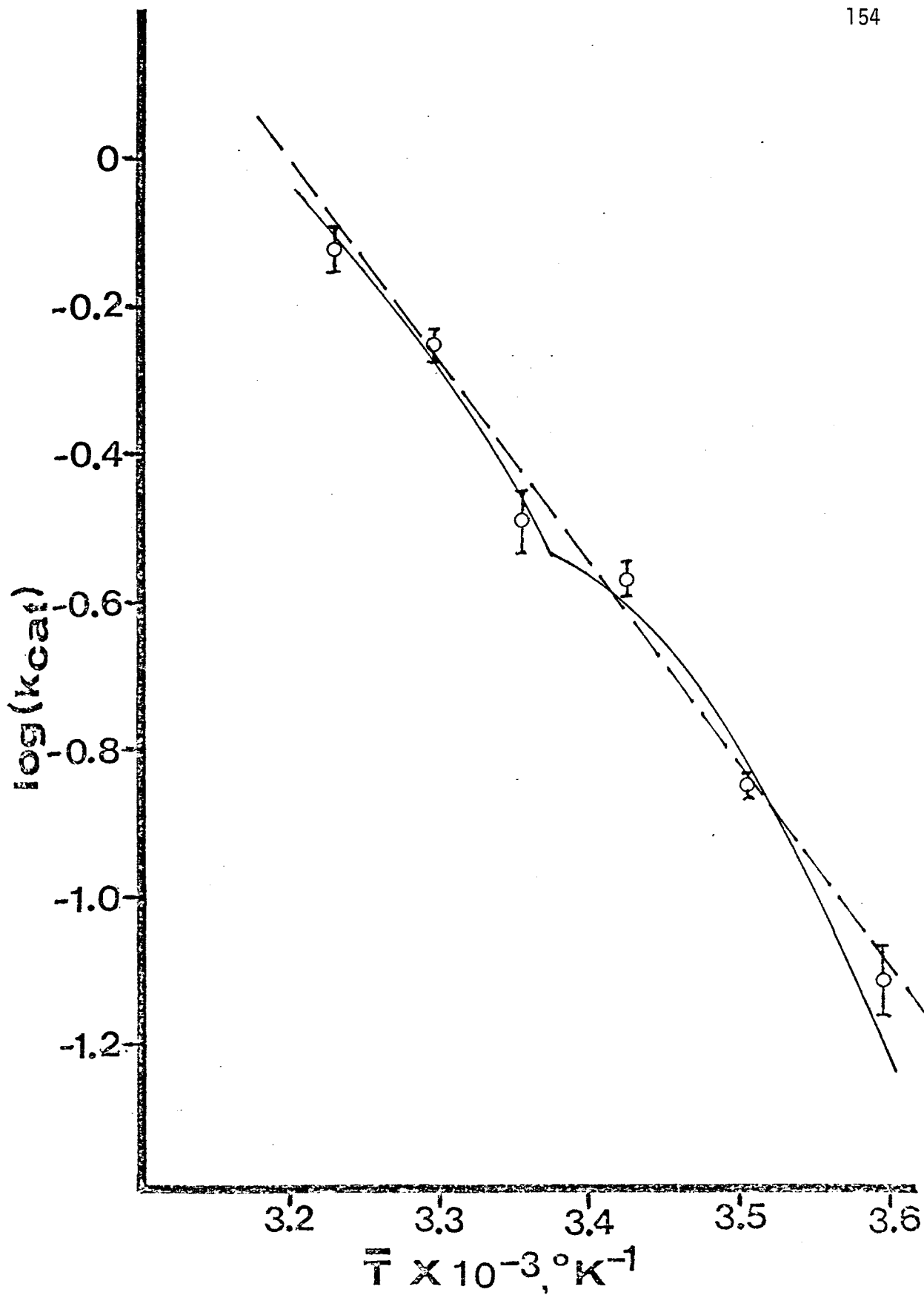
LEGEND

Figure 24. Arrhenius Plot of the Temperature Dependence of the Catalytic Rate Constant (k_{cat}) of N-Ac-Phe-NH₂.



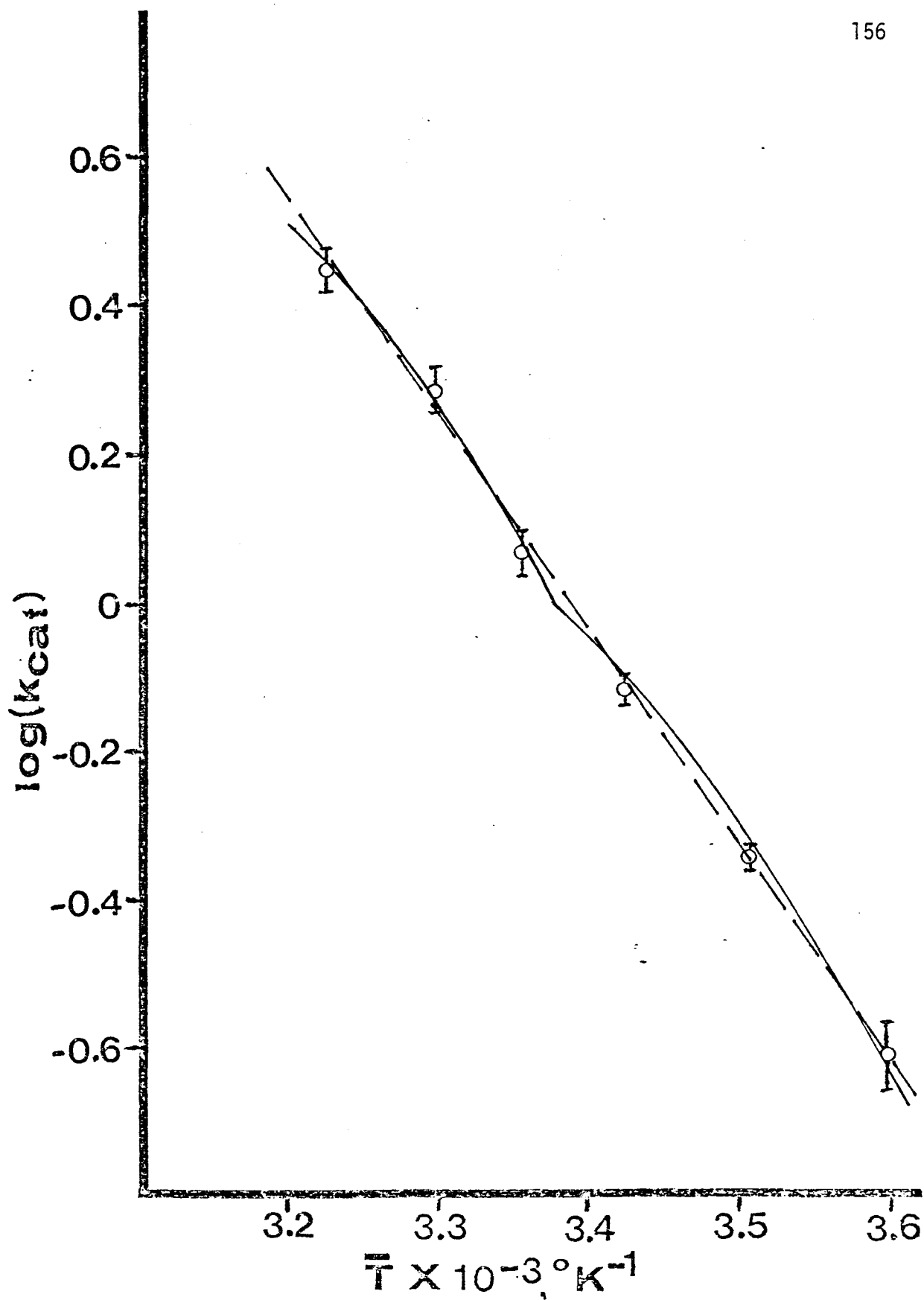
LEGEND

Figure 25. Arrhenius Plot of the Temperature Dependence of the Catalytic Rate Constant (k_{cat}) of N-Ac-Pro-Phe-NH₂.



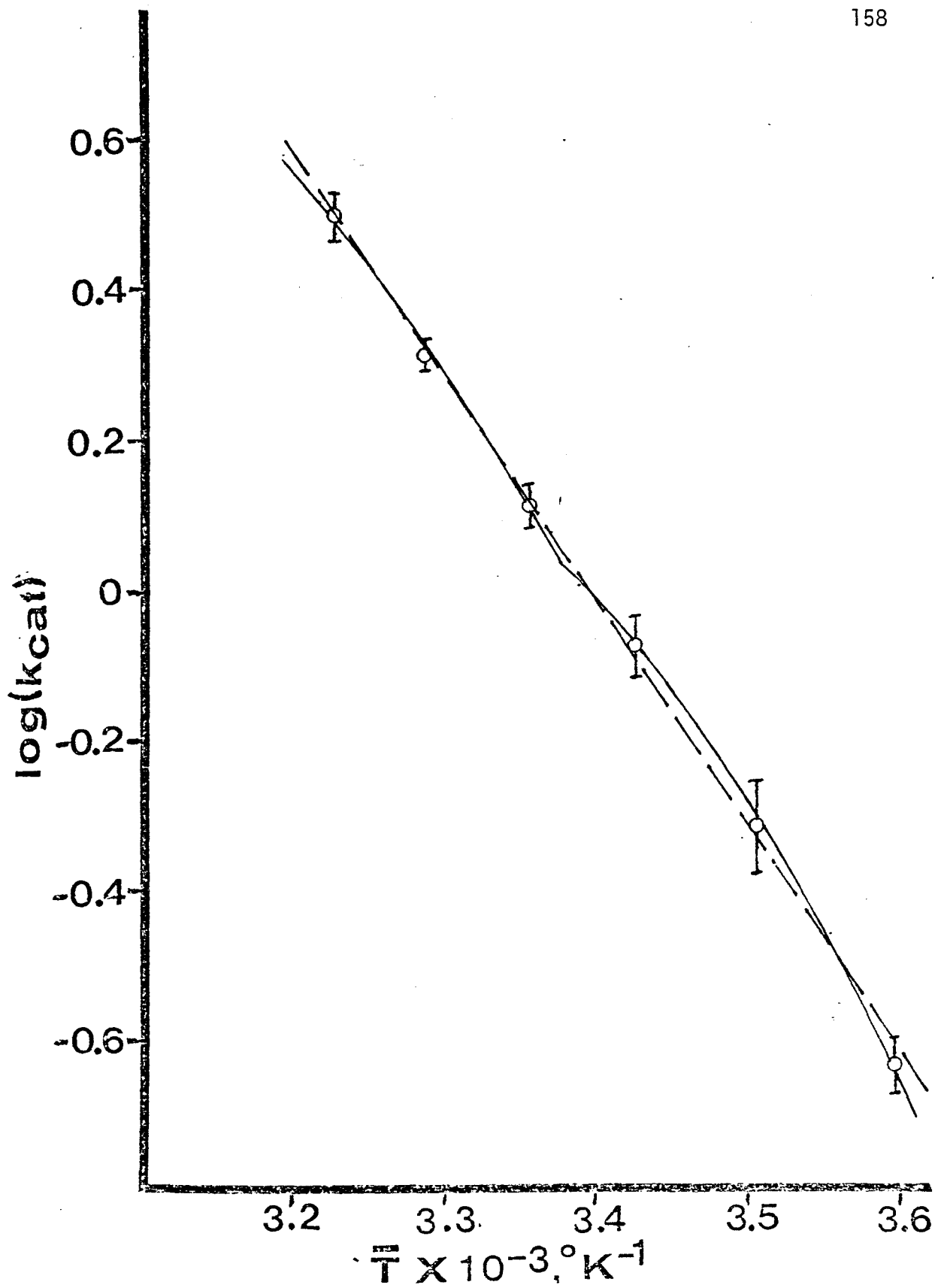
LEGEND

Figure 26. Arrhenius Plot of the Temperature Dependence of the Catalytic Rate Constant (k_{cat}) of N-Ac-Ala-Pro-Phe-NH₂.



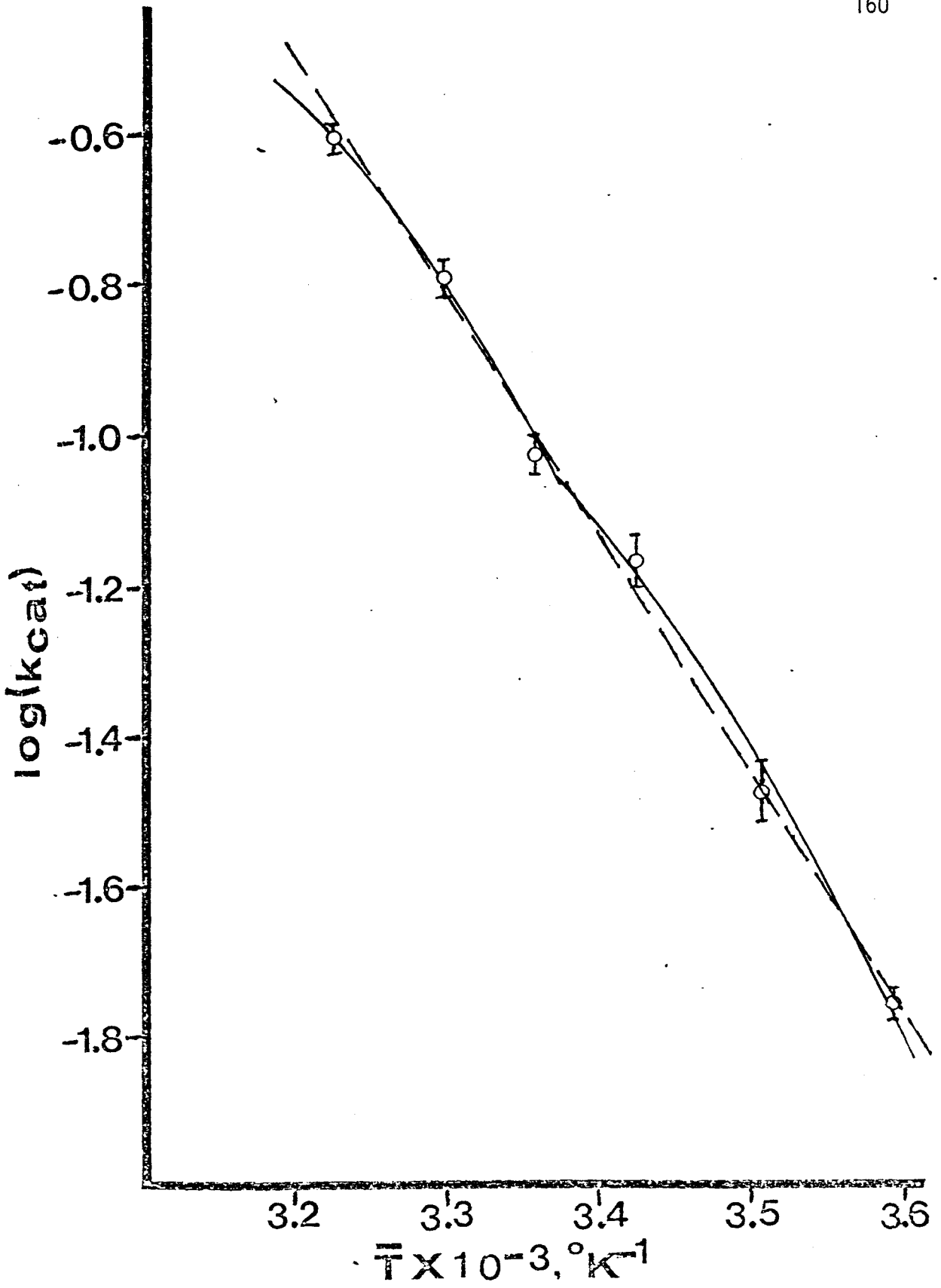
LEGEND

Figure 27. Arrhenius Plot of the Temperature Dependence of the Catalytic Rate Constant (k_{cat}) of N-Ac-Pro-Ala-Pro-Phe-NH₂.



LEGEND

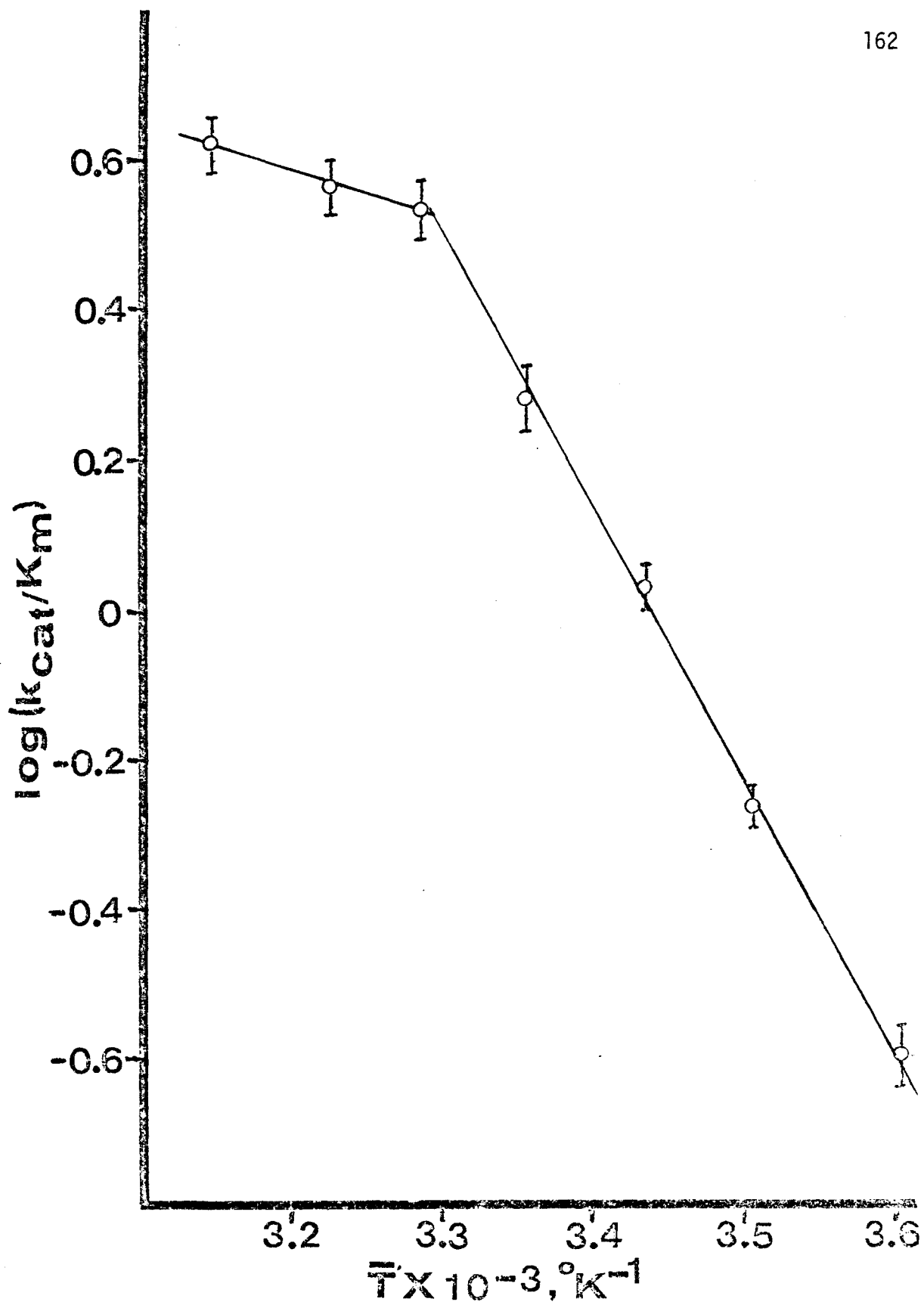
Figure 28. Arrhenius Plot of the Temperature Dependence of the Catalytic Rate Constant (k_{cat}) of N-Ac-Phe-Gly-NH₂.



LEGEND

Figure 29. Arrhenius Plot of the Temperature Dependence of
the Second Order Rate Constant (k_{cat}/K_m) of N-Ac-
Phe-NH₂.

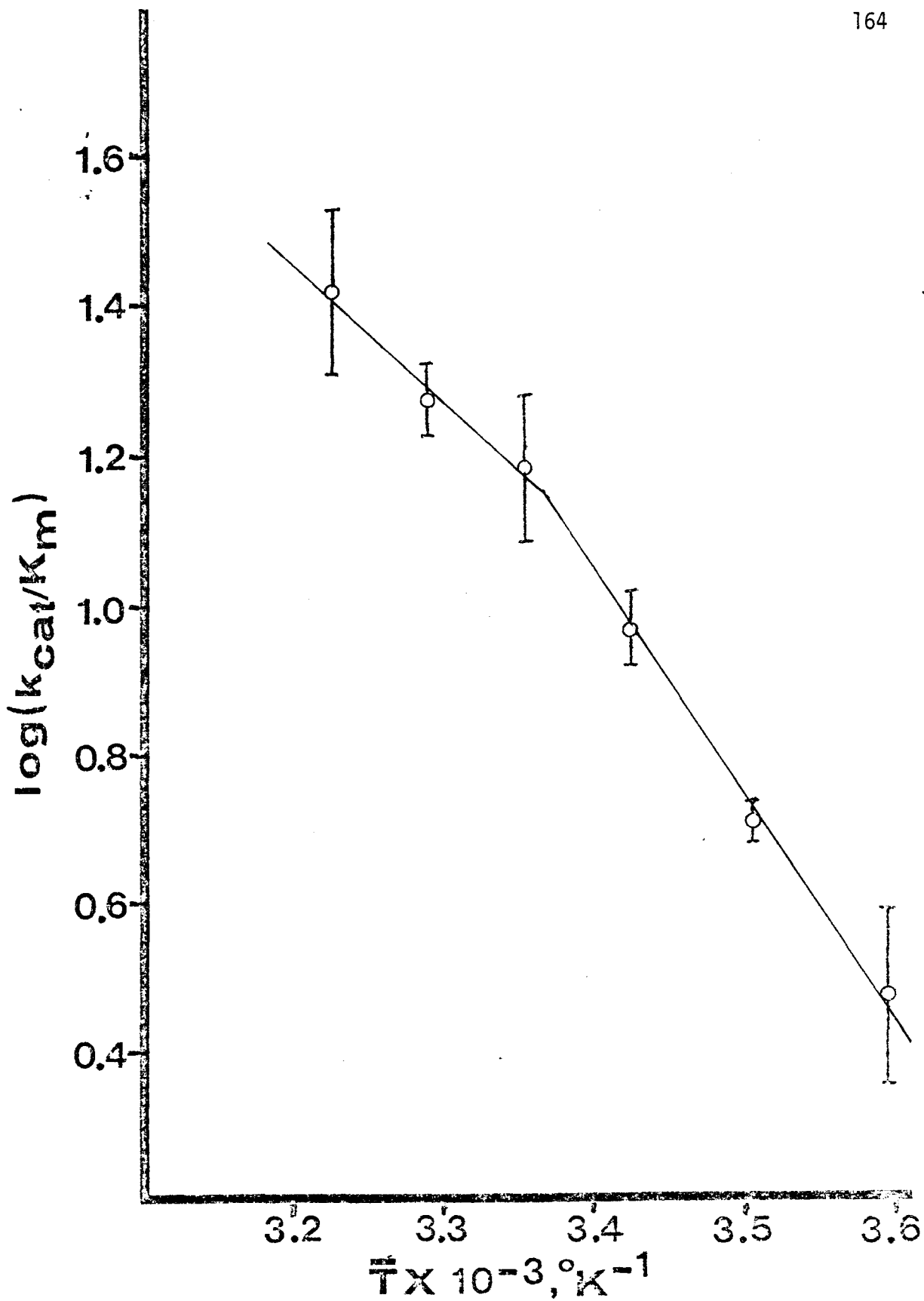
See text for details.



LEGEND

Figure 30. Arrhenius Plot of the Temperature Dependence of the Second Order Rate Constant (k_{cat}/K_m) of N-Ac-Pro-Phe-NH₂.

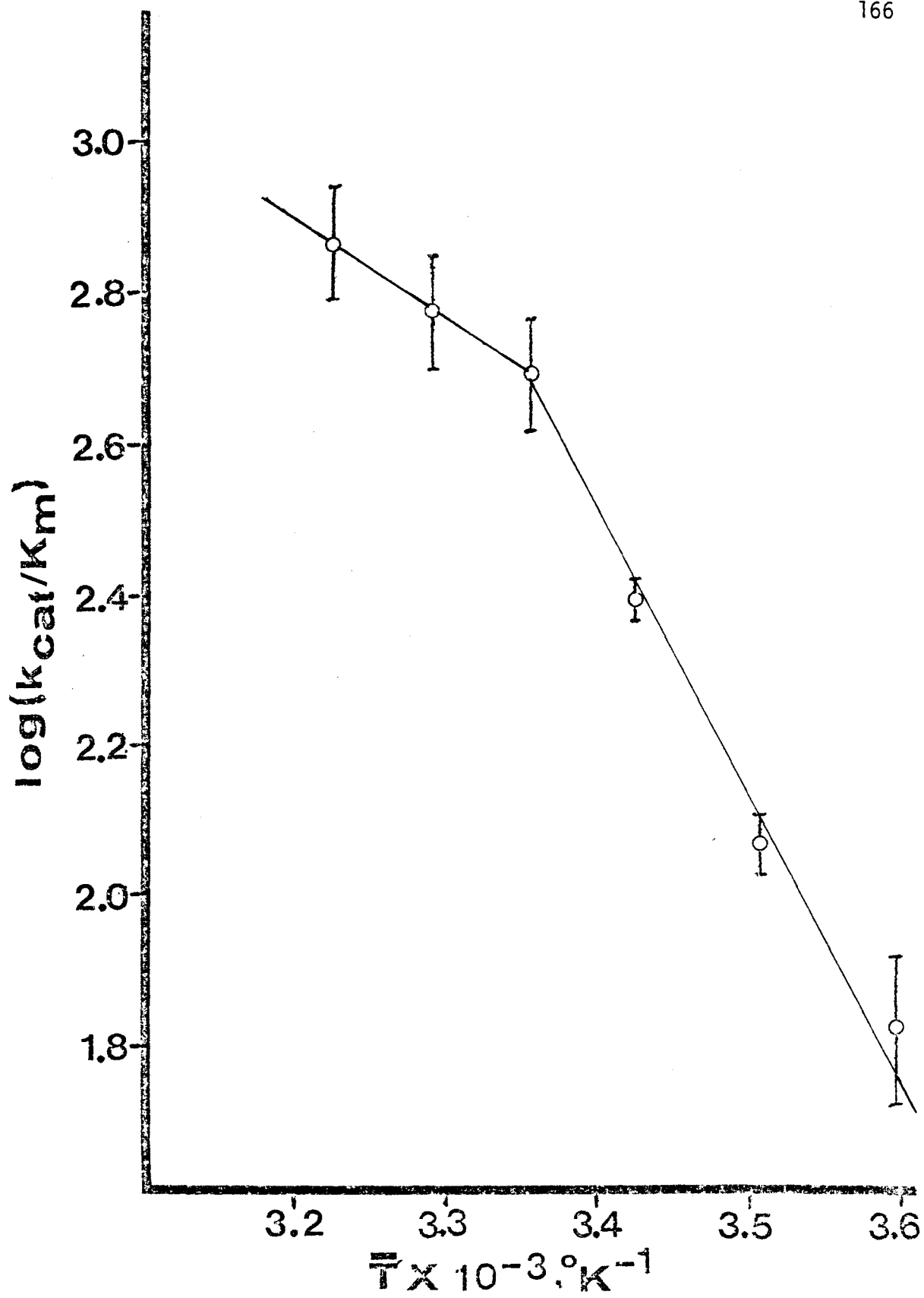
See text for details.



LEGEND

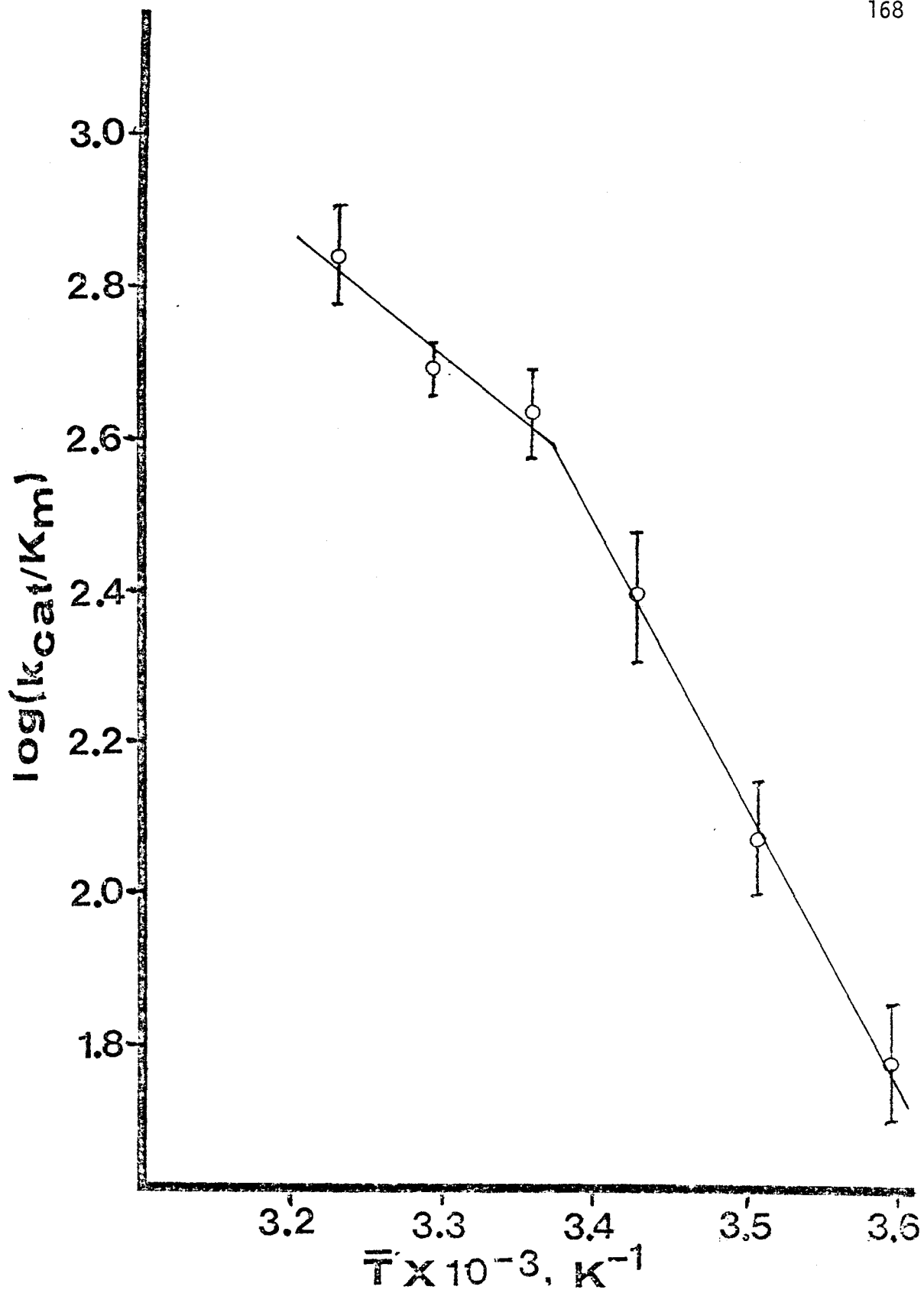
Figure 31. Arrhenius Plot of the Temperature Dependence of the Second Order Rate Constant (k_{cat}/K_m) of N-Ac-Ala-Pro-Phe-NH₂.

See text for details.



LEGEND

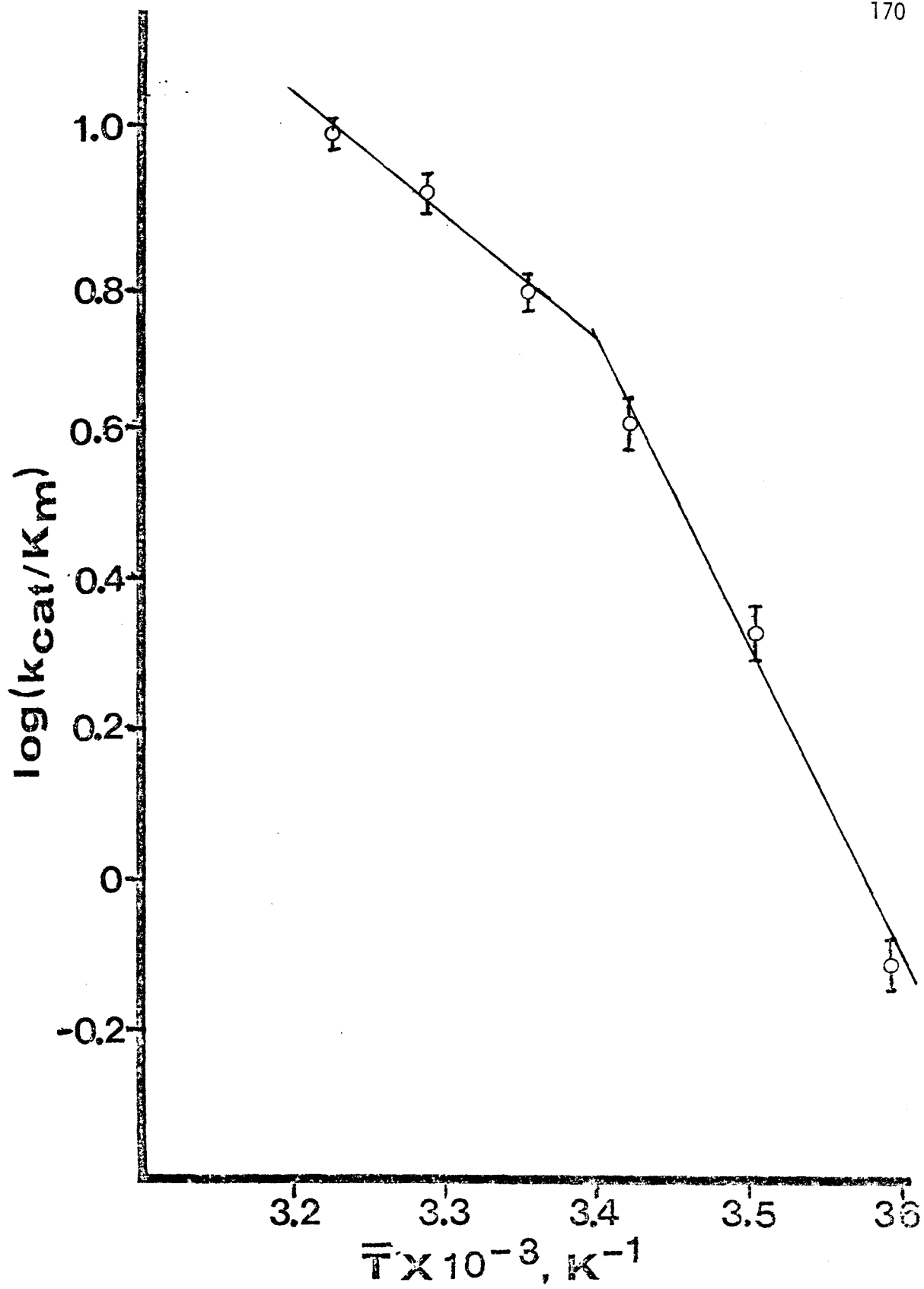
Figure 32. Arrhenius Plot of the Temperature Dependence of the Second Order Rate Constant (k_{cat}/K_m) of N-Ac-Pro-Ala-Pro-Phe-NH₂.
See text for details.



LEGEND

Figure 33. Arrhenius Plot of the Temperature Dependence of the Second Order Rate Constant (k_{cat}/K_m) of N-Ac-Phe-Gly-NH₂.

See text for details.



III B-2. Thermodynamics of the Steady-State Association and Catalysis
of N-Acyl-L-Phenylalanine Amide Substrates by α -Chymotrypsin.

van't Hoff plots of the temperature dependence of the dissociation constant K_m , for the five peptide and amide substrates (figs. 19-23) all indicate a discontinuity correlating with two temperature dependent forms of the enzyme as discussed in section II B-1.

The van't Hoff plot of the substrate N-ac-Phe-NH₂ (fig. 19) appears to best correlate with the existence of two curved lines ($\Delta C_p < 0$), with a crossover point (discontinuity) at about 30°C. Alternatively, if a straight line is drawn through all the points the data points at 31° and 5°C are more than a standard deviation from the least square line. In addition, the repetitivity of the pattern for all five peptide substrates studied strongly indicates that the correct plots through the data are curvilinear. The slope of the curve drawn as in fig. 19 at temperatures immediately below the discontinuity is negative, giving an apparent positive ΔH_a^0 and ΔS_a^0 (Table 16). The slope of the curve at temperatures immediately above the discontinuity is positive, giving an apparent negative ΔH_a^0 and ΔS_a^0 (Table 16). The two temperature dependent forms of the enzyme then have very different thermodynamic parameters for the binding process around the discontinuity (Table 17). This is in agreement with the change in ΔH and ΔS for water sorption by Cht around 25°C as shown by Ruegg and co-workers (50,62). Furthermore, if we start from 5°C for N-ac-Phe-NH₂ and move toward the discontinuity both ΔH_a^0 and ΔS_a^0 go from negative to positive values. Similarly, as we decrease the temperature from 37°C the values are positive and become negative as the temperature is decreased towards

TABLE 16

THERMODYNAMICS OF THE STEADY-STATE ASSOCIATION OF AMIDE AND PEPTIDE SUBSTRATES BY

 α -CHYMOTRYPSIN AT 25°C

COMPOUND	LOW TEMP. FORM			HIGH TEMP. FORM		
	ΔG_a^0 kcal/mole	ΔH_a^0 kcal/mole	ΔS_a^0 e.u.	ΔG_a^0 kcal/mole	ΔH_a^0 kcal/mole	ΔS_a^0 e.u.
N-ac-Phe-NH ₂	-2.09±0.03	+ 4.38±0.58	+21.9 ±2.05	(-2.50±0.06)	-15.51±4.0	-43.64±13.62
N-ac-Pro-Phe-NH ₂	(-2.33±0.10)	+10.64±2.0	+43.50±7.04	-2.29±0.08	-11.44±1.2	-30.69± 4.29
N-ac-Ala-Pro-Phe-NH ₂	(-3.65±0.08)	+12.37±0.9	+53.75±3.29	-3.57±0.06	-11.81±0.9	-27.64± 3.22
N-ac-Pro-Ala-Pro-Phe-NH ₂	(-3.57±0.08)	+11.51±0.9	+50.58±3.29	-3.44±0.05	-13.76±0.9	-34.48± 3.19
N-ac-Phe-Gly-NH ₂	(-2.52±0.05)	+ 6.46±1.1	+30.12±3.89	-2.46±0.03	-10.06±0.9	-25.49± 3.12

^a ΔG_a^0 in parenthesis is calculated from the projected curve for that form of the enzyme at 25°C.

ΔH_a^0 is calculated from the tangent to the curves for the 2 forms at 25°C.

ΔS_a^0 is calculated from the formula $\Delta G = \Delta H - T \Delta S$.

TABLE 17

DIFFERENCES IN THERMODYNAMIC PARAMETERS AT 25°C FOR THE
ASSOCIATION OF AMIDE AND PEPTIDE SUBSTRATES WITH THE TWO
TEMPERATURE DEPENDENT FORMS OF α -CHYMOTRYPSIN

COMPOUND	$(\Delta G_a^\circ)_H - (\Delta G_a^\circ)_L$ kcal/mole	$(\Delta H_a^\circ)_H - (\Delta H_a^\circ)_L$ kcal/mole	$(\Delta S_a^\circ)_H - (\Delta S_a^\circ)_L$ e.u.
N-ac-Phe-NH ₂	-0.41±0.09	-19.89±4.58	-65.54±15.67
N-ac-Pro-Phe-NH ₂	0.04±0.18	-22.08±3.20	-74.19±11.33
N-ac-Ala-Pro-Phe-NH ₂	0.08±0.14	-24.18±1.80	-81.39± 6.51
N-ac-Pro-Ala-Pro-Phe-NH ₂	0.13±0.13	-25.27±1.8	-85.06± 6.48
N-ac-Phe-Gly-NH ₂	0.06±0.09	-16.52±2.0	-55.61± 7.01

^a Difference in values (high-low) taken from Table 16.

the discontinuity (fig. 34).

van't Hoff plots of the four remaining peptide substrates follow a similar pattern (figs. 20-23; Table 16). The "W" pattern is less pronounced as we progress to longer substrates and the discontinuity appears near 25°C instead of 31°C. However, all appear to be characterized by significant positive heat capacity changes, ΔC_p^0 , for both the low and high temperature forms of the enzyme (Table 18, fig. 34). In addition, the plot of the dipeptide N-ac-Phe-Gly-NH₂ cannot be drawn as two curves (fig. 23), as the 5°C point is off the low temperature curve. This observation indicates that binding in the S₁' site may involve a different mechanism.

van't Hoff plots of the temperature dependence of the rate constant k_{cat} for the amide and peptide substrates show a corresponding discontinuity near 31°C for N-ac-Phe-NH₂ and near 25°C for the remaining four substrates (figs. 24-28). The discontinuity is clearly demonstrated in the plots of the two dipeptide substrates (figs. 25,28). These data also appear to fit two curved lines, intersecting near 25°C. According to this analysis, large differences in the thermodynamic parameters at 25°C for the two forms will be found for the k_{cat} step, as for the association step (Table 19). The high temperature form is characterized by a more positive ΔH^\ddagger and ΔS^\ddagger than the low temperature form, which is opposite to the pattern for ΔH_a^0 and ΔS_a^0 for the association step in the high and low temperature forms, respectively (Table 16).

Several trends are apparent on comparing the association and activation steps for the two temperature dependent forms. In the low

LEGEND

Figure 34. Change in the Enthalpy of Association (ΔH_a^0) with Temperature for the Five Specific Amide and Peptide Substrates.

Data points were taken from tangents to the van't Hoff plots for the association step (figs. 19-23.)

1, N-ac-Phe-NH₂; 2, N-ac-Pro-Phe-NH₂; 3, N-ac-Ala-Pro-Phe-NH₂; 4, N-ac-Pro-Ala-Pro-Phe-NH₂; 5, N-ac-Phe-Gly-NH₂.

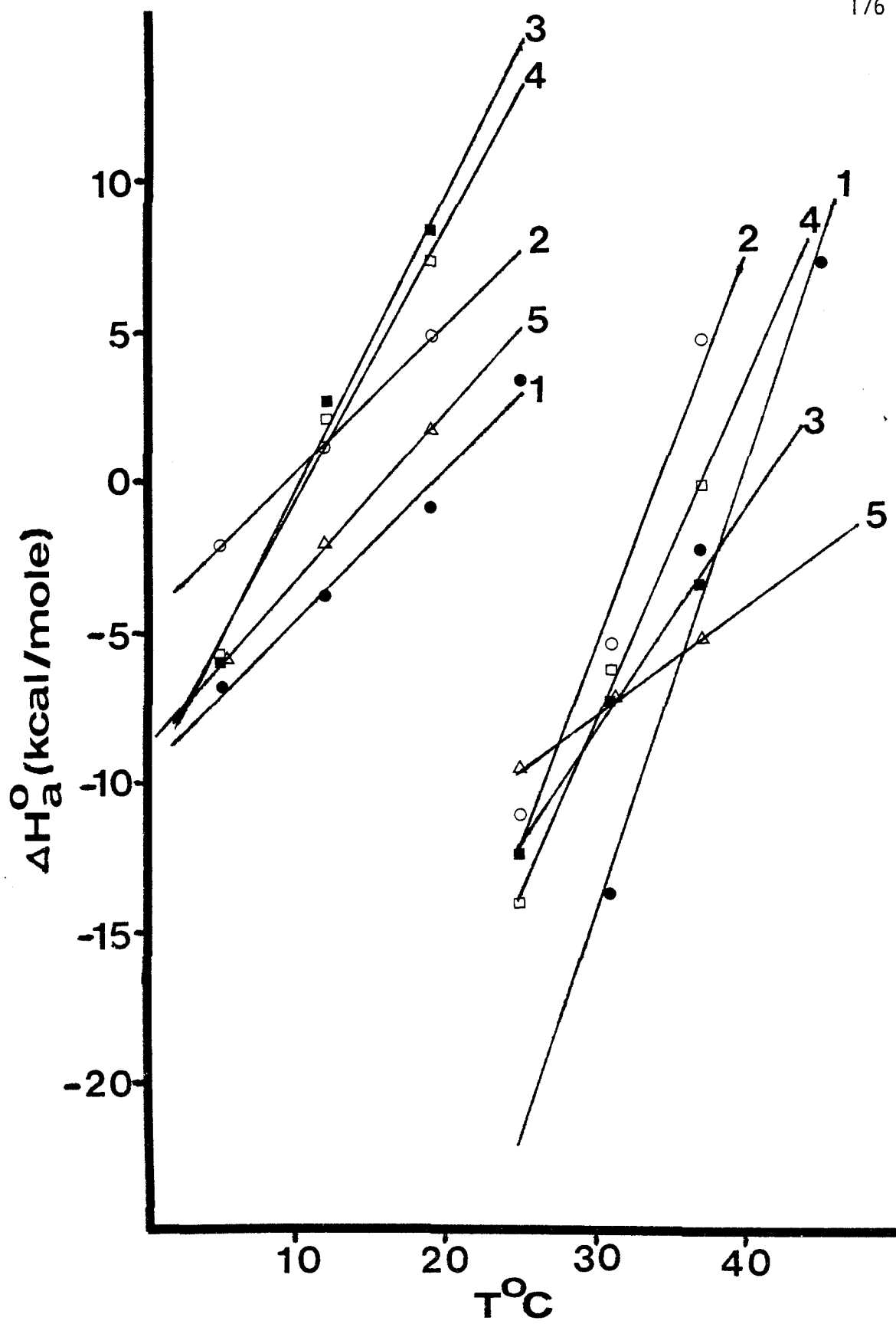


TABLE 18
CHANGE IN HEAT CAPACITY DUE TO ASSOCIATION OF AMIDE AND
PEPTIDE SUBSTRATES WITH α -CHYMOTRYPSIN

COMPOUND	LOW TEMP. FORM ^a	ΔC_p° (cal/°C)	HIGH TEMP. FORM ^b
N-ac-Phe-NH ₂	505 ± 46		1491 ± 196
N-ac-Pro-Phe-NH ₂	499 ± 22		1330 ± 215
N-ac-Ala-Pro-Phe-NH ₂	1026 ± 121		748 ± 54
N-ac-Pro-Ala-Pro-Phe-NH ₂	923 ± 105		1156 ± 78
N-ac-Phe-Gly-NH ₂	541 ± 315		357 ± 18

^a Determined from tangents to the plot $\log 1/K_m$ vs $1/T$ at 5°, 12° and 19°C except for N-ac-Phe-NH₂ which was determined at 5°, 12°, 19° and 25°C and N-ac-Phe-Gly-NH₂ at 12° and 19°C.

^b Determined from tangents at 25°, 31°, and 37°C except for N-ac-Phe-NH₂ which was determined at 31°, 37° and 45°C. Error was estimated by drawing a family of tangents at a particular temperature and is expressed as standard error.

TABLE 19

THERMODYNAMICS OF ACTIVATION FOR THE STEADY-STATE CATALYSIS OF AMIDE AND PEPTIDE SUBSTRATES BY
 α -CHYMOTRYPSIN AT 25°C

COMPOUND	LOW TEMP. FORM			HIGH TEMP. FORM		
	ΔG^\ddagger kcal/mole	ΔH^\ddagger kcal/mole	ΔS^\ddagger e.u.	ΔG^\ddagger kcal/mole	ΔH^\ddagger kcal/mole	ΔS^\ddagger e.u.
N-ac-Phe-NH ₂	19.10 \pm 0.03	12.62 \pm 0.68	-21.73 \pm 2.38	(19.16 \pm 0.47)	20.02 \pm 4.0	+2.88 \pm 14.99
N-ac-Pro-Phe-NH ₂	(18.07 \pm 0.06)	4.68 \pm 1.5	-44.9 \pm 5.23	18.07 \pm 0.05	15.87 \pm 1.0	-7.38 \pm 3.52
N-ac-Ala-Pro-Phe-NH ₂	(17.35 \pm 0.05)	6.49 \pm 1.1	-36.42 \pm 3.86	17.31 \pm 0.05	15.94 \pm 0.9	-4.6 \pm 3.19
N-ac-Pro-Ala-Pro-Phe-NH ₂	(17.28 \pm 0.05)	7.55 \pm 1.1	-32.63 \pm 3.86	17.25 \pm 0.03	14.77 \pm 0.9	-8.32 \pm 3.12
N-ac-Phe-Gly-NH ₂ ^b	(18.80 \pm 0.04)	8.09 \pm 1.1	-35.92 \pm 3.82	18.79 \pm 0.03	16.72 \pm 1.0	-6.95 \pm 3.45

^a ΔG^\ddagger in parenthesis is calculated from the projected curve for that form of the enzyme at 25°C.

ΔH^\ddagger is calculated from the tangent to the curves of the two forms at 25°C.

ΔS^\ddagger is calculated from the formula $\Delta G = \Delta H - T\Delta S$.

^b Catalysis occurs at the Phe-Gly bond.

temperature form the association step has a large positive ΔH_a^0 and ΔS_a^0 at 25°C, the activation step has both a more negative ΔH^\ddagger and ΔS^\ddagger than the high temperature form. In contrast, the high temperature form at 25°C appears to have a negative ΔH_a^0 and ΔS_a^0 coupled with a more positive ΔH^\ddagger and ΔS^\ddagger than the low temperature form. In fact, in some cases the ΔS^\ddagger for the high temperature form is greater than zero (Table 19).

The data indicate that both temperature-dependent forms of the enzyme have a large positive ΔH term in either the association or the activation step, which reflects either bond distortion upon binding or distortion upon formation of the transition state, respectively (2-4). In addition, both temperature dependent forms of the enzyme have a large negative ΔS term in either the association or the activation step, which has been related to an ordering process of either enzyme and/or substrate (2-4).

Plots of the second order rate constant k_{cat}/K_m in turn, shows an amelioration of the curves found in the association and activation plots to linear relationships (figs. 29-33). Two linear temperature dependent forms of the enzyme are found, with a transition temperature from one form to the other near the temperatures of the discontinuities found in the van't Hoff and Arrhenius plots. The high and low temperature forms both show a decreased positive ΔG^\ddagger , as the substrate size and specificity is increased (Table 20). The low temperature form of the enzyme is characterized by a large positive ΔH^\ddagger and a small variable ΔS^\ddagger which range from negative to positive values. The high temperature form is characterized by a small positive ΔH^\ddagger and a large negative ΔS^\ddagger .

TABLE 20

THERMODYNAMICS OF ACTIVATION FOR THE SECOND ORDER RATE CONSTANT k_{cat}/K_m AT 25°C

COMPOUND	LOW TEMP. FORM			HIGH TEMP. FORM		
	ΔG^\ddagger kcal/mole	ΔH^\ddagger kcal/mole	ΔS^\ddagger e.u.	ΔG^\ddagger kcal/mole	ΔH^\ddagger kcal/mole	ΔS^\ddagger e.u.
N-ac-Phe-NH ₂	17.02 \pm 0.06	15.81 \pm 0.52	- 4.05 \pm 1.95	16.73 \pm 0.09	2.32 \pm 0.26	-48.38 \pm 1.17
N-ac-Pro-Phe-NH ₂	15.83 \pm 0.15	12.37 \pm 0.60	-11.59 \pm 2.52	15.78 \pm 0.10	7.71 \pm 1.28	-27.1 \pm 4.63
N-ac-Ala-Pro-Phe-NH ₂	13.84 \pm 0.12	14.81 \pm 1.53	3.26 \pm 5.53	13.73 \pm 0.08	5.42 \pm 0.11	-27.89 \pm 0.64
N-ac-Pro-Ala-Pro-Phe-NH ₂	13.81 \pm 0.11	16.06 \pm 0.69	7.54 \pm 2.68	13.82 \pm 0.07	6.78 \pm 2.02	-23.61 \pm 7.01
N-ac-Phe-Gly-NH ₂	16.14 \pm 0.08	18.64 \pm 2.19	8.36 \pm 7.61	16.34 \pm 0.05	6.73 \pm 1.04	-32.24 \pm 3.66

^a ΔG^\ddagger is calculated from the second order rate constant at 25°C (Table 14) or from the value on the projected line.

III C. Nonapeptide.

III C-1. pH Stat Titration of Nonapeptide.

Titration of the nonapeptide in 0.1N NaCl under N₂ at 25°C was carried out on a radiometer pH stat titrator against 0.01N NaOH. A difference plot of the quantity of NaOH added versus pH for the nonapeptide minus the quantity of NaOH used to titrate a 0.1N NaCl solution versus pH was calculated (fig. 35). The difference plot showed a pKa for the higher acid group of 6.4 ± 0.2 and a second pKa for the lower acid group of 4.4 ± 0.2 (Table 21). This compares with a pKa of 6.6 for the nonapeptide imidazolium as determined by NMR (Table 21). Free histidine shows a pKa of 6.11 (corrected for ionic strength (142)) and a pKa of 6.8 for the His-57 in Cht (141).

III C-2. Kinetics of Nonapeptide Catalyzed Hydrolysis of p-Nitrophenyl Acetate.

The rate of hydrolysis of p-nitrophenyl acetate by the nonapeptide in 0.05M sodium phosphate, pH 7.0 buffer was followed at 400nm ($\epsilon = 1.06 \times 10^4 / \text{M/cm}$). Similarly the rates of hydrolysis of pNPA by α -chymotrypsin and histidine were also studied. An observed second order rate constant was calculated by equation 3.1

$$k_{\text{II(app)}} = \frac{k_{\text{obs}}}{(\text{pNPA})(C)}, \quad (3.1)$$

where k_{obs} is the observed initial rate corrected for the spontaneous hydrolysis rate, pNPA the p-nitrophenyl acetate concentration, and C the catalyst concentration. A pH independent rate constant ($k_{\text{II(lim)}}$)

LEGEND

Figure 35. pH Stat Titration of Nonapeptide.

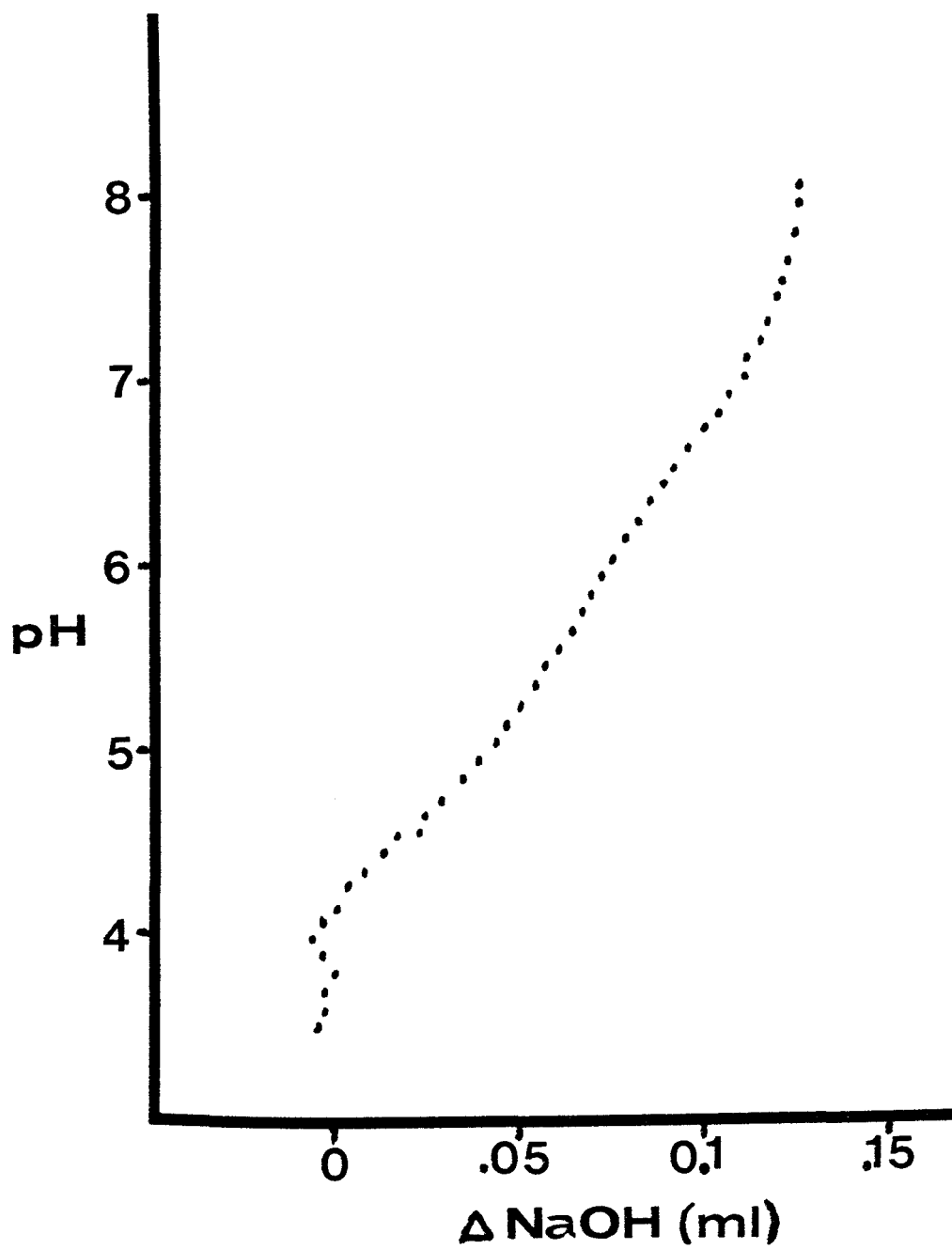


TABLE 21

PROFLAVIN BINDING CONSTANTS AND SECOND ORDER RATE CONSTANTS FOR THE
HYDROLYSIS OF p-NITROPHENYL ACETATE BY THE NONAPEPTIDE:
COMPARISON WITH α -CHYMOTRYPSIN AND MODEL SYSTEMS.

COMPOUND	pNPA ^a		PROFLAVIN
	pKa _{IM}	k _{II(lim)} (M ⁻¹ S ⁻¹)	K _I (M)
Nonapeptide	6.4 ^b	6.61 x 10 ⁻²	1.3 x 10 ⁻³ ^d
	6.4 ^c	7.38 x 10 ⁻²	2.8 x 10 ⁻⁴ ^e
Histidine	6.11 ^f	3.69 x 10 ⁻²	-----
Cht	6.8	1.73 x 10 ¹	2.7 x 10 ⁻⁵
N-Acetyl-Tryptophane	--	-----	1.4 x 10 ⁻¹

^a 25°C, 0.05M sodium phosphate, 0.1N NaCl.

^b pKa determined by NaOH titration.

^c pKa determined by NMR titration, corrected for D₂O effect (143).

^d K_I calculated using difference extinction coefficient from Cht (9).

^e K_I calculated using difference extinction coefficient from N-Acetyl-Tryptophane (9).

^f Free histidine in distilled water shows a pKa of 6.0 (144), at ionic strength (μ) of 0.1 pKa = 6.11 (143).

was then calculated by equation 3.2:

$$k_{II(lim)} = k_{II(app)} \left[1 + \frac{(H^+)}{K_a} \right], \quad (3.2)$$

where K_a is the acid dissociation constant of the imidazolium group in the catalyst. A pK_a of 6.11 was used for histidine, pK_a 's of 6.4 and 6.8 (in D_2O) for the imidazolium of the nonapeptide, and a pK_a of 6.8 for Cht (Table 21).

The second order rate constants reported in Table 21 show that the nonapeptide catalyzed hydrolysis of pNPA is 1.8 to 2.0 fold faster than that of histidine, while the Cht-catalyzed hydrolysis is approximately 250 fold faster than that found for the nonapeptide.

III C-3. Proflavin Binding to Nonapeptide.

Proflavin binding studies were done with the nonapeptide by Richard M. Schultz (145) by procedures previously described (9,44). The K_I or binding constant of proflavin is calculated at 465nm by the equation

$$K_I = \frac{\left[P_0 - \frac{\Delta A_{465}}{\Delta E_{465}} \right] \left[C_0 - \frac{\Delta A_{465}}{\Delta E_{465}} \right]}{\frac{A_{465}}{\Delta E_{465}}}, \quad (3.3)$$

where ΔE_{465} is the difference extinction coefficient for the proflavin-peptide complex, P_0 the initial proflavin concentration, and C_0 the initial nonapeptide concentration. As the ΔE_{465} for the proflavin-peptide complex is not known, the ΔE_{465} previously found for the complex of proflavin and Cht ($\Delta E_{465} = 2.23 \times 10^4 / M/cm$ (9)) and for the complex

of proflavin with the acetylated mon-amino acid N-Acetyl-L-tryptophane (AcTry) ($\Delta E_{465} = 5.83 \times 10^3 / \text{M/cm}$ (9)) were utilized as approximations for the ΔE_{465} of proflavin-peptide. These two extinction coefficients may serve as extremes for the boundaries of the possible difference extinction coefficient for the complex of proflavin with nonapeptide in which two phenyl rings may complex with proflavin.

Based on an observed ΔA_{465} of 0.014 for the proflavin-peptide complex, the K_I values calculated are $1.3 \times 10^{-3} \text{ M}$ and $2.8 \times 10^{-4} \text{ M}$. As the K_I values previously found for proflavin association to AcTrp is $1.4 \times 10^{-1} \text{ M}$ and to Cht is $2.7 \times 10^{-5} \text{ M}$ (9), the peptide appears to bind proflavin two to four orders of magnitude stronger than AcTrp and one to two orders of magnitude less strongly than Cht.

CHAPTER IV

DISCUSSION

IV A. Conclusions.

Several conclusions can be drawn based upon the results of this dissertation.

- i) There are two temperature dependent forms of α -chymotrypsin. The existence of two temperature dependent forms of Cht is based upon the van't Hoff and Arrhenius plots of the binding constants (K_s) and catalytic constants (k_{cat}/K_m) for N-acyl peptide substrates, which show a sharp discontinuity.
- ii) The physiological temperature in vivo for Cht is 37°C. However, most physical and kinetic studies of Cht are done at 25°C where the concentration of the two forms of Cht are approximately in equimolar amounts. The results would, therefore, be 'averaged' data composed of components from both forms.
- iii) van't Hoff and Arrhenius plots of the binding and catalytic constants may best fit curvilinear lines showing a significant positive ΔC_p^0 in the binding step and a negative ΔC_p^0 in the catalytic step.
- iv) Both the enthalpy and entropy of association for both the high and low temperature forms of Cht show a large temperature dependence with a positive increase in both values with increasing temperature for the two forms. However, the large increases in enthalpy and entropy are compensating and result in significant

small changes in the free energy.

- v) Association-activation mechanisms are not observed in the free energy of substrate association (i.e. $\Delta G_{a(\text{obs})} = \Delta G_i + \Delta G_{aa}$). An alternative or more complex thermodynamic mechanism must, therefore, be put forth to account for association-activation.
- vi) There appears to be a coupled inverse relationship in the respective amount of ordering carried out in the binding and catalytic steps. For example, substrates binding to the high temperature form of Cht at 25°C have larger negative entropies of binding and less negative (more positive) entropies of activation for the catalytic step, following the binding step. In contrast, substrate binding to the low temperature form of Cht has large positive entropies of binding and large negative entropies of activation for the catalytic step.
- vii) The peptide substrates that bind to the S_1 , S_2 , and S_3 sites showed a greater specificity for Cht than peptide substrates that associate only at S_1 , as shown by the second order rate constant k_{cat}/K_m . Binding to the S_4 site showed a slight decrease in k_{cat}/K_m due to a small increase in k_{cat} , with a larger unfavorable increase in K_m . Longer chain substrates were entropically more specific at all temperatures, requiring less ordering overall in the binding and catalytic step.
- viii) The positive ΔC_p^0 observed for the binding step K_s and negative ΔC_p^0 observed for the catalytic step k_2 cancel out for the second order rate constant (k_{cat}/K_s), which correlates with the process



Thus it is the ES complex that appears to demonstrate the variation of enthalpy with temperature.

- ix) The significant differences in enthalpy and entropy for the association and catalysis of substrates by the two conformational forms of Cht whose concentration is temperature-dependent implies that there exists two different mechanisms for the binding and catalysis of substrates, both of which give similar rates of catalysis.

IV. B. Two Temperature Dependent Forms of α -Chymotrypsin.

IV. B-1. Kinetic and Thermodynamic Evidence for Two Temperature Dependent Forms of α -Chymotrypsin.

This work supports the hypothesis of two temperature dependent forms of Cht (Section III B, Results Section). The existence of two temperature dependent forms of Cht has been proposed previously (Section I C-4, Introduction Section).

Previous investigators (45,52,55,57) have proposed two temperature dependent forms of Cht with a transition temperature around 25°C, based upon difference in the thermodynamic parameters above and below 25°C. Similar discontinuous differences were found in this work for the kinetic parameters K_s , k_2/K_s and possibly k_2 (figs. 19-33).

van't Hoff plots of the association step K_m (figs. 19-23) indicate a minimum of six data points that can best be resolved to two curvilinear lines with a minima. Although, Arrhenius plots of the catalytic constant k_2 (kcat) appear more linear, they may be resolvable into two curvilinear lines which display maxima instead of minima. However, these plots of two curvilinear figures appear to be resolved to two straight line relationships in an Arrhenius plot of the second order rate constant, k_{cat}/K_m (figs. 29-33).

It has been argued by Kumamoto et al. (146) and Londesborough (147) that sharply bent or discontinuous Arrhenius plots could be caused by different temperature dependencies for the rate constants of the different steps of an enzymatic reaction. However, of the workers who have proposed two temperature dependent forms of Cht, based upon their kinetic

results, all have argued that the discontinuity is not due to a change in the rate determining step of the reaction (45,52,55,57).

Direct physical methods which are independent of kinetic rate controlling steps, also indicate two temperature dependent forms of Cht. Spectrophotometric studies have shown sharp changes in the temperature dependence of both the fluorescence and absorbance of Cht above and below 25°C (58-60). The temperature dependence of the oxidation of surface methionine showed a sharp increase at 25°C for Cht and 30°C for chymotrypsinogen (61). Recently, Matta et al. (148) studied Cht with NMR techniques and showed two signals were present for Cht which had been labeled with carbon-13 on the methionine-192 residue. They interpreted these results to be indicative of two conformational forms of Cht at pH 7.0.

One of the most interesting studies of Cht was done by Ruegg and co-workers (50,62) who studied the thermodynamics of the water sorption process of Cht. They found distinct differences in the thermodynamic parameters above and below the temperature range 295-298°K for the water sorption process of the first or primary monolayer of water (denoted as V_m , the monolayer volume). Changes in the partial molar enthalpy for the water sorption process below the V_m (70 moles H_2O /mole Cht) were opposite in sign for the high temperature form (295.5-313°K) versus the low temperature form (283-295.5°K). Above the V_m , the changes in enthalpy and entropy terms showed a parallel decrease in value. In addition, all changes in the enthalpy were accompanied by a covariant compensating change in the entropy term. These data led Ruegg and co-workers to propose a temperature transition in the enzyme protein structure similar to what we are suggesting based upon our kinetic and binding data.

IV B-2. Enthalpy and Entropy Change Effects in Generating a Non-Linear van't Hoff Plot.

The proposal of the existence of two temperature dependent forms of Cht based upon both kinetic and physical methods has been described (37,38,45,50,52,55,57-62) and is strongly supported in this work (III B, Results Section).

If, indeed, a temperature dependent equilibrium between a high and low temperature form of Cht exists, with physical and chemical differences, then a mathematical model of the system can be proposed based upon these differences to explain the contribution of each of the forms to an observed phenomena. For example, Kim and Lumry have proposed such a model to explain the temperature dependent changes in the intrinsic fluorescence of Cht (58).

This work has proposed two temperature dependent forms of Cht based upon the temperature dependence of binding and catalysis of a series of highly specific peptide amide substrates (Section III B). Furthermore, this work proposes that the binding step exhibits a positive heat capacity change for both forms of the enzyme. In addition, binding to the high temperature form of the enzyme at 25°C is characterized by a more negative enthalpy of binding (ΔH_a^0) than binding to the low temperature form at 25°C (Tables 16,17; fig. 34). Lastly, the temperature dependent positive changes in the enthalpy of binding (heat capacity changes) exhibited by both forms are accompanied by a concomitant compensatory positive, temperature dependent change in entropy resulting in only small changes in the free energy of binding. This compensatory change in enthalpy and entropy with resultant small changes in free energy on substrate analog association has been also observed by other workers (9,35,36,44,45).

A theoretical model will be constructed to show how changes in enthalpy and/or entropy for two temperature dependent forms of a model enzyme 'X' can give observed (overall) van't Hoff plots similar to those found for Cht (figs. 19-23).

A temperature dependent equilibrium is defined for enzyme X between a high and low temperature conformational form



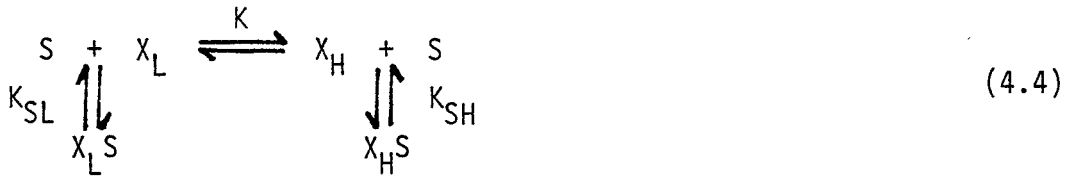
with an equilibrium constant K

$$K = \frac{(X_H)}{(X_L)} \quad (4.2)$$

If we arbitrarily assume that temperature dependent changes in K result in a -10 kcal/mole change in the standard free energy change for the equilibrium process over the forty degree temperature range of 5° to 45°C, and the concentration of the two forms is equal at 25° (K=1), we can construct a table from equation 4.3 giving the percent of enzyme X in the high and low temperature conformations at a given temperature (Table 22).

$$\Delta G^{\circ} = -RT \ln K \quad (4.3)$$

The constant K is the equilibrium constant for the equilibrium process between the low and high temperature forms of free enzyme X. If substrate S is then added to the two enzyme conformation system and S can bind to both forms of enzyme X, we have the equilibrium defined in equation 4.4



where K_{SL} and K_{SH} are the binding constants (Michaelis dissociation constants, equation 1.7) for the low and high temperature forms, respectively. The new equilibrium relationship between the two forms is expressed as

$$K' = \frac{X_H + X_H S}{X_L + X_L S} \quad (4.5)$$

where K' is the equilibrium constant for the total enzyme in the high and low temperature forms, X_H and X_L is free enzyme, and $X_H S$ and $X_L S$ are the respective enzyme substrate Michaelis complexes for the high and low temperature forms. The relationship between K and K' (equation 4.6) has been derived in appendix A. The relationship

$$K' = K \frac{\left(1 + \frac{S}{K_{SH}}\right)}{\left(1 + \frac{S}{K_{SL}}\right)} \quad (4.6)$$

shows the dependence of K' on the substrate concentration. If we take the limit of equation 4.6 both as substrate goes to zero or to infinity, we find that at low substrate concentrations

$$\lim_{S \rightarrow 0} K' = K \quad (4.7)$$

while at high substrate concentration

$$\lim_{S \rightarrow \infty} K' = K \frac{(K_{SL})}{(K_{SH})} \quad (4.8)$$

The observed enzymatic velocity will be equal to the sum of the velocities of the high and low temperature forms of X,

$$v_{\text{obs}} = v_l + v_h = \frac{V_L(S)}{K_{SL} + (S)} + \frac{V_H(S)}{K_{SH} + (S)} \quad (4.9)$$

Also at high substrate concentrations, with $(S) \gg K_{SL}$ and K_{SH}

$$V_{\text{max(obs)}} = V_L + V_H \quad (4.10)$$

where V_L and V_H are the V_{max} for the low and high temperature forms of the enzyme. Since from equation 1.8, and

$$v = \frac{k_{\text{cat}}(E)(S)}{K_m + S}; \quad k_{\text{cat}}(E) = V_{\text{max}}$$

substituting equation 1.8 into 4.5 we find

$$\frac{V_{\text{max(obs)}}(S)}{K_{m(\text{obs})} + S} = \frac{V_L(S)}{K_L + S} + \frac{V_H(S)}{K_H + S} \quad (4.11)$$

where $V_{\text{max(obs)}}$ and $K_{m(\text{obs})}$ are the observed maximum velocity and binding constant for the mixed reaction, and K_L and K_H are the binding constants for the low and high temperature forms of enzyme X, respectively. After a simple algebraic manipulation, we can show the

$$\frac{V_{\text{max(obs)}}}{\frac{K_{m(\text{obs})}}{(S)} + 1} = \frac{V_L}{\frac{K_L}{(S)} + 1} + \frac{V_H}{\frac{K_H}{(S)} + 1} \quad (4.12)$$

which shows that the equation is complex. Conversion to a Lineweaver-Burk plot of $1/v$ vs $1/S$ (equation 1.10) shows that in the regions of $(S) = K_L$ and K_H , a curvilinear plot would be expected. This problem is less complicated if we restrict our model system to high substrate concentrations relative to both K_L and K_H . Frankfater (151) and others (152,153) have shown that at high substrate concentrations (as $1/S \rightarrow 0$) the Lineweaver-Burk plot takes the following form of equation 4.13 (see appendix B for entire derivation)

$$\frac{1}{v} = \frac{K_L V_L + K_H V_H}{(V_L + V_H)^2} \left(\frac{1}{(S)} + \frac{1}{V_L + V_H} \right) \quad (4.13)$$

Equation 4.13 resembles the common Lineweaver-Burk equation (equation 1.10)

$$\frac{1}{v} = \frac{K_m}{k_{cat}} \left(\frac{1}{(S)} + \frac{1}{V_{max}} \right)$$

From the reciprocal of equation 4.10 we know that

$$\frac{1}{V_{max(obs)}} = \frac{1}{V_L + V_H} \quad (4.14)$$

Combining equations 4.13, 1.10, and 4.14 we find that at high substrate concentrations where $(S) \gg K_L$ and K_H

$$K_m = \frac{K_L V_L + K_H V_H}{V_L + V_H} \quad (4.15)$$

We can consider three cases using different thermodynamic parameters to describe a two enzyme equilibrium system under conditions of $(S) \gg K_L$ and K_H and a 10 kcal/mole free energy change for K (equation 4.2, Table 22). In the first case we will give only a positive heat capacity

TABLE 22

EFFECT OF CHANGES IN ΔG° ON THE EQUILIBRIUM OF ENZYME X BETWEEN A
HIGH AND LOW TEMPERATURE FORM.

TEMP. °C	ΔG° kcal/mole	K $(x_H)/(x_L)$	LOW TEMP. %	HIGH TEMP. %
5	+ 5,000	0.00012	99.99	0.01
10	+ 3,750	0.00127	99.9	0.1
15	+ 2,500	0.0127	98.7	1.3
20	+ 1,250	0.117	89.5	10.5
25	0	1.00	50.0	50.0
30	- 1,250	7.94	11.2	88.8
35	- 2,500	59.17	1.7	98.3
40	-3,750	416.7	0.2	99.8
45	- 5,000	2,703.	0.04	99.96

change to the two enzyme forms and set the entropy for the process equal to zero, so that the K_m will vary with the change in ΔH^0 only. If we set $\Delta C_p^0 = 25 \text{ cal/mole/}^\circ\text{C}$ and start with values of ΔH^0 that give us binding constants in the region of from 5 to 50 mM we can generate a table of values (Table 23) showing the K_m at every 5°C for both forms (K_L and K_H). A K_m observed for the two enzyme form system can then be calculated from equations 4.2, 4.3, and 4.8. Graphing the system (fig. 36) gives a complex van't Hoff plot not unlike that found for the peptide amide substrates (figs. 19-23).

In a second, more relative case, the model system is given both a positive heat capacity ($\Delta\Delta H$)_T and a positive covariant temperature dependent compensating change in entropy ($\Delta\Delta S$)_T. Again, values were picked to keep within a certain range of K_m . However, a heat capacity change 20 times larger than that in case one, of $500 \text{ cal/mole/}^\circ\text{C}$, is used. A compensating ΔS^0 of $1.65 \text{ e.u./}^\circ\text{C}$ and $1.5 \text{ e.u./}^\circ\text{C}$ was used for the low and high temperature forms of Cht to keep the observed K_m in the range of 10 to 30 mM (Table 24). Graphing the resultant K_m observed data from Table 25 (fig. 37) gives a figure shaped somewhat like a 'W' as was found for the peptide amide substrates.

A third case of a constant ΔH^0 and a positive temperature dependent change in ΔS^0 would give a figure similar to figure 37 since the entropy contribution would become more favorable with increasing temperature and the K_m would, therefore, decrease.

In addition, if the transition between the high and low temperature forms of Cht occurred over a smaller temperature range due to a greater ΔC_p^0 for the equilibrium K (equation 4.2) such as suggested by Kim and Lumry (58) or even a 3° range as suggested by Adams and Swart (55), the

TABLE 23

CHANGES IN K_m DUE TO A POSITIVE HEAT CAPACITY CHANGE^a

TEMP. °C	ΔH_L^0 cal/mole	K_L^0 (mM)	ΔH_H^0 cal/mole	K_H^b (mM)	K'^c	K_m (app) ^d (mM)
5	- 2,550	9.91	- 3,225	2.92	0.0004	9.91
10	- 2,425	13.43	- 3,100	4.05	0.0042	13.39
15	- 2,300	18.00	- 2,975	5.54	0.0412	17.51
20	- 2,175	23.9	- 2,850	7.5	0.373	19.45
25	- 2,050	31.42	- 2,725	10.05	3.125	15.23
30	- 1,925	40.94	- 2,600	13.35	24.39	14.44
35	- 1,800	52.88	- 2,475	17.56	178.6	17.76
40	- 1,675	67.75	- 2,350	22.9	1,235.	22.94
45	- 1,550	86.13	- 2,225	29.61	7,874.	29.61

^a $C_p^0 = 25$ cal/mole/°C for both forms of enzyme.

^b $\Delta G^0 = \Delta H^0$ and K_L and K_H are calculated from $\Delta G^0 = -RT \ln K$.

^c Based upon equilibrium in Table 22 and equation 4.8.

^d Calculated from equation 4.15, assuming $k_{cat_L} = k_{cat_H}$.

LEGEND

Figure 36. Change in Binding Constants of Two Temperature Dependent Forms of Enzyme 'X' Due to a Positive Heat Capacity Change.

Low temperature form ● ; high temperature form ■ ; combined or $K_{m(\text{app})}$ ○. Data from Table 23.

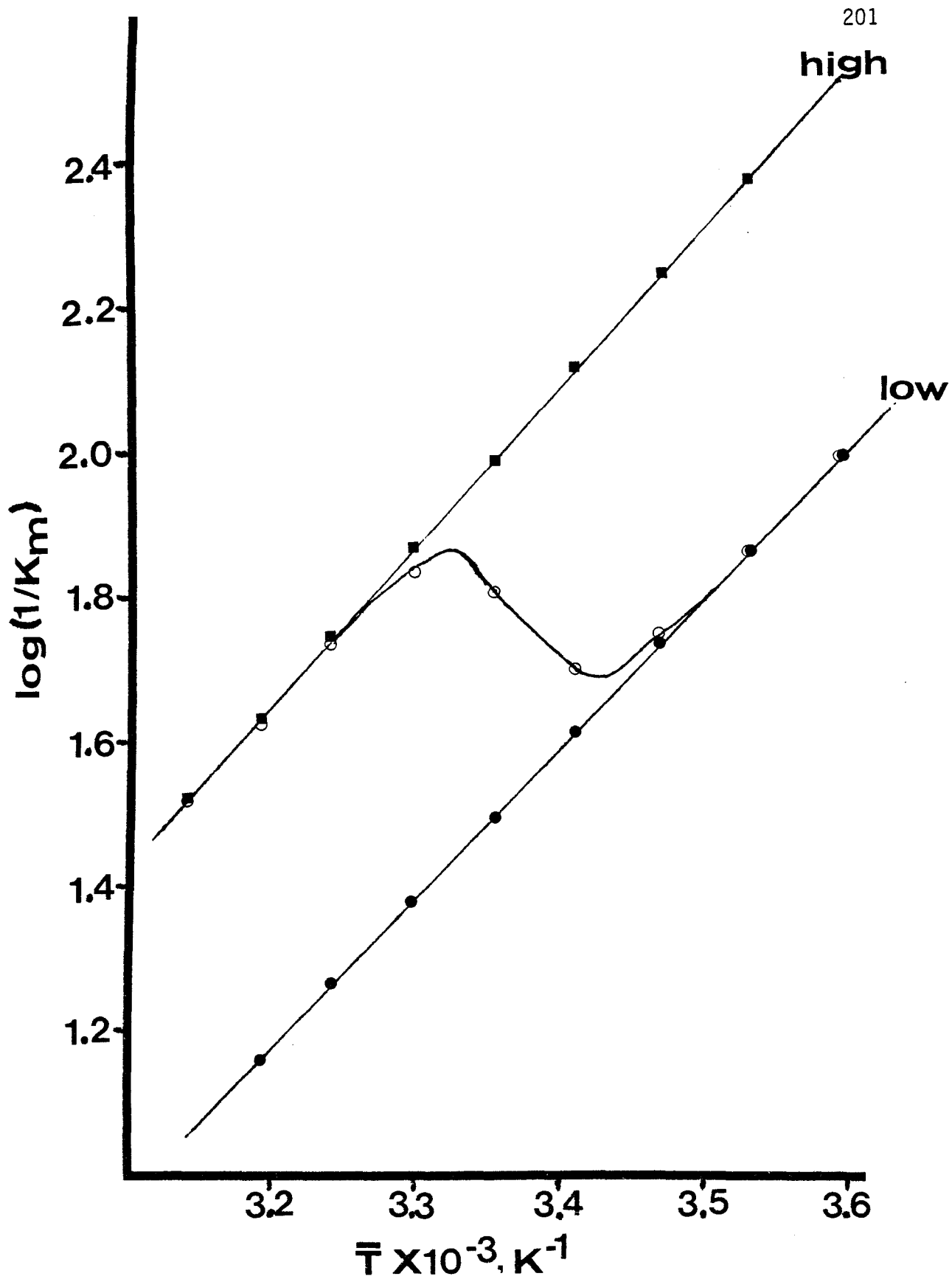


TABLE 24

THERMODYNAMIC PARAMETERS FOR TWO TEMPERATURE DEPENDENT FORMS OF ENZYME 'X' BASED UPON

COMPENSATING CHANGES IN ΔH° AND ΔS° .^a

TEMP. °C	ΔC_{L}° ^b cal/mole	ΔH_{L}° cal/mole	ΔS_{L}° e.u.	$-T \Delta S_{L}^{\circ}$ cal/mole	ΔG_{H}° ^b cal/mole	ΔH_{H}° cal/mole	ΔS_{H}° e.u.	$-T \Delta S_{H}^{\circ}$ cal/mole
5	- 2,500	- 5,000	- 9.0	+ 2,500	- 4,542	- 15,000	- 37.6	+ 10,458
10	- 2,288	- 2,500	- 0.75	+ 212	- 3,977	- 12,500	- 30.1	+ 8,523
15	- 2,161	0	+ 7.5	- 2,161	- 3,488	- 10,000	- 22.6	+ 6,512
20	- 2,117	+ 2,500	+ 15.75	- 4,617	- 3,073	- 7,500	- 15.1	+ 4,427
25	- 2,156	+ 5,000	+ 24.0	- 7,156	- 2,734	- 5,000	- 7.6	+ 2,266
30	- 2,277	+ 7,500	+ 32.25	- 9,777	- 2,470	- 2,500	- 0.1	+ 30
35	- 2,480	+ 10,000	+ 40.5	- 12,480	- 2,284	0	+ 7.4	- 2,280
40	- 2,766	+ 12,500	+ 48.75	- 15,266	- 2,166	+ 2,500	+ 14.9	- 4,666
45	- 3,134	+ 15,000	+ 57.00	- 18,134	- 2,400	+ 5,000	+ 22.4	- 7,400

^a $\Delta C_{p}^{\circ} = +500$ cal/mole/°C for both forms. $\Delta \Delta S^{\circ} = +1.65$ e.u./°C for the low temperature form and +1.5 e.u./°C for the high temperature form.

^b ΔG° calculated from $\Delta G^{\circ} = \Delta H^{\circ} - T \Delta S^{\circ}$.

CHANGES IN K_m DUE TO A POSITIVE HEAT CAPACITY CHANGE AND A
POSITIVE TEMPERATURE DEPENDENT CHANGE IN ΔS° .^a

TEMP. °C	K_L^b (mM)	K_H^b (mM)	K^c	$K_{m(app)}^d$ (mM)
5	10.85	0.27	0.00474	10.80
10	17.13	0.85	0.0257	16.72
15	22.95	2.26	0.129	20.59
20	26.4	5.11	0.606	18.39
25	26.27	9.9	2.65	14.38
30	22.82	16.56	10.94	17.08
35	17.42	24.0	42.9	23.85
40	11.73	30.77	159.	30.65
45	7.02	22.45	847.	22.43

^a $\Delta C_p^\circ = +500$ cal/mole/°C for both forms. $\Delta \Delta S^\circ = +1.65$ e.u./°C. for low temperature form and $+1.5$ e.u./°C for high temperature form.

^b Calculated from ΔG° values in Table 24 using equation $\Delta G^\circ = -RT \ln K$.

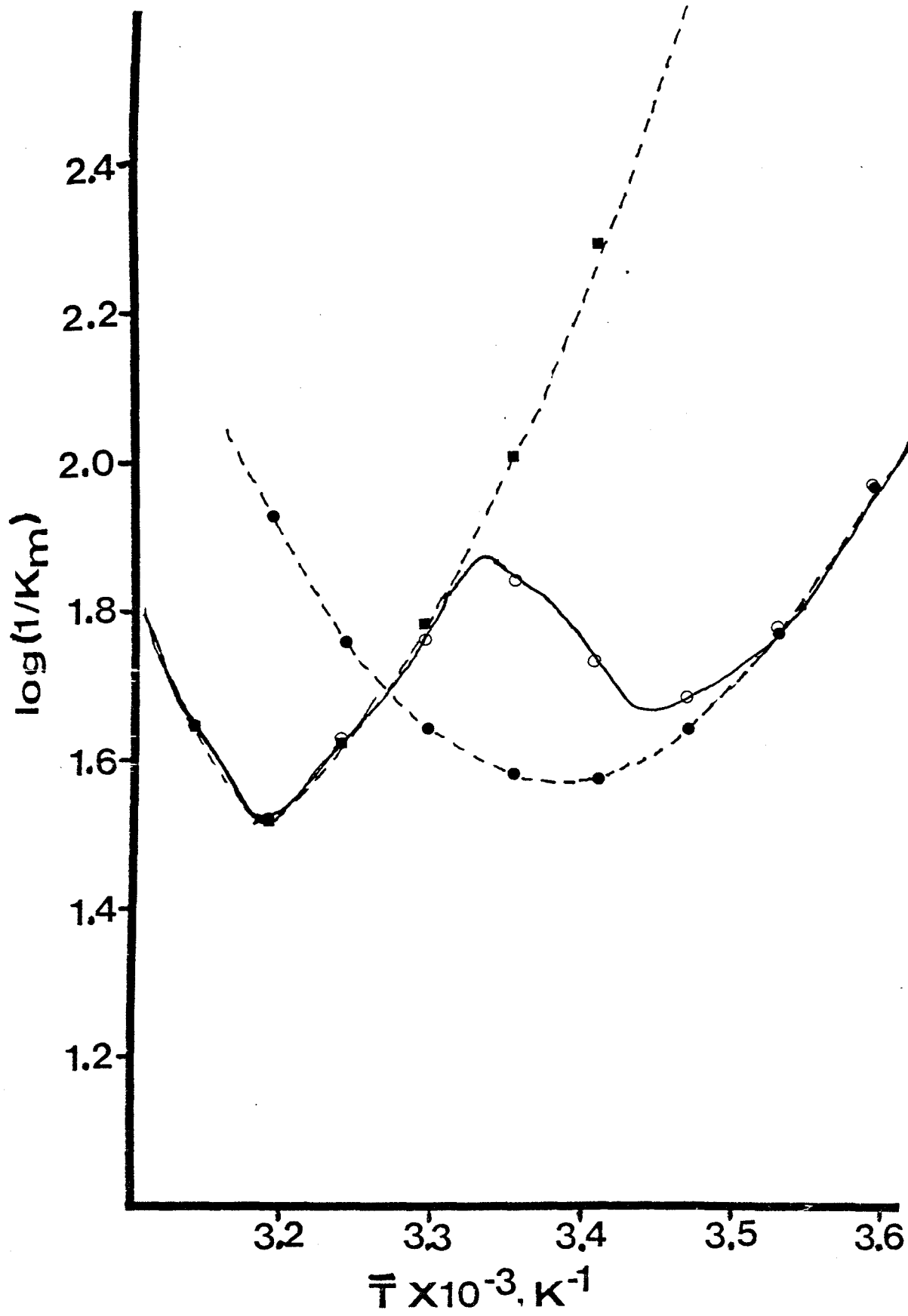
^c Based upon equilibrium in Table 22 and equation 4.8.

^d Based upon equation 4.15.

LEGEND

Figure 37. van't Hoff Plot of Binding Constants of Two Temperature Dependent Forms of Enzyme 'X' Due to a Positive Heat Capacity Change and a Compensating Positive Temperature Dependent Change in ΔS^0 with ΔH^0 .

Low temperature form ●; high temperature form ■; combined or $K_{m(\text{app})}$ ○. Data from Table 25.



discontinuity would be much sharper and over a smaller temperature range.

A more realistic calculation would utilize experimentally determined values for the temperature dependency of ΔH and the compensatory changes in ΔS for the two enzyme forms. Accordingly, for any of the peptide substrates one can calculate $\Delta\Delta H/\Delta T (= \Delta C_p)$ and the $\Delta\Delta S/\Delta T$ in the temperature regions where only the low or high temperature dependent enzyme form predominates. These calculated values of $\Delta\Delta H_a^0/\Delta T$ and $\Delta\Delta S_a^0/\Delta T$ can then be used to obtain extrapolated values for the binding constants of each form into the temperature region in which the other form predominates. An overall van't Hoff plot can then be calculated for the combined forms in equilibrium as in case two and the similarity to the actual plot for that substrate can be determined.

Analysis of the van't Hoff plot for the association of the substrate N-acetyl-Alanine-Proline-Phenylalanine-amide with Cht (fig. 21) indicates a high and low temperature form of Cht with a temperature dependent enthalpy and entropy of association assuming a constant ΔC_p^0 and ΔS_a^0 over the temperature range (Table 26). The enthalpies and entropies of association for the low temperature form of Cht was extrapolated from the temperature dependent change in ΔH_a^0 and ΔS_a^0 between 5° and 12° where the concentration of the high temperature form of Cht will make an insignificant contribution to the thermodynamic and kinetic data. Similarly, the high temperature form enthalpies and entropies of association were generated from the temperature dependent changes in ΔH_a^0 and ΔS_a^0 between 31° and 37°C where the concentration of the low temperature conformational form will make a minimum contribution. Accordingly, the more realistic equilibrium constant K' can be calculated from equation 4.6 for each temperature from the extrapolated binding constants (using 6mM as a substrate

TABLE 26

THERMODYNAMIC PARAMETERS AND ASSOCIATION CONSTANTS FOR THE ASSOCIATION OF N-Ac-Ala-Pro-Phe-NH₂
WITH THE TWO TEMPERATURE DEPENDENT FORMS OF CHT FROM 5° TO 37°C,^a

TEMP. °C	LOW TEMPERATURE FORM ^b				HIGH TEMPERATURE FORM ^c			
	ΔG_a° cal/mole	ΔH_a° cal/mole	ΔS_a° e.u.	K_L (mM)	ΔG_a° cal/mole	ΔH_a° cal/mole	ΔS_a° e.u.	K_H (mM)
5	- 3,087	- 5,830	- 9.86	3.75±0.58	- 5,416	- 24,180	- 67.46	0.06
12	- 3,135	2,820	20.88	3.95±0.2	- 4,605	- 19,595	- 52.57	0.3
19	- 3,609	11,472	51.62	2.0	- 4,005	- 15,010	- 37.67	1.01
25	- 4,359	18,888	77.97	0.64	- 3,656	- 11,080	- 24.9	2.09
31	- 5,422	26,304	104.31	0.13	- 3,462	- 7,150	- 12.13	3.25±0.35
37	- 6,804	33,720	130.66	0.02	- 3,420	- 3,220	0.64	3.89±0.38

^a Two forms were calculated using 5° and 12°C data and extrapolating for the low temperature form and 31° and 37°C data for the high temperature form.

^b $\Delta H_a^{\circ}/T = 1,236$ cal/mole/°C; $\Delta S_a^{\circ}/T = 4.391$ e.u./°C.

^c $\Delta H_a^{\circ}/T = 655$ cal/mole/°C; $\Delta S_a^{\circ}/T = 2.128$ e.u./°C.

concentration since the range of substrate was 1.33 to 9.48 mM (Table 14)). In this way, an observed K_m for the combined process can then be calculated from equation 4.15 using the K values calculated for the equilibrium between the high and low temperature forms of Cht in Table 22 (Table 27).

A van't Hoff plot of the data (fig. 38) generates a figure similar to that found for the real enzyme substrate data (fig. 21). In addition, the model shows that the concentration of the low temperature form decreases by 75%, while the concentration of the high temperature form increases by 75% in the temperature range of 19° to 31°C. This correlates well with the large changes in fluorescence (58,59) and other parameters (45,50,52,55,57,60-62) for Cht over a relatively small temperature range.

Thus, models based on a temperature controlled equilibrium process between two temperature dependent forms of Cht may generate a van't Hoff plot similar to those observed for our substrates.

TABLE 27

PREDICTED OBSERVED ASSOCIATION CONSTANT FOR N-Ac-Ala-Pro-Phe-NH₂ WITH CHT BASED UPON TWO TEMPERATURE DEPENDENT FORMS OF CHT IN EQUILIBRIUM.^a

TEMP. °C	^b K $\frac{(E_L)}{(E_H)}$	^c K $\frac{(E_{LT})}{(E_{HT})}$	% LOW	% HIGH	^d K _{m(app)} ($\frac{M}{M}$)
5	0.00012	0.000706	99.93	0.07	3.75
12	0.00323	0.00974	99.04	0.96	3.92
19	0.0757	0.1214	89.17	10.83	3.05
25	1.00	0.935	51.68	48.32	2.35
31	11.97	6.14	14.01	85.99	2.98
37	130.1	33.2	2.92	97.08	3.80

^a See text.

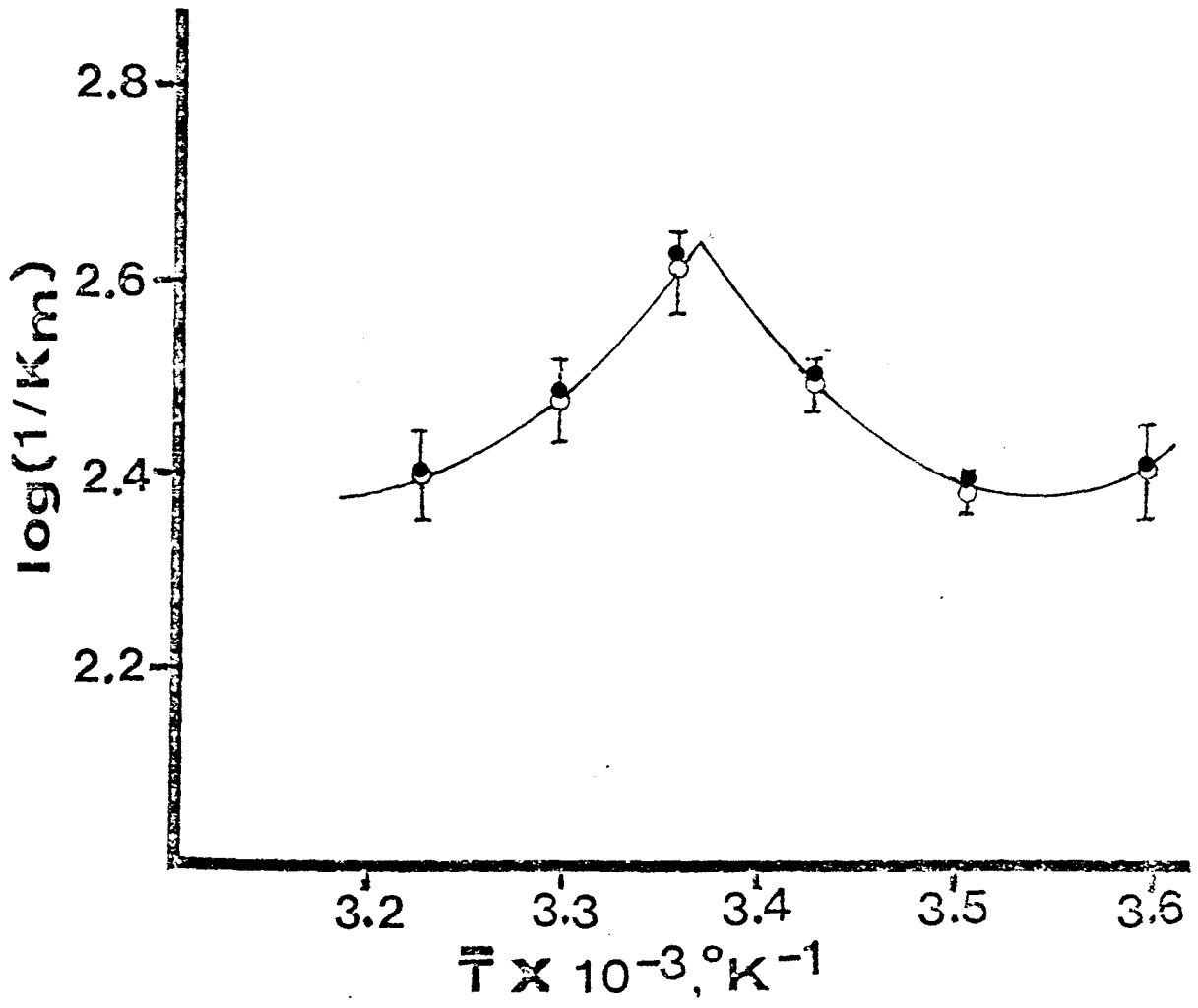
^b From Table 22.

^c From equation 4.6.

^d From Table 26 and equation 4.15.

LEGEND

Figure 38. van't Hoff Plot of Predicted Observed Binding Constants for N-Ac-Ala-Pro-Phe-NH₂ with Cht Versus Actual Observed Data.
Actual data from figure 21, ○; predicted data, ●.



IV B-3. Interpretation of Curved Van't Hoff Plots.

The van't Hoff equation or isochore

$$\frac{d \ln k}{d 1/T} = - \frac{\Delta H^0}{R} \quad (4.16)$$

can be found in any standard thermodynamic text (149,150). The equation holds for a two state equilibrium process at constant pressure and concentration (the equilibrium system is a closed system where reactants can only go from A \rightarrow B and B \rightarrow A). The change in the log of the equilibrium constant K with respect to the change in the reciprocal of the temperature in 0K is controlled by the value of the enthalpy term for the process. One can in turn, calculate the enthalpy term for the process from a plot of $\ln K$ vs $1/T$ (149,150). If the enthalpy change for the process varies with temperature the resultant van't Hoff plot will be curved (2,34,149,150).

Van't Hoff plots of the model partition data in Section III A (figs. 9-17) all showed a linear relationship for the transfer process, showing that the enthalpy for the process is constant over the temperature range measured. However, van't Hoff plots of the temperature dependence of the binding constant K_m to Cht (figs. 19-23) show a complicated discontinuous curvilinear relationship for the five peptide amide substrates studied.

The thermodynamic analysis presented in the Results Section (III B-2) was based upon a straightforward analysis of the van't Hoff plots, with the ΔH_a^0 determined from the slope of the graph in linear areas or from the tangents to the line in non-linear areas. However, our analysis in the previous section shows that analysis of the van't Hoff plot in the

region of intermediate temperatures (15° to 30°C) is probably complex. For example, the first model was based upon the hypothesis of two temperature dependent forms of the enzyme with a transition point around 25°C , as is suggested by our analysis of the data in Section III B. This gives a system composed of more than two states over the temperature range studied, with the concentrations of the two enzyme forms, E_L and E_H , changing with temperature. At low temperatures, the equilibrium process for the binding constant K_m would consist of a two state system with free substrate S and enzyme E_L in equilibrium with the complex $E_L S$. At middle temperatures, where both enzyme forms are present, we would have both free S, E_L and E_H in equilibrium with the complexes $E_L S$ and $E_H S$, respectively. At high temperatures the system would be composed of both free S and E_H in equilibrium with the complex $E_H S$. Accordingly, only the data from the high and low temperature extremes of the experiment can be clearly interpreted using a van't Hoff analysis.

IV B-4. Model Partition Studies Versus Enzyme-Substrate Association.

Interpretation of enthalpy and entropy data for the association of enzyme with substrate is, at best, a speculative venture. Thermodynamic values observed for the association process may represent a composite of complex processes including desolvation of substrate and the enzyme binding site with the resultant changed solvation of the complex, as well as reflect contributions from non-covalent interactions between the enzyme and substrate. In addition, changes in conformation of the enzyme and/or substrate may also contribute to the observed enthalpy-entropy data. Furthermore, according to association-activation theories of enzymatic catalysis, a part of the binding energy is used to lower the energy of activation for the catalytic process. Elucidation of the contributions of each of these processes is necessary for a thorough understanding of enzymatic binding and catalysis (1-5,9).

Partition studies between aqueous and hydrophobic solvents have been used to study the energy of transfer for both hydrophobic and hydrophilic molecules (34,100,101,155-157). Aromatic and alkyl compounds have been found to prefer an organic or hydrophobic environment while polar or charged groups prefer an aqueous environment. Similar results have been found for the polar and non-polar side chains of amino acid residues (100, 101,135). Peptide bonds have been shown to be relatively hydrophilic moieties, with the transfer from carbon tetrachloride to aqueous or N-methylacetamide characterized by free energies of transfer of -3.9 kcal/mole and -4.1 kcal/mole (101 and 156, respectively). The transfer of the peptide unit to water is enthalpy driven (-7.4 and -7.8 kcal/mole (101, 156), respectively) and show a negative entropy value for the ordering of solvent water molecules (2).

Thermodynamic parameters resulting from transfer processes from aqueous to organic phases are temperature dependent with hydrophobic moieties showing a positive heat capacity change and a decrease in the entropy term with temperature (34,158). Electrostatic or polar groups on transfer from aqueous to organic phase show an opposite negative heat capacity change, with a similar decrease in the positive entropy term with increasing temperature (158). Based upon these observations some authors have interpreted their results showing temperature dependent positive heat capacity changes in processes involving proteins as being indicative of hydrophobic forces playing a major role in these processes (83,84,89). Accordingly, the already well elucidated major role of hydrophobic interactions in the binding of substrate with Cht (28,29) may be given added support by the observation of large positive heat capacity changes for the binding process in this work (Table 18).

The role of water in the binding process has received much attention. Amidon et al. (155) have carried out model studies of the gas phase transfer of alkyl and aromatic groups from an organic to an aqueous phase. They found that the organic molecules showed little preference for the organic phase over the aqueous phase based upon a free energy per unit area change and argued that desolvation of a substrate by the active site of an enzyme and the concomitant desolvation of the active site would add little or even be an unfavorable factor in the binding process (155). Richards and Richmond, however, argue that the primary monolayer of solvating water is very different from bulk water and that water in the binding groove of an enzyme is higher energy than bulk water. The displacement of water from the active site groove would, therefore, contribute significant favorable energy to the binding process (159). Some authors have argued that an en-

enthalpy-entropy compensation process observed for K_m and k_{cat} for the Cht catalyzed hydrolysis of substrates is due to changes in the solvation of the enzyme (45,55,58,160) or are due to observed intrinsic changes in the physical and thermodynamic properties of water from 15° to 35°C (34,58,161).

Water has been shown to play an important role in the enzymatic process (1-7,11,12). Studies of catalysis of ATEE by Cht in nine different aqueous solutions perturbed by different concentrations of salt and organic solvents by Glick (45) have shown significant differences in the rates of Cht catalyzed hydrolysis of ATEE at different temperatures. Similarly, studies of the Hofmeister series of anion salts that are thought to effect protein structure by their structure making or breaking effects on water structure have shown significant changes in the binding and catalytic steps of Cht (145,162).

Studies of binding of substrate and inhibitors by Cht in solvent perturbed by the organic solvent DMSO (dimethylsulfoxide) have shown increases (poorer binding) in the observed binding constants (165-167). Fink found a 40% increase in the binding constant for the substrate N-acetyl-L-tryptophan p-nitrophenyl ester (165) and a similar increase in the binding constant of the competitive inhibitor proflavin (166) in solutions containing up to 65% DMSO. Kennedy and Schultz found increases in the binding constant of the inhibitor N-acetyl-L-phenylalaninal (aldehyde) of up to 35% with 12.5% DMSO solutions (167).

However, the data for the model partition studies of the phenylalanine analog series showed no significant differences (except in one case) between an aqueous buffer/ $CHCl_3$ system containing no DMSO versus an aqueous buffer containing 5% DMSO/ $CHCl_3$ system (Tables 8 and 9). The one exception was for the cyclized compound L-(-)-KCAQ. The data showed a

large increase in both the enthalpy and entropy terms for the transfer process of L-(-)-KCAQ to CHCl_3 when the aqueous phase is perturbed by 5% DMSO (2.7 ± 0.5 kcal/mole and 9.2 ± 1.9 e.u., respectively) while the free energy term showed a slight decrease in the positive term from 750 ± 5 cal/mole to 695 ± 45 cal/mole. The change in the enthalpy-entropy data can be interpreted as an increase in solvent ordering and hydrogen bonding (2) around the cyclized KCAQ molecule by water when the 5% DMSO is present.

The sensitivity of ester hydrolysis to solvent is demonstrated in a recent study by Holterman and Engberts on the hydrolysis of two acyl activated esters in water rich 2-n-butoxyethanol-water mixtures (168). Arrhenius plots of $-\ln(k/T)$ versus $1/T$ in mixtures of 2-n-butoxyethanol and water showed linear relationships for the hydrolysis of the two esters in solution where the mole fraction of water was equal to 1.00 and 0.95. However, at the intermediate "magic mole fraction" (168) of 0.98, they found that the plot was now curvilinear with a maximum at 23°C and a positive heat capacity change of 224 and 342 ± 51 cal/mole/ $^\circ\text{C}$ for the hydrolysis of the two esters. The enthalpy-entropy partition data of this work and other data (45,162-164,168) similarly show that chemical reactions and simple physical processes such as partitioning may be sensitive to small perturbations to the composition and make-up of the solvent.

As has been previously discussed, association of substrate with enzyme is a complex process involving desolvation of the substrate and transfer to the binding site, desolvation of the binding site, and possibly a concomitant conformational change in the enzyme and/or substrate upon association. Partition studies, where molecules are transferred from an aqueous to a hydrophobic organic solvent can be thought of as an analogous process to some of the process involved in the total enzyme-substrate

association process. Both processes involve desolvation of the substrate, transfer of the molecule to a hydrophobic environment, with a "resolution" of the substrate by a liquid organic phase with low dielectric constant (169). The subtraction of the model partition from the enzymatic process would normalize the different substrates for desolvation and hydrophobicity effects, thus emphasizing the specificity of the enzyme binding site for the substrate and conformational changes in the enzyme and/or substrate upon substrate binding.

Model partition studies have been shown to have a good predictive value for the free energy of binding small molecular weight aromatic compounds to the S_1 aromatic binding site of Cht. Wildnauer and Canady found almost identical linear relationships for plots of free energy of transfer between aqueous and organic solvent and the binding of compounds to the S_1 site of Cht for the non-specific series of aromatic compounds: benzene, toluene, ethylbenzene, etc. (99). Bauer et al. (71) found a free energy of transfer of -2.2 kcal/mole for the benzyl side chain of phenylalanine to the S_1 site of Cht, which agrees well with values of -2.6, -2.32, and -1.8 kcal/mole for the transfer of the benzyl side chain of phenylalanine to pure ethanol, ethylene glycol, and n-hexanol, respectively (100, 101). However, the model studies do not quantitatively predict the enthalpy and entropy for substrate transfer from aqueous to non-polar phase in the enzymatic processes. Berezin et al. (98) found that the transfer of benzene from aqueous buffer (pH 8.0) to the S_1 site of Cht at 25°C was characterized by a $\Delta G_t^0 = -3.0$ kcal/mole, $\Delta H_t^0 = -4.5$ kcal/mole, and $\Delta S_t^0 = -5$ e.u. (unitary units) which compares with thermodynamic parameters for the transfer of benzene from aqueous to benzene of $\Delta G_t^0 = -4.6$ kcal/mole, $\Delta H_t^0 = -0.5$ kcal/mole, and a $\Delta S_t^0 = +14$ e.u. (97). The transfer of ben-

zene to an organic solvent is an entropy driven process, while the transfer of benzene to the S_1 site of Cht is an enthalpy driven process. Berezin et al. (98) and others (2,3,9,11,28,29,36-40) have taken these and similar enthalpy and entropy values to mean that a conformational change occurs in Cht upon binding of substrate to the aromatic binding site of S_1 .

Predictions based upon the partition studies can be made for the hydrophobic component of substrate binding. The cyclized oxygen analog CADIC has a free energy of transfer -2,720 cal/mole more negative compared to the nitrogen cyclized analog L(-)-KCAQ (Table 8) and this component would be expected to increase its binding 100 fold with respect to the cyclized nitrogen analog. The cyclized nitrogen analog L(-)-KCAQ has a free energy of transfer 715 cal/mole more positive than its non-cyclized analog, N-ac-Phe-NH₂, and the solvation effect may, therefore, act to decrease its binding constant by a factor of 3.3 times with respect to the non-cyclized analog's binding constant. The cyclized oxygen substrate CADIC has a free energy of transfer 380 cal/mole more positive than the non-cyclized oxygen analog, O-acetoxy-L-phenyllactic amide, which effects their relative binding constants by a factor of two. The non-cyclized oxygen analog, O-acetoxy-L-phenyllactic amide, has a free energy transfer of -2,385 cal/mole more negative than its nitrogen analog N-ac-Phe-NH₂ and the transfer process should contribute to its binding constant by a factor of 56 times with respect to the binding constant of N-ac-Phe-NH₂.

Detailed thermodynamic data for binding of these amide analogs with Cht is not now available. However, by looking at binding data for the L and D conformers as well as methyl and p-nitrophenyl esters a comparison can be made to determine whether these hydrophobic factors are

dominant. Comparison of literature values for the analogs in Table 28 shows that the transfer model is probably a poor predictor for the strength of binding to Cht. The apparent affinity of CADIC to the enzyme is only 0.3 to 2.2 times poorer than KCAQ (D and L conformations, respectively), significantly different than the relative affinity predicted by the transfer model alone of 100 times better (123). The cyclized nitrogen analog, KCAQ, apparently binds 9 times poorer than the non-cyclized nitrogen analog N-ac-Phe-OMe (model partition predicts 3.3 times poorer), while the cyclized D isomer of KCAQ bound a factor of 4.7 times better than the non-cyclized D isomer. The non-cyclized amide oxygen analog, O-acetoxy-D-Phenyl-lactic amide, has a binding constant only 1.16 times better than the non-cyclized nitrogen analog, N-ac-D-Phe-NH₂, while the transfer of the oxygen analog was 56 times better in the model system. However, a problem in these comparisons is that $K_{m(\text{obs})}$ does not equal K_s for ester substrates (12). Accordingly, the comparison of only D versus L isomers and the amide series may be valid.

Thus, the non-stereospecific partition model appears a poor predictor for the strength of binding of these asymmetric substrates to Cht. This is due to the inability of the model to account for favorable non-covalent polar interactions as well as the constraints put upon binding asymmetric substrate molecules to the well defined asymmetric, stereospecific binding site of Cht (5,9,11,12,28,29,122,123,160,170). Furthermore, invoking the association-activation hypotheses, the part of the binding energy which may be used to lower the energy of activation for the bond breaking and/or making step (1-4,9) in the enzyme case, will not appear in the model study.

The partition model also fails to predict both the binding strength and the binding order for the peptide amide series: N-ac-Phe-, Pro-Phe-,

TABLE 28

COMPARISON OF BINDING CONSTANTS FOR THE PHENYLALANINE
SUBSTRATE ANALOGS

COMPOUND	ISOMER	MODEL HYDROPHOBIC BINDING AFFINITY ^a	ENZYME BINDING AFFINITY ^b	REF.
CADIC-methyl ester	D	98.6	40	123
	L	98.6	1	123
KCAQ-methyl ester	D	1	52.8	123
	L	1	2.2	123
N-ac-Phe-OMe	D	3.3	11.2	140
	L	3.3	20	123
O-acetoxy-Phenyllactic-NH ₂	D	187	3.15	122
N-ac-Phe-NH ₂	D	3.3	2.64	122
O-acetoxy-Phenyllactic- p-nitrophenyl ester	L	187	4591	122
N-ac-Phe-p-nitrophenyl ester	L	3.3	5834	122

^a Relative affinity of compound for hydrophobic phase. Larger number is greater affinity. Normalized to an affinity of 1 is equal to a mole fraction ratios of 0.283 from Table 8 for amide substrates at 25°C.

^b Relative association constants. Larger number means greater affinity. Normalized to an affinity of 1 is a K_m of 28.0 mM. However, for esters,

$$K_m = K_s \left(\frac{k_3}{k_2 + k_3} \right).$$

Ala-Pro-Phe-, and Pro-Ala-Pro-Phe-NH₂. Partition data predicts that the binding order should be di- > tetra- > mono- > tri- (Table 11). However, at 25°C, pH 7.8 the actual order for binding with Cht is tri- > tetra- > di- > mono- (Table 14).

It is not surprising that the model may be a poor predictor as the model fails to account for the contribution of the substrate peptide backbone which forms a β structure with the protein when bound (31,32). The model only allows for hydrophobic contributions to the transfer process. Studies of the binding of glycine containing peptides to Cht (66,70,74-77; Table 2) have shown that the peptide backbone can contribute favorably to the binding process at almost all of the binding subsites (S_4 , S_3 , S_2 , S_1' , S_3' , S_4'). The failure of this model to predict the contribution of the amino acid residues of the peptide substrates (Table 29) is due once again to inability to account for the effects of specificity in the interaction of the binding site with the substrate.

However, the model was studied only as a "handle" on the transfer process. The successes of this model is that it indicates to us that the binding site (especially the extended binding site) may not be controlled solely by hydrophobic bonding forces. Indeed, the enthalpy and entropy data to be presented in the next section will show us that the enzymatic process is very different thermodynamically from simple hydrophobic processes. However, these data can be used to normalize the enzyme data for relative inherent differences in hydrophobicity (desolvation interactions) that occur on the respective binding of these different substrates to the enzyme active site.

TABLE 29

COMPARISON OF MODEL PARTITION AND α -CHYMOTRYPSIN BINDING FREE
ENERGY DATA FOR THE CONTRIBUTION OF PEPTIDE RESIDUES OF THE PEPTIDE
AMIDE SUBSTRATE SERIES AT 25°C.^a

AMINO ACID RESIDUE	POSITION ^b	Model ^c $\Delta G_t^{\circ} = \text{cal/mole}$	^d Cht $\Delta G_a^{\circ} = \text{cal/mole}$	
			LOW	HIGH
N-ac-Phe-NH ₂	P ₁	35 ± 30	-4470± 30	-4880± 60
Pro	P ₂	- 785 ± 40	- 240±130	+ 210±140
Ala	P ₃	+ 840 ± 35	-1320±180	-1280±140
Pro	P ₄	- 490 ± 35	+ 80±160	+ 130±110

^a ΔG° is unitary units (34). Calculated values by subtracting lower peptide from higher to get difference due to residue.

^b Nomenclature according to Schechter and Berger (27).

^c From Table 11.

^d From Table 16 converted to unitary units (34).

IV B-5. Thermodynamics of Peptide Substrate Binding and Catalysis:
Productive Binding, Association-Activation.

IV B-5a. Association-Activation is Not Observed in the Free Energy of
Binding.

Simple hydrophobic bond formation has been shown to be characterized thermodynamically by a negative free energy term, an enthalpy near zero, and a positive entropy term and is, therefore, an entropy driven process (2,34,97). Productive binding refers to non-covalent association of enzyme and substrate which results in catalysis. Productive binding has been studied extensively for Cht (see Section I C-2) and believed to be characterized thermodynamically by a negative free energy term, a negative enthalpy term, and a negative entropy term. Accordingly, it is an enthalpy driven process, unlike simple hydrophobic bond formation (9,35,36,44) that the negative entropies found for productive binding are indicative of the enzyme-substrate complex being ordered for catalysis upon formation of the Michaelis complex. This is a type of association-activation mechanism (Section I B-3). It is argued that this ordering process is paid for by utilization of some of the actual or intrinsic favorable free energy of binding (ΔG_i), so that the observed free energy of binding (ΔG_o) is less than the intrinsic free energy of binding by the amount used to lower the energy of activation (ΔG_{aa}) for the catalytic step following binding (1-4,9,11; Section I B-3).

In the case of non-productive binding, catalysis does not occur so that the observed binding free energy is expected to be more negative than the observed free energy for productive binding. However, only small increases of from -300 to -700 cal/mole have been observed for non-pro-

ductive binding of D isomers (inhibitors) and for binding of inhibitors and substrates to pH and chemically modified forms of Cht (9,30,35,36,44, 172,173), while ΔG^\ddagger for k_{cat} are significantly higher (greater than 3 to 5 kcal/mole) for the less specific substrates. This conflicts with the energetic expectations predicted for association-activation (9,44).

IV B-5b. Can Association-Activation be Observed in the Enthalpy and Entropy of Binding?

If we predict that the complex is ordered for catalysis in the association step, then the catalytic step should, in turn, be characterized by a relatively positive entropy term with respect to non-enzymatic reactions. However, systematic kinetic and thermodynamic data of the individual steps of catalysis for a kinetically specific series of substrates for an enzyme were not available prior to this point in time to permit a detailed thermodynamic analysis of the catalytic process in terms of this and other association-activation mechanisms (see Section I C-3). Therefore, the data presented in this work may be a valuable contribution to understanding the catalytic process.

van't Hoff and Arrhenius plots (figs. 19-33) of the kinetic data (Table 14) for the peptide series: N-ac-Phe-NH₂, N-ac-Pro-Phe-NH₂, N-ac-Ala-Pro-Phe-NH₂, N-ac-Pro-Ala-Pro-Phe-NH₂, and N-ac-Phe-Gly-NH₂ indicate two temperature dependent forms of Cht in solution (Sections I C-4, III B, and IV B). As discussed in Section IV B-1, the data may best fit two curvilinear lines drawn through the points of the van't Hoff plots (figs. 19-23) for substrate binding of all five substrates. Similarly, two curvilinear lines appear to best fit the Arrhenius plots (figs. 24-28) of the catalytic rate constants (kcat).

The model of the hypothetical enzyme 'X' as developed in Section IV B-2 indicates that the enthalpy for each of the forms cannot be obtained by drawing tangents to the curves near the middle temperature range of 15^o to 30^oC (Section III B) as the observed van't Hoff in this region represents the sum of substrate binding to two independent enzyme forms. However, as can be seen in Section IV B-2, on extrapolating the actual

binding data for a substrate from the low and high temperature regions, the values obtained from the van't Hoff plots should be good approximations for the actual thermodynamic values of the two temperature dependent forms of Cht in the middle temperature range. Furthermore, all the plots were analyzed for this discussion in the same manner, and reservations about the accuracy of the data may not be significant for comparisons of the different peptide substrates which appear to bind by similar thermodynamic processes.

Surprisingly, thermodynamic data for binding of the five peptide substrates with Cht at 25°C shows that the low temperature form is characterized by positive enthalpy and entropy terms, while the high temperature form is characterized by negative enthalpy and entropy terms. The binding process to the low temperature form at 25°C is, therefore, entropy driven while binding to the high temperature form at 25°C is an enthalpy driven process. If we look at the van't Hoff plots of the four peptide amide substrates (figs. 19-22) at 5°C, all four have a positive slope (negative enthalpy) for the binding process to the low temperature form of Cht. Accordingly, the binding is enthalpy driven at 5°C and becomes entropy driven at 25°C. Similarly, all the substrates show an enthalpy of association near zero for binding to the high temperature form of Cht at 37°C. The peptide N-ac-Phe-Gly-NH₂, unlike the series of four peptide amides, binds to the S₁' site. The van't Hoff plot (fig. 23) indicates that binding at the S₁' site may be more complicated as the 5°C temperature data point cannot be included in a simple curve with the 12°C and 19°C points as for the peptide amide series substrates.

Heat capacity changes have already been well discussed (Section I C-6) in relation to hydrophobic bond formation (2,34), for quaternary

structure formation in hemoglobin (81,83,84), in denaturation of proteins (82,89), in the association of hormones with receptors (90), in protein dimerization (91), in the binding of large protein proteinase inhibitors (96), and in hapten-antibody association. For example, Mukkur and co-workers (86-88) have shown hapten-antibody association to be characterized by a large positive heat capacity change ($\Delta C_p = 470 \text{ cal/mole/}^\circ\text{C}$ over the temperature range -3° to 67°C ($\Delta H^\circ = -14.22 \text{ kcal/mole}$, $\Delta S^\circ = -18.34 \text{ e.u.}$ and $\Delta H^\circ = +18.88 \text{ kcal/mole}$, $\Delta S^\circ = +90.69 \text{ e.u.}$, respectively at -3° and 67°C).

According to entropy theories of association-activation, the formation of the enzyme-substrate complex should be ordered with respect to the free enzyme and substrate (1-4,9,11); and therefore, the binding step should be characterized by a negative entropy of association (ordering) with relatively positive entropy values characterizing the activation energies for k_{cat} . However, these data (Table 16) show that binding to the enzyme at particular temperatures is characterized by positive enthalpy and entropy values in the binding step. This is unexpected, theoretically and from previous substrate analog binding data.

Several explanations for the apparent conflict are possible. First, the observed values may be due to enthalpy-entropy processes in the water of solvation as has been previously discussed (34,45,55,58,160,161; Section IV B-4). "Productive" binding characterized by negative enthalpies and entropies of association with concomitant activation of the complex towards catalysis may, in fact occur, but is hidden by the larger thermodynamic processes occurring in the solvent water. These processes in water may be compensating and have no significant effect on the free energy of binding and catalysis for the two enzyme forms. A second explana-

tion is that the two enzyme forms activate their respective substrates by different mechanisms. This latter possibility will be pursued in the discussion below.

IV B-5c. Is Substrate Specificity Enthalpy or Entropy Determined?

As large changes in the physical and chemical properties of many proteins have been noted at temperatures above or below the physiologic temperature of the particular protein (159,174), a thermodynamic analysis of Cht at its physiologic temperature of 37°C, where the contribution from the low temperature form should be minimal may be of interest. A comparison of the enthalpy and entropy values of association at 37°C show no trends as substrates of increasing length bind (Table 30). The association step shows vasculatory positive and negative values for the entropy and enthalpy terms with increasing peptide length. All five substrates, in turn, are characterized by fairly large negative entropy values for the catalytic step (-22.4 to -35.7 e.u.), with an increasingly more positive entropy of activation with increasing substrate specificity. The enthalpy of activation does not vary consistently, and thus, specificity in kcat is determined by variations in entropy.

Furthermore, we can see from the van't Hoff plots of the association step (figs. 19-23) that at 5°C, where contributions from the high temperature form should be minimal, the association step would be characterized by a negative enthalpy and entropy of association. Arrhenius plots (figs. 24-29) of the catalytic step k_2 , in turn, give a large positive enthalpy of activation with an entropy of activation near zero for the five peptide amide substrates. The enthalpy and entropy values found at 5°C are, therefore, similar to those found for the high temperature form at 25°C.

The temperature dependence in the enthalpy and entropy terms observed in this work may help explain seemingly conflicting data found in the literature. Inagami et al. (54) studied the Cht catalyzed hydrolysis

of N-acetyl-L-tyrosine anilides at 15⁰, 25⁰, and 35⁰C. They found enthalpy values near zero and positive entropy values for the association step at 25⁰C while the k_2 step showed large positive enthalpy values (10-17 kcal/mole) and small negative entropy values for the analogs studied (-3 to -8 e.u.). Reexamination of their data, however, shows that the association data does in fact, best fit van't Hoff plots with curvilinear lines and not straight lines. In fact, van't Hoff plots of the data for several of their less substituted analide substrates would give figures shaped like an inverted "V" with a maximum at 25⁰C, similar to what was found in this work for the peptide amide substrate series (figs. 19-23). Similarly, Kunugi et al. (56) found an enthalpy of association near zero and a positive entropy of association for the substrate N-(2-furyl) acryloyl-L-phenylalanine methyl ester and N-acetyl-L-tryptophan p-nitrophenyl ester. However, their reported results were also based upon a linear interpretation. Reexamination of their data shows that experiments were only carried out at 25⁰C and below, and both sets of data could better fit van't Hoff plots with curvilinear lines similar to those found for the association of the low temperature form of Cht with substrate as found in this work (figs. 19-22). These conflicts between the data presented in this work and that found in the literature (54,56) then, is apparently due to other investigators failing to realize that there are two temperature dependent forms of Cht and the possibility of heat capacity changes in the binding and catalytic steps. This failure has resulted in their reported "averaged" data over temperature ranges that are too short, too widely spaced temperature intervals, or at temperature ranges that only cover one temperature dependent form of Cht.

Specificity for the binding step of the peptide substrates (i.e.

whether enthalpy or entropy controlled) was found in this work to be dependent on the temperature at which the binding process is studied. At 37°C there is no clear distinction as to whether specificity is enthalpy or entropy controlled (Table 30). It appears from Table 30 that each residue added in the five peptide substrates express their contribution to the binding energy in characteristically different ways. For instance, the addition of the amino acid proline in both the P₂ and P₄ position (Table 30) makes a positive enthalpy contribution to the binding energy (unfavorable) and a positive entropy contribution (favorable). Addition of alanine in the P₃ position and glycine to the P₁' position both show a negative enthalpy and entropy contribution to the binding energy (Table 30).

Comparison of these thermodynamic contributions at 25°C with the values calculated from the model partition data (Table 31) shows significant differences in the thermodynamic values for the enzyme versus model. Addition of P₂ proline shows significantly more positive enthalpy and entropy terms for the binding to enzyme versus transfer from an aqueous to a non-polar solvent phase (Table 31). While other amino acid residues in the P₂ site (66,72,175) have shown greater increases in specificity (as determined by k_{cat}/K_m), Bauer et al. (72) and others (65,66,71,79,80) have argued that proline in the P₂ position of the substrate prevents non-productive modes of binding (see Section I C-5). Addition of proline in the P₂ position leads to a tenfold increase in k_{cat} (Table 14) with little or no change in K_m . In addition, addition of P₂ proline shows the largest difference in enthalpy and entropy values of binding and catalysis and amino acid residues added after P₂ proline show smaller differences in the observed enthalpy and entropy data (Tables 16,19,20,30-32). For ex-

TABLE 30

THERMODYNAMIC PARAMETERS FOR THE ASSOCIATION AND ACTIVATION OF FIVE SPECIFIC PEPTIDE AMIDE SUBSTRATES

WITH α -CHYMOTRYPSIN AT 37°C,^a

COMPOUND	ΔG_a° kcal/mole	ΔH_a° kcal/mole	ΔS_a° e.u.	ΔG^\ddagger kcal/mole	ΔH^\ddagger kcal/mole	ΔS^\ddagger e.u.
N-ac-Phe-NH ₂ ^b	- 2.12	- 3.89 (- 2.1)	- 5.7 (0.06)	19.49	8.42 (4.15)	- 35.7 (- 49.5)
N-ac-Pro-Phe-NH ₂	- 2.2	4.98	23.15	18.36	10.15	- 26.5
N-ac-Ala-Pro-Phe-NH ₂	- 3.42	- 3.22	0.64	17.54	9.17	- 27.0
N-ac-Pro-Ala-Pro-Phe-NH ₂	- 3.32	0.0	10.7	17.47	10.51	- 22.4
N-ac-Phe-Gly-NH ₂	- 2.26	- 5.20	- 9.48	19.03	9.85	- 29.6

^a Enthalpy of association and activation are calculated from the tangents to figures 19-28.

^b For comparison purposes, data for N-ac-Phe-NH₂ was calculated without the 45°C point included and new curves drawn to the remaining points. Data in parenthesis are calculated with 45°C point included.

TABLE 31

^a

MODEL PARTITION VERSUS ENZYMIC CONTRIBUTIONS TO THE ENERGY OF BINDING BY AMINO ACID RESIDUES AT 25°C.

RESIDUE	POSITION	PARTITION DATA ^b			ENZYME DATA ^c		
		ΔG_u^0 kcal/mole	ΔH_u^0 kcal/mole	ΔS_u^0 e.u.	ΔG_u^0 kcal/mole	ΔH_u^0 kcal/mole	ΔS_u^0 e.u.
<u>LOW TEMPERATURE FORM</u>							
N-ac-Phe-NH ₂	P ₁	35 _{±30}	3,570 _{±80}	11.8 _{±0.4}	-4,470 _{±30}	4,380 _{±580}	29.88 _{±2.05}
Pro	P ₂	-785 _{±40}	-1,370 _{±280}	-1.8 _{±1.1}	-240 _{±130}	6,260 _{±2,580}	21.6 _{±9.09}
Ala	P ₃	840 _{±35}	2,800 _{±770}	6.6 _{±2.7}	-1,320 _{±180}	1,730 _{±2,900}	10.25 _{±10.33}
Pro	P ₄	-490 _{±35}	-400 _{±815}	0.2 _{±2.8}	80 _{±160}	-860 _{±1,800}	-3.17 _{±6.58}
<u>HIGH TEMPERATURE FORM</u>							
N-ac-Phe-NH ₂	P ₁	35 _{±30}	3,570 _{±80}	11.8 _{±0.4}	-4,880 _{±60}	-15,510 _{±4,000}	-35.66 _{±13.62}
Pro	P ₂	-785 _{±40}	-1,370 _{±280}	-1.8 _{±1.1}	210 _{±140}	4,070 _{±5,200}	12.95 _{±17.91}
Ala	P ₃	840 _{±35}	2,800 _{±770}	6.6 _{±2.7}	-1,280 _{±140}	-370 _{±2,100}	3.05 _{±7.51}
Pro	P ₄	-490 _{±35}	-400 _{±815}	0.2 _{±2.8}	130 _{±110}	-1,950 _{±1,800}	-6.84 _{±6.41}

^a Contributions for residue Pro (P₂) calculated by (N-ac-Pro-Phe-NH₂)-(N-ac-Phe-NH₂) = Pro, etc.

^b From Table 11.

^c From Table 16, changed to unitary units (34).

ample, addition of P₃ alanine shows an increase in favorable binding free energy (-1.3 kcal/mole) with favorable increases in the entropy terms for both forms of Cht while the enthalpy term increased 1.7 kcal/mole for the low temperature form and -0.37 kcal/mole for the high temperature form.

Specificity of the acylation step at 25⁰C shows a decrease in the enthalpy of activation for the more specific substrates by both forms of Cht (Table 19), and is, therefore, an enthalpy controlled process with the enthalpy varying positively and negatively while the entropy term became more positive (favorable) with addition of amino acid residues to the substrate (Table 30). Kunugi et al. found the acylation step for specific substrates to be entropy controlled. However, they were comparing the methyl ester of furylacryloyl-L-phenylalanine and the p-nitrophenyl ester of acetyl-L-tryptophan (56). These two analogs may not be comparable as the p-nitrophenyl ester may contribute a unique interaction between the enzyme and substrate that is lacking in the methyl ester (52). Furthermore, the kinetic meaning of k_{cat} and K_m for ester substrates is complex.

The second order rate constants (k_{cat}/K_m ; Tables 14, 20, and 32) show an increasing rate with N-ac-Ala-Pro-Phe-NH₂ > N-ac-Pro-Phe-NH₂. These data show the longer more specific peptides have, in general, less negative entropies of activation at all temperatures.

TABLE 32

THERMODYNAMIC PARAMETERS FOR THE SECOND ORDER RATE
CONSTANTS FOR THE CHT CATALYZED HYDROLYSIS OF FIVE
PEPTIDE AMIDE SUBSTRATES AT 37°C.^a

COMPOUND	ΔG^\ddagger kcal/mole	ΔH^\ddagger kcal/mole	ΔS^\ddagger e. u.
N-ac-Phe-NH ₂	17.37 ± 0.09	2.32 ± 0.26	-48.53 ± 1.17
N-ac-Pro-Phe-NH ₂	16.16 ± 0.10	7.71 ± 1.28	-27.25 ± 4.63
N-ac-Ala-Pro-Phe-NH ₂	14.12 ± 0.08	5.42 ± 0.11	-28.03 ± 0.64
N-ac-Pro-Ala-Pro-Phe-NH ₂	14.15 ± 0.07	6.78 ± 2.02	-23.76 ± 7.01
N-ac-Phe-Gly-NH ₂	16.78 ± 0.05	6.73 ± 1.04	-32.39 ± 3.66

^a ΔH^\ddagger calculated from slope of the high temperature form of k_{cat}/K_m plots (figs. 29-33).

ΔG^\ddagger calculated from data in Table 14 by equation 1.22.

ΔS^\ddagger calculated from $\Delta G = \Delta H - T \Delta S$.

IV B-6. Model Partition Corrections for Substrate Desolvation in the Enzyme-Substrate Association Process.

Enzyme-substrate association can be broken down into several concomitant processes. As discussed in the previous two sections these processes may include desolvation of the substrate and binding site with the resultant changed solvation of the complex as well as enzyme and/or substrate conformational changes. The model partition studies would give us a measure of the natural affinity of the substrates for a non-specific hydrophobic environment. Desolvation of the substrate occurs in the model partition studies similar to the desolvation process that is alleged to occur on substrate binding to enzyme. Subtraction of the thermodynamic contribution of the model substrate transfer process from the enzymatic process will theoretically yield the thermodynamic parameters that characterize the specific interaction of the enzyme with the substrate and/or enzyme/substrate conformational changes.

As enzymatic processes are usually calculated in the 1M standard state (5) converting the data from Table 16 to unitary units (Table 33) requires the addition of 7.98 e.u. to the entropy data and -2.38 kcal/mole to the free energy data to eliminate the contribution due to unmixing (two molecules coming together to form one with the loss of translational and rotational degrees of freedom with respect to each other (34,82,89)).

The enthalpy and entropy terms for the model partition experiments were positive in value (Table 11). Subtraction of these terms from the enzymatic data in unitary units (Table 33) results in a negative increase in the enthalpy (favorable) and entropy (unfavorable) values for the as-

TABLE 33

THERMODYNAMIC PARAMETERS IN UNITARY UNITS^a FOR THE STEADY-STATE ASSOCIATION OF AMIDE
AND PEPTIDE SUBSTRATES BY CHT AT 25°C.

COMPOUND	LOW TEMPERATURE FORM			HIGH TEMPERATURE FORM		
	$\Delta G_{\text{au}}^{\circ}$ kcal/mole	$\Delta H_{\text{au}}^{\circ}$ kcal/mole	$\Delta S_{\text{au}}^{\circ}$ e. u.	$\Delta G_{\text{au}}^{\circ}$ kcal/mole	$\Delta H_{\text{au}}^{\circ}$ kcal/mole	$\Delta S_{\text{au}}^{\circ}$ e. u.
N-ac-Phe-NH ₂	-4.47	+ 4.38	+29.88	-4.88	-15.51	-35.66
N-ac-Pro-Phe-NH ₂	-4.61	+10.64	+51.48	-4.67	-11.44	-22.71
N-ac-Ala-Pro-Phe-NH ₂	-6.03	+12.37	+61.73	-5.95	-11.81	-19.66
N-ac-Pro-Ala-Pro-Phe-NH ₂	-5.95	+11.51	+58.56	-5.82	-13.76	-26.50
N-ac-Phe-Gly-NH ₂	-4.90	+ 6.46	+38.10	-4.84	-10.06	-17.51

^a See section III A-1 (34). Calculated from Table 16. Subscript 'au' denotes that these parameters are for the association step and are in unitary units.

sociation process (Table 34). As seen for the enzymatic data, before normalizing for the model study (Tables 16,19), the binding process for the low temperature form of Cht at 25⁰C is characterized by a positive entropy term (disordering) and a positive enthalpy term, while the high temperature form at 25⁰C is characterized by a negative enthalpy and entropy (ordering) of association. After converting to unitary units and normalizing the association data for the model desolvation process we find no qualitative change in the enthalpy-entropy data. However, the normalized enthalpy-entropy data for the association of substrate with Cht shows the enthalpy terms are now more negative by -0.9 to -5.0 kcal/mole and the entropy terms are also more negative by -3.1 to -8.7 e.u. (Tables 16 and 34). Accordingly, more ordering appears to be associated with the binding process of substrate to enzyme after normalizing for desolvation of the substrate.

TABLE 34

THERMODYNAMIC PARAMETERS^a FOR THE ASSOCIATION OF AMIDE SUBSTRATES TO CHT AT 25°C CORRECTED FOR THERMODYNAMIC CONTRIBUTIONS DUE TO THE TRANSFER PROCESS AS FOUND BY MODEL PARTITION STUDIES.

COMPOUND	LOW TEMPERATURE FORM			HIGH TEMPERATURE FORM		
	ΔG_{an}° kcal/mole	ΔH_{an}° kcal/mole	ΔS_{an}° e.u.	ΔG_{an}° kcal/mole	ΔH_{an}° kcal/mole	ΔS_{an}° e.u.
N-ac-Phe-NH ₂	-4.51	+0.81	+18.8	-4.87	-19.08	-47.46
N-ac-Pro-Phe-NH ₂	-3.86	+8.44	+41.48	-3.92	-13.64	-32.71
N-ac-Ala-Pro-Phe-NH ₂	-6.12	+7.37	+45.13	-5.91	-16.81	-36.26
N-ac-Pro-Ala-Pro-Phe-NH ₂	-5.91	+6.91	+41.78	-5.78	-14.66	-43.3

^a Subscript "an" denotes that these parameters are for the association step, are in unitary units, and have been "normalized" by subtracting out the contribution to the binding process as found by the model partition studies (Table 11).

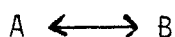
IV B-7. Catalytic Efficiency in α -chymotrypsin from a Thermodynamic and Evolutionary Perspective.

There is now ample evidence for the existence of two temperature dependent forms of Cht based upon the work presented in this dissertation and evidence cited in the literature (section I C-4). van't Hoff and Arrhenius plots of K_m (figs. 19-23), k_{cat} (figs. 24-28), and k_{cat}/K_m (figs. 29-33) clearly can be drawn as two temperature dependent figures for each substrate. If we look at the Arrhenius plots of $\log k_{cat}$ versus $1/T$ for the peptide substrates we see that as the temperature increases from 5° to 25°C there is a steady increase in k_{cat} which can be fit to follow a curvilinear relationship (see section III B-1 and figs. 24-28). As we approach 25°C , however, the rate of rise of k_{cat} starts to decrease (slope becomes less negative) and as we cross the range of 23° to 25°C (around 30° for N-ac-Phe-NH₂) we see an increase in the slope (more negative) for the change in $\log k_{cat}$ versus $1/T$. Thus, the efficiency of catalysis decreases slightly near 25°C and then begins to increase again. Correlating with the free energy changes in k_{cat} are enthalpy and entropy changes. At low temperatures ($\ll 25^\circ\text{C}$), the binding process is characterized by positive enthalpy and entropy values, and association is an entropy driven process. The corresponding low temperature catalytic step shows a low positive enthalpy of activation and a relatively high negative entropy indicating ordering of the substrate and/or enzyme for catalysis did not occur in the binding step. The reverse is seen for the high temperature form at 25°C , where the binding process is characterized by a negative enthalpy and entropy (enthalpy driven) and the proceeding catalytic step shows an entropy of activation near zero

(Tables 16 and 19). An explanation based upon evolutionary and thermodynamic grounds is possible to explain the reversal in thermodynamic values for the binding and catalytic steps for the high and low temperature forms of Cht.

The function of an enzyme is to increase the rate of catalysis of a reaction (2,5,11,12). Since the highest energy barrier in the catalytic pathway will determine the rate of a reaction, successful evolutionary design of the "fittest" enzyme would be aimed at lowering this high energy barrier (2,5,11,12,176,177). The other steps in the catalytic reaction pathway with lower energy barriers may be directed towards lowering the energy barrier of the rate determining step. The acylation step is the rate limiting step for the Cht catalyzed hydrolysis of peptides and peptide amides (23,30). Peptides are, in turn, the natural substrate of Cht (17) and, therefore, evolutionary improvements would go towards improving the efficiency of this step.

It has been shown in this work that the acylation step for the five peptide amide substrates was characterized by relatively low enthalpy barriers and high entropy barriers for the low temperature form of Cht at 25°C ($\Delta H^\ddagger = 4.68$ to 12.62 kcal/mole and $\Delta S^\ddagger = -21.73$ to -44.9 e.u.; Table 19). The acylation step for the high temperature form was found in turn, to be characterized by high enthalpy barriers and very small entropy barriers ($\Delta H^\ddagger = 14.77$ to 20.02 kcal/mole and $\Delta S^\ddagger = -8.32$ to 2.88 e.u.; Table 19). Positive enthalpy values indicate endothermic or heat absorbing processes (2,6,7,146,147). Processes that are characterized by a positive enthalpy values show an increase with increasing temperature (2,6,7,146,147). For instance, if the process:



is characterized by a positive enthalpy term for the forward reaction of $A \longrightarrow B$, and a negative enthalpy term for $B \longrightarrow A$, then as the temperature is increased more B will be formed (2,6,7,146,147). Therefore, processes characterized by a large positive unfavorable enthalpy term will be favored over a similar process involving a large negative unfavorable entropy term as the temperature is increased. This is what is found for Cht in this work: high enthalpy barriers for the high temperature form and lower enthalpy barriers with high entropy barriers for the low temperature form (Table 19).

The binding step of the high temperature form is characterized by a large negative entropy of association, thus little or no ordering may be necessary in the catalytic step (k_2). In contrast, the binding step for the low temperature form is characterized by a large positive enthalpy and entropy and the ordering is apparently carried out in the catalytic step. This is correlated with the smaller ΔH^\ddagger (less positive) for the low temperature form as compared with the ΔH^\ddagger of the high temperature form.

One additional bit of evidence should be mentioned. As the just proposed theory for the low and high temperature forms of Cht represent two extremes for the reaction thermodynamics, with the high temperature form showing high enthalpy and low entropy of activation and the low temperature form showing low enthalpy and high entropy of activation, it is interesting that the non-enzymatic pathway for the hydrolysis of amide bonds shows intermediate enthalpy and entropy values. Bejaud et al. (178) studied the hydrolysis of amide bonds at 25⁰C by hydroxide ion (pH 10). They studied the compounds alanine-NH₂, N-methyl-alanine-NH₂ and propyl-NH₂. They found enthalpies of activation of from 12.8 to 13.5 ± 0.8 kcal/mole and entropies of activation of from -18 to -21 ± 2 e.u. (178). This

compares with mean values from the two enzyme forms calculated from the enthalpies and entropies of activation found for the five peptide amide substrates by this work at 25°C (Table 19) of $\Delta H^\ddagger = 7.89 \pm 2.95$ kcal/mole and $\Delta S^\ddagger = -34.32 \pm 8.37$ e.u. for the low temperature form and $\Delta H^\ddagger = 16.66 \pm 2.0$ kcal/mole and $\Delta S^\ddagger = -4.87 \pm 4.55$ e.u. for the high temperature form. The average values of $\Delta H^\ddagger = 12.28$ kcal/mole and $\Delta S^\ddagger = -19.6$ e.u. which are well within experimental error of the values of Bejaud et al. (Table 35).

The observed values of ΔH^\ddagger and ΔS^\ddagger for a reaction have been proposed to represent the values characterizing the median or optimal pathway along the reaction coordinates (6,7,149,150,179). Furthermore, as the mean enzymatic and non-enzymatic values observed at 25°C are within experimental error and are very similar to the values found at 37°C for the enzymatic catalysis of the five peptide substrates studied (Table 30), the enzyme appears to be "designed" to catalyze along the optimal pathway at the physiologic temperature (37°C).

TABLE 35

COMPARISON OF THE THERMODYNAMICS OF α -CHYMOTRYPSIN^a
CATALYZED HYDROLYSIS OF THE AMIDE BOND
WITH NON-CATALYZED^b HYDROLYSIS AT 25°C.

SYSTEM	ΔG^\ddagger kcal/mole	ΔH^\ddagger kcal/mole	ΔS^\ddagger e.u.
Cht - Low Temp. Form	18.12 \pm 5.44	7.89 \pm 2.95	-34.32 \pm 8.37
Cht - High Temp. Form	18.11 \pm 3.36	16.66 \pm 2.0	- 4.87 \pm 4.55
Average Cht - High			
and Low	18.115 \pm 4.4	12.28 \pm 2.5	-19.6 \pm 6.46
Base Hydrolysis	19.13 \pm 0.8	13.13 \pm 0.8	-19.67 \pm 2.0

^a Thermodynamic values are the mean and standard deviation for the five peptide amide compounds.

^b Thermodynamic values are the mean and standard deviation for three compounds (178). Hydroxide catalyzed hydrolysis at pH 10. See text.

IV B-8. Evidence and a Unifying Theory for the Association-Activation Mechanisms.

The work presented in this dissertation is the most complete, systematic, thermodynamic study of productive binding by specific substrates to an enzyme to date. The observation of two temperature dependent forms of Cht with negative enthalpies and entropies of association for the high temperature form and positive enthalpies and entropies of association for the low temperature form at 25°C (Table 16) appear to be conflicting and may support any one of the above mentioned theories of association-activation mechanisms (1-4,9,11,44).

Studies of substrates and substrate analogs that associate in potentially productive and non-productive binding modes with Cht have led investigators to propose that productive binding is characterized by a negative enthalpy and entropy of association and non-productive binding is characterized by a more positive enthalpy and entropy for the association process (9,11,35-40). Many authors have taken the values to be indicative of a conformational change upon substrate association (2,3,9,11, 28,29,36-40). These results may have led to the proposal that this conformational change orders or activates the enzyme-substrate complex towards the transition state, thus lowering the activation energy barrier and increasing the rate of the enzymatically catalysed reaction (2,3,9, 11; figs. 2 and 3). The activation by mechanisms of strain and distortion (1,2), orientation (3), and/or restrictions in translational and rotational degrees of freedom (4) would, in turn, be paid for by using a part of the association free energy (see sections I B-3, I C-2, and IV B-5 for a more detailed discussion).

In the case of non-productive binding of the inactive D isomers of specific amino acid substrates of Cht (inhibitors) or of binding of substrate to chemically or pH modified catalytically inactive forms of Cht, one might expect to see the true or intrinsic binding free energy term which would be the sum of the free energy that would normally have been used to activate the enzyme-substrate complex toward catalysis on formation of the Michaelis complex plus the observed binding free energy for productive association (equation 1.32). However, these expected increases of -3 to -5 kcal/mole (2,11,12) over the observed free energy for productive binding were not observed. Only small increases in the free energy of binding of -300 to -700 cal/mole are observed (9,30,35,36,44, 172,173).

This failure to observe the expected changes in free energy led Schultz et al., in 1977 to propose a different mechanism for the association-activation process (9). Based upon their data (Table 1), Schultz et al., concluded, that the enzyme-substrate complex was activated for catalysis by association of substrate with enzyme and that this association-activation process was characterized by large negative enthalpies and entropies of association (-10 kcal/mole and -30 e.u., respectively), however, these large changes in enthalpy and entropy are compensating and are, therefore, not observed in the free energy of binding (9). In 1979 Schultz et al. refined their theory further by proposing that upon association of substrate, the ground state free energy of the enzyme-substrate complex (ES) is raised or increased at the active site (see figures 1,2, and 3 for a perspective) thus lowering the activation energy barrier. However, they proposed a coupled process whereby this increase in free energy must be paid for by a decrease in free energy somewhere else in

the enzyme molecule as it is not directly observable in differences in the free energy of binding. Thus the change in free energy leading to substrate activation in the association step is characterized by large compensating changes in enthalpy and entropy, indicative of this coupled process.

Additional evidence can be found in the literature in support of the compensating enthalpy-entropy hypothesis of Schultz and co-workers (9,44). Bauer et al. studied the binding and catalysis by Cht and SGP3 (Streptomyces griseus protease 3) of a series of peptides of the sequence N-ac-Pro-Ala-Pro-X-NH₂, where X was either Gly, Ala, Val, Leu, Phe, or Tyr (71). Since the difference between the amino acids glycine and phenylalanine is the aromatic benzyl side chain of phenylalanine then the difference in binding and catalysis between the peptide substrates containing Gly and Phe is due to the binding of the aromatic benzyl side chain in the S₁ site of Cht and SGP3. They found that the benzyl side chain contributed -2,2 kcal/mole of binding energy to both enzymes (71; Table 36). However, model partition studies of phenylalanine have shown the benzyl side chain would contribute -2.6 kcal/mole for transfer to 100% ethanol (100), about -2.7 kcal/mole to chloroform, and a maximum of -3.02 kcal/mole to the highly non-polar solvents carbon tetrachloride (101). Accordingly, the average value for the transfer of a benzyl side chain to a hydrophobic environment is -2.73 kcal/mole.

Association-activation mechanism argues that some of the binding free energy is used to lower the free energy of activation of the catalytic step (1-4,11). This is depicted by equation 1.32:

$$\Delta G_{\text{obs}} = \Delta G_i + \Delta G_{\text{aa}},$$

where ΔG_{obs} is the observed binding free energy, ΔG_i is the actual in-

trinsic or true binding free energy, and ΔG_{aa} is the binding free energy utilized to activate the enzyme-substrate complex towards the transition state for step k_2 following binding. Rearranging equation 1.32 to:

$$\Delta G_{aa} = \Delta G_{obs} - \Delta G_i, \quad (4.17)$$

it becomes clear that the difference in free energy between the observed and intrinsic binding free energy is equal to the contribution of binding free energy used to lower the free energy of activation of the catalytic step. If we take the difference between the observed binding free energy of the benzyl side chain (-2.2 kcal/mole) (71) and the average free energy of transfer of "binding" to a non-specific hydrophobic environment ($\Delta G_{\ddagger}^0 = -2.73$ kcal/mole) (100,101), we calculate the probable contribution of binding free energy to the lowering of the free energy of activation as only -0.53 kcal/mole.

However, from the free energy of activation for the catalysis of the glycine and phenylalanine analogs by Cht and SGP3 (Table 36), we find that the binding of the benzyl side chain of phenylalanine to the S_1 site of Cht lowered the free energy of activation (ΔG_{\ddagger}^0) a minimum of -2.48 kcal/mole (they were unable to get a good k_{cat} for Cht with the glycine analog so this value represents the smallest possible change in the free energy of activation). The binding of the benzyl side chain to the S_1 site of SGP3 lowered the free energy of activation by -3.81 kcal/mole (Table 37).

Therefore, a small difference between ΔG_{obs} and ΔG_i of -0.53 kcal/mole apparently lowered the free energy of activation by large differences of -2.48 and -3.81 kcal/mole for Cht and SGP3, respectively (Table 37). Accordingly, the association-activation theories that con-

TABLE 36

FREE ENERGIES OF BINDING AND ACTIVATION FOR SIX PEPTIDES OF THE SERIESN-ac-Pro-Ala-Pro-X-NH₂

RESIDUE X	K_m (mM)	ΔG_a° cal/mole	k_{cat} s ⁻¹	ΔG^\ddagger cal/mole
<u>α-Chymotrypsin^b</u>				
Gly	120	- 1,306	< 0.05 ^d	> 20,024
Ala	75	- 1,596	< 0.05 ^d	> 20,024
Val	55	- 1,787	< 0.05 ^d	> 20,024
Leu	18 ± 3	- 2,476	0.56 ± 0.05	18,535
Phe	3.4 ± 0.4	- 3,502	2.8 ± 0.2	17,543
Tyr	3.0 ± 0.1	- 3,580	7.4 ± 0.2	16,944
<u>SGP3^c</u>				
Gly	20 ± 5	- 2,411	0.012 ± 0.002	20,903
Ala	8.0 ± 0.5	- 2,976	0.30 ± 0.01	18,919
Val	4.0 ± 0.3	- 3,403	0.130 ± 0.005	19,435
Leu	0.79 ± 0.04	- 4,402	1.80 ± 0.02	17,815
Phe	0.54 ± 0.03	- 4,637	5.8 ± 0.1	17,094
Tyr	1.4 ± 0.1	- 4,050	10.1 ± 0.2	16,752

^a Data of Bauer *et al.* (71).

^b pH 8.0, 37°C.

^c pH 9.0, 37°C.

^d Rates were too slow to measure.

TABLE 37

MODEL PARTITION DATA VERSUS ENZYME BINDING DATA FOR p₁ RESIDUE SIDE CHAINS OF SIX PEPTIDES OF THE SERIESN-ac-Pro-Ala-Pro-X-NH₂

RESIDUE ^a	ΔG_{tss}° ^b cal/mole	ΔG_{ass}° ^c cal/mole	ΔG° ^d cal/mole	ΔG^{\ddagger} ^e cal/mole	"FREE" ΔG^{\ddagger} ^f cal/mole
<u>α-Chymotrypsin</u>					
Ala	- 520	- 290	- 230	g	g
Val	- 1,475	- 481	- 994	g	g
Leu	- 2,245	- 1,170	- 1,075	- 1,489	- 414
Phe	- 2,600	- 2,196	- 404	- 2,481	- 2,077
Tyr	- 2,390	- 2,274	- 116	- 3,080	- 2,964
<u>SGP3</u>					
Ala	- 520	- 562	+ 45	- 1,984	- 2,029
Val	- 1,475	- 992	- 483	- 1,468	- 985
Leu	- 2,245	- 1,991	- 254	- 3,088	- 2,834
Phe	- 2,600	- 2,226	- 374	- 3,809	- 3,435
Tyr	- 2,390	- 1,639	- 751	- 4,151	- 3,400

^a From data of Bauer et al. (71), Table 36. See text. ^b Data of Nozaki and Tanford (100) for transfer of side chains to ethanol. ^c Contribution of side chain of residue X to binding. Calculated by subtracting binding energy of glycine containing peptide from peptide with given residue, Table 36. ^d Difference between binding energies of enzyme and model. ^e Difference in activation free energy of glycine containing peptide and peptide with the given residue. ^f Energy unaccounted for after subtracting the "lost" binding energy. ^g Rates were too slow to measure.

tend that part of the binding free energy is used to lower the free energy of activation (1-4,11) fail to account for the large lowering of ΔG_{aa} (i.e. $\Delta G_{obs} - \Delta G_i$). A similar analysis is carried out for the side chain contributions to lowering the free energy of activation of the remaining four amino acids studies by Bauer et al. (Tables 36 and 37). All showed similar unaccounted large decreases in the free energy of activation for both enzymes that are not accounted for by predicted increases in the observed free energy of binding as compared to the expected intrinsic free energy of binding (equation 4.17). The observed relationship is:

$$\Delta G_{aa} = \Delta G_{obs} - \Delta G_i. \quad (4.18)$$

Additional evidence comes from studies of non-productive association of Cht with the D-amino-acid isomers (inhibitors) and from the binding of the L isomers (substrates) to chemically and pH modified forms of Cht. Proponents of association-activation theories argue that a portion of the binding free energy is used to lower the free energy of activation (1-4,11). Therefore, the contribution of the free energy of binding to lowering the free energy of activation should be equal to the difference between the free energy of productive binding of substrates (L isomers) to active enzyme and the free energy of non-productive binding of D isomers (inhibitors) to active enzyme. Expected increases in the free energy of binding of -3 to -5 kcal/mole (2) for the D-inhibitors over the L-substrates were not observed. Only small increases of -0.30 to -0.70 kcal/mole were observed for non-productive binding of D isomers of substrates to Cht (9,30,35,36,44,172,173).

Therefore by two independent calculations, the contribution of binding free energy to be approximately -0.5 kcal/mole (Tables 36 and 37) and -0.3 to -0.7 kcal/mole (9,30,35,44,172,173), yet the ΔG^\ddagger for k_{cat} is substantially lower (> 2 kcal/mole) for productive association as compared to less productive association.

Schultz and co-workers have argued that a compensating enthalpy-entropy process can result in an increase in free energy at the active site coupled with changes in the rest of the molecule (9,44). This mechanism can explain the decrease in the free energy of activation that appears to be unaccounted for in the binding free energy. The initial "price" of -0.5 kcal/mole of binding free energy may be the initial activating energy for this enthalpy-entropy or linked free energy compensation process.

Furthermore, as the thermal denaturation of the 154 amino acid protein myoglobin at 25°C is characterized by changes in enthalpy and entropy of $\Delta H = 42$ kcal/mole and $\Delta S = +95$ e.u. (89), the observed changes in the binding enthalpy and entropy of the high and low temperature forms of $\Delta H_a^0 = 20$ to 24 kcal/mole and $\Delta S_a^0 = 65$ to 85 e.u. represents significant thermodynamic changes. Support for the existence of significant changes in the enzyme comes from X-ray crystallographic data of Cht which showed significant changes in the location of over 40 amino acid residues when substrate was bound (32). Accordingly, I feel that these changes represent more than the change in position of the His-57 and Ser-195 side chains as has been proposed to occur upon substrate binding (9,44). These values may, in fact, represent compensating enthalpy-entropy changes

in the enzyme between the active site and the rest of the protein molecules as suggested by Schultz et al. (44). Enthalpy-entropy compensation phenomena as described by Schultz et al. would, in turn, give a role to the rest of the enzyme molecule away from the active site.

Theories stipulating that the binding step acts as an entropy trap may explain thermodynamic parameters found to characterize the high temperature form of Cht. They do not explain the thermodynamic values characterizing catalysis by the low temperature form ($\Delta H_a^0 > 0, \Delta S_a^0 > 0$). Even the enthalpy-entropy compensation theory of Schultz and co-workers (9,44) may not explain the thermodynamics of binding and catalysis of the low temperature form of Cht.

Predictions for the enthalpy and entropy of association can be made for the common association-activation hypotheses of orientation (29, 123), substrate distortion (94), and induced fit (180-182) that would correlate with the particular hypothesis. However, none of these predictions explains the radical differences in the enthalpy-entropy of association found for in either the low and high temperature form of Cht (Tables 16 and 19).

The overall hydrolysis of a peptide bond is a favorable energy process (2,6,7,11,46). The bond is stable at room temperature between pH 2 and 12 due to a high energy of activation (section IV B-7). For example, Bejaud et al. (178) found average energies of activation for the bond breaking step of $\Delta G^\ddagger = 19.13 + 0.8$ kcal/mole, $\Delta H^\ddagger = 13.13 + 0.8$ kcal/mole, and $\Delta S^\ddagger = -19.67 + 2.0$ e.u. (Table 35). The positive enthalpy value has been generally interpreted to represent bond strain or distortion on formation of the transition state from the ground state while the negative entropy term represents a greater ordering of the transition

state with respect to the ground state (2,6,7,11,46). The observed ΔH^\ddagger and ΔS^\ddagger represents the mean or average value of the ΔH^\ddagger and ΔS^\ddagger for the various pathways that will successfully break the bond under the particular experimental conditions (6,7,146,147). Therefore, some pathways with higher enthalpy and lower entropy (less negative) requirements as well as with lower enthalpy and higher entropy (more negative) than the average observed value are possible (179). A truly unifying theory would have to be able to account for possible contributions from association-activation theories (1-4,9,11,44), orientation theories (3,39,123), substrate distortion theories (1,2,94), induced-fit theories (3,180-182), and propinquity effects (2,4) to the free energy, enthalpy, and entropy of substrate association and catalysis.

The rate of a reaction could be increased by preorienting the reactants in the binding step and then allowing the reaction to proceed by the lowest enthalpy pathway in the catalytic step. This mechanism would predict a relatively negative ΔS^0 for the association step and an intermediate enthalpy of activation for the catalytic step. However, if the association of enzyme and substrate were, in turn, to strain or distort the substrate towards the transition state in the binding step, then the enthalpy of binding should show a positive term (1,2). The enthalpy of activation requirements of the catalytic step, in turn, would be reduced with respect to the non-catalytic pathway since the substrate bond would be distorted towards the transition state structure prior to the catalytic step. Entropy of activation requirements may still be high in the catalytic step compared to the non-catalytic pathways, unless an orientation simultaneously occurs with distortion of the substrate in the ground

state. Accordingly, the distortion mechanism of association-activation would be characterized by a positive ΔH^0 for the association step and a relatively small positive enthalpy of activation for the catalytic step while the orientation mechanism would be characterized by a negative ΔH^0 for the association and a relatively larger positive enthalpy term for the catalytic step.

The thermodynamic data found in this work for the low temperature form of Cht at 25°C provides evidence for a strain and distortion mechanism on association (1,2). The association of the peptide amide substrates with Cht shows a large positive enthalpy of binding coupled with a large positive entropy (Tables 16 and 34) which may be interpreted as distortion of the substrate. This positive ΔH for distortion is paid for by a large favorable entropy process occurring elsewhere in the enzyme molecule. The positive entropy process may drive the unfavorable enthalpy process at the active site as suggested by Schultz et al. (44). The catalytic step for the low temperature form of Cht then shows enthalpies of activation lower by 4.5 kcal/mole than the non-enzymatic amide hydrolysis (Table 35). The entropies of activation of the catalytic step of the low temperature form of Cht show a large negative value indicating that significant amounts of ordering are necessary to reach the transition state of the catalytic step.

If, on the other hand, the function of the association step were to order the enzyme-substrate complex along the catalytic pathway (3), one would expect to see large negative entropy of association values indicative of the ordering process in the binding step. The entropies of activation seen in the catalytic step would, in turn, be smaller than those observed for the non-enzymatic process. Accordingly, the enthalpy

of activation would be relatively high compared to a strain and distortion association-activation mechanism (2,4).

The thermodynamic data for the high temperature form of Cht at 25°C correlates with an orientation and/or an induced fit mechanism (3). The binding step of the five peptide amide substrates was characterized by a large negative entropy term indicating an ordering process upon binding (Tables 16 and 34). The catalytic step, in turn, showed an entropy term near zero (Tables 19 and 35) which indicates that the ordering of the enzyme-substrate complex is carried out prior to the catalytic step (1-4, 9,11). The catalytic step, in turn showed a large positive enthalpy term, indicating that significant bond distortion had not occurred prior to the catalytic step (Tables 19 and 35). Comparison of the thermodynamic values found in the high temperature enzymatic form with the non-enzymatic hydrolysis of amide bonds in Table 35, reveals that the entropy term is 15 e.u. more positive than the non-enzymatic catalysis and the enthalpy of activation term shows an increase of 3.5 kcal/mole.

Furthermore, as the physiologic temperature of 37°C is approached it was found that the high enthalpy of activation is decreasing and the entropy of activation is becoming more negative (Table 30; figs. 24-28). The enthalpy and entropy binding terms, in turn, are both becoming more negative (Tables 16,34, and 35). This may imply that at this temperature, the enzyme used contributions from both the strain or distortion and the orientation mechanisms. Accordingly, this implies that there exists a continuum along the reaction pathway in which the ground state of the substrate with respect to the enzyme active site is raised in energy by mechanisms of either distortion or orientation, or both. Whether these

processes occur in the binding step and to what extent they occur is dependent on the temperature and the enzyme form. In any case, the same transition state is achieved, though the pathways to the transition may differ.

The data presented in this work suggest the mechanism of Cht catalysis involves elements of both strain or distortion and of orientation. Furthermore, the contribution from these two processes are temperature dependent with varying contributions to the catalytic mechanisms.

IV C. The Nonapeptide as a Synthetic Catalyst.

Model building techniques have shown the cyclized nonapeptide synthesized in this work (Section II C) to possess a hydrophobic binding pocket and charge relay system (145) similar to that proposed for the serine protease α -chymotrypsin (see Section I C-1). The hydrophobic binding pocket consists of the residues L-Phe-2 and D-Phe-5. This hydrophobic binding pocket is situated next to the charge relay system consisting of His-1, Ser-6, and Glu-8 (fig. 39).

However, as can be seen from the data in Table 21 the nonapeptide binds proflavin one to two orders of magnitude less strongly than Cht. In addition, the rate of nonapeptide catalyzed hydrolysis of pNPA is only 1.8 to 2.0 times faster than the rate of histidine alone (Table 21).

These preliminary results show that the nonapeptide is not a good catalyst for the hydrolysis of pNPA. This lack of catalytic rate enhancement may be due to several factors including lack of activation of the complex for catalysis upon association of substrate, solvation effects upon the substrate and charge relay system of the nonapeptide, and/or a less productive orientation of the nonapeptide active site residues.

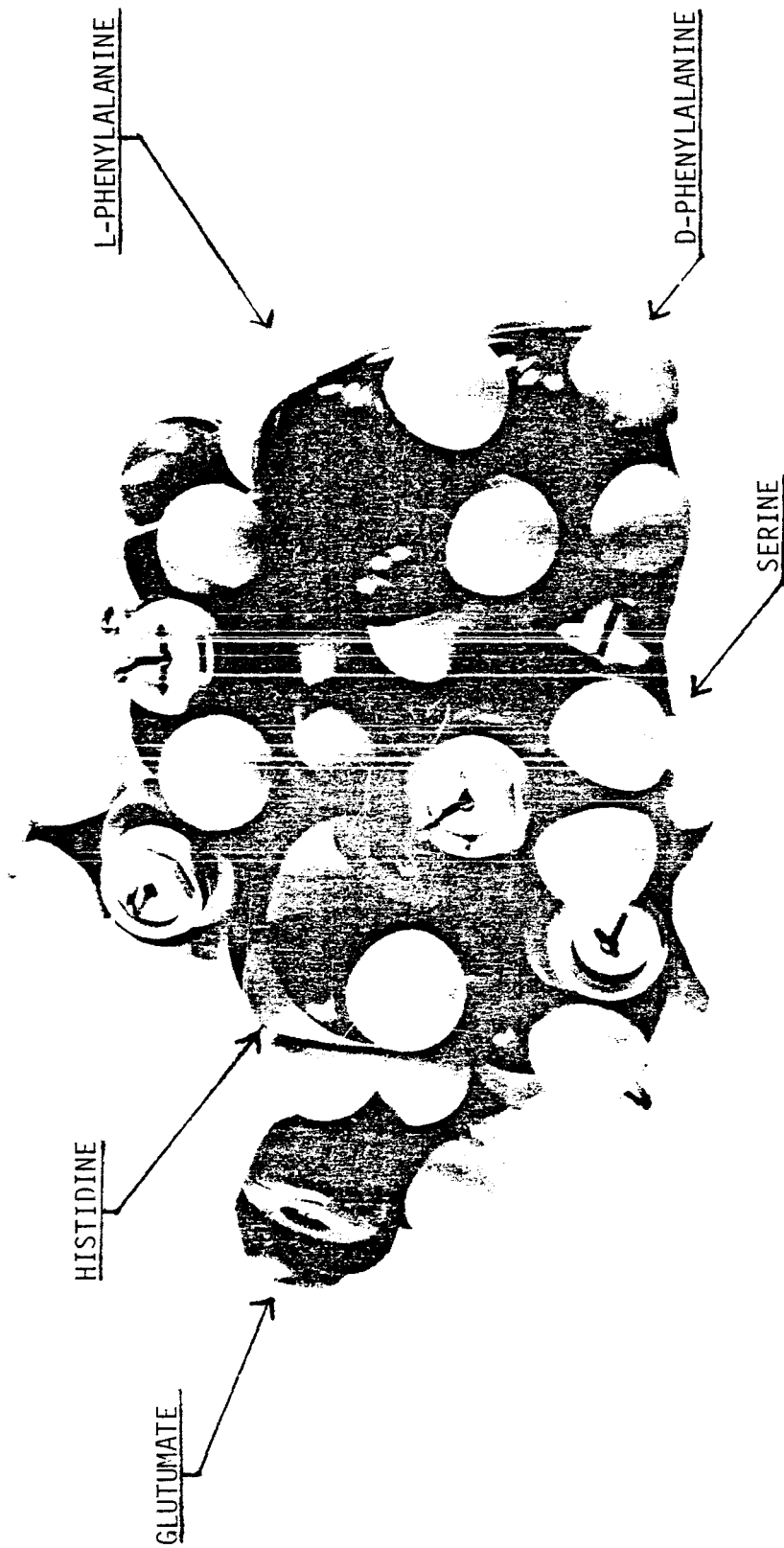
If a compensating enthalpy-entropy mechanism is a major contributor to the catalytic rate enhancement of Cht as proposed by Schultz and co-workers (9,44) then it is not surprising that the nonapeptide is a poor catalyst. Since this proposed type of association-activation mechanism argues that the rest of the large protein molecule away from the active site undergoes a favorable energy process to drive an unfavorable energy process at the active site we might not expect the small nonapeptide to exhibit this compensating process. In addition, the geometrical arrangement at the active site may not be optimal for catalysis or for an

association-activation mechanism to operate.

Solvating water molecules may also play an important role in this lack of catalysis. As the active site of the nonapeptide is more highly accessible to solvating water molecules (fig. 39) than the active site groove of Cht (see Section I C-1) these solvating water molecules may stabilize the reactants and disrupt the charge relay system. The pKa of free histidine is 6.11 (Table 21) while the pKa of the nonapeptide has been found to be 6.4. However, the pKa of histidine which has been incorporated into a peptide backbone has been shown to be 6.4 (183). This suggests that the glutamate in the nonapeptide, which is highly accessible to solvent water unlike the buried Asp-102 of Cht, is not forming a charge relay system in the nonapeptide due to either solvating or geometric effects.

LEGEND

Figure 39. The Nonapeptide Active Site.



REFERENCES

1. Eyring, H., Lumry, R. and Spikes, J.D. (1954) The Mechanisms of Enzyme Action. (Johns Hopkins Press, Baltimore, MD.).
2. Jencks, W.P. (1969) Catalysis in Chemistry and Enzymology. (McGraw Hill, New York, N.Y.).
3. Koshland, D.E. and Neet, K.E. (1969) *Ann. Rev. Biochem.* 37, 359-410. "The catalytic and regulatory properties of enzymes".
4. Page, M.I. and Jencks, W.P. (1971) *Proc. Nat'l. Acad. Sci. USA* 68, 1678-1683. "Entropic contributions to rate accelerations in enzymatic and intramolecular reactions and the chelate effect".
5. Dixon, M. and Webb, E.C. (1971). Enzymes. (Spooniswoode, Ballantyne and Co., Ltd. Longhams, England).
6. Laidler, K.J. (1965). Chemical Kinetics, 2nd Edition. (McGraw Hill Book Co., New York, N.Y.).
7. Laidler, K.J. (1969). Theories of Chemical Reaction Rates. (McGraw Hill Book Co., New York, N.Y.).
8. Walter, C. (1965) Steady-State Applications in Enzyme Kinetics. (The Ronald Press Co., New York, N.Y.).
9. Schultz, R.M., Konovessi-Panayotatos, A. and Peters, J.R. (1977) *Biochem.* 16, 2194-2202. "Thermodynamics of binding to native α -chymotrypsin and to forms of α -chymotrypsin in which catalytically essential residues are modified: a study of "productive" and "non-productive" associations".
10. Thompson, R.C. and Blout, E.R. (1973) *Biochem.* 12, 57-65. "Dependence of the kinetic parameters for elastase catalyzed amide hydrolysis on the length of peptide substrates".
11. Jencks, W.P. (1975) *Adv. in Enz.* 43, 219-410. "Binding energy, specificity, and enzymatic catalysis: The circe effect".
12. Fersht, A. (1977). Enzyme Structure and Mechanism. (W.H.Freeman and Co., San Francisco, CA.).
13. Pauling, L. (1946) *Chem. Eng. News* 24, 1375-1383. "Configuration and electronic structure of molecules with some applications to natural products".
14. Fersht, A.R. (1974) *Proc. Royal Soc. (London)* 187, 397-407. "Catalysis, binding and enzyme substrate complementarity".
15. Northrop, H.H., Kunitz, M., and Herriott, R.M. (1948). Crystalline Enzymes, 2nd Edition. (Columbia University Press, N.Y.).

16. Bergmann, M. and Fruton, J.S. (1941) *Adv. In Enz.* 1, 63-98. "The specificity of proteinases".
17. Bensen, J.A. Jr. and Rampone, A.J. (1966) *Ann. Rev. Physiol.* 28, 201-226. "Gastrointestinal absorption".
18. Desnuelle, P. in Boyer, P.F., Tardy, H. and Myrback, K., Editors, (1960). The Enzymes, 2nd Edition, Vol. 4, Chapter 5. (Academic Press, N.Y.).
19. Hartley, B.S. and Kauffman, D.L. (1966) *Biochem. J.* 101, 229-231. "Corrections to the amino acid sequence of bovine chymotrypsinogen-A".
20. Hess, G.P. in Boyer, P.D., Editor (1971). The Enzymes. 3rd Edition, Vol. 3, p. 213. (Academic Press, N.Y.).
21. Blow, D.M., Birkoft, J.J. and Hartley, B.S. (1969) *Nature* 221, 337-340. "Role of a buried acid group in the mechanism of action of chymotrypsin".
22. Bender, M.L., Kezdy, F.J. and Gunther, C.R. (1964) *J. Amer. Chem. Soc.* 86, 3714-3721. "The anatomy of an enzymatic catalysis. α -chymotrypsin".
23. Himoe, A., Brandt, K.G., DeSa, R.J., and Hess, G.P. (1969) *J. Biol. Chem.* 244, 3483-3493. "Investigations of the chymotrypsin-catalyzed hydrolysis of specific substrates".
24. Bruice, T.C. and Benkovic, S. (1966). Bioorganic Mechanisms, Vol. 1, chapter 2. (W.A. Benjamin Publisher, N.Y.).
25. Hartley, B.S. and Shotton, D.M. in Boyer, P.D., Editor (1971). The Enzymes, 3rd Edition, Vol. 3, p. 323. (Academic Press, N.Y.).
26. Neurath, H. and Schwert, G.W. (1950) *Chem. Rev.* 46, 69-153. "The mode of action of the crystalline pancreatic proteolytic enzymes".
27. Schechter, I. and Berger, A. (1967) *Biochem. Biophys. Res. Commun.* 27, 157-162. "On the size of the active site in proteases".
28. Hein, G.E. and Niemann, C. (1961) *Proc. Nat. Acad. Sci. USA* 47, 1341-1355. "An interpretation of the kinetic behavior of model substrates of α -chymotrypsin".
29. Cohen, S.G. (1969) *Trans. N.Y. Acad. Sci. Ser. II* 31, 705-719. "On the active site and specificity of α -chymotrypsin".
30. Zerner, B. and Bender, M.L. (1964) *J. Amer. Chem. Soc.* 86, 3669-3674. "The kinetic consequences of the acyl-enzyme mechanism for the reactions of specific substrates with chymotrypsin".

31. Blow, D.M. in Boyer, P.D., Editor (1971). The Enzymes, 3rd Edition, Vol. 3, p. 185. (Academic Press, N.Y.).
32. Tulinsky, A., Mavridis, I. and Mann, R.F. (1978) J. Biol. Chem. 253, 1074-1078. "Expression of functionality of α -chymotrypsin".
33. Matthews, D.A., Alden, R.A., Birktoft, J.J., Freer, S.T. and Kraut, J. (1977) J. Biol. Chem. 252, 8875-8883. "Re-examination of the charge relay system in subtilisin and comparison with other serine proteases".
34. Tanford, C. (1980). The Hydrophobic Effect, 2nd Edition. (John Wiley and Sons, N.Y.).
35. Vaslow, F. and Doherty, D.G. (1953) J. Amer. Chem. Soc. 75, 928-931. "Thermodynamic study of some enzyme-inhibitor complexes of α -chymotrypsin II".
36. Shiao, D.D.F. (1970) Biochem. 9, 1083-1090. "Calorimetric investigations of the binding of inhibitors to α -chymotrypsin II. A systematic comparison of the thermodynamic functions of a variety of inhibitors to α -chymotrypsin".
37. Lumry, R. and Biltonen, R. in Timasheff, S.N. and Fasman, G.D., Editors (1969). Structure and Stability of Biological Macromolecules, p. 65. (Marcel Dekker, Inc. N.Y.).
38. Lumry, R. and Rajender, S. (1970) Biopolymers 9, 1125-1227. "Enthalpy-entropy compensation phenomena in water solutions of proteins and small molecules: a ubiquitous property of water".
39. Lumry, R. and Rajender, S. (1971) J. Phys. Chem. 75, 1387-1401. "Studies of the chymotrypsinogen family of proteins XVI. Enthalpy-entropy compensation phenomenon of α -chymotrypsin and the temperature of minimum sensitivity".
40. Lumry, R. (1974) Ann. N.Y. Acad. Sci. 227, 46-73. "Conformational mechanisms for free energy transductions in protein systems: old ideas and new facts".
41. Ako, H., Foster, R.J. and Ryan, C.A. (1974) Biochem. 13, 132-139. "Mechanism of action of naturally occurring proteinase inhibitors. Studies with anhydrotrypsin and anhydrochymotrypsin purified by affinity chromatography".
42. Ryan, D.S. and Feeney, R.E. (1975) J. Biol. Chem. 250, 843-847. "The interaction of inhibitors of proteolytic enzymes with 3-methyl-histidine-57-chymotrypsin".
43. Fastrez, J. and Houyet, N. (1977) Eur. J. Biochem. 81, 515-522. "Mechanism of chymotrypsin: acid/base catalysis and transition-state solvation by the active site".

44. Schultz, R.M., Varma-Nelson, P., Peters, J.R. and Treadway, W.J. Jr. (1979) *J. Biol. Chem.* 254, 12411-12418. "Effect of modification of the essential catalytic residues in α -chymotrypsin on the thermodynamics of substrate analog association".
45. Glick, D.M. (1971) *Biochem. Biophys. Acta* 250, 390-394. "Effects of solutes on the temperature dependence of chymotryptic hydrolysis".
46. Lefler, J.E. and Grunwald, E. (1963). Rates and Equilibria of Organic Reactions, p. 315. (John Wiley and Sons, Inc. N.Y.).
47. Krug, R.R., Hunter, W.G. and Grieger, R.A. (1976) *J. Phys. Chem.* 80, 2335-2341. "Enthalpy-entropy compensation. I. Some fundamental statistical problems associated with the analysis of van't Hoff and Arrhenium data".
48. Krug, R.R., Hunter, W.G. and Grieger, R.A. (1976) *J. Phys. Chem.* 80, 2341-2351. "Enthalpy-entropy compensation. II. Separation of the chemical from the statistical effects".
49. Exner, O. (1973) *Progr. Phys. Org. Chem.* 10, 411-482. "Enthalpy-entropy relationships".
50. Luscher, M., Ruegg, M. and Schindler, P. (1978) *Biochem. Biophys. Acta* 536, 27-37. "Thermodynamic studies of the interactions of α -chymotrypsin with water. II. Statistical analyses of the enthalpy-entropy compensation effect".
51. Marshall, T.H. and Chen, V. (1973) *J. Amer. Chem. Soc.* 95, 5400-5405. "Activation parameters of elastase and chymotrypsin catalyzed hydrolysis. Differential role of favorable enthalpy in determining reactivity".
52. Baggott, J.E. and Klapper, M.H. (1976) *Biochem.* 15, 1473-1481. "Rate enhancement specificity with α -chymotrypsin: temperature dependence of deacylation".
53. Rajender, S., Lumry, R., and Han, M. (1971) *J. Phys. Chem.* 75, 1375-1386. "Studies of the chymotrypsinogen family of proteins. XV. pH and temperature dependence of the α -chymotryptic hydrolysis of N-acetyl-L-tryptophan ethyl ester".
54. Inagami, T., Patchornik, A. and York, S.S. (1969) *J. Biochem.* 65, 809-819. "Participation of an acidic group in the chymotrypsin catalysis".
55. Adams, P.A. and Swart, E.R. (1977) *Biochem. J.* 161, 83-92. "The effects of temperature on the individual stages of the hydrolysis of non-specific p-nitrophenyl esters by α -chymotrypsin".

56. Kunugi, S., Hirohara, H. and Ise, N. (1979) *J. Amer. Chem. Soc.* 101, 3640-3646. "Kinetic and thermodynamic study of the specificity in the elementary steps of α -chymotrypsin-catalyzed hydrolysis reaction".
57. Wedler, F.C., Uretsky, L.S., McClune, G. and Cencula, J. (1975) *Arch. Biochem. Biophys.* 170, 476-484. "Conformational states of chymotrypsin at high pH: Temperature effects on catalysis and binding".
58. Kim, Y.D. and Lumry, R. (1971) *J. Amer. Chem. Soc.* 93, 1003-1013. "Studies of the chymotrypsinogen family. XII. "A" type substrates of α -chymotrypsin at neutral and alkaline pH values".
59. Kennedy, W.P. (1980) Ph.D. Dissertation, Loyola University of Chicago.
60. Havesteen, B., Labousse, B. and Hess, G. (1963) *J. Amer. Chem. Soc.* 85, 796-802. "Evidence for conformational changes in α -chymotrypsin catalyzed reactions. VII. Thermally induced reversible changes of conformation at pH 2.0".
61. Wasi, S. and Hofmann, T. (1973) *Can. J. Biochem.* 51, 797-805. "The conformational state of methionine residues in the temperature controlled transition of chymotrypsinogen and α -chymotrypsin".
62. Luscher, M. and Ruegg, M. (1978) *Biochem. Biophys. Acta* 533, 428-439. "Thermodynamic studies of the interaction of α -chymotrypsin with water. I. Determination of the isosteric enthalpies and entropies of eater binding to the native enzyme".
63. Fruton, J.S., in Reich, E., Rifkin, D.B. and Shaw, E., Editors (1975). Proteases and Biological Control. (Cold Springs Harbor Laboratory, N.Y.).
64. Morihara, K. and Oka, T. (1973) *Arch. Biochem. Biophys.* 156, 764-771. "Effect of secondary interaction on the enzymatic activity of trypsin-like enzymes from *Streptomyces*".
65. Segal, D. (1972) *Biochem.* 11, 349-356. "A kinetic investigation of the crystallographically deduced binding substrates of bovine chymotrypsin A".
66. Bauman, W.K., Bizzozero, S.A. and Dutler, H. (1973) *Eur. J. Biochem.* 39, 381-391. "Kinetic investigation of the α -chymotrypsin-catalyzed hydrolysis of peptide substrates".
67. Morihara, K. and Oka, T. (1973) *FEBS Letters* 33, 54-56. "Effects of secondary interactions on the enzymatic activity of Subtilisin BPN': comparison with α -chymotrypsin, trypsin, and elastase".
68. Fruton, J.S. (1970) *Adv. Enzymol.* 33, 401-443. "The specificity and mechanism of pepsin action".

69. Magnusson, S. in Boyer, P.D., Editor (1971) The Enzymes 3rd Edition, Vol. III, p. 277-321. (Academic Press, N.Y.).
70. Yoshida, N., Yamamoto, T. and Izumiya, N. (1968) Arch. Biochem. Biophysics. 123, 165-171. "Action of chymotrypsin on synthetic substrates. VII. Hydrolysis of oligopeptides containing glycine and tyrosine".
71. Bauer, C.A., Thompson, R.C. and Blout, E.R. (1976) Biochem. 15, 1296-1299. "The active centers of Streptomyces Griseus protease 3, α -chymotrypsin, and elastase: enzyme-substrate interactions close to the scissile bond".
72. Bauer, C., Thompson, R. and Blout, E. (1976) Biochem. 15, 1291-1295. "The active centers of Streptomyces Griseus protease 3 and α -chymotrypsin: enzyme-substrate interactions remote from the scissile bond".
73. Wright, H.T. (1977) Eur. J. Biochem. 73, 567-578. "Secondary and conformational specificity of trypsin and chymotrypsin".
74. Yoshida, N. and Ishii, S. (1972) J. Biochem. 71, 185-191. "Specificity determining site of α -chymotrypsin. I. Kinetic investigation of aromatic amino compounds and phenylalanine ester derivatives in α -chymotrypsin-catalyzed hydrolysis.
75. Yamamoto, T. and Izumiya, N. (1966) Arch. Biochem. Biophys. 114, 459-464. "Action of chymotrypsin on synthetic substrates. VI. The action of α -chymotrypsin on glycyL-aminoacyl-L-tyrosine ethyl esters".
76. Baumann, W.K., Bizzozero, S.A. and Dutter, H. (1970) FEBS Letters 8, 257-260. "Specificity of α -chymotrypsin dipeptide substrates".
77. Izumiya, N. and Yamashita, T. (1959) J. Biochem. 46, 19-30. "Action of chymotrypsin on synthetic substrates. I. Action of α -chymotrypsin on aminoacyl-L-tyrosinamides".
78. Segal, D.M., Powers, J.C., Cohen, G.H., Davies, D.R. and Wilcox, P.E. (1971) Biochem. 10, 3728-3738. "Substrate binding site in chymotrypsin A. A crystallographic study using peptide chloromethyl ketones as site-specific inhibitors".
79. Steitz, T.A., Henderson, R. and Blow, D.M. (1969) J. Mol. Biol. 46, 337-348. "Structure of crystalline α -chymotrypsin. III. Crystallographic studies of substrates and inhibitors bound to the active site of α -chymotrypsin".
80. Thompson, R.C. and Blout, E.R. (1973) Biochem. 12, 51-57. "Restrictions on the binding of proline-containing peptides to elastase".
81. Mills, F.C., Ackers, G.K., Gaud, H.T. and Gill, S.J. (1979) J. Biol. Chem. 254, 2875-2880. "Thermodynamic studies on ligand binding and subunit association of human hemoglobins".

82. Kauzmann, W. (1959) *Adv. Prot. Chem.* 14, 1-63. "Some factors in the interpretation of protein denaturation".
83. Valdes, R., Jr. and Ackers, G.K. (1977) *J. Biol. Chem.* 252, 74-81. "Thermodynamic studies on subunit assembly in human hemoglobin. Self-association of oxygenated chains (α^{SH} and β^{SH}): determination of stoichiometrics and equilibrium constants as a function of temperature".
84. Ip, S.H.C. and Ackers, G.K. (1977) *J. Biol. Chem.* 252, 82-87. "Thermodynamic studies on subunit assembly in human hemoglobin. Temperature dependence of the dimer-tetramer association constants for oxygenated and unliganded hemoglobins".
85. Monod, J., Wyman, J. and Changeaux, J.P. (1965) *J. Mol. Biol.* 12, 88-112. "On the nature of allosteric transition: a plausible model".
86. Szewczuk, M.R. and Mukkur, T.K.S. (1977) *Immunology* 32, 111-119. "Enthalpy-entropy compensation in dinitrophenyl-anti dinitrophenyl antibody interactions".
87. Szewczuk, M.R. and Mukkur, T.K.S. (1977) *Immunology* 33, 11-16. "Thermodynamics of the interaction of ϵ -dinitrophenyl-L-lysine and the subunits (Fab) of bovine colostrum immunoglobulin GI anti-dinitrophenyl antibody".
88. Mukkur, T.K.S. (1980) *Trends in Biochem. Sciences* 5, 72-74. "Thermodynamics of hapten-antibody interaction(s)".
89. Tanford, C. (1968) *Adv. Prot. Chem.* 23, 122-283. "Protein denaturation".
90. Cuatrecasas, P. (1971) *J. Biol. Chem.* 246, 7265-7274. "Properties of the insulin receptor of isolated fat cell membranes".
91. Aune, K.C., Goldsmith, L.C. and Timasheff, S.N. (1971) *Biochem.* 10, 1617-1622. "Dimerization of α -chymotrypsin. II. Ionic strength and temperature dependence".
92. Laskowski, M. Jr. and Sealock, R.W. in Boyer, P.D., Editor (1971) *The Enzymes*, 3rd Edition, Vol. 3, chap. 11. (Academic Press, N.Y.).
93. Blow, D.M., Wright, C.S., Kukla, D., Ruhlmann, A., Steigemann, W. and Huber, R. (1972) *J. Mol. Biol.* 69, 137-144. "A model for the association of bovine pancreatic trypsin inhibitor with chymotrypsin and trypsin".
94. Ruhlmann, A., Kukla, D., Schwager, P., Barteles, K. and Huber, R. (1973) *J. Mol. Biol.* 77, 417-436. "Structure of the complex formed by bovine trypsin and bovine pancreatic trypsin inhibitor".
95. Vincent, J.P. and Lazdunski, M. (1973) *Eur. J. Biochem.* 38, 365-372. "The interactions between α -chymotrypsin and pancreatic trypsin inhibitor (Kunitz inhibitor)".

96. Quast, U., Engel, J., Heumann, H., Krause, G. and Steffen, E. (1974) *Biochem.* 13, 2512-2520. "Kinetics of the interaction of bovine pancreatic trypsin inhibitor (Kunitz) with α -chymotrypsin".
97. Gill, S.J., Nichols, N.F. and Wadso, I. (1976) *J. Chem. Thermo.* 8, 445-452. "Calorimetric determination of enthalpies of solution of slightly soluble liquids. II. Enthalpy of solution of some hydrocarbons in water and their use in establishing the temperature dependence of their solubilities".
98. Berezin, I.V., Levashor, A.V. and Martinek, K. (1970) *Eur. J. Biochem.* 16, 472-474. "Thermodynamics of α -chymotrypsin-inhibitor complex formation".
99. Wildnauer, R. and Canady, W.J. (1966) *Biochem.* 5, 2885-2892. "A hydrocarbon-water model for the formation of the enzyme-inhibitor complex in the case of α -chymotrypsin".
100. Nozaki, Y. and Tanford, C. (1971) *J. Biol. Chem.* 246, 2211-2217. "The solubility of amino acids and two glycine peptides in aqueous ethanol and dioxane solutions".
101. Nandi, P.K. (1976) *Inter. J. Pept. Prot. Res.* 8, 253-264. "Thermodynamic parameters of transfer of N-acetyl ethyl esters of different amino acids from organic solvents to water".
102. Yatsimirski, A.K., Martinek, K. and Berezin, I.V. (1971) *Tetrahedron* 27, 2855-2868. "Mechanism of micellar effects on acylation of aryl oximes by p-nitrophenyl carboxylates".
103. Hogan, J.C. and Gandour, R.D. (1980) *J. Amer. Chem. Soc.* 102, 2865-2866. "The remarkable catalytic power of glymes in ester aminolysis carried out in nonpolar media".
104. Breslow, R., Czarniecki, M.F., Emert, J. and Hamaguchi, H. (1980) *J. Amer. Chem. Soc.* 102, 762-770. "Improved acylation rates within cyclodextrin complexes from flexible capping of the cyclodextrin and from adjustment of the substrate geometry".
105. Klotz, I.M., Royer, G.P. and Scarpa, I.S. (1971) *Proc. Nat. Acad. Sci. USA* 68, 263-264. "Synthetic derivatives of polyethyleneimines with enzyme-like catalytic activity (Synzymes)".
106. Mirejovsky, D. (1979) *J. Org. Chem.* 44, 4881-4886. "Behavior of imidazole on poly (ethylenimine) derivatives; Hydrolysis of p-nitrophenyl caproate".
107. Fridkin, M. and Goren, H.J. (1974) *Eur. J. Biochem.* 41, 273-283. "Synthesis and catalytic properties of the heptapeptide L-seryl-L-prolyl-L-cysteinyl-L-seryl- α -L-glytanyl-L-threonyl-L-tyrosine".
108. Petz, D. and Schneider, F. (1976) *FEBS Letters* 67, 32-35. "Catalytic properties of peptides without hydrolytic activity".

109. Goren, H.J., Fletcher, T., Fridkin, M. and Katchalski-Katzir, E. (1978) *Biopolymers* 17, 1679-1692. "Poly (L-histidinyl-L-alanyl-L-glutamic acid). II. Catalysis of p-nitrophenyl acetate hydrolysis".
110. Katchalski, E., Fasman, G.D., Simons, E., Blout, E.R., Gurd, F.R.N. and Koltun, W. (1960) *Arch. Biochem. Biophys.* 88, 361-365. "Synthetic histidine-containing polypeptides as catalysts for the hydrolysis of p-nitrophenyl acetate".
111. Yapel, A., Han, M., Lumry, R., Rosenberg, A. and Shiao, D.F. (1966) *J. Amer. Chem. Soc.* 88, 2573-2584. "Studies of the chymotrypsinogen family. V. The effect of small molecule contaminants on the kinetic behavior of α -chymotrypsin".
112. Dixon, G.H. and Neurath, H. (1957) *J. Biol. Chem.* 225, 1049-1059. "Acylation of the enzymatic site of α -chymotrypsin by esters, acid anhydrides and acid chlorides".
113. Greenstein, J.P. and Winitz, M. (1961) Chemistry of the Amino Acids, Vol. 2 (John Wiley and Sons, New York, N.Y.).
114. Schwarz, H., Bumpus, F.M. and Page, I.H. (1957) *J. Amer. Chem. Soc.* 79, 5697-5703. "Synthesis of a biologically active octapeptide similar to natural isoleucine angiotonin octapeptide".
115. Huang, H.T., Foster, R.J., and Niemann, C., (1952) *J. Amer. Chem. Soc.* 74, 105-109. "The kinetics of α -chymotrypsin-catalyzed hydrolysis of acetyl- and nicotinyl-L-phenylalaninamide in aqueous solution at 25°C and pH 7.9".
116. Vaughn, J.R., Jr. and Osato, R.L. (1952) *J. Amer. Chem. Soc.* 74, 676-679. "The preparation of peptides using mixed carbonic-carboxylic acid anhydrides".
117. Anderson, G.W. (1972). Progress in Peptide Research. Vol. II. S. Lande (Editor) 343-345. (Gordon and Breach Publisher, New York). "Steric hindrance associated with triethylamine use in peptide synthesis by the mixed carbonic anhydride method".
118. Tilak, M.A., Hendricks, M.L. and Wedel, D.S. (1972). Progress in Peptide Research. Vol. II. S. Lande (Editor) 351-359. (Gordon and Breach Publisher, New York), "Excess mixed anhydride method for rapid synthesis of peptides in high yield and purity with minimum purification".
119. Pettit, G.R. (1970) Synthetic Peptides. Vol. I. (Van Nostrand Reinhold Company, New York),
120. Sheehan, J.C. and Yang, D.H. (1958) *J. Amer. Chem. Soc.* 80, 1154-1158. "The use of N-formylamino acids in peptide synthesis".
121. Dakin, H.D. and Dudley, H.W. (1914) *J. Biol. Chem.* 18, 29-51. "The formation of amino- and hydroxy-acids from glyoxals in the animal organism".

122. Ingles, D.W. and Knowles, J.R. (1968) *Biochem. J.* 108, 561-569. "The stereospecificity of α -chymotrypsin".
123. Cohen, S.G. and Schultz, R.M. (1968) *J. Biol. Chem.* 243, 2607-2617. "The active site in α -chymotrypsin".
124. Bodanszky, M., Klausner, Y. and Ondetti, M. (1976) Peptide Synthesis, 2nd Edition. (John Wiley and Sons, New York).
125. Randerath, K. (1966) Thin-Layer Chromatography, 2nd Edition. (Academic Press, New York).
126. Dyckes, D.F., Nestor, J.J.Jr., Ferger, M.F. and duVigneaud, V. (1974) *J. Med. Chem.* 17, 250-252. "(1-B-Mercapto-B, B-diethylpropionic acid)-8-lysine-vasopressin, a potent inhibitor of 8-lysine vasopressin and oxytocin".
127. Sifferd, R.H. and du Vigneaud, V. (1935) *J. Biol. Chem.* 108, 753-761. "A new synthesis of cornasine, with some observations on the splitting of the benzyl group from carbobenzoxy derivatives and from benzylthio ethers".
128. Ellman, G.L. (1959) *Arch. Biochem. Biophys.* 82, 70-77. "Tissue sulfhydryl groups".
129. Smith, C.W. and Hruby, V.J. (1974) *J. Med. Chem.* 17, 873-876. "Four cyclic disulfide pentapeptides possessing the ring of isotocin and glutitocin".
130. Moore, S. and Stein, W. (1954) *J. Biol. Chem.* 211, 907-913. "A modified ninhydrin reagent for the photometric determination of amino acids and related compounds".
131. Blackburn, S. (1969) Amino Acid Determination Methods and Techniques. (Marcel Dekker, Inc. New York).
132. Sehwert, G.W. and Takenaka, Y. (1955) *Biochem. Biophys. Acta* 16, 570-575. "A spectrophotometric determination of trypsin and chymotrypsin".
133. Bender, M.L., Begue-Canton, M.L., Blakeley, R.L., Brubacher, L.J., Feder, J., Gunther, C.R., Kezdy, F.J., Killheffer, J.V.Jr., Marshall, T.H., Moller, C.G., Roseske, R.W. and Stoops, J.K. (1966) *J. Amer. Chem. Soc.* 88, 5890-5913. "The determination of the concentration of hydrolytic enzyme solutions: α -chymotrypsin, trypsin, papain, elastase, subtilisin and acetylcholinesterase".
134. Schonbaum, G., Zerner, B. and Bender, M. (1961) *J. Biol. Chem.* 236, 2930-2935. "The spectrophotometric determination of the operational normality of an α -chymotrypsin solution".

135. Bull, H.B. and Breese, K. (1974) Arch. Biochem. Biophys. 161, 665-670. "Surface tension of amino acid solution. A. Hydrophobicity scale of the amino acid residues".
136. Tanford, C. (1962) J. Amer. Chem. Soc. 84, 4240-4247. "Contributions of hydrophobic interactions to the stability of the globular conformation of proteins".
137. Pandit, M.W. and Narasinga-Rao, M.S. (1974) Biochem. 13, 1048-1055. "Studies on self-association of proteins. The self-association of α -chymotrypsin at pH 8.3 and ionic strength 0.05".
138. Kumar, S. and Hein, G.E. (1970) Biochem. 9, 291-297. "Concerning the mechanism of autolysis of α -chymotrypsin".
139. Taylor, R.P., Vatz, J.B. and Lumry, R. (1973) Biochem. 12, 2933-2940. "Control of conformation of α -chymotrypsin through chemical modifications".
140. Foster, R.J. and Niemann, C. (1955) J. Amer. Chem. Soc. 77, 1886-1892. "Reevaluation of kinetic constants of previously investigated specific substrates of α -chymotrypsin".
141. Bender, M.L., Clement, G.E., Kezdy, F.J. and d'A Heck, H. (1964) J. Amer. Chem. Soc. 86, 3680-3690. "The correlation of the pH (pD) dependence and stepwise mechanism of α -chymotrypsin-catalyzed reactions".
142. Segel, I.H. (1976) Biochemical Calculations, 2nd Edition (John Wiley and Sons, New York).
143. Personal communication. Dr. Yuriel Olsher, Harvard Medical School.
144. CRC Handbook of Chemistry and Physics, 58th Edition (1977-1978). (CRC Press, Inc., Cleveland, Ohio USA).
145. Personal communication. Dr. Richard M. Schultz, Loyola-Stritch School of Medicine.
146. Kumamoto, J., Raison, J.K. and Lyons, J.M. (1971) J. Theor. Biol. 31, 47-51. "Temperature breaks in Arrhenius plots: a thermodynamic consequence of a phase change".
147. Londesborough, J. (1980) Eur. J. Biochem. 105, 211-215. "The causes of sharply bent or discontinuous Arrhenius plots for enzyme-catalyzed reactions".
148. Matta, M.S., Landis, M.E., Patrick, T.B., Henderson, P.A., Russo, M.W. and Thomas, R.L. (1980) J. Amer. Chem. Soc. 102, 7151-7152. "¹³C-enriched S-methyl probe at the active site of an enzyme (S-(¹³C)methylmethionine-192)- α -chymotrypsin (MSMC)".

149. Andrews, F.C. (1971) Thermodynamics: Principles and Applications. (John Wiley and Sons, Inc. New York).
150. Castellan, G.W. (1971) Physical Chemistry, 2nd Edition (Addison-Wesley Publishing Co., Reading, Mass. USA).
151. Frankfater, A. (1968). Ph.D. dissertation, Duke University.
152. Kistakowsky, G.B. and Rosenberg, A.J. (1952) J. Amer. Chem. Soc. 74, 5020-5025. "The kinetics of urea hydrolysis by urease".
153. Alberty, R.A., Massey, V., Frieden, C. and Fuhlbridge, A.R. (1954) J. Amer. Chem. Soc. 76, 2485-2493. "Studies of the enzyme fumarase. III. The dependence of the kinetic constants at 25°C upon the concentration and pH of phosphate buffers".
154. Segel, I H. (1975) Enzyme Kinetics. (John Wiley and Sons, Inc., New York, N.Y.).
155. Amidon, G.L., Pearlman, R.S. and Anik, S.T. (1979) J. Theor. Biol. 77, 161-170. "The solvent contributions to the free energy of protein-ligand interactions".
156. Kresheck, G.C. and Klotz, I.M. (1969) Biochem. 8, 8-12. "The thermodynamics of transfer of amides from an apolar to an aqueous solution".
157. Wolfenden, R. (1978) Biochem. 17, 201-204. "Interaction of the peptide bond with solvent water: a vapor phase analysis".
158. Sturtevant, J.M. (1977) Proc. Nat. Acad. Sci. USA 74, 2236-2240. "Heat capacity and entropy changes in processes involving proteins (thermodynamics/hydrophobic effects/vibrational mode/conformations)".
159. Richards, F.M. and Richmond, T. (1978) in Molecular Interactions and Activity in Proteins, chap. 2 (Excerpta Medica Publisher, N.Y.).
160. Cohen, S., Vaidya, V. and Schultz, R. (1970) Proc. Nat. Acad. Sci. USA 66, 249-256. "Active site of α -chymotrypsin. Activation by association-desolvation.
161. Ling, G.N. (1967) in Thermobiology, chap. 2 (Academic Press, New York, N.Y.).
162. Somer, G.N., Neubauer, M. and Low, P.S. (1977) Arch. Biochem. Biophysics. 181, 438-446. "Neutral salt effects on the velocity and activation volume of the lactate dehydrogenase reaction: evidence for enzyme hydration changes during catalysis".

163. Von Hippel, P.H. and Wong, K.Y. (1964) *Science* 145, 577-580. "Neutral salts: the generality of their effects on the stability of macromolecular conformations".
164. Von Hippel, P.H. and Schleich, T. in Timasheff, S.N. and Fasman, G.D., Editors (1969) Structure and Stability of Biological Macromolecules, Vol. II, p.417 (Marcel Dekker Inc., New York, N.Y.).
165. Fink, A.L. (1973) *Biochem.* 12, 1736-1742. "The α -chymotrypsin catalyzed hydrolysis of N-acetyl-L-tryptophan p-nitrophenyl ester in dimethyl sulfoxide at subzero temperatures".
166. Fink, A.L. (1974) *Biochem.* 13, 277-280. "Effect of dimethyl sulfoxide on the interaction of proflavine with α -chymotrypsin".
167. Kennedy, W.P. and Schultz, R.M. (1979) *Biochem.* 18, 349-356. "Mechanism of association of a specific aldehyde "Transition state analogue" to the active site of α -chymotrypsin".
168. Holterman, H.A.J. and Engberts, J.B.F.N. (1980) *J. Amer. Chem.Soc.* 102, 4256-4257. "Hydrolysis of two acyl activated esters in water-rich 2-n-butoxyethanol-water mixtures. Effects of hydrophobic interactions on enthalpies, entropies, and heat capacities of activation".
169. Cooper, A. (1976) *Proc. Nat. Acad. Sci. USA* 73, 2740-2741. "Thermodynamic fluctuations in protein molecules".
170. Ingles, D.W. and Knowles, J.R. (1967) *Biochem. J.* 104, 369-377. "Specificity and stereospecificity of α -chymotrypsin".
171. Lipscomb, W.N. (1978) in Molecular Interactions and Activity in Proteins, chap. 1. (Excerpta Medica Publisher, New York).
172. Brandt, K.G., Himoe, A. and Hess, G.P. (1967) *J. Biol. Chem.* 242, 3973-3982. "Investigation of the chymotrypsin-catalyzed hydrolysis of specific substrates".
173. Bosshard, H.R. (1974) *FEBS Letters* 38, 139-142. "The interaction of D-amino acid residues with the aromatic binding site of α -chymotrypsin".
174. Ptitsyn, O.B. (1978) *FEBS Letters* 93, 1-4. "Inter-domain mobility in proteins and its probable functional role".
175. Bauer, C.A. (1980) *Eur. J. Biochem.* 105, 565-570. "Active centers of α -chymotrypsin and of Streptomyces Griseus proteases 1 and 3. S₂-P₂ enzyme-substrate interactions".
176. Alberty, W.J. and Knowles, J.R. (1976) *Biochem.* 15, 5631-5640. "Evolution of enzyme function and the development of catalytic efficiency".

177. Darwin, C. (1897). The Origin of Species by Means of Natural Selection or the Preservation of Favored Races in the Struggle for Survival. (D. Appleton and Co., Publishers, New York, N.Y.).
178. Bejoud, M., Mion, L., Taillades, J. and Commeyres, A. (1975) Tetrahedron 31, 403-410. "Systems de strecker et apparentes - IV".
179. Lefler, J.E. and Grunwald, E (1963) Rates and Equilibria of Organic Reactions, p. 62-65. (John Wiley and Sons, Inc. New York, N.Y.).
180. Fink, A.L. (1976) Biochem. 15, 1580-1586. "Cryoenzymology of chymotrypsin: the detection of intermediates in the catalysis of a specific anilide substrate".
181. Havesteen, B.H. (1967) J. Biol. Chem. 242, 769-776. "The Kinetics of the two-step interaction of chymotrypsin with proflavin".
182. Cruickshank, W.H. and Kaplan, H. (1975) Biochem. J. 147, 411-416. "Properties of the histidine residues of indole-chymotrypsin".
183. Sachs, D.H., Schechter, A.N. and Cohen, J.S. (1971) J. Biol. Chem. 246, 6576-6580. "Nuclear Magnetic Resonance Titration Curves of Histidine Ring Protons".

APPENDIX A

Derivation of an Equation to Describe the Effect on the Equilibrium Between Two Conformations of an Enzyme upon Addition of Substrate.

The equilibrium system between a high and low temperature form of an enzyme E can be described by



where E_L and E_H are the low and high temperature forms of the free enzyme in solution, respectively, and K is the equilibrium constant for the process

$$K = \frac{(E_H)}{(E_L)} \quad (2)$$

If substrate is added to the system removing free enzyme from the equilibrium pool, then the free enzyme remaining must change according to equation 1 to satisfy the equilibrium (Eq. 2).

After addition of substrate the total enzyme (E_T) bound and unbound for each form can be described as

$$E_{LT} = E_L + E_L S \quad (3)$$

and

$$E_{HT} = E_H + E_H S \quad (4)$$

Since from equation 2 we know

$$K(E_L) = (E_H) \quad (5)$$

we can substitute 5 into 4

279

$$E_{HT} = K(E_L) + E_H S \quad (6)$$

From basic enzyme kinetics (5) and equation 1.1 we know

$$K_S = \frac{(E)(S)}{(ES)} \quad (7)$$

and rearranging

$$(ES) = \frac{(E)(S)}{K_S} \quad (8)$$

and substituting into equations 3 and 4 we get

$$E_{LT} = E_L + \frac{(E_L)(S)}{K_{SL}} \quad (9)$$

and

$$E_{HT} = K(E_L) + \frac{(E_H)(S)}{K_{SH}} \quad (10)$$

and substituting equation 5 into 10 we get

$$E_{HT} = K(E_L) + \frac{K(E_L)(S)}{K_{SH}} \quad (11)$$

The new equilibrium established for bound and free enzyme in the two forms can be written as

$$K' = \frac{E_H + E_H S}{E_L + E_L S} = \frac{E_{HT}}{E_{LT}} \quad (12)$$

Substituting equations 9 and 11 into 12 we get

$$K' = \frac{K(E_L) + \frac{K(E_L)(S)}{K_{SH}}}{(E_L) + \frac{(E_L)(S)}{K_{SL}}} \quad (13)$$

Rearranging we get

$$K' = \frac{K(E_L) \left(1 + \frac{(S)}{K_{SH}}\right)}{(E_L) \left(1 + \frac{(S)}{K_{SL}}\right)} \quad (14)$$

After cancelling the enzyme concentration we find that the equilibrium constant for total enzyme bound and free is

$$K' = K \frac{\left(1 + \frac{(S)}{K_{SH}}\right)}{\left(1 + \frac{(S)}{K_{SL}}\right)} \quad (15)$$

which shows that the equilibrium constant will vary according to the size of the respective binding constants K_{SL} and K_{SH} and according to the substrate concentration.

We can find the relationship at very high and low substrate concentrations by taking the limits of equation 15 with respect to S . So at low substrate concentration we find that the limit of $S \rightarrow 0$ is

$$\lim_{S \rightarrow 0} K' = K \quad (16)$$

At high substrate concentration we find that

$$\lim_{S \rightarrow \infty} K' = K \frac{\left(\frac{1}{K_{SH}}\right)}{\left(\frac{1}{K_{SL}}\right)} \quad (17)$$

or rearranging

$$\lim_{S \rightarrow \infty} K' = K \frac{K_{SL}}{K_{SH}} \quad (18)$$

APPENDIX B

Appendix B: Rate Equations for Enzymes Possessing Two
Catalytic Sites¹

To obtain a rate equation for an enzyme possessing two non-interacting catalytic sites characterized by different kinetic parameters, we need only sum two Michaelis-Menten equations. Thus

$$v = \frac{V_1}{\frac{K_1}{(S)} + 1} + \frac{V_2}{\frac{K_2}{(S)} + 1}$$

and

$$v = \frac{V_1 \left(\frac{K_2}{(S)} + 1 \right) + V_2 \left(\frac{K_1}{(S)} + 1 \right)}{\frac{K_1 K_2}{(S)^2} + \frac{K_1 + K_2}{(S)} + 1} \quad (1)$$

The reciprocal of this equation is given by

$$\frac{1}{v} = \frac{\frac{K_1 K_2}{(S)^2} + \frac{K_1 + K_2}{(S)} + 1}{V_1 \left(\frac{K_2}{(S)} + 1 \right) + V_2 \left(\frac{K_1}{(S)} + 1 \right)} \quad (2)$$

¹ Reproduced from the dissertation of Dr. Allen Frankfater (151).

Equation (1) is similar in form to an equation derived by Kistiakowsky and Rosenberg (152) to describe this same model. V_1 and V_2 are the contributions made by each site at saturating levels of substrate. Thus V_{max} is equal to $(V_1 + V_2)$.

Kistiakowsky and Rosenberg (152) have also derived an expression describing a model possessing two initially equivalent but interacting catalytic sites. This equation may be rewritten as

$$v = \frac{V_1 \frac{2K_2}{(S)} + 2V_2}{\frac{K_1K_2}{(S)^2} + \frac{2K_2}{(S)} + 1} \quad (3)$$

In reciprocal form equation (3) is

$$\frac{1}{v} = \frac{\frac{K_1K_2}{(S)^2} + \frac{2K_2}{(S)} + 1}{V_1 \frac{2K_2}{(S)} + 2V_2} \quad (4)$$

where V_1 is a maximum velocity term describing the hypothetical situation in which only one site is saturated, and $2V_2$ describes the contribution made by both sites at saturating levels of substrate and is therefore equal to V_{max} .

It is characteristic of equations (2) and (4) that different Lineweaver and Burk plots with different slopes and intercepts are approached at high

and low substrate concentrations (153). It is possible to derive equations which describe these linear segments. This method will be illustrated using equation (2).

$$\frac{1}{v} = \frac{\frac{K_1 K_2}{(S)^2} + \frac{K_1 + K_2}{(S)} + 1}{\frac{K_2 V_1 + K_1 V_2}{(S)} + V_1 + V_2} \quad (2a)$$

Then to determine the slope of this equation we differentiate. Thus

$$\frac{d \left(\frac{1}{v} \right)}{d \left(\frac{1}{S} \right)} = \frac{\left[\frac{K_2 V_1 + K_1 V_2}{(S)} + V_1 + V_2 \right] \left[\frac{2K_1 K_2}{(S)} + K_1 + K_2 \right] - \left[\frac{K_1 K_2}{(S)^2} + \frac{K_1 + K_2}{(S)} + 1 \right] \left[K_2 V_1 + K_1 V_2 \right]}{\left(\frac{K_2 V_1 + K_1 V_2}{(S)} + V_1 + V_2 \right)^2} \quad (5)$$

To evaluate this slope at infinite substrate concentration we take the limit of equation (5) as $1/(S) \rightarrow 0$.

Thus

$$\lim_{\frac{1}{S} \rightarrow 0} \frac{d \left(\frac{1}{v} \right)}{d \left(\frac{1}{S} \right)} = \frac{(V_1 + V_2) \cdot (K_1 + K_2) - V_1 K_2 + V_2 K_1}{(V_1 + V_2)^2}$$

or

$$\lim_{\frac{1}{(S)} \rightarrow 0} \frac{d \left(\frac{1}{V} \right)}{d \left(\frac{1}{(S)} \right)} = \frac{K_1 V_1 + K_2 V_2}{(V_1 + V_2)^2} \quad (6)$$

To determine the slope of equation (2) at the limit of zero substrate concentration we multiply the top and bottom of the right hand term of equation (5) by $(S)^2$ and evaluate it as $(S) \rightarrow 0$.

Thus

$$\left[K_2 V_1 + K_1 V_2 + (V_1 + V_2) (S) \right] \left[2K_1 K_2 + (K_1 + K_2) (S) \right] -$$

$$\frac{d \left(\frac{1}{V} \right)}{d \left(\frac{1}{(S)} \right)} = \frac{\left[K_1 K_2 + (K_1 + K_2) (S) + (S)^2 \right] \left[K_2 V_1 + K_1 V_2 \right]}{\left(K_2 V_1 + K_1 V_2 + (V_1 + V_2) (S) \right)^2}$$

then

$$\lim_{(S) \rightarrow 0} \frac{d \left(\frac{1}{V} \right)}{d \left(\frac{1}{(S)} \right)} = \frac{(K_2 V_1 + K_1 V_2) (2K_1 K_2) - K_1 K_2 (K_2 V_1 + K_1 V_2)}{(K_2 V_1 + K_1 V_2)^2}$$

$$\lim_{(S) \rightarrow 0} \frac{d \left(\frac{1}{V} \right)}{d \left(\frac{1}{(S)} \right)} = \frac{K_1 K_2}{K_2 V_1 + K_1 V_2} \quad (7)$$

To obtain the equation describing the straight line segment at high substrate

$$\frac{\frac{1}{v_2} - \frac{1}{v_1}}{\frac{1}{(S_2)} - \frac{1}{(S_1)}} = \frac{K_1V_1 + K_2V_2}{(V_1 + V_2)^2}$$

then

$$\frac{1}{v_2} - \frac{1}{v_1} = \frac{K_1V_1 + K_2V_2}{(V_1 + V_2)^2} \frac{1}{(S_2)} - \frac{K_1V_1 + K_2V_2}{(V_1 + V_2)^2} \frac{1}{(S_1)} \quad (8)$$

Combining equations (2) and (8) we have

$$\frac{1}{v_2} - \frac{\frac{K_1K_2}{(S_1)^2} + \frac{K_1 + K_2}{(S_1)} + 1}{\frac{K_2V_1 + K_1V_2}{(S_1)} + V_1 + V_2} = \frac{K_1V_1 + K_2V_2}{(V_1 + V_2)^2} \frac{1}{(S_2)} - \frac{K_1V_1 + K_2V_2}{(V_1 + V_2)^2} \frac{1}{(S_1)}$$

then

$$\frac{1}{v_2} = \frac{\left[\frac{K_1V_1 + K_2V_2}{(V_1 + V_2)^2} \frac{1}{(S_2)} \right] \left[\frac{K_2V_1 + K_1V_2}{(S_1)} + V_1 + V_2 \right] - \left[\frac{K_1V_1 + K_2V_2}{(V_1 + V_2)^2} \frac{1}{(S_1)} \right] \left[\frac{K_2V_1 + K_1V_2}{(S_1)} + V_1 + V_2 \right] + \frac{K_1K_2}{(S_1)^2} + \frac{K_1 + K_2}{(S_1)} + 1}{\frac{K_2V_1 + K_1V_2}{(S_1)} + V_1 + V_2}$$

when $1/(S_1) \rightarrow 0$

$$\frac{1}{v_2} = \frac{\frac{K_1 V_1 + K_2 V_2}{(V_1 + V_2)^2} \frac{1}{(S_2)} (V_1 + V_2) + 1}{(V_1 + V_2)}$$

or

$$\frac{1}{v} = \frac{K_1 V_1 + K_2 V_2}{(V_1 + V_2)^2} \frac{1}{(S)} + \frac{1}{V_1 + V_2} \quad (9)$$

Similarly, to obtain the equation for the straight line segment at low substrate concentrations we assume that to a good approximation

$$\frac{\frac{1}{v_2} - \frac{1}{v_1}}{\frac{1}{(S_2)} - \frac{1}{(S_1)}} = \frac{K_1 K_2}{K_2 V_1 + K_1 V_2}$$

then

$$\frac{1}{v_2} - \frac{1}{v_1} = \frac{K_1 K_2}{K_2 V_1 + K_1 V_2} \frac{1}{(S_2)} - \frac{K_1 K_2}{K_2 V_1 + K_1 V_2} \frac{1}{(S_1)} \quad (10)$$

Combining equation (2) and equation (10) we have.

$$\frac{1}{v_2} = \frac{\frac{K_1 K_2}{(S_1)^2} + \frac{K_1 K_2}{(S_1)} + 1}{\frac{K_2 V_1 + K_1 V_2}{(S_1)} + V_1 + V_2} = \frac{K_1 K_2}{K_2 V_1 + K_1 V_2} \frac{1}{(S_2)} - \frac{K_1 K_2}{K_2 V_1 + K_1 V_2} \frac{1}{(S_1)}$$

$$\frac{1}{v_2} = \left[\frac{K_1 K_2}{K_2 V_1 + K_1 V_2} \frac{1}{(S_2)} \right] \left[\frac{K_2 V_1 + K_1 V_2}{(S_1)} + V_1 + V_2 \right] - \left[\frac{K_1 K_2}{K_2 V_1 + K_1 V_2} \frac{1}{(S_1)} \right] \left[\frac{K_2 V_1 + K_1 V_2}{(S_1)} + V_1 + V_2 \right] +$$

$$\frac{K_1 K_2}{(S_1)^2} + \frac{K_1 + K_2}{(S_1)} + 1$$

$$\frac{K_2 V_1 + K_1 V_2}{(S_1)} + V_1 + V_2$$

$$\frac{1}{v_2} = \left[\frac{K_1 K_2}{K_2 V_1 + K_1 V_2} \frac{1}{(S_2)} \right] \left[\frac{K_2 V_1 + K_1 V_2}{(S_1)} + V_1 + V_2 \right] - \frac{K_1 K_2}{(S_1)^2} \frac{K_1 K_2 (V_1 + V_2)}{K_2 V_1 + K_1 V_2} \frac{1}{(S_1)} +$$

$$\frac{K_1 K_2}{(S_1)^2} + \frac{K_1 K_2}{(S_1)} + 1$$

$$\frac{K_2 V_1 + K_1 V_2}{(S_1)} + V_1 + V_2$$

multiplying the top and bottom of the right hand term by (S_1) we have

$$\left[\frac{K_1 K_2}{K_2 V_1} K_1 V_2 \frac{1}{(S_2)} \right] \left[K_2 V_1 K_1 V_2 + V_1 + V_2 (S_1) \right] - \frac{K_1 K_2 (V_1 + V_2)}{K_2 V_1 + K_1 V_2} +$$

$$\frac{1}{v_2} = \frac{K_1 + K_2 + (S_1)}{K_2 V_1 + K_1 V_2 + (V_1 + V_2) (S_1)}$$

then as $S_1 \rightarrow 0$.

$$\frac{1}{v_2} = \frac{\left[\frac{K_1 K_2}{K_2 V_1 + K_1 V_2} \frac{1}{(S_2)} \right] \left[K_2 V_1 + K_1 V_2 \right] - \frac{K_1 K_2 (V_1 + V_2)}{K_2 V_1 + K_1 V_2} + K_1 + K_2}{K_2 V_1 + K_1 V_2}$$

or

$$\frac{1}{v} = \frac{K_1 K_2}{K_2 V_1 + K_1 V_2} \frac{1}{(S)} + \frac{1}{K_2 V_1 + K_1 V_2} \left(K_1 + K_2 - \frac{K_1 K_2 (V_1 + V_2)}{K_2 V_1 + K_1 V_2} \right) \quad (11)$$

To determine the coordinates of the point of intersection of the straight line segments at high and low substrate concentrations described by equations (9) and (11) we set both equations equal to each other. Thus

$$\frac{K_1V_2 + K_2V_2}{(V_1 + V_2)^2} \frac{1}{(S)} + \frac{1}{V_1 + V_2} =$$

$$\frac{K_1K_2}{K_2V_1 + K_1V_2} \frac{1}{(S)} + \frac{1}{K_2V_1 + K_1V_2} \left(K_1 + K_2 - \frac{K_1K_2(V_1 + V_2)}{K_1V_2 + K_1V_2} \right)$$

then

$$\frac{1}{(S)} = \frac{\frac{K_1 + K_2}{K_2V_1 + K_1V_2} - \frac{K_1K_2(V_1 + V_2)}{(K_2V_1 + K_1V_2)^2} - \frac{1}{V_1 + V_2}}{}$$

$$\frac{K_1V_1 + K_2V_2}{(V_1 + V_2)^2} - \frac{K_1K_2}{K_2V_1 + K_1V_2}$$

$$\frac{1}{(S)} = \frac{(V_1 + V_2) \left[(K_1 + K_2) (K_2V_1 + K_1V_2) - K_1K_2 (V_1 + V_2) - K_2V_1 + K_1V_2 \right]}{(V_1V_2) (K_2V_1 + K_1V_2)^2}$$

$$\frac{(K_1V_1 + K_2V_2) (K_2V_1 + K_1V_2) - K_1K_2(V_1 + V_2)^2}{(K_2V_1 + K_1V_2) (V_1 + V_2)^2}$$

$$\frac{1}{S} = \frac{(V_1 + V_2) \left[(K_1 + K_2) (K_1V_2 + K_1V_2) (V_1 + V_2) - K_1K_2(V_1 + V_2)^2 - (K_2V_1 + K_1V_2)^2 \right]}{K_2V_1 + K_1V_2 \left[(K_1V_1 + K_2V_2) (K_2V_1 + K_1V_2) - K_1K_2 (V_1 + V_2)^2 \right]}$$

since

$$\begin{aligned} (K_1 + K_2) (K_2V_1 + K_1V_2) (V_1 + V_2) - K_1K_2(V_1 + V_2)^2 - (K_2V_1 + K_1V_2)^2 &= \\ (K_1V_1 + K_2V_2) (K_2V_1 + K_1V_2) - K_1K_2(V_1 + V_2)^2 & \end{aligned}$$

then at the point of intersection

$$\frac{1}{(S)} = \frac{V_1 + V_2}{K_2V_1 + K_1V_2} \quad (12)$$

substituting equation (12) into equation (9) we have

$$\frac{1}{v} = \left[\frac{K_1V_1 + K_2V_2}{(V_1 + V_2)^2} \right] \left[\frac{(V_1 + V_2)}{K_2V_1 + K_1V_2} \right] + \frac{1}{V_1 + V_2}$$

$$\frac{1}{v} = \frac{K_1V_1 + K_2V_2 + K_2V_1 + K_1V_2}{(V_1 + V_2)(K_2V_1 + K_1V_2)}$$

$$\frac{1}{v} = \frac{K_1(V_1 + V_2) + K_2(V_1 + V_2)}{(V_1 + V_2)(K_2V_1 + K_1V_2)}$$

Then at the point of intersection

$$\frac{1}{v} = \frac{K_1 + K_2}{K_2V_1 + K_1V_2} \quad (13)$$

Using this same technique, it is possible to demonstrate that for equation

(4) the line at high substrate concentration is given by

$$\frac{1}{v} = \frac{2K_2V_2 - K_2V_1}{2V_2^2} \frac{1}{(S)} + \frac{1}{2V_2} \quad (14)$$

and at low substrate concentration

$$\frac{1}{v} = \frac{K_1}{2V_1} \frac{1}{(S)} + \frac{1}{V_1} \left(1 - \frac{K_1 V_2}{2K_2 V_1} \right) \quad (15)$$

and at the point of intersection

$$\frac{1}{v} = \frac{1}{V_1} \quad (16)$$

and

$$\frac{1}{S} = \frac{V_2}{K_2 V_1} \quad (17)$$

APPROVAL SHEET

The dissertation submitted by John Paul Huff has been read and approved by the following committee:

Dr. Richard M. Schultz, Director
Associate Professor, Biochemistry and Biophysics, Loyola

Dr. Elliott J. Burrell
Associate Professor, Chemistry, Loyola

Dr. Allen Frankfater
Associate Professor, Biochemistry and Biophysics, Loyola

Dr. Charles F. Lange
Professor, Microbiology, Loyola

Dr. Robert V. Miller
Associate Professor, Biochemistry and Biophysics, Loyola

The final copies have been examined by the director of the dissertation and the signature which appears below verifies the fact that any necessary changes have been incorporated and that the dissertation is now given final approval by the Committee with reference to content and form.

The dissertation is therefore accepted in partial fulfillment of the requirements for the degree of Doctor of Philosophy.

4/24/81

Date

Richard M. Schultz

Director's Signature